UNIVERSITEIT VAN PRETORIA
UNIVERSITY OF PRETORIA
YUNIBESITHI YA PRETORIA

Faculty of Health Sciences
School of Health Care Sciences
Department of Radiography

Radiosensitising efficacy of histone deacetylase inhibitors CUDC-101 and SAHA in breast cell lines

Thesis in publication format for PhD (Radiography)

Student name: Elsie Neo Seane

Student number: 04309510

Supervisor: **Prof** AM Joubert
Department of Physiology, School of Medicine
Faculty of Health Sciences
University of Pretoria
Pretoria
South Africa

Co-supervisors:
Dr C Vandevoorde
GSI Helmholtzzentrum für Schwerionenforschung,
Department of Biophysics
Germany

Dr S Nair
Radiation Biophysics Division
NRF iThemba LABS
Cape Town
South Africa

Date: 19 November 2024

Declaration

I, Elsie Neo Seane, student number 04309510 hereby declare that:

1. this thesis, "*Radiosensitising efficacy of histone deacetylase inhibitors CUDC-101 and SAHA in breast cell lines,*" is submitted in accordance with the requirements for the Doctoral degree in Radiography (Radiation Therapy) at University of Pretoria.
2. I understand what plagiarism is and am aware of the University's policy in this regard. The Thesis is presented in the form of manuscripts that have been published, therefore Turn-it-in report is not included.
3. I declare that this thesis is my own original work. Where other people's work has been used (either from a printed source, Internet or any other source), this has been properly acknowledged and referenced in accordance with departmental requirements.
4. I have not used work previously produced by another student or any other person to hand in as my own.
5. I have not allowed and will not allow anyone to copy my work with the intention of passing it off as his or her own work.
6. I declare that I did not use artificial intelligence (AI) tools neither in the preparation of presented manuscripts nor in the preparation of the thesis.

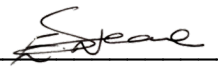

Elsie Neo Seane

Witness

Dr Aladdin Speelman

19 November 2024

Ethics Statement

The author, Elsie Neo Seane, whose name appears on the title page of this dissertation, has obtained, for the research described in this work, the applicable research ethics approval.

The author declares that she has observed the ethical standards required in terms of the University of Pretoria's Code of ethics for researchers and the Policy guidelines for responsible research.

Ethics Number: 689/2021

Ethics clearance certificates for years 2022- 2024 are included as **Annexure A**

Dedication

I dedicate this research to:

- My late family, my mother Galeboe Margaret Seane, and my sisters Ditshebo Khutswane, Seasebeng “Summer” Seane and Kelebogile Seane.

“When you all left me one after the other in a short space of time, I asked God to also take me rather than to leave me alone, but the answer I got was that my purpose is not yet served. They say time heals all wounds, but my wounds are too deep to heal. Will forever be in my heart”

- All the women who have succumbed breast cancer, particularly my aunt Mary Mogapi who passed on from metastatic breast cancer while the study was in progress.

Acknowledgements

To have achieved this milestone in my life, I would like to express my sincere gratitude to the following people:

- **Prof Annie Joubert**, my supervisor who provided me the strength, knowledge and perseverance to complete this study. Most importantly, the warmth and love of a mother figure that she radiates;

- **Dr Charlot Vandevoorde** and **Dr Shankari Nair**, my co-supervisors, for their guidance, invaluable advice, expertise and inspiring motivation during difficult times during the study;

- **The management of NRF iThemba laboratories** and the **Radiobiology laboratory team**. This project could not have been completed without the support, particularly support to access and to complete the proton experiments in Trento;

- **Dr Alessandra Bisio** from Cellular, Computational and Integrative Biology (CIBIO) laboratory (Italy) and the staff of Trento Institute of fundamental Physics and application (TIFPA) proton facility for hosting us and going an extra mile to support us to complete all the proton irradiations and laboratory work;

- **Peter Du Plessis**, my laboratory partner and friend. They say choosing a lab partner is more important than choosing a life partner, and I agree. You were there from the beginning to the end, and most importantly you made me laugh through the challenges of the journey;

- **Aladdin Speelman, Valdiela Daries** and **Rika and Victor Boshoff**, my support system, I couldn't have done it without your encouragement, and continued love and support;

- **Kopano Seane**, my daughter who had to keep up with my moods during this challenging journey;

- Last, but not the least – **Funders**, Department of Higher Education and Training (IQP grant and USDP grant) and NRF iThemba Laboratories.

Abstract

Introduction: Photon-based radiation therapy remains to be an important treatment modality in the management of breast cancers. However, proton therapy has attracted a lot of interest due to the ability to reduce dose to healthy tissues. It is rapidly evolving as a radiation therapy tool for women with left-sided breast cancer in order to limit unnecessary dose to the heart and reduce the risk of long-term cardiac morbidity. In addition to the evolution in radiation therapy modalities, increasing evidence shows that histone deacetylase inhibitors (HDACi) are able to sensitise cancer cells to ionising radiation with little effect on healthy cells. Studies on radiosensitising capabilities of HDACi in combination with proton irradiation remain limited. To date, the published manuscripts presented in this thesis were the first to be published on radiosensitising capabilities of HDACi in combination with proton therapy in breast cell lines.

Aim and hypothesis: The study aimed to compare *in vitro* radiosensitising capacities of two different HDACi, suberoylanilide hydroxamic acid (SAHA) and CUDC-101, to photon and proton irradiation in multiple breast cell lines. CUDC-101 is an inhibitor of histone deacetylases (HDACs), epidermal growth factor receptor (EGFR) and human epidermal growth factor receptor 2 (HER2) and was therefore expected to be a more effective radiosensitiser than SAHA.

Research design: The study followed a factorial experimental design with three main effects (HDACi, cell types, radiation types) with three repeats and 180 observations.

Methods: MCF-7, MCF-10A and MDA-MB-231 human breast cell lines were utilised to conduct cell proliferation, clonogenic survival, gamma-Histone subtype H2A isoform X (γ-H2AX), cell migration, apoptosis and cell cycle analysis assays. Cells were pre-treated with HDACi and each sample irradiated at room temperature with varying doses of 184 MeV proton irradiation or 250Kvp X-rays. Data analysis was conducted using Graphpad Prism software. For statistical analysis, unpaired Student *t*-tests were used to test for significance. Testing was done at the 0.05 level of significance.

Significance of the study: The study contributes new knowledge on HDACi-mediated sensitisation of breast cell lines to proton irradiation. The results highlighted the role of CUDC-101 as a potent radiosensitizer and a promising strategy to mitigate breast cancer metastasis. The results also add to the ongoing efforts to clarify the mechanisms that underlie the radiosensitising effects of HDACi particularly to proton irradiations.

Results: Both HDACi, SAHA and CUDC-101 are able to enhance the radiation-induced cytotoxicity in the MCF-7 and MDA-MB-231 breast cancer cell lines when combined with either X-rays or protons. In the triple negative MDA-MB-231 cell line, increased DNA DSB induction and retention following treatment with CUDC-101 or SAHA monotherapy and in combination treatments with 2Gy protons or X-rays. An unexpected finding in the study was the increase in migration and invasion after SAHA treatment in the MCF-7 cell line, whereas both SAHA and CUDC-101 reduced migration and invasion in the triple negative MDA-MB-231 cells.

Key terms /concepts: histone deacetylase inhibitor, radiosensitising efficacy, photon therapy, proton therapy, metastasis and relative biological effectiveness

List of Abbreviations/ Acronyms

Abbreviation / acronym	Meaning
ºC	Degree Celsius
%	Percentage
µg/mL	Micrograms per millilitre
µM	Micromolar
γ-H2AX	gamma-Histone subtype H2A isoform X
Ac-histone	Acetylated histone
Ac-tubulin	Acetylated tubulin
ANOVA	Analysis of Variance
ATCC	American Type Culture Collection
BSA	Bovine serum albumin
CDK	Cyclin-dependent kinase
CO_2	Carbon dioxide
CSA	Colony survival assay
CUDC-101	7-(4-(3-Ethynylphenylamino)-7-methoxyquinazolin-6-yloxy)-*N*-hydroxyheptanamide
DAPI	4′,6-Diamidino-2-phenylindole dihydrochloride
DDR	DNA damage repair
DMEM	Dulbecco's Modified Eagle's Medium
DMSO	Dimethyl sulfoxide
DNA	Deoxyribonucleic acid
DNA-PK's	DNA-dependent protein kinases
DSB	Double strand break
DTT	Dithiothreitol
EGFR	Epidermal growth factor receptor
ELISA	Enzyme-linked immunosorbent assay
ER	Estrogen receptor
FACS	Fluorescence-activated cell sorting
FBS	Fetal bovine serum
FDA	Food and Drug Administration
FITC	Fluorescein isothiocyanate
HATs	Histone acetyltransferase
G1	Gap 1
G2	Gap 2
Gy	Gray
H2AX	Histone subtype H2A isoform X
HCC	Hepatocellular carcinoma
HDAC	Histone deacetylase
HDACi	Histone deacetylase inhibitors
HER2	Human epidermal growth factor receptor 2

HR	Homologous repair
IAEA	International Atomic Energy Agency
ISO/IEC	International Standards Organisation and International Electrotechnical Commission
IC_{50}	Half-maximal inhibitory concentration
IQP	Improvement of qualifications programme
L	Litre
MCF-7	Michigan Cancer Foundation-7
MCF-10A	Michigan Cancer Foundation-10A
Mcl-1	Myeloid cell leukemia-1
MDA-MB-231	M.D. Anderson Metastatic Breast cancer
MeV	Mega electron volt
mL	Millilitre
mM	Millimolar
M-phase	Mitosis
MTT	Thiazolyl blue tetrazoliumbromide
MRN	MRE11, Rad50 and NBS1 complex
MV	Megavoltage
NaCl	Sodium chloride
NEHJ	Non-homologous end joining
nM	Nanomolar
NMISA	National meteorology institute of South Africa
NSCLC	Non-small cell lung cancer
OAR	Organs at risk
p21	Cyclin-dependent kinase inhibitor
p53	Tumour suppressor protein
PE	Platting efficiency
p-ERK	Phosphorylated extracellular signal regulated kinase
PFA	Paraformaldehyde
PI	Propidium iodide
PR	Progesterone receptor
PRAVO	Pelvic radiotherapy and vorinostat
PVDF	Polyvinylidene difluoride
Rb	Retinoblastoma
RBE	Relative biological effectiveness
RECIST	Response evaluation criteria in solid tumours
RIPA	Radio immunoprecipitation
RNA	Ribonucleic acid
RNase	Ribonuclease
SA	South Africa
SAHA	Suberoylanilide hydroxamic acid
SER	Sensitisation enhancement ratio

S-phase	Synthesis phase
SDS	Sodium dodecyl sulphate
SSD	Source skin distance
TNBC	Triple-negative breast cancer
Tris-HCl	Trisaminomethane hydrochloride
UCDG	University Capacity Development Grant
USA	United States of America

Table of Contents

List of Figures

CHAPTER 1: INTRODUCTION

1.1 BACKGROUND AND CONTEXT

Breast cancer remains the most common cancer in females in sub-Saharan Africa[1-3] and the second leading cause of death in females worldwide.[4] Majority of breast cancer deaths are attributed to metastasis.[5] Despite improved detection and treatment facilities in South Africa as compared to other sub-Saharan African countries, overall survival rates remain to be low with 5-years expected survival of 50%.[4, 6] The South African National Department of Health's breast cancer treatment guidelines (2018) recommends surgery, radiation therapy and systematic therapy as the main treatment modalities, and all are offered in public and private health care systems.[3, 6] Data from randomised clinical trials has indicated that giving radiation therapy post- breast conserving surgery improves long term local control and overall survival with good cosmetic outcomes as compared to mastectomy.[7]

Although breast cancer irradiation using megavoltage (MV) photons is widely available and has improved treatment outcomes, it is also associated with late effects such as secondary malignancies and cardiopulmonary toxicities which can impact on overall survival.[4] Proton therapy is a form of particle radiation therapy with unique physical characteristics as illustrated in Figure 1.[4, 8] Proton therapy allows conformal irradiation of the tumour with a low entrance dose and low doses to the normal tissues proximal to the tumour, while there is no dose deposited beyond the Bragg peak. This allows significant dose reduction for surrounding normal tissue and organs at risk (OAR) compared to conventional photon-based radiotherapy.

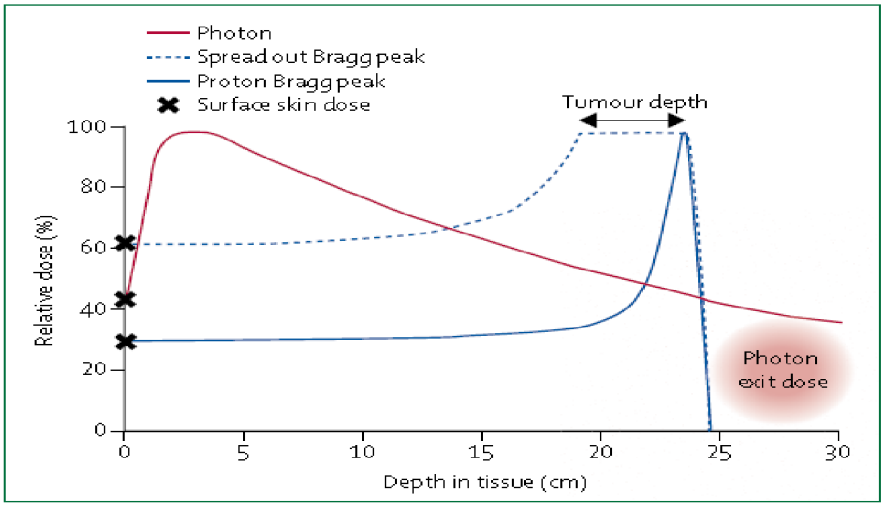

Figure 1: Physical Depth dose curve for MV photons is shown in red. The solid blue and dashed blue lines represent proton Bragg peak and proton spread-out Bragg peak, respectively.[9]

In terms of biologic effectiveness, both X-rays and protons are classified as low linear energy transfer (LET) types of radiation, and have comparable relative biological effectiveness (RBE) values.[10,11] RBE is a concept that compares the different biological activities of particle therapy such as carbon ions and protons to that of X-rays when the same physical dose is used.[12] Previously, a standard RBE value of 1.1 was assumed for protons, however, growing evidence supports that the RBE of protons differs under different circumstances such as cell line, proton beam energy, dose per fraction and chemotherapeutic or targeted therapy agents used.[11-13] This lends support to the fact that proton RBE values should be determined for different cell lines and for different therapy combinations.

Evidence from pre-clinical studies has revealed that the combination of radiation and histone deacetylases inhibitors (HDACi) results in increased cell kill in a number of cell lines including lung, colon and breast, to name a few.[14-24] To date, five HDACi SAHA (generic name vorinostat), belinostat, panabinostat, chidamide, romidepsin have been approved by the Food and Drug Administration (FDA) for cancer therapy.[25, 26] More than 20 different HDACi are in different phases of clinical trials as monotherapy for melanoma, prostate, glioma, colon, non-small cell lung cancer (NSCLC), osteosarcoma and breast in combination with other deoxyribonucleic acid (DNA) damaging agents.[27] HDACi are classified into several classes according to their chemical structure namely benzamides (e.g. chidamide, entinostat), hydroxamic acids (e.g. SAHA, belinostat, panabinostat, CUDC-101), cyclic tetrapeptides (e.g. romidepsin) and aliphatic acids (e.g. butyrate, valproic acid).[17, 28] Of these classes, hydroxamic acids is the main class that has been used and continues to be used in most studies.[29] Hydroxamic acids are preferred as they inhibit a broad range of histone deacetylases (HDACs) (HDACs1-11), and they can cause cellular effects at low (nM) concentrations.[27] HDACi can also be classified into pan-HDACi that can inhibit all HDAC classes (e.g. SAHA), selective HDACi, that targets a specific HDACs and multi-target inhibitors that inhibit HDACs and other targets (e.g. CUDC-101).

When used as monotherapy, HDACi have shown promising therapeutic outcomes in haematological malignancies such as leukaemia, multiple myeloma and lymphoma, with disappointing results in solid tumours.[25-27, 30, 31] The molecular basis for the poor clinical outcomes in solid tumours are still unclear, but are thought to be due to the short drug half-life of HDACi which leads to poor drug distribution, poor HDAC isoform selectivity, and poor patient selection.[25, 27] As a result, combination therapies either with radiation or other DNA damaging agents have been suggested as ideal strategy to improve their efficacy in solid tumours.[17, 26, 30]

The radiosensitising capabilities of HDACi using photon irradiation has been assessed in a number of pre-clinical and clinical studies. Evidence from pre-clinical shows that different classes of HDACi are able to sensitise tumour types such as melanoma, metastatic breast, prostate, colorectal, head and neck squamous cell, non-small cell lung cancers and glioblastoma mutliforme to photon irradiation.[14, 32-36] As an example, in a pre-clinical study by Moertl *et al*[36] the radiosentising effect of multi-target HDACi CUDC-101, was compared with SAHA in human pancreatic tumour cell lines. Enhancement of radiation-induced cytotoxicity was observed with both HDACi. CUDC-101 was, however, determined to be a more effective radiosensitiser than SAHA.[36] The increased effectiveness of CUDC-101 could be attributed to inhibition of epidermal growth factor receptor (EGFR) which is often overexpressed in pancreatic tumours.[37] The study was conducted using photons.

In an *in vitro* study by Schlaff *et al*[38] CUDC-101 was reported to enhance sensitivity of glioblastoma cells and an MDA-MB-231 cell line to photon irradiation with no effect on normal fibroblasts. The *in vitro* study was followed by an *in vivo* study and the results of the *in vitro* study could not be replicated *in vivo* due to high toxicity. This is in contradiction to an earlier *in vivo* study by Bashnagel *et al*[21] where mice implanted with MDA-MB-231 breast cells using intracranial implant models were treated with SAHA and photon irradiation. The authors reported that SAHA and photon irradiation had a greater additive effect on tumour growth delay with minimal signs of toxicity.[21] The discrepancy in the results of the two studies might be due to the fact that CUDC-101, which was hypothesised to be a more effective radiosensitiser than SAHA in the current study, was used in the study by Schlaff *et al*.[38] In another *in vitro* study, Chiu *et al*[20] investigated the anti-cancer effects of SAHA combined with photon radiation using MCF-7 and MDA-MB-231 breast cancer cell lines. The study reported SAHA in combination with photon radiation as having an increased therapeutic efficacy compared to either treatment alone.[20]

A small number of Phase I clinical trials have also been conducted to establish the maximum tolerated dose of HDACi SAHA and panabinostat in combination with photon irradiation in the treatment of brain[39], gastro-intestinal [40]oesophagus, head and neck, prostate[41], refractory neuroblastoma.[42] Results from Phase I studies revealed a daily dose of 300mg for SAHA to be well tolerated. Results of the trial using panabinostat have not been published. In Phase II study using SAHA and photon irradiation in non-small cell lung cancer, objective response to treatment could not be observed in any of the patients using the response evaluation criteria for solid tumours (RECIST). The authors highlighted that the RECIST criteria might not be

suitable in assessing the efficacy of targeted agents.[43] Another Phase II study using combination of valproic acid, temozolomide and radiation therapy in glioblastoma tumours was shown to improve progression free survival from 19.3 months when using radiation therapy and temozolomide to 29.6 months when HDACi valproic acid combined with radiation therapy and temozolomide. [44]

Studies on the radiosensitising abilities of HDACi using particle therapy are still limited. SAHA increased the sensitivity of glioblastoma cell lines (LN18, U251)[45], sarcoma and lung cell lines[46] to irradiation with carbon ions as compared to irradiation with photon irradiation.[11] In pre-clinical studies using proton irradiation, HDACi valproic acid enhanced sensitivity of hepatocellular carcinoma (HCC) Hep3B cells to proton irradiation as compared to photon irradiation by enhancing apoptosis and prolonged DNA damage induction.[12] However, the homologous recombination (HR) repair genes were not observed to be altered after proton irradiation.[12] This is in contradiction to an earlier study where the HR pathway was found to be crucial for proton-induced DNA damage repair following treatment with SAHA in A549 lung cell line.[47] These findings could suggest that choice of repair pathway is not only dependent on the type of radiation type used, but might be dependent on HDACi and cell line used. In a follow-up study, HDACi panabinostat was found to increase the RBE_{37} (RBE determined at 37% cell survival) of protons from 1.33 to 1.44 and from 1.18 to 1.30 in HCC (Hep3Band Huh7) cell lines.[11]. The increase in RBE was attributed to the downregulation of Mcl-1 which in turn impaired the HR pathway. These first results indicate that more studies are needed to clarify the mechanisms of HDACi-mediated sensitisation to proton irradiation.

1.2 PROBLEM STATEMENT

Proton therapy has emerged as an exciting radiotherapy modality for breast cancer due to the ability to minimise dose to normal organs such as the lungs, heart, coronary arteries and to reduce chances of secondary malignancies.[4] However, questions remain around the radiobiology of protons.[48, 49] On the other hand, HDACi have also emerged as promising agents that can enhance radiation response and improve tumour control. Accumulating evidence from pre-clinical and clinical studies indicates that radiation therapy (protons or photons) may be a suitable combination modality with HDACi in a number of cancer types.[11, 18, 24, 50] Ample evidence exists to support the radiosensitising effect of HDACi SAHA in combination with X-rays on MCF-7, MDA-MB-231 and 4T1 cell lines [20], but combination treatments of HDACi, particularly CUDC-101 and particle therapies remain limited. Further, the molecular mechanisms that contribute to the radiosensitising effect of HDACi are poorly understood, particularly when combined with proton therapy.[11]

1.3 RESEARCH QUESTION(S), AIMS AND OBJECTIVES

Aim of the study

The study aimed to investigate *in vitro* radiosensitising efficacy of multi-target HDACi CUDC-101 and pan-HDACi SAHA in malignant (MCF-7), spontaneously immortalised (MCF-10A) and triple-negative (MDA-MB-231) breast cancer cell lines.

The objectives of the research study were

1. to quantify relative cell survival upon treatment with different concentrations of HDACi (SAHA or CUDC-101), in combination with proton and photon irradiations;
2. to quantify the proportion of cells in G1, S and G2/M phases of the cell cycle as a result of treatment with HDACi in combination with proton and photon irradiations;
3. to quantify gamma-H2AX foci formation and retention post-treatment with HDACi in combination with proton and photon irradiations;
4. to quantify the fraction of apoptotic cells after treatment with HDACi in combination with proton and photon irradiations and
5. to determine cell migratory and invasion capacity post treatment with HDACi in combination with proton and photon irradiations.

1.4 DEFINITION OF KEY TERMS / CONCEPTS

Radiosensitising efficacy

Conceptual definition: The relative ability of the pharmacological agent in increasing the cell's susceptibility to damage by radiation.[51]

Operational definition: Radiosensitising efficacy will be calculated at survival fraction of 10% (D_{10}) using sensitisation enhancement ratio (SER). [11, 13, 46]

$$SER = \frac{Dose\ of\ radiation\ that\ reduces\ cell\ survival\ to\ 10\%\ without\ sensitiser}{Dose\ of\ radiation\ that\ reduces\ cell\ survival\ to\ 10\%\ with\ sensitiser} \quad \text{(Eq.1)}$$

Relative biological effectiveness (RBE)

Conceptual definition: The ratio of doses required of a reference type of radiation (photons) over a test type radiation (protons) to induce the same level of biological effect.[11]

Operational definition: RBE will be determined from data from clonogenic survival assays at survival fraction of 10% (D_{10}) and 37% (D_{37}).[11, 13, 46]

$$RBE = \frac{Dose\ of\ photon\ radiation}{Dose\ of\ proton\ radiation}\ that\ reduce\ fraction\ of\ surviving\ cells\ to\ 10\% \quad \text{(Eq.2)}$$

Histone deacetylase inhibitor

Conceptual definition: Chemical compounds that inhibit the action of histone deacetylases.[15]

Operational definition: The inhibition capacity of the HDACi will be measured using by determining the half maximum inhibitory concentration (IC_{50}).[52]

Photon Therapy

Conceptual definition: A type of ionising radiation therapy that uses electromagnetic radiation (x-rays or gamma rays). X-rays are generated from a linear accelerator and gamma rays are emitted as radioactive Cobalt-60 source decays. [53]

Operational definition: Irradiation using photons causes DNA damage which results in abnormal cell function and cell death. Cell death will be measured by determining the fraction of cells that survive the different radiation doses.[54]

Proton Therapy

Conceptual definition: Type of radiation therapy that uses particles with an electric charge of +1 and mass of 1 atomic mass unit. Protons are generated in a cyclotron.[53]

Operational definition: Irradiation with protons causes DNA damage which results in abnormal cell function and cell death. The response of cells to protons irradiation will be measured by determining the fraction of cells that survive the different radiation doses.[54]

1.5 SETTING

The study was laboratory-based using human breast cell lines. All the X-ray experiments were conducted at Radiation biology section of iThemba Laboratory for Accelerators Based Sciences (LABS), Faure, Cape Town, South Africa (SA). Proton beam was generated at Trento Institute of Fundamental Physics and Applications (TIFPA), Azienda Provinciale per i Servizi Sanitari, Trento, Italy. All the proton experiments were conducted at the Department of Cellular, Computational and Integrative Biology (CIBIO) Laboratories, Via Sommarive, 9, Povo, 38123 Trento, Italy.

1.6 DELINEATION

The study was limited to human breast cell lines (MCF-7, MCF-10A and triple-negative cell cancer line MDA-MB-231). The scope of the study was limited to treatments with two HDACi, SAHA and CUDC-101 in combination with two types of radiation, protons and X-rays. Experiments conducted were *in vitro* and results of the study cannot be extrapolated to *in vivo*.

1.7 SIGNIFICANCE OF THE STUDY

Proton therapy centres have increased exponentially and continue to increase across the globe and the use of proton therapy treatments for breast cancer is increasing, but limited data exist on the benefit of proton therapy in breast cancer.[8] Also, since the discovery of HDACi as potential radiosensitisers, the focus of most studies has been on combination therapies of HDACi and X-rays. Therefore, this *in vitro* study presents new knowledge about the response of MCF-7, MDA-MB-231 and MCF-101A cell lines to proton irradiation, as well as the efficacy of HDACi SAHA and CUDC-101 in sensitising breast cell lines to proton and photon irradiation. The results are not limited to the local effects but also include new knowledge on the systematic effects of HDACi, either as monotherapy or in combination with both types of radiation. The study outcomes also contribute in clarifying the mechanisms that underlie HDACi-mediated radiosensitisation, particularly when combined with proton irradiation.

1.8 OVERVIEW OF THE CHAPTERS

Chapter One provides context to the study with respect to proton therapy, histone deacetylase inhibitors (HDACi) and existing knowledge on the combination therapies of HDACi and radiation. Chapter Two is presented in the form of a published literature review, according to specific journal format. An additional published literature review is included as Annexure B. The published papers highlight the known cellular effects of HDACi as well, the continuing ambiguities around their mechanisms of action, and applications of HDAC targeted imaging. The published literature also highlights the inconsistencies in the methods used in the previous studies, which has contributed to challenges in interpretation of existing data. Chapter Three is also presented in the form of a published paper and addresses objectives 1- 4 using CUDC-101. Chapter Four is presented in the form of a submitted manuscript (published in the pre-prints) which addresses objective 5. Chapter Five presents a draft manuscript which is intended to be submitted in January 2025 and includes data for objectives 1- 4 using SAHA. Chapter Six contains the general discussions and summarises the publications presented and recommendations for future research are also highlighted.

1.9 CONCLUSION

Chapter one provided the context to the study and highlighted the nature of the problem that motivated the study. The research question as well as the objectives that guided the study, were outlined. The key terms and concepts were defined to provide clarity to the reader. The study setting and the *in vitro* nature of the study were clarified, and the significance of the study was also highlighted.

CHAPTER 2: LITERATURE REVIEW

Published Literature Review Article 1:

Seane EN, Nair S, Vandevoorde C, Joubert A. Mechanistic Sequence of Histone Deacetylase Inhibitors and Radiation Treatment: An Overview. Pharmaceuticals (Basel). 2024 May 8;17(5):602. doi: 10.3390/ph17050602. PMID: 38794172; PMCID: PMC11124271.

Published Literature Review Article 2

Everix L, **Seane EN**, Ebenhan T, Goethals I, Bolcaen J. Introducing HDAC-Targeting Radiopharmaceuticals for Glioblastoma Imaging and Therapy. Pharmaceuticals (Basel). 2023 Feb 1;16(2):227. doi: 10.3390/ph16020227. PMID: 37259375; PMCID: PMC9967489.

pharmaceuticals

MDPI

Review

Mechanistic Sequence of Histone Deacetylase Inhibitors and Radiation Treatment: An Overview

Elsie Neo Seane [1,2,3,*], Shankari Nair [3], Charlot Vandevoorde [4] and Anna Joubert [5]

[1] Department of Radiography, School of Health Care Sciences, Faculty of Health Sciences, University of Pretoria, Pretoria 0028, South Africa
[2] Department of Medical Imaging and Therapeutic Sciences, Faculty of Health and Wellness, Cape Peninsula University of Technology, Cape Town 7530, South Africa
[3] Radiation Biophysics Division, Separate Sector Cyclotron (SSC) Laboratory, iThemba LABS, Cape Town 7131, South Africa; shankari.nair.dr@gmail.com
[4] GSI Helmholtz Centre for Heavy Ion Research, Department of Biophysics, 64291 Darmstadt, Germany; c.vandevoorde@gsi.de
[5] Department of Physiology, School of Medicine, Faculty of Health Sciences, University of Pretoria, Pretoria 0028, South Africa; annie.joubert@up.ac.za
* Correspondence: seanee@cput.ac.za

Abstract: Histone deacetylases inhibitors (HDACis) have shown promising therapeutic outcomes in haematological malignancies such as leukaemia, multiple myeloma, and lymphoma, with disap- pointing results in solid tumours when used as monotherapy. As a result, combination therapies either with radiation or other deoxyribonucleic acid (DNA) damaging agents have been suggested as ideal strategy to improve their efficacy in solid tumours. Numerous in vitro and in vivo studies have demonstrated that HDACis can sensitise malignant cells to both electromagnetic and particle types of radiation by inhibiting DNA damage repair. Although the radiosensitising ability of HDACis has been reported as early as the 1990s, the mechanisms of radiosensitisation are yet to be fully understood. This review brings forth the various protocols used to sequence the administration of radiation and HDACi treatments in the different studies. The possible contribution of these various protocols to the ambiguity that surrounds the mechanisms of radiosensitisation is also highlighted.

Citation: Seane, E.N.; Nair, S.; Vandevoorde, C.; Joubert, A. Mechanistic Sequence of Histone Deacetylase Inhibitors and Radiation Treatment: An Overview. *Pharmaceuticals* **2024**, *17*, 602. https://doi.org/10.3390/ph17050602

Academic Editor: Irina Velikyan

Received: 27 March 2024
Revised: 28 April 2024
Accepted: 6 May 2024
Published: 8 May 2024

1. Introduction

Histone deacetylase inhibitors (HDACis) have attracted a lot of interest as potential radiosensitisers that have selective effects on malignant cells with little effect on healthy cells [1,2]. The radiosensitising capabilities of HDACis in combination with photon irradiation have been well studied [3–12], while studies in combination with proton and carbon ion irradiation remain limited [13–18]. The exact mechanisms that underlie the radiosensitisation potential of these drugs for both photons and particle types of radiation also remain a matter of research. The effect of HDACis on the DNA damage repair (DDR) pathways as well as the effect they have on chromatin structure have been suggested as the main mechanisms [19–24]. However, the temporal sequence of HDACis in combination with radiation, as well as the optimal duration of HDACi treatment during a radiotherapy course, remains an elusive subject. As a result, different administration times and sequences have been used in *in vitro* studies so far, which makes the interpretation of results complex. Data on HDACi and radiation treatment from clinical studies and clinical trials are very limited [25–28]. In this review, the cellular effects of HDACis as well as the proposed mechanisms of radiosensitisation by HDACis are briefly reviewed, followed by the review of temporal sequences of radiation and HDACis used in different *in vitro* studies. The durations of incubation with HDACis before or after radiation in these studies are also reviewed.

2. Epigenetic Modulation by HDACs and HDAC Inhibitors

During the process of malignant transformation in cells, genes that encode for his- tone acetyl transferases (HATs) can be amplified, translocated, or mutated leading to the inactivation of HATs. Consequently, histone deacetylase (HDACs) become overactive in malignant cells, resulting in the accumulation of deacetylated proteins. The overexpression of HDACs has been found in multiple human tumours such as lymphoma, prostate, gastric, leukaemia, colon, and breast [3,4,6–12,29]. HDACs have thus been recognised as promising targets to modify and reverse the aberrant epigenetic control in cancer cells [7]. HDACs are classified into four classes: Class I (HDACs 1, 2, 3, 8), Class II (HDACs 4, 5, 6, 7, 9, 10), Class III (Sirtuins 1-7), and Class IV (HDAC 11) [30]. To this effect, HDACis have emerged as anti-cancer agents aimed at reversing the aberrant histone modification control in tumours [20,31,32]. The inhibition of HDAC activity results in the accumulation of acetylated proteins leading to cellular effects such as cell cycle arrest, differentiation, altered gene expression, and the inhibition of angiogenesis, metastasis, and apoptosis in a cell-type-dependent manner, as shown in Figure 1 [31,33,34].

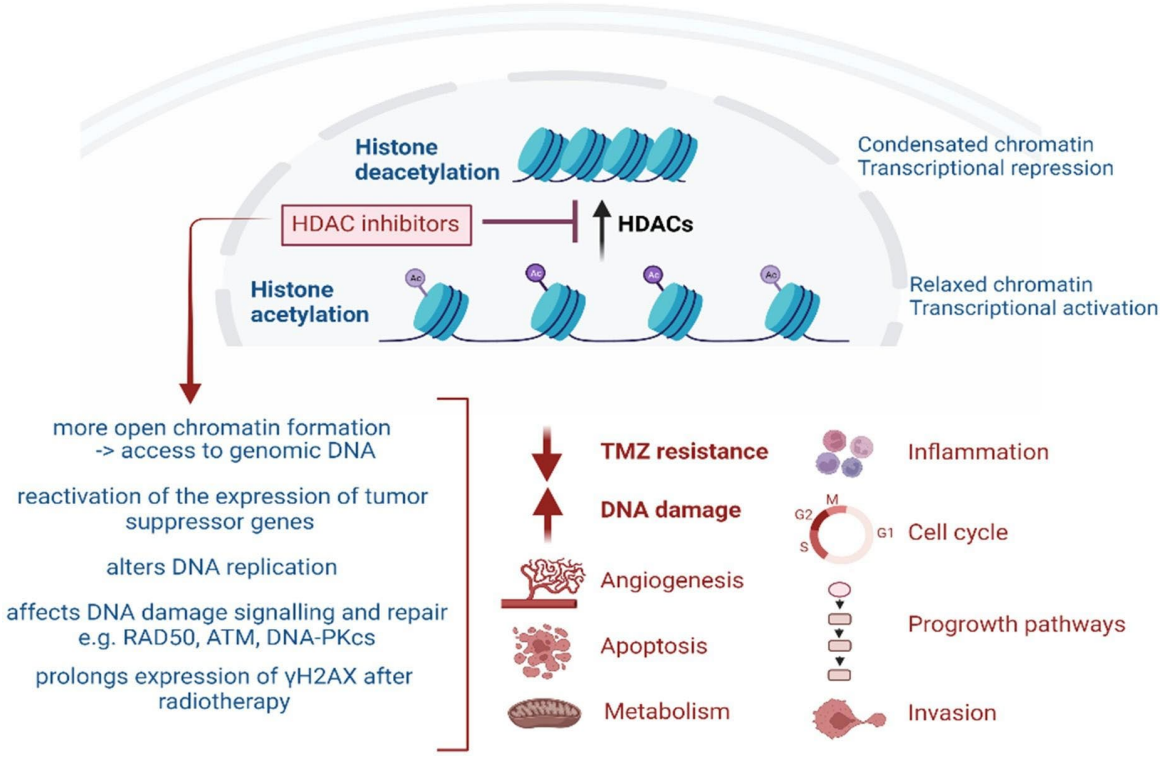

Figure 1. Overview of the broad effects of HDAC inhibitors [35].

The mechanism of action of HDACis has been linked to the structure and class of HDACis. In brief, HDACis are classified according to structure into benzamides (e.g., chidamide and entinostat), hydroxamic acids (e.g., vorinostat (SAHA), belinostat, panabinostat, and CUDC-101), cyclic tetrapeptides (e.g., romidepsin), and aliphatic acids (e.g., butyrate and valproic acid) [6,36,37]. Of these classes, hydroxamic acids are the main class that has been used and continues to be used in most studies [38]. Hydroxamic acids are preferred as they inhibit a broad range of HDACs (HDACs1-11), and they can cause cellular effects at low (nM) concentrations [37].

Earlier studies proposed histone hyper-acetylation and subsequent alterations in gene expression to be the main mechanism through which HDACis mediate their antiproliferative effect. Histone acetylation was reported to increase at 6 h post-treatment, reaching a maximum between 24 and 48 h after treatment with HDACi MS-275 in prostate carcinoma (DU145) and glioma (U251) cell lines [4]. However, this hypothesis could not explain the high specificity of HDACis for tumour cells. Subsequently, the hyper- acetylation of non-chromatin and non-histone proteins involved in cell death, proliferation, cell migration, inflammation, angiogenesis, cell cycle control, and DNA repair were acknowledged [13,32,33]. HDACi-

induced cell death is mediated by several mechanisms, including apoptosis, autophagy, necrosis, and cell cycle arrest in a cell-type-dependent manner [31,33,34].

2.1 HDACi-Induced Apoptosis and Autophagy

The induction of apoptosis was initially recognised as the predominant mode of HDACi-induced cell death [39–41]. A number of studies reported HDACi-induced apoptosis through both the intrinsic and extrinsic pathways [20,31–33,39,42–44]. In particular, the intrinsic (mitochondria-related) apoptotic pathway has been supported by many studies as the main pathway that is activated by HDACi [20,31,33,39,42–44]. In brief, HDACi increases the production of reactive oxygen species (ROS), which leads to the loss of mem- brane potential. The loss of membrane potential enables cytochrome *c* to be released from the mitochondria to the cytoplasm, leading to the activation of caspase 9 and initiation of apoptosis [45]. The activation of both p53-dependent and -independent apoptotic pathways post-HDACi treatment has been reported, which would be beneficial for the treatment of p53 mutant tumours [2]. The role of the extrinsic apoptotic pathway and caspase- independent pathways in HDACi-induced apoptosis have long been acknowledged but remain poorly understood [32,39]. However, a possible link between autophagy and the extrinsic apoptotic pathway has been reported [46]. It is possible that since autophagic cell death in cancer is not well understood, some autophagic cell death may have previously been attributed to caspase-independent apoptotic death [47].

The role of autophagy in cancer is complex and remains controversial [48]. Traditionally, autophagy was regarded as a cell death mechanism which eliminates damaged organelles, proteins, macromolecules, and breakdown products from cells, thereby suppressing tumour progression. Hence, autophagy was referred to as cell death type II [2]. Later evidence suggested that autophagy can also act as a cell survival mechanism to promote tumour growth [49]. A conceivable explanation of the dynamic nature of autophagy in cancer elucidated that the role of autophagy depends on the stage, type of tumour, and genetic pre-disposition of the tumour [2,49,50]. In the early tumour stages, autophagy plays a protective role by preventing the accumulation of damaged organelles and macro- molecules. In the late tumour stages, autophagy assumes the role of a survival mechanism by recycling degraded metabolites and counteracting the effect of chemotherapy treatment as well as oxygen and nutrient deprivation in hypoxic tumour areas, maintaining tumour growth [2,50]. It is appealing to associate the role of autophagy in late-stage tumours to the role of mammalian target of rapamycin (mTOR). mTOR plays a crucial role in metabolism and regulates autophagy by deactivating human autophagy initiation kinase ULK1, a component of upstream autophagic signalling pathway [2].

It comes as no surprise that HDACi-induced autophagy is also a highly debated topic. The proposed working mechanisms of HDACi-mediated autophagy include acetylation and upregulation of numerous autophagy-related proteins such as p53, p21, ATG3, ATG 7, ULK1, and Nuclear Factor kappa B (NF-κB). The inhibition of mTOR, transcription of FOX 01, inactivation of apoptosomes, upregulation of death-associated protein kinase (DAPK), and accumulation of reactive oxygen species (ROS) have also been suggested as possible mechanisms [2]. Several studies have reported a molecular shift between autophagy and apoptosis as well as dual induction of apoptosis and autophagy following HDACi treatment in different cell lines [2,30,47]. As an example, in chronic myeloid leukemia (CLL), reduced activation of autophagy treatment with HDACi mocetinostat was reported, whereas the upregulation of autophagy was reported in MCF-7 cell line using the same HDACi [41,51]. Also, in HeLa cells, SAHA and sodium butyrate induced both autophagy and apoptosis [47]. The type of cell, genetic pre-disposition of the tumour, duration, and dose of HDACis have been put forward as deciding factors of whether HDACi-induced autophagy acts as a pro-survival or pro-cell death mode [41]. If this stands true, this could in part explain the diverse results observed in different studies using different cell lines and different HDACi, as well as the uncertainty that surrounds the mechanisms of HDACi-induced cell death.

2.2 HDACi-Induced Upregulation of p21 and Cell Cycle Arrest

HDACi-induced apoptosis has been associated with the upregulation of cyclin-dependent kinase (CDK) inhibitor p21 and cell cycle arrest [2]. Transcriptional re-activation of p53 and the subsequent upregulation of p21 by HDACis have been reported in different cell lines [2,32,52]. Activation of p53 induces the expression of p21 to induce cell cycle arrest mainly in the gap 1 (G1) phase. An earlier report by Richon et al. alluded that HDACis are gene-specific after having observed only the upregulation of p21 and no alteration in the expression of either p27, also a CDK inhibitor, or γ-actin genes [53]. Cell cycle arrest in the G2/M phase of the cell cycle has also been reported and is accomplished by downregulating the expression of cyclin A by HDACis [31,54–56].

2.3 HDACi-Induced Inhibition of Angiogenesis

Studies on the effect of HDACis on angiogenesis remain limited. The inhibition of angiogenesis by HDACis was reported in nucleus polposus cells of interverbal discs, endothelial progenitor cells, human embryonic kidney (HEK) 293, and epithelial fibrosarcoma (HT1080) cells [57–60]. The inhibition of angiogenesis was evidenced by attenuation of vascular endothelial growth factor (VEGF), hyper-acetylation of hypoxia-inducible factor 1 (HIF-1α), and

degradation of hypoxia-induced transcription factor [57,58,61]. Altered expression of pro- and anti-angiogenic genes following HDACi treatment has also been reported [60,62].

3. Radiosensitisation by HDAC Inhibitors

Evidence from pre-clinical studies has revealed that the combination of radiation and HDACis results in increased cell death in a number of cell lines, including lung, melanoma, prostate, glioma, colon, non-small cell lung cancer (NSCLC), osteosarcoma, and breast [3–12,14,15,17,18,63]. When used as monotherapy, HDACis have shown promising therapeutic outcomes in haematological malignancies such as leukaemia, multiple myeloma, and lymphoma, with disappointing results in solid tumours [20,31,37,64,65]. The molecular basis for the poor clinical outcomes in solid tumours is still unclear, but is thought to be due to the short drug half-life of HDACis, which leads to poor drug distribution, poor HDAC isoform selectivity, and poor patient selection [13,38]. HDACi-induced radiosensitisation is mainly attributed to their role in DNA damage response (DDR) and their effect on chromatin structure [12]. As a result, combination therapies either with radiation or other DNA-damaging agents have been suggested as an ideal strategy to improve their efficacy in solid tumours [5,14,36].

3.1 DNA DSB Induction and DNA Damage Repair (DDR)

Following the induction of DNA, double-strand breaks by radiation pathways that sense, respond, and repair the damage are activated [66]. DNA double-strand breaks are repaired using two basic mechanisms, homologous recombination (HR) or non-homologous end joining (NHEJ). During the initial stages of both HR and NHEJ, ATM promotes the processing of the broken DNA ends by the MRE11/NBS/Rad50 (MRN) complex to resect the broken ends into 3′DNA single-strand tails [67]. The choice of repair pathway is dictated in part by the presence or absence of p53 binding protein 1 (53BP1). In the presence of 53BP1, HR is inhibited and NHEJ is initiated. During NHEJ, Ku70 and Ku80 heterodimer bind to the DNA ends and block the resection of the 5′ end. Ku70/80 recruits DNA PKs to the broken ends. In the final steps, the DNA PK complex recruits a ligase complex consisting of X-ray repair complementing defective in Chinese Hamster 4 (XRCC4), XRCC4-like factor- DNA ligase 4 (XLF-LIGIV), and polynucleotide kinase (PNK) to perform the ligation of broken ends [21,68]. NHEJ is an error-prone mechanism which is active throughout the cell cycle, mainly in the G1 phase [21,69].

During HR, the damaged DNA ends are resected by the Mre11-Rad50-Nbs1(MRN) complex to form 3′prime ends. The 3′prime ends are coated by replication protein A (RPA) to form a nucleoprotein filament to which HR proteins (breast cancer tumour suppressor (BRCA1), RAD51, and RAD52) can bind [66]. RAD51 is a key protein in HR that facilitates strand exchange with the complementary undamaged DNA strand to form the holiday junction. The

resolution of the holiday junction into two DNA duplexes is carried out by MMS4 and MUS81 [68]. HR requires the presence of an undamaged DNA strand (sister chromatid or chromosomes) to use as a template for repair. Sister chromatids are only available during the late S-and G2 phases after DNA replication, thus HR is active during these phases. The use of a DNA template for repair facilitates accurate repair which makes HR an error-free pathway [68,69]. HDACis have been observed to repress DNA repair proteins such as MRE11/Rad50/NBS1 (MRN) complex and Rad51 involved in HR and ku70, ku80, DNA PK involved in NHEJ [12,19,22,70].

3.2 Role of HDACs and HDACi in the Early Stages of the DNA Damage Response (DDR)

The DDR consists of a complex network of signalling pathways that involves the activation of cell cycle checkpoints, DNA repair, transcriptional programmes, and programmed cell death [71]. Cell cycle checkpoints monitor the progression of the cell cycle by stopping entry into S-phase (G1/S checkpoint), delaying S-phase progression (intra-S checkpoint), or preventing entry into mitosis (G2/M checkpoint) in response to DNA damage by exogenous agents such as radiation or due to replication stress [71]. At the G1/S checkpoint, ataxia-telengiectasia mutated (ATM) is autophosphorylated and initiates the DNA damage signalling cascade by activating Chk 2. Chk2 phosphorylates cell division cycle (CDC)25A phosphatase, which inhibits the activation of Cyclin E/A and its binding to Cdk 2 to induce rapid cell cycle arrest. At the G2/M checkpoint, ATR is autophosphorylated and initiates Chk1 which phosphorylates (CDC)25A, -B, and -C phosphatases. The maintenance of cell cycle arrest is promoted by the phosphorylation of p53 by Chk 2, which in turn induces the accumulation of Cdk inhibitor p21. The binding of p21 to the cyclin D and Cdk 4 complex keeps the retinoblastoma protein (pRb) in an unphosphorylated state and promotes its association with the E2F1 transcription factor, maintaining cell cycle arrest, as shown in Figure 2. HDAC1 has been reported to repress p21, and the inhibition of HDAC1 activity, therefore, activates p21 to induce and maintain cell cycle arrest [72]. Earlier studies have also pointed out that the interaction between HDAC1/2 and E2F transcription factors is important for the G1-S cell cycle transition [73,74]. A recent study conducted in colon cancer (HCT116) cells reported that the pRb-E2F complex does not necessarily require HDAC activity to induce rapid cell cycle arrest, but HDAC activity might be required for complete cell cycle arrest and to maintain arrest [75].

Evidence suggests that HDACs play a role in regulating ATM. HDAC1 was observed to interact with ATM, particularly after exposure to gamma-radiation in fibroblast cells [76]. In support of this observation, the reduced activation of ATM after treatment with HDACi SAHA was reported in breast (MCF-7, T-47D), melanoma (SK-MEL-28), human osteosarcoma

(Saos-2), and A549 cell lines [76]. This observation was further corroborated by reports of accumulation of HDAC1 and 2 at the damaged sites within 5 min of DNA damage induction and dissociation at 30 min after radiation treatment [77]. The rapid accumulation and dispersal of HDAC1 and 2 were associated with the rapid deacetylation of Histone3 lysine 56 (H3K56) and Histone4 lysine 16 (H4K16) which favours non-homologous end-joining (NHEJ), followed by histone acetylations that favours homologous repair (HR) [77]. The authors also observed that the acetylation levels of H3K56 were reduced upon the induction of DNA damage without treatment with HDACis [77]. HDAC1 and 2 bind to CDK inhibitors p21 and p27, thereby reducing their activity and resulting in cell cycle progression from G1 to S-phase [39,40,42]. The inhibition of HDAC1, therefore, restores the activity of p21, leading to G1 cell cycle arrest [40]. The depletion of HDAC1 was also reported to partially contribute to G2/M arrest and cell cycle arrest [40,43]. HDAC4 was reported to co-localise with another DDR indicator, 53BP1, at DSB sites in fibroblast (FT169A and YZ5 cells). Furthermore, DNA damage-induced G2 checkpoint was inactivated and the levels of 53BP1 were observed to be reduced when HDAC4 was knocked down, leading to the conclusion that HDAC4 is critical in maintaining G2 checkpoint [47,78]. The roles of the different HDACs in the DDR are summarised in Table 1.

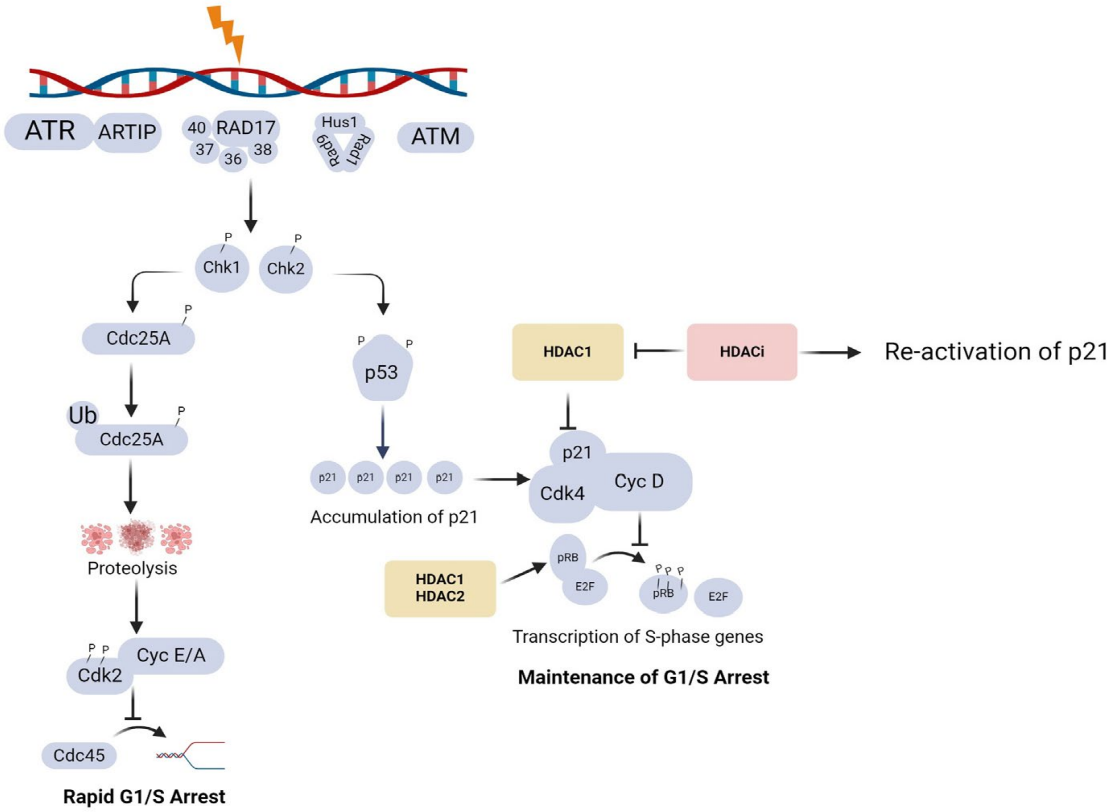

Figure 2. Illustration of the role of HDACs in cell cycle regulation (created with BioRender.com https://app.biorender.com/illustrations/6420e9f530ff29832d070b3f) (accessed 23 April 2024).

Table 1. Roles of HDACs in the DDR.

HDAC	Role	Reference
HDAC 1 and 2	DNA-damage signalling	
	Stabilise broken ends during NHEJ	[77]
	Influence persistence of Ku70 and Artemis at DNA damage sites- promoting NHEJ	[13]
	Deactivates the function of p21 and p27	[79,80]
	Hypo-phosphorylation of RB gene	[81]
HDAC 3	Maintenance of chromatin structure and genomic stability	[82]
	Essential for DNA DSB repair	[13]
	Recruits Xeroderma Pigmentosum C (XPC) during Nucleotide excision repair (NER)	[83]
HDAC 4	Silencing of chromatin near broken ends.	[78]
	Co-localises with 53BP foci, and contributes to the stability of 53BP	[13]
HDAC 6	Reduces cellular sensitivity to damaging agents	[84]
	Repair of DNA mismatch	[13]
HDAC 9 and 10	DSB repair via the HR pathway	[13]
	G2/M transition regulates transcription of cyclin A2	[80]
	Reduces activity of p53	
SIRT1	Modulation of γ-H2AX foci, BBRCA1, Rad51, and NBS foci formation	[85]
SIRT6	Facilitates DSB repair by activating PARP1	[80]

4. Impact of Chromatin Structure on Radiation Response

The architecture of chromatin during DNA damage induction, recognition, signalling, and repair is an important factor that can dictate the successful repair or misrepair of DNA double-strand breaks [23]. However, the topic has received little attention over the years, partly due to a lack of efficient *in vitro* systems for the manipulation of long chromatin and quantitative detection for DSBs [66]. As early as 1991, Smerdon proposed the “access- repair-restore” model to describe the impact of chromatin structure on DNA repair. In brief, the model proposed that in order for DNA damage to be repaired, DNA damage in different chromatin structures should be detected, and local chromatin structure needs to be remodeled to allow repair proteins to have access to damaged sites and to be restored after repair [86].

For the purposes of this review, a brief description of chromatin structure is justified. Chromatin is organised in structures named nucleosomes. Each nucleosome consists of DNA wrapped around histone octamer which consists of histones, H2A, H2B, H3, and H4. The nucleosome is then connected to a linker DNA and histone H1 [87]. The amino terminus tails of the histones protrude from the histone core and are open to various histone post-translational modifications such as acetylation, ubiquitination, or methylation. The two forms of chromatin, heterochromatin and euchromatin, are regulated by post- translation modification (PMT) of histones. Some of the post-translational modifications that occur on the histone tails play an important role in the DDR [87,88].

4.1 Influence of Chromatin Structure on DNA Damage Induction, Detection, and Repair

It has long been accepted that heterochromatin has a protective effect on DNA against ionising radiation [23,24,89]. Cowel et al. observed that γ-H2AX foci, a marker of DSB, were absent from areas which contained heterochromatin markers HP1α and H3K9Me3 in the nuclei of MCF-7 cells [90]. Similarly, Kim et al. reported an increased number of γ-H2AX foci in areas of open chromatin [91]. A similar observation was made by Takata et al., who reported a 5–50-fold decrease in DSB induction by γ-rays in condensed chromatin as compared to decondensed chromatin [23]. Clearly, there is agreement that heterochromatin confers protection against DNA DSB induction by radiation. However, the underlying mechanisms around this protective effect remain a matter of debate. Warters et al. argued that the protective effect against radiation is dependent on the level of chromatin-associated non-histone proteins in heterochromatin rather than on the concentration of chromatin [89]. In other words, the more proteins carried by the chromatin, the higher the protection of chromatin from ionising radiation. The authors observed a 70 times higher yield of DSB in deproteinised DNA as compared to intact nuclei. Elia and Bradley concluded that chromatin domains that differ in tertiary structure and protein composition may also differ in their susceptibility to DNA double-strand breaks induced by ionising radiation [23]. However, in both studies, the protective effect offered by chromatin compaction was acknowledged.

Nygren et al. investigated the role of DNA-bound proteins in the protective effect and they reported an increase in the protective effect of a factor of 14 in single-strand breaks and a factor of 5 in double-strand breaks when DNA-bound proteins were removed [92]. They concluded that DNA-bound proteins protect chromatin to a limited extent by acting as free radical scavengers. The greater part of the protection was attributed to the fact that DNA in

the chromatin is made up of large, compact aggregates where the distance between separate aggregates exceeds the effective range of the hydroxyl (·OH) radicals. Further, inside the large aggregates, the amount of DNA damaging ·OH radicals produced are less due to reduced water content as compared to when DNA is more evenly distributed in a given volume [92]. Similarly, Takata et al. observed that the level and composition of proteins were similar between condensed and decondensed chromatin in HeLa cells and concluded that the protective effect is due to the concentration of chromatin and not the level of chromatin-associated proteins as previously proposed [23]. They reasoned that a lower chromatin concentration contains more water molecules, with subsequent increases in reactive radicals that are formed. It remains contentious whether the opposing observations between Takata et al. and Warters et al. could be due to the different chromatin manipulation methods used in the respective studies [23,89].

4.2 DNA Damage Induced Chromatin Modifications

Evidence from earlier biochemical studies pointed out that the induction of double- strand breaks causes the remodeling of chromatin structure around the damaged site [87,93]. Subsequently, Lisby et al. reported that in yeast *Saccharomyces cerevisiae*, DNA DSB localises to repair foci which contain Rad52 protein, suggesting that multiple DSBs can be repaired by a Rad52 repair foci [94]. These findings implied that the mobility of chromatin allows DSBs to localise at one repair site [94,95]. The authors, however, acknowledged that the localisation and interaction of DSB observed in the yeast *Saccharomyces cerevisiae* might be due to the small nuclear size in yeast as compared to the nuclei of mammalian cells, rather than due to the mobility of chromatin. Also, as compared to mammalian cells, homologous recombination is a dominant repair mechanism in yeast, which would explain the co-localisation of Rad52 foci in yeast and not in mammalian cells [93,94]. Similarly, in a later study, the relocalisation of DSB to the nuclear periphery before the recruitment of Rad51 was reported in Drospohlilla [96].

A contradictory observation was made by Kruhlak et al. in mammalian cells. The authors noted that remodeling of chromatin architecture at DSB sites does not involve large- scale mobility of chromatin to assemble at repair centres but rather small-scale mobility in the micrometre range [93]. The authors reported chromatin expansion at 20 s after irradiation which lasted up to 180 s after UV irradiation in HeLa cells. In an attempt to explain the local expansion in chromatin that was observed in the area around the DSB, the authors conceptualised that after DSB formation, the break causes the damaged chromatin region to unfold, relieving the torsional stress exerted by the packaging of DNA, thus resulting in the expansion and relaxation of chromatin. They concluded that the observed chromatin relaxation and

expansion might be due to the presence of DSB sensor proteins which exhibit chromatin unwinding properties [93]. Indeed, the increased acetylation of DDR proteins histones H2A and H4 at DSB sites was reported to lead to the rapid formation of open chromatin by a number of studies [97,98]. Perhaps, the reasoning offered by Takata et al., that chromatin relaxation after DSB induction was part of the evolutionary conservation of the genome to allow access for repair protein, should be given consideration [23].

Another important observation made was an increase in the size of foci as chromatin becomes open [91]. A reasonable explanation was later offered by Kruhlak *et al.* that the time-dependent increase in the size of individual foci which was noted was not due to the merging of multiple DSBs as a result of the mobility of chromatin, but rather due to spreading of H2AX phosphorylation over large chromatin area, which subsequently acts as a docking site for DNA damage proteins [93]. An akin reasoning was given by Krawczyk et al. that the mobility of foci might simply be due to the relaxation of chromatin and not due to the mobility of chromatin [99].

4.3 Chromatin Modification and Type of Radiation

The protective effect of heterochromatin against DSB induction has been linked to the type of radiation, i.e., low or high linear energy transfer (LET) radiation [23]. Earlier reports associated the protective effect with low LET radiation. This was because the radiolysis of water molecules with subsequent formation of hydroxyl radicals has long been acknowledged as the major contributor to DNA damage, particularly when low LET radiation is used. It was therefore argued that since heterochromatin has fewer water molecules per chromatin, fewer hydroxyl radicals are produced, as discussed in Section 4.2. The opposite is true for decondensed chromatin [23]. However, Takata et al. reported that heterochromatin protects against DNA damage not only from low LET radiation but from heavy ions as well. The authors made this conclusion after observing a 7-fold increase in radioprotection in heterochromatin when carbon ion was used in HeLa cells [23]. Furthermore, using Monte Carlo simulations, the complexity of DNA damage induction caused by low and high LET types of radiation was observed to be the same in heterochromatin, as well as in euchromatin. However, inefficient repair was noted in heterochromatin [23,87]. This lends support to the arguments presented by Takata et al. that the protective effect of heterochromatin hinders the efficient repair of DSB [23].

5. Sequencing of HDACi Treatment and Radiation

The use of HDAC inhibitors in combination with radiation therapy remains to be a matter of ongoing research. Evidence from numerous studies suggests that there is agreement on

HDACi treatment before radiation (pre-irradiation HDACi protocol), with only a few studies having investigated the HDACi post-irradiation (post-irradiation HDACi protocol) [7,100,101]. In the studies using pre-irradiation HDACi protocols, HDACi treatment was given at different timepoints (3, 6, 16, 18, 24, and 48 h) before irradiation in different studies [7,10,11,14,17,18,63,70,102–108]. Kim et al. determined that 18 and 24 h of pre-irradiation incubation of the A549 cell line with trichostatin A (TSA) resulted in enhanced radiation sensitisation to 2–8 Gy X-rays as compared to HDACi treatment at 3, 6, and 12 h post-irradiation [100]. In U251 glioma cell lines, dose enhancement factors of 1.38, 1.4, and 1.46 were reported when cells were exposed to 1.5 mmol/L valproic acid (VPA) at 6 h, 24 h, and immediately after irradiation, respectively [6]. A greater dose enhancement factor of 1.71 was noted with a 16 h pre- and post-incubation in VPA leading to a conclusion that pre-and post-exposure to HDACis is necessary for maximal radiosensitisation [7]. It is noteworthy to mention that a higher dose enhancement factor (1.46) was reported when VPA was administered immediately after radiation, as compared to when VPA was administered 6 h and 24 h post-irradiation. It is tempting to speculate that the modestly higher dose enhancement factor might be in part due to radiation-induced chromatin modifications. As set forth by numerous studies [24,86–88,91,96], following the induction of DSB by radiation, chromatin relaxation around the DSB occurs. Therefore, one could mechanistically reason that the addition of HDACis immediately post-IR, coincides with the rapid chromatin changes that occur post-irradiation. In support, Kruhlak et al. reported chromatin changes as early as 20 s after irradiation [93].

Van Nifterik reported a dose enhancement factor of 1.3 and 1.4 for D384 medulloblastoma cells and 1.7 and 1.5 for T98 glioblastoma cells for 24 and 48 h pre-incubation periods with 5 mM VPA [101]. The authors further reported that they did not observe any enhancement, with dose enhancement factors of 1.1 for D384 cells and 1.0 for T98 cells, when cells were incubated in VPA for 24 h post-irradiation only. It is tempting to speculate that the difference in radiosensitivity between the pre-and post-irradiation HDACi protocols may in part be due to two important factors, i.e., different plating methods, (pre-irradiation plating (pre-IR plating) and post-irradiation plating (post-IR plating)) and the incubation period in HDACis. Typically, radiation sensitivity studies are conducted using colony survival assays [109]. In the pre-IR plating setting, cells are seeded, allowed to attach, and treated. In the post-IR setting, cells are treated followed by trypsinisation, and the required numbers of cells are seeded in plates. In addition, the post-IR plating method has two methods that can be used, immediate plating (IP) and delayed plating (DP). In the IP method, cells are seeded immediately after radiation, and in the DP method, cells are seeded hours after irradiation. Of the two post-IR plating methods, IP was observed to exhibit a lower survival than DP [110,111]. The difference

between the resultant cell survival curves when using the two methods was explained by the cell's capacity to repair potentially lethal damage [110,111]. Moreover, in most studies, it is not specified whether DP or IP was used, which also poses a challenge for data integration. Oike et al. reported consistent SF_2, SF_4, SF_6, SF_8, SF_{10}, D_{10}, and D_{50} values between pre-IR plating and post-IR plating methods, using lung cancer (A549) and submandibular gland (HSG) cells [109]. The study, however, did not investigate the possible impact of delayed plating in the post-IR plating setting [109]. It remains undetermined whether consistent results observed by Oike et al. can extrapolate to other cell lines, and most importantly, in the context of this review, whether the results can be applied to the combination treatment of HDACis and radiation.

Furthermore, whether a post-IR HDACi protocol or pre-IR HDACi protocol is used, the total period of HDACi incubation used in the various studies is different. As an example, Chinnaiyan et al. evaluated both pre- and post-IR HDACi protocols. In the post-IR HDACi protocol, cells were seeded in 6-well plates, and VPA was added immediately 6 h and 24 h after irradiation. Cells were incubated in VPA-containing media for the remainder of the assay [7]. When using the pre-irradiation HDACi protocol, the cells were treated with VPA for 16 h, irradiated, and rinsed with PBS before fresh HDACi-free media was added. In the pre- and post-protocol, cells were pre-treated with VPA for 16 h and returned for incubation post-IR. The authors reported improved radiosensitisation (factor of 1.7) when cells were exposed to VPA pre- and post-irradiation, as compared to factors of 1.3 when VPA was administered pre-IR only. This suggests that the removal of VPA-containing media at plating could be the reason for the observed non-enhancement. Also, taking into account the modes of HDACi-induced cell death in Section 2.1, HDACi-induced autophagy is reported to depend on the duration and dose of HDACis [2]. It is enticing to speculate that different periods of HDACi incubation, as well as different HDACi concentrations noted in the different studies, might have played a role in the mode of cell death, with subsequent differences in the observed results.

6. Conclusions

The combination therapy of HDACis and radiation is complex. The matter is further complicated by the pleiotropic effects of HDACis on histone and non-histone targets in cells. The biological rationale for this combination therapy relies on the ability of HDACis to modulate epigenetics to maximise the radiation effect. Mechanistically, pre-IR HDACi treatment induces chromatin relaxation to facilitate increased DSB induction by radiation. However, from existing reports, different temporal sequencing protocols of HDACis and radiation have been used. Some studies employed the pre-IR HDACi protocol and others used post-IR HDACi protocol. The different plating methods, i.e., pre-IR or post-IR plating, delayed plating, or immediate

plating, also pose a challenge with the integration of data from different studies. Considering the ability of radiation and HDACis to modify chromatin structure, as well as the paradoxical relationship between apoptosis and autophagy under different conditions, the molecular interplay of the two modalities is bound to be complex.

Several reports have emphasised that HDACi treatment depends on the cell type, period of incubation with HDACis, as well as the dose of HDACi. To date, evidence suggests that incubation for 24–48 h pre-irradiation is the most optimal sequence. The mechanisms involved remain elusive. The inhibition of DNA DSB repair has traditionally been hailed as the main mechanism of HDACi-induced radiosensitisation; however, emerging evidence from different cell lines suggests otherwise. For example, numerous studies reported that HDACis impair DSB repair as evidenced by the prolonged appearance of the γ-H2AX foci. However, Moertl et al. reported not having observed any prolongation of foci after treatment with SAHA and CUDC-101 in pancreatic cell lines (Su.86.86, MIA Paca-2, and T3M-4) [100]. Clearly, more studies using different cell lines and different HDACis are required to fully unravel the mechanisms of radiosensitisation. For future studies, analysis of DSB repair proteins in addition to the appearance of γ-H2AX foci, as well as investigation of other modes of cell death such as autophagy and ROS production, may aid in fully elucidating the mechanisms involved.

In view of the complex mechanism of action of HDACis under different conditions, it seems reasonable to recommend that the optimal temporal sequencing protocol of HDACi and radiation, as well as the optimal period of HDACi incubation, should be first determined for each cell and each HDACi used for *in vitro* studies. Mechanistically, this would allow sufficient time for chromatin to be remodelled to allow increased DSB induction by radiation. For combination therapy of HDACi and radiation in the clinic, it is also recommended that HDACi be administered hours before radiation.

Author Contributions: Conceptualization, E.N.S.; writing—original draft preparation, E.N.S.; writing—review and editing, E.N.S., S.N., C.V. and A.J. All authors have read and agreed to the published version of the manuscript.

Funding: This research was funded by the Department of Higher Education and Training (DHET), Grant number: UCDP/Y649.

Institutional Review Board Statement: Not applicable.

Informed Consent Statement: Not applicable.

Data Availability Statement: Data sharing is not applicable.

Acknowledgments: This review includes an image from a previous publication from our research group. Pharmaceuticals 2023, 16(2), 227; https://doi.org/10.3390/ph16020227 (accessed on 20 February 2024). Biorender was used for creating the images.

Conflicts of Interest: The authors declare no conflicts of interest.

Ethics Number: 689/2021

References

1. Lee, J.H.; Choy, M.L.; Ngo, L.; Foster, S.S.; Marks, P.A. Histone deacetylase inhibitor induces DNA damage, which normal but not transformed cells can repair. *Proc. Natl. Acad. Sci. USA* **2010**, *107*, 14639–14644. [CrossRef] [PubMed]
2. Mrakovcic, M.; Bohner, L.; Hanisch, M.; Fröhlich, L.F. Epigenetic Targeting of Autophagy via HDAC Inhibition in Tumor Cells: Role of p53. *Int. J. Mol. Sci.* **2018**, *19*, 3952. [CrossRef] [PubMed]
3. Camphausen, K.; Scott, T.; Sproull, M.; Tofilon, P.J. Enhancement of xenograft tumor radiosensitivity by the histone deacetylase inhibitor MS-275 and correlation with histone hyperacetylation. *Clin. Cancer Res.* **2004**, *10 Pt 1*, 6066–6071. [CrossRef] [PubMed]
4. Camphausen, K.; Tofilon, P.J. Inhibition of histone deacetylation: A strategy for tumor radiosensitization. *J. Clin. Oncol.* **2007**, *25*, 4051–4056. [CrossRef] [PubMed]
5. Groselj, B.; Sharma, N.L.; Hamdy, F.C.; Kerr, M.; Kiltie, A.E. Histone deacetylase inhibitors as radiosensitisers: Effects on DNA damage signalling and repair. *Br. J. Cancer* **2013**, *108*, 748–754. [CrossRef] [PubMed]
6. Damaskos, C.; Garmpis, N.; Valsami, S.; Kontos, M.; Spartalis, E.; Kalampokas, T.; Kalampokas, E.; Athanasiou, A.; Moris, D.; Daskalopoulou, A.; et al. Histone Deacetylase Inhibitors: An Attractive Therapeutic Strategy Against Breast Cancer. *Anticancer Res.* **2017**, *37*, 35–46. [CrossRef] [PubMed]
7. Chinnaiyan, P.; Cerna, D.; Burgan, W.E.; Beam, K.; Williams, E.S.; Camphausen, K.; Tofilon, P.J. Postradiation sensitization of the histone deacetylase inhibitor valproic acid. *Clin. Cancer Res.* **2008**, *14*, 5410–5415. [CrossRef]
8. Schlaff, C.D.; Arscott, W.T.; Gordon, I.; Tandle, A.; Tofilon, P.; Camphausen, K. Radiosensitization Effects of Novel Triple-Inhibitor CUDC-101 in Glioblastoma Multiforme and Breast Cancer Cells *In Vitro*. *Int. J. Radiat. Oncol. Biol. Phys.* **2013**, *87*, S650. [CrossRef]
9. Chiu, H.W.; Yeh, Y.L.; Wang, Y.C.; Huang, W.J.; Chen, Y.A.; Chiou, Y.S.; Ho, S.Y.; Lin, P.; Wang, Y.J. Suberoylanilide hydroxamic acid, an inhibitor of histone deacetylase, enhances radiosensitivity and suppresses lung metastasis in breast cancer *in vitro* and in vivo. *PLoS ONE* **2013**, *8*, e76340. [CrossRef]
10. Baschnagel, A.; Russo, A.; Burgan, W.E.; Carter, D.; Beam, K.; Palmieri, D.; Steeg, P.S.; Tofilon, P.; Camphausen, K. Vorinostat enhances the radiosensitivity of a breast cancer brain metastatic cell line grown *in vitro* and as intracranial xenografts. *Mol. Cancer Ther.* **2009**, *8*, 1589–1595. [CrossRef]

11. Chen, X.; Wong, P.; Radany, E.; Wong, J.Y. HDAC inhibitor, valproic acid, induces p53-dependent radiosensitization of colon cancer cells. *Cancer Biother. Radiopharm.* **2009**, *24*, 689–699. [CrossRef] [PubMed]
12. Munshi, A.; Kurland, J.F.; Nishikawa, T.; Tanaka, T.; Hobbs, M.L.; Tucker, S.L.; Ismail, S.; Stevens, C.; Meyn, R.E. Histone deacetylase inhibitors radiosensitize human melanoma cells by suppressing DNA repair activity. *Clin. Cancer Res.* **2005**, *11*, 4912–4922. [CrossRef]
13. Antrobus, J.; Parsons, J.L. Histone Deacetylases and Their Potential as Targets to Enhance Tumour Radiosensitisation. *Radiation* **2022**, *2*, 149–167. [CrossRef]
14. Gerelchuluun, A.; Maeda, J.; Manabe, E.; Brents, C.A.; Sakae, T.; Fujimori, A.; Chen, D.J.; Tsuboi, K.; Kato, T.A. Histone Deacetylase Inhibitor Induced Radiation Sensitization Effects on Human Cancer Cells after Photon and Hadron Radiation Exposure. *Int. J. Mol. Sci.* **2018**, *19*, 496. [CrossRef]
15. Barazzuol, L.; Jeynes, J.C.; Merchant, M.J.; Wéra, A.C.; Barry, M.A.; Kirkby, K.J.; Suzuki, M. Radiosensitization of glioblastoma cells using a histone deacetylase inhibitor (SAHA) comparing carbon ions with X-rays. *Int. J. Radiat. Biol.* **2015**, *91*, 90–98. [CrossRef]
16. Johnson, A.M.; Bennett, P.V.; Sanidad, K.Z.; Hoang, A.; Jardine, J.H.; Keszenman, D.J.; Wilson, P.F. Evaluation of Histone Deacetylase Inhibitors as Radiosensitizers for Proton and Light Ion Radiotherapy. *Front. Oncol.* **2021**, *11*, 735940. [CrossRef] [PubMed]
17. Yu, J.I.; Choi, C.; Shin, S.W.; Son, A.; Lee, G.H.; Kim, S.Y.; Park, H.C. Valproic Acid Sensitizes Hepatocellular Carcinoma Cells to Proton Therapy by Suppressing NRF2 Activation. *Sci. Rep.* **2017**, *7*, 14986. [CrossRef]
18. Choi, C.; Lee, G.H.; Son, A.; Yoo, G.S.; Yu, J.I.; Park, H.C. Downregulation of Mcl-1 by Panobinostat Potentiates Proton Beam Therapy in Hepatocellular Carcinoma Cells. *Cells* **2021**, *10*, 554. [CrossRef]
19. Groselj, B.; Kerr, M.; Kiltie, A.E. Radiosensitisation of bladder cancer cells by panobinostat is modulated by Ku80 expression.*Radiother. Oncol.* **2013**, *108*, 429–433. [CrossRef]
20. Jenke, R.; Ressing, N.; Hansen, F.K.; Aigner, A.; Buch, T. Anticancer Therapy with HDAC Inhibitors: Mechanism-Based Combination Strategies and Future Perspectives. *Cancers* **2021**, *13*, 634. [CrossRef]
21. Maier, P.; Hartmann, L.; Wenz, F.; Herskind, C. Cellular Pathways in Response to Ionizing Radiation and Their Targetability for Tumor Radiosensitization. *Int. J. Mol. Sci.* **2016**, *17*, 102. [CrossRef] [PubMed]

22. Shabason, J.E.; Tofilon, P.J.; Camphausen, K. Grand rounds at the National Institutes of Health: HDAC inhibitors as radiation modifiers, from bench to clinic. *J. Cell. Mol. Med.* **2011**, *15*, 2735–2744. [CrossRef] [PubMed]
23. Takata, H.; Hanafusa, T.; Mori, T.; Shimura, M.; Iida, Y.; Ishikawa, K.; Yoshikawa, K.; Yoshikawa, Y.; Maeshima, K. Chromatin Compaction Protects Genomic DNA from Radiation Damage. *PLoS ONE* **2013**, *8*, e75622. [CrossRef]
24. Venkatesh, P.; Panyutin, I.V.; Remeeva, E.; Neumann, R.D.; Panyutin, I.G. Effect of Chromatin Structure on the Extent and Distribution of DNA Double Strand Breaks Produced by Ionizing Radiation; Comparative Study of hESC and Differentiated Cells Lines. *Int. J. Mol. Sci.* **2016**, *17*, 58. [CrossRef] [PubMed]
25. Chan, E.; Arlinghaus, L.R.; Cardin, D.B.; Goff, L.; Berlin, J.D.; Parikh, A.; Abramson, R.G.; Yankeelov, T.E.; Hiebert, S.; Merchant, N.; et al. Phase I trial of vorinostat added to chemoradiation with capecitabine in pancreatic cancer. *Radiother. Oncol.* **2016**, *119*, 312–318. [CrossRef] [PubMed]
26. Galanis, E.; Anderson, S.K.; Miller, C.R.; Sarkaria, J.N.; Jaeckle, K.; Buckner, J.C.; Ligon, K.L.; Ballman, K.V.; Moore, D.F., Jr.; Nebozhyn, M.; et al. Phase I/II trial of vorinostat combined with temozolomide and radiation therapy for newly diagnosed glioblastoma: Results of Alliance N0874/ABTC 02. *Neuro-Oncol.* **2017**, *20*, 546–556. [CrossRef] [PubMed]
27. Gurbani, S.S.; Yoon, Y.; Weinberg, B.D.; Salgado, E.; Press, R.H.; Cordova, J.S.; Ramesh, K.K.; Liang, Z.; Vega, J.V.; Voloschin, A.; et al. Assessing Treatment Response of Glioblastoma to an HDAC Inhibitor Using Whole-Brain Spectroscopic MRI. *Tomography* **2019**, *5*, 53–60. [CrossRef] [PubMed]
28. Teknos, T.N.; Grecula, J.; Agrawal, A.; Old, M.O.; Ozer, E.; Carrau, R.; Kang, S.; Rocco, J.; Blakaj, D.; Diavolitsis, V.; et al. A phase 1 trial of Vorinostat in combination with concurrent chemoradiation therapy in the treatment of advanced staged head and neck squamous cell carcinoma. *Investig. New Drugs* **2019**, *37*, 702–710. [CrossRef] [PubMed]
29. Zhang, C.; Richon, V.; Ni, X.; Talpur, R.; Duvic, M. Selective induction of apoptosis by histone deacetylase inhibitor SAHA in cutaneous T-cell lymphoma cells: Relevance to mechanism of therapeutic action. *J. Investig. Dermatol.* **2005**, *125*, 1045–1052. [CrossRef]
30. Passaro, E.; Papulino, C.; Chianese, U.; Toraldo, A.; Congi, R.; Del Gaudio, N.; Nicoletti, M.M.; Benedetti, R.; Altucci, L. HDAC6 Inhibition Extinguishes Autophagy in Cancer: Recent Insights. *Cancers* **2021**, *13*, 6280. [CrossRef]
31. Li, Y.; Seto, E. HDACs and HDAC Inhibitors in Cancer Development and Therapy. *Cold Spring Harb. Perspect. Med.* **2016**, *6*, a026831. [CrossRef] [PubMed]

32. Mrakovcic, M.; Kleinheinz, J.; Frohlich, L.F. Histone Deacetylase Inhibitor-Induced Autophagy in Tumor Cells: Implications for p53. *Int. J. Mol. Sci.* **2017**, *18*, 1883. [CrossRef] [PubMed]
33. Bolden, J.E.; Peart, M.J.; Johnstone, R.W. Anticancer activities of histone deacetylase inhibitors. *Nat. Rev. Drug Discov.* **2006**, *5*, 769–784. [CrossRef]
34. Fotheringham, S.; Epping, M.T.; Stimson, L.; Khan, O.; Wood, V.; Pezzella, F.; Bernards, R.; La Thangue, N.B. Genome-wide loss-of-function screen reveals an important role for the proteasome in HDAC inhibitor-induced apoptosis. *Cancer Cell* **2009**, *15*, 57–66. [CrossRef] [PubMed]
35. Everix, L.; Seane, E.N.; Ebenhan, T.; Goethals, I.; Bolcaen, J. Introducing HDAC-Targeting Radiopharmaceuticals for Glioblastoma Imaging and Therapy. *Pharmaceuticals* **2023**, *16*, 227. [CrossRef] [PubMed]
36. Dokmanovic, M.; Clarke, C.; Marks, P.A. Histone Deacetylase Inhibitors: Overview and Perspectives. *Mol. Cancer Res.* **2007**, *5*, 981–989. [CrossRef] [PubMed]
37. Smalley, J.P.; Cowley, S.M.; Hodgkinson, J.T. Bifunctional HDAC Therapeutics: One Drug to Rule Them All? *Molecules* **2020**, *25*, 4394. [CrossRef] [PubMed]
38. Rajak, H.; Singh, A.; Raghuwanshi, K.; Kumar, R.; Dewangan, P.K.; Veerasamy, R.; Sharma, P.C.; Dixit, A.; Mishra, P. A structural insight into hydroxamic acid based histone deacetylase inhibitors for the presence of anticancer activity. *Curr. Med. Chem.* **2014**, *21*, 2642–2664. [CrossRef] [PubMed]
39. Zhang, J.; Zhong, Q. Histone deacetylase inhibitors and cell death. *Cell. Mol. Life Sci.* **2014**, *71*, 3885–3901. [CrossRef]
40. Frew, A.J.; Johnstone, R.W.; Bolden, J.E. Enhancing the apoptotic and therapeutic effects of HDAC inhibitors. *Cancer Lett.* **2009**,*280*, 125–133. [CrossRef]
41. Mrakovcic, M.; Kleinheinz, J.; Fröhlich, L.F. p53 at the Crossroads between Different Types of HDAC Inhibitor-Mediated Cancer Cell Death. *Int. J. Mol. Sci.* **2019**, *20*, 2415. [CrossRef] [PubMed]
42. Insinga, A.; Minucci, S.; Pelicci, P.G. Mechanisms of selective anticancer action of histone deacetylase inhibitors. *Cell Cycle* **2005**, *4*, 741–743. [CrossRef] [PubMed]
43. Peart, M.J. Novel mechanisms of apoptosis induced by histone deacetylase inhibitors. *Cancer Res.* **2003**, *63*, 4460–4471. [PubMed]
44. Gong, P.; Wang, Y.; Jing, Y. Apoptosis Induction byHistone Deacetylase Inhibitors in Cancer Cells: Role of Ku70. *Int. J. Mol. Sci.***2019**, *20*, 1601. [CrossRef] [PubMed]
45. Bao, L.; Diao, H.; Dong, N.; Su, X.; Wang, B.; Mo, Q.; Yu, H.; Wang, X.; Chen, C. Histone deacetylase inhibitor induces cell apoptosis and cycle arrest in lung cancer cells via mitochondrial injury and p53 up-acetylation. *Cell Biol. Toxicol.* **2016**, *32*, 469–482. [CrossRef] [PubMed]

46. Yang, Z.J.; Chee, C.E.; Huang, S.; Sinicrope, F.A. The role of autophagy in cancer: Therapeutic implications. *Mol. Cancer Ther.***2011**, *10*, 1533–1541. [CrossRef] [PubMed]
47. Shao, Y.; Gao, Z.; Marks, P.A.; Jiang, X. Apoptotic and autophagic cell death induced by histone deacetylase inhibitors. *Proc. Natl. Acad. Sci. USA* **2004**, *101*, 18030–18035. [CrossRef] [PubMed]
48. Rebecca, V.W.; Amaravadi, R.K. Emerging strategies to effectively target autophagy in cancer. *Oncogene* **2016**, *35*, 1–11. [CrossRef]
49. Kimmelman, A.C. The dynamic nature of autophagy in cancer. *Genes Dev.* **2011**, *25*, 1999–2010. [CrossRef]
50. Pagotto, A.; Pilotto, G.; Mazzoldi, E.L.; Nicoletto, M.O.; Frezzini, S.; Pastò, A.; Amadori, A. Autophagy inhibition reduces chemoresistance and tumorigenic potential of human ovarian cancer stem cells. *Cell Death Dis.* **2017**, *8*, e2943. [CrossRef]
51. El-Khoury, V.; Pierson, S.; Szwarcbart, E.; Brons, N.H.; Roland, O.; Cherrier-De Wilde, S.; Plawny, L.; Van Dyck, E.; Berchem,G. Disruption of autophagy by the histone deacetylase inhibitor MGCD0103 and its therapeutic implication in B-cell chronic lymphocytic leukemia. *Leukemia* **2014**, *28*, 1636–1646. [CrossRef]
52. Gilardini Montani, M.S.; Granato, M.; Santoni, C.; Del Porto, P.; Merendino, N.; D'Orazi, G.; Faggioni, A.; Cirone, M. Histone deacetylase inhibitors VPA and TSA induce apoptosis and autophagy in pancreatic cancer cells. *Cell. Oncol.* **2017**, *40*, 167–180. [CrossRef]
53. Richon, V.M.; Sandhoff, T.W.; Rifkind, R.A.; Marks, P.A. Histone deacetylase inhibitor selectively induces p21WAF1 expression and gene-associated histone acetylation. *Proc. Natl. Acad. Sci. USA* **2000**, *97*, 10014–10019. [CrossRef]
54. Dong, Z.; Yang, Y.; Liu, S.; Lu, J.; Huang, B.; Zhang, Y. HDAC inhibitor PAC-320 induces G2/M cell cycle arrest and apoptosis in human prostate cancer. *Oncotarget* **2018**, *9*, 512–523. [CrossRef]
55. Lee, H.A.; Chu, K.B.; Moon, E.K.; Kim, S.S.; Quan, F.S. Sensitization to oxidative stress and G2/M cell cycle arrest by histone deacetylase inhibition in hepatocellular carcinoma cells. *Free Radic. Biol. Med.* **2020**, *147*, 129–138. [CrossRef]
56. Hrgovic, I.; Doll, M.; Kleemann, J.; Wang, X.-F.; Zoeller, N.; Pinter, A.; Kippenberger, S.; Kaufmann, R.; Meissner, M. The histone deacetylase inhibitor trichostatin a decreases lymphangiogenesis by inducing apoptosis and cell cycle arrest via p21-dependent pathways. *BMC Cancer* **2016**, *16*, 763. [CrossRef] [PubMed]
57. Schoepflin, Z.R.; Shapiro, I.M.; Risbud, M.V. Class I and IIa HDACs Mediate HIF-1α Stability Through PHD2-Dependent Mechanism, While HDAC6, a Class IIb Member, Promotes HIF-1α Transcriptional Activity in Nucleus Pulposus Cells of the Intervertebral Disc. *J. Bone Min. Res.* **2016**, *31*, 1287–1299. [CrossRef] [PubMed]

58. Jeong, J.W.; Bae, M.K.; Ahn, M.Y.; Kim, S.H.; Sohn, T.K.; Bae, M.H.; Yoo, M.A.; Song, E.J.; Lee, K.J.; Kim, K.W. Regulation and destabilization of HIF-1alpha by ARD1-mediated acetylation. *Cell* **2002**, *111*, 709–720. [CrossRef] [PubMed]
59. Deroanne, C.F.; Bonjean, K.; Servotte, S.; Devy, L.; Colige, A.; Clausse, N.; Blacher, S.; Verdin, E.; Foidart, J.M.; Nusgens, B.V.; et al. Histone deacetylases inhibitors as anti-angiogenic agents altering vascular endothelial growth factor signaling. *Oncogene* **2002**, *21*, 427–436. [CrossRef]
60. Liu, T.; Kuljaca, S.; Tee, A.; Marshall, G.M. Histone deacetylase inhibitors: Multifunctional anticancer agents. *Cancer Treat. Rev.***2006**, *32*, 157–165. [CrossRef]
61. Iordache, F.; Buzila, C.; Constantinescu, A.; Andrei, E.; Maniu, H. Histone deacetylase (HDAC) inhibitors down-regulate endothelial lineage commitment of umbilical cord blood derived endothelial progenitor cells. *Int. J. Mol. Sci.* **2012**, *13*, 15074–15085. [CrossRef] [PubMed]
62. Ellis, L.; Pili, R. Histone Deacetylase Inhibitors: Advancing Therapeutic Strategies in Hematological and Solid Malignancies.*Pharmaceuticals* **2010**, *3*, 2411–2469. [CrossRef] [PubMed]
63. Munshi, A.; Tanaka, T.; Hobbs, M.L.; Tucker, S.L.; Richon, V.M.; Meyn, R.E. Vorinostat, a histone deacetylase inhibitor, enhances the response of human tumor cells to ionizing radiation through prolongation of γ-H2AX foci. *Mol. Cancer Ther.* **2006**, *5*, 1967–1974. [CrossRef] [PubMed]
64. Ediriweera, M.K.; Tennekoon, K.H.; Samarakoon, S.R. Emerging role of histone deacetylase inhibitors as anti-breast-cancer agents.*Drug Discov. Today* **2019**, *24*, 685–702. [CrossRef] [PubMed]
65. Luu, T.H.; Morgan, R.J.; Leong, L.; Lim, D.; McNamara, M.; Portnow, J.; Frankel, P.; Smith, D.D.; Doroshow, J.H.; Wong, C.; et al. A phase II trial of vorinostat (suberoylanilide hydroxamic acid) in metastatic breast cancer: A California Cancer Consortium study. *Clin. Cancer Res.* **2008**, *14*, 7138–7142. [CrossRef] [PubMed]
66. Vitti, E.T.; Parsons, J.L. The Radiobiological Effects of Proton Beam Therapy: Impact on DNA Damage and Repair. *Cancers* **2019**,*11*, 946. [CrossRef] [PubMed]
67. Bian, L.; Meng, Y.; Zhang, M.; Li, D. MRE11-RAD50-NBS1 complex alterations and DNA damage response: Implications for cancer treatment. *Mol. Cancer* **2019**, *18*, 169. [CrossRef] [PubMed]
68. Hall, E.J.; Giaccia, A.J. *Radiobiology for the Radiologist*, 7th ed.; Lippincott Williams & Wilkins: Philadelphia, PA, USA, 2012;pp. 18–22.
69. Fontana, A.O.; Augsburger, M.A.; Grosse, N.; Guckenberger, M.; Lomax, A.J.; Sartori, A.A.; Pruschy, M.N. Differential DNA repair pathway choice in cancer cells after proton- and photon-irradiation. *Radiother. Oncol.* **2015**, *116*, 374–380. [CrossRef] [PubMed]

70. Kachhap, S.K.; Rosmus, N.; Collis, S.J.; Kortenhorst, M.S.; Wissing, M.D.; Hedayati, M.; Shabbeer, S.; Mendonca, J.; Deangelis, J.; Marchionni, L.; et al. Downregulation of homologous recombination DNA repair genes by HDAC inhibition in prostate cancer is mediated through the E2F1 transcription factor. *PLoS ONE* **2010**, *5*, e11208. [CrossRef]
71. Bose, P.; Dai, Y.; Grant, S. Histone deacetylase inhibitor (HDACI) mechanisms of action: Emerging insights. *Pharmacol. Ther.* **2014**,*143*, 323–336. [CrossRef]
72. Scotto, L.; Serrano, X.J.; Zullo, K.; Kinahan, C.; Deng, C.; Sawas, A.; Bates, S.; O'Connor, O.A. ATM inhibition overcomes resistance to histone deacetylase inhibitor due to p21 induction and cell cycle arrest. *Oncotarget* **2020**, *11*, 3432–3442. [CrossRef] [PubMed]
73. Brehm, A.; Miska, E.A.; McCance, D.J.; Reid, J.L.; Bannister, A.J.; Kouzarides, T. Retinoblastoma protein recruits histone deacetylase to repress transcription. *Nature* **1998**, *391*, 597–601. [CrossRef] [PubMed]
74. Ferreira, R.; Magnaghi-Jaulin, L.; Robin, P.; Harel-Bellan, A.; Trouche, D. The three members of the pocket proteins family share the ability to repress E2F activity through recruitment of a histone deacetylase. *Proc. Natl. Acad. Sci. USA* **1998**, *95*, 10493–10498. [CrossRef] [PubMed]
75. Barrett, A.; Shingare, M.R.; Rechtsteiner, A.; Wijeratne, T.U.; Rodriguez, K.M.; Rubin, S.M.; Müller, G.A. HDAC activity is dispensable for repression of cell-cycle genes by DREAM and E2F:RB complexes. *bioRxiv* **2023**. [CrossRef] [PubMed]
76. Thurn, K.T.; Thomas, S.; Raha, P.; Qureshi, I.; Munster, P.N. Histone deacetylase regulation of ATM-mediated DNA damage signaling. *Mol. Cancer Ther.* **2013**, *12*, 2078–2087. [CrossRef]
77. Miller, K.M.; Tjeertes, J.V.; Coates, J.; Legube, G.; Polo, S.E.; Britton, S.; Jackson, S.P. Human HDAC1 and HDAC2 function in the DNA-damage response to promote DNA nonhomologous end-joining. *Nat. Struct. Mol. Biol.* **2010**, *17*, 1144–1151. [CrossRef]
78. Kao, G.D.; McKenna, W.G.; Guenther, M.G.; Muschel, R.J.; Lazar, M.A.; Yen, T.J. Histone deacetylase 4 interacts with 53BP1 to mediate the DNA damage response. *J. Cell Biol.* **2003**, *160*, 1017–1027. [CrossRef] [PubMed]
79. Yamaguchi, T.; Cubizolles, F.; Zhang, Y.; Reichert, N.; Kohler, H.; Seiser, C.; Matthias, P. Histone deacetylases 1 and 2 act in concert to promote the G1-to-S progression. *Genes Dev.* **2010**, *24*, 455–469. [CrossRef]
80. Hai, R.; He, L.; Shu, G.; Yin, G. Characterization of Histone Deacetylase Mechanisms in Cancer Development. *Front. Oncol.* **2021**,*11*, 700947. [CrossRef]
81. Valenzuela-Fernández, A.; Cabrero, J.R.; Serrador, J.M.; Sánchez-Madrid, F. HDAC6: A key regulator of cytoskeleton, cell migration and cell-cell interactions. *Trends Cell Biol.* **2008**, *18*, 291–297. [CrossRef]

82. Bhaskara, S.; Knutson, S.K.; Jiang, G.; Chandrasekharan, M.B.; Wilson, A.J.; Zheng, S.; Yenamandra, A.; Locke, K.; Yuan, J.L.; Bonine-Summers, A.R.; et al. Hdac3 is essential for the maintenance of chromatin structure and genome stability. *Cancer Cell* **2010**, *18*, 436–447. [CrossRef] [PubMed]
83. Nishimoto, K.; Niida, H.; Uchida, C.; Ohhata, T.; Kitagawa, K.; Motegi, A.; Suda, T.; Kitagawa, M. HDAC3 Is Required for XPC Recruitment and Nucleotide Excision Repair of DNA Damage Induced by UV Irradiation. *Mol. Cancer Res.* **2020**, *18*, 1367–1378. [CrossRef] [PubMed]
84. Zhang, M.; Xiang, S.; Joo, H.Y.; Wang, L.; Williams, K.A.; Liu, W.; Hu, C.; Tong, D.; Haakenson, J.; Wang, C.; et al. HDAC6 Deacetylates and Ubiquitinates MSH2 to Maintain Proper Levels of MutSα. *Mol. Cell* **2014**, *55*, 31–46. [CrossRef] [PubMed]
85. Wang, R.-H. Impaired DNA Damage Response, Genome Instability, and Tumorigenesis in SIRT1 Mutant Mice. *Cancer Cell* **2008**,
14, 312–323. [CrossRef] [PubMed]
86. Polo, S.E.; Almouzni, G. Chromatin dynamics after DNA damage: The legacy of the access-repair-restore model. *DNA Repair* **2015**, *36*, 114–121. [CrossRef] [PubMed]
87. Fortuny, A.; Polo, S.E. The response to DNA damage in heterochromatin domains. *Chromosoma* **2018**, *127*, 291–300. [CrossRef]
88. Etier, A.; Dumetz, F.; Chéreau, S.; Ponts, N. Post-Translational Modifications of Histones Are Versatile Regulators of Fungal Development and Secondary Metabolism. *Toxins* **2022**, *14*, 317. [CrossRef] [PubMed]
89. Warters, R.L.; Lyons, B.W. Variation in radiation-induced formation of DNA double-strand breaks as a function of chromatin structure. *Radiat. Res.* **1992**, *130*, 309–318. [CrossRef]
90. Cowell, I.G.; Sunter, N.J.; Singh, P.B.; Austin, C.A.; Durkacz, B.W.; Tilby, M.J. gammaH2AX foci form preferentially in euchromatin after ionising-radiation. *PLoS ONE* **2007**, *2*, e1057. [CrossRef]
91. Kim, J.A.; Kruhlak, M.; Dotiwala, F.; Nussenzweig, A.; Haber, J.E. Heterochromatin is refractory to gamma-H2AX modification in yeast and mammals. *J. Cell Biol.* **2007**, *178*, 209–218. [CrossRef]
92. Nygren, J.; Ljungman, M.; Ahnström, M. Chromatin Structure and Radiation-induced DNA Strand Breaks in Human Cells: Soluble Scavengers and DNA-bound Proteins Offer a Better Protection Against Single- than Double-strand Breaks. *Int. J. Radiat. Biol.* **1995**, *68*, 11–18. [CrossRef] [PubMed]
93. Kruhlak, M.J.; Celeste, A.; Dellaire, G.; Fernandez-Capetillo, O.; Müller, W.G.; McNally, J.G.; Bazett-Jones, D.P.; Nussenzweig, A. Changes in chromatin structure and mobility

in living cells at sites of DNA double-strand breaks. *J. Cell Biol.* **2006**, *172*, 823–834. [CrossRef] [PubMed]

94. Lisby, M.; Mortensen, U.H.; Rothstein, R. Colocalization of multiple DNA double-strand breaks at a single Rad52 repair centre. *Nat. Cell Biol.* **2003**, *5*, 572–577. [CrossRef] [PubMed]
95. Aten, J.A.; Stap, J.; Krawczyk, P.M.; van Oven, C.H.; Hoebe, R.A.; Essers, J.; Kanaar, R. Dynamics of DNA double-strand breaks revealed by clustering of damaged chromosome domains. *Science* **2004**, *303*, 92–95. [CrossRef] [PubMed]
96. Amaral, N.; Ryu, T.; Li, X.; Chiolo, I. Nuclear Dynamics of Heterochromatin Repair. *Trends Genet.* **2017**, *33*, 86–100. [CrossRef] [PubMed]
97. Murr, R.; Loizou, J.I.; Yang, Y.G.; Cuenin, C.; Li, H.; Wang, Z.Q.; Herceg, Z. Histone acetylation by Trrap-Tip60 modulates loading of repair proteins and repair of DNA double-strand breaks. *Nat. Cell Biol.* **2006**, *8*, 91–99. [CrossRef] [PubMed]
98. Xu, Y.; Sun, Y.; Jiang, X.; Ayrapetov, M.K.; Moskwa, P.; Yang, S.; Weinstock, D.M.; Price, B.D. The p400 ATPase regulates nucleosome stability and chromatin ubiquitination during DNA repair. *J. Cell Biol.* **2010**, *191*, 31–43. [CrossRef]
99. Krawczyk, P.M.; Borovski, T.; Stap, J.; Cijsouw, T.; ten Cate, R.; Medema, J.P.; Kanaar, R.; Franken, N.A.; Aten, J.A. Chromatin mobility is increased at sites of DNA double-strand breaks. *J. Cell Sci.* **2012**, *125 Pt 9*, 2127–2133. [CrossRef] [PubMed]
100. Kim, J.H.; Kim, I.H.; Shin, J.H.; Kim, H.J.; Kim, I.A. Sequence-Dependent Radiosensitization of Histone Deacetylase Inhibitors Trichostatin A and SK-7041. *Cancer Res. Treat.* **2013**, *45*, 334–342. [CrossRef]
101. Van Nifterik, K.A.; Van den Berg, J.; Slotman, B.J.; Lafleur, M.V.; Sminia, P.; Stalpers, L.J. Valproic acid sensitizes human glioma cells for temozolomide and gamma-radiation. *J. Neurooncol.* **2012**, *107*, 61–67. [CrossRef]
102. Moertl, S.; Payer, S.; Kell, R.; Winkler, K.; Anastasov, N.; Atkinson, M.J. Comparison of Radiosensitization by HDAC Inhibitors CUDC-101 and SAHA in Pancreatic Cancer Cells. *Int. J. Mol. Sci.* **2019**, *20*, 3259. [CrossRef] [PubMed]
103. Adimoolam, S.; Sirisawad, M.; Chen, J.; Thiemann, P.; Ford, J.M.; Buggy, J.J. HDAC-inhibitor-PCI24781-decreases-RAD51- expression-and-inhibits-homologous-recombination. *Proc. Natl. Acad. Sci. USA* **2007**, *104*, 19482–19487. [CrossRef] [PubMed]
104. Mueller, S.; Yang, X.; Sottero, T.L.; Gragg, A.; Prasad, G.; Polley, M.Y.; Weiss, W.A.; Matthay, K.K.; Davidoff, A.M.; DuBois, S.G.; et al. Cooperation of the HDAC inhibitor vorinostat and radiation in metastatic neuroblastoma: Efficacy and underlying mechanisms. *Cancer Lett.* **2011**, *306*, 223–229. [CrossRef] [PubMed]

105. Flatmark, K.; Nome, R.V.; Folkvord, S.; Bratland, A.; Rasmussen, H.; Ellefsen, M.S.; Fodstad, O.; Ree, A.H. Radiosensitization of colorectal carcinoma cell lines by histone deacetylase inhibition. *Radiat. Oncol.* **2006**, *1*, 25. [CrossRef]
106. Saelen, M.G.; Ree, A.H.; Kristian, A.; Fleten, K.G.; Furre, T.; Hektoen, H.H.; Flatmark, K. Radiosensitization by the histone deacetylase inhibitor vorinostat under hypoxia and with capecitabine in experimental colorectal carcinoma. *Radiat. Oncol.* **2012**, *7*,165. [CrossRef] [PubMed]
107. Shoji, M.; Ninomiya, I.; Makino, I.; Kinoshita, J.; Nakamura, K.; Oyama, K.; Nakagawara, H.; Fujita, H.; Tajima, H.; Takamura, H.; et al. Valproic acid, a histone deacetylase inhibitor, enhances radiosensitivity in esophageal squamous cell carcinoma. *Int. J. Oncol.* **2012**, *40*, 2140–2146. [CrossRef] [PubMed]
108. Perona, M.; Thomasz, L.; Rossich, L.; Rodriguez, C.; Pisarev, M.A.; Rosemblit, C.; Cremaschi, G.A.; Dagrosa, M.A.; Juvenal, G.J. Radiosensitivity enhancement of human thyroid carcinoma cells by the inhibitors of histone deacetylase sodium butyrate and valproic acid. *Mol. Cell. Endocrinol.* **2018**, *478*, 141–150. [CrossRef]
109. Oike, T.; Hirota, Y.; Dewi Maulany Darwis, N.; Shibata, A.; Ohno, T. Comparison of Clonogenic Survival Data Obtained by Pre- and Post-Irradiation Methods. *J. Pers. Med.* **2020**, *10*, 171. [CrossRef] [PubMed]
110. Frankenberg-Schwager, M.; Frankenberg, D.; Harbich, R. Potentially lethal damage repair is due to the difference of DNA double-strand break repair under immediate and delayed plating conditions. *Radiat. Res.* **1987**, *111*, 192–200. [CrossRef]
111. Reddy, N.M.; Kapiszewska, M.; Lange, C.S. Detection of X-ray damage repair by the immediate versus delayed plating technique is dependent on cell shape and cell concentration. *Scanning Microsc.* **1992**, *6*, 543–555, discussion 556–559.

pharmaceuticals

MDPI

Review

Introducing HDAC-Targeting Radiopharmaceuticals for Glioblastoma Imaging and Therapy

Liesbeth Everix [1], Elsie Neo Seane [2], Thomas Ebenhan [3,4,5], Ingeborg Goethals [6] and Julie Bolcaen [7,*]

[1] Molecular Imaging Center Antwerp (MICA), University of Antwerp, 2610 Antwerpen, Belgium
[2] Department of Medical Imaging and Therapeutic Sciences, Cape Peninsula University of Technology, Cape Town 7530, South Africa
[3] Pre-Clinical Imaging Facility (PCIF), (NuMeRI) NPC, Pretoria 0001, South Africa
[4] Department of Science and Technology/Preclinical Drug Development Platform (PCDDP), North West University, Potchefstroom 2520, South Africa
[5] Nuclear Medicine, University of Pretoria, Pretoria 0001, South Africa
[6] Department of Nuclear Medicine, Ghent University Hospital, 9000 Ghent, Belgium
[7] Radiation Biophysics Division, SSC laboratory, iThemba LABS, Cape Town 7131, South Africa
* Correspondence: jbolcaen@tlabs.ac.za; Tel.: +27(0)218431217

Citation: Everix, L.; Seane, E.N.; Ebenhan, T.; Goethals, I.; Bolcaen, J. Introducing HDAC-Targeting Radiopharmaceuticals for Glioblastoma Imaging and Therapy. *Pharmaceuticals* **2023**, *16*, 227. https://doi.org/10.3390/ ph16020227

Academic Editors: Martina Benešová and Gábor Bakos

Received: 20 December 2022

Revised: 24 January 2023

Accepted: 26 January 2023

Published: 1 February 2023

Abstract: Despite recent advances in multimodality therapy for glioblastoma (GB) incorporating surgery, radiotherapy, chemotherapy and targeted therapy, the overall prognosis remains poor. One of the interesting targets for GB therapy is the histone deacetylase family (HDAC). Due to their pleiotropic effects on, e.g., DNA repair, cell proliferation, differentiation, apoptosis and cell cycle, HDAC inhibitors have gained a lot of attention in the last decade as anti-cancer agents. Despite their known underlying mechanism, their therapeutic activity is not well-defined. In this review, an extensive overview is given of the current status of HDAC inhibitors for GB therapy, followed by an overview of current HDAC-targeting radiopharmaceuticals. Imaging HDAC expression or activity could provide key insights regarding the role of HDAC enzymes in gliomagenesis, thus identifying patients likely to benefit from HDACi-targeted therapy.

Keywords: glioblastoma; histone deacetylases inhibitors; radiopharmaceuticals; theranostics

1. Introduction

Glioblastoma multiforme (GB) is the most malignant tumor in the central nervous system (CNS). Despite recent advances in multimodality therapy for GB incorporating surgery, radiotherapy (RT), chemotherapy and targeted therapy, the overall prognosis remains poor. Almost all tumors recur with a more aggressive form, and there is no standard of care for recurrent GB. The survival rate at 5 years postdiagnosis remains at only 5.8% [1–3]. Novel molecular markers were identified improving GB classification and providing powerful prognostic information [4]. However, therapy resistance remains a hurdle. Precision oncology incorporating personalized targeted therapy holds much promise in developing more efficacious and tolerable therapies [3]. One of the interesting targets for GB-targeted therapy is the histone deacetylase family (HDAC). Due to their pleiotropic effects on, e.g., DNA repair, cell proliferation, differentiation, apoptosis and senescence, they have gained a lot of attention in the last decade as anti-cancer agents. In addition, HDAC inhibitors (HDACi) have been applied for the treatment of metabolic disorders and psychiatric or neurodegenerative diseases [5]. The HDAC family contains 18 family members, categorized as following: class I (HDAC1,2,3,8), IIa (HDAC 4,5,7,9), IIb (HDAC 6,10), III (nicotinamide adenine dinucleotide (NAD+)-dependent sirtuins (SIRTs) and IV (HDAC11) [6,7]. Two groups of enzymes control the acetylation and deacetylation of histones: histone acetyltransferase (HAT) and HDACs. The transfer or removal of acetyl groups by HATs and HDACs induce a more open and accessible chromatin structure or chromatin condensation and transcriptional repression [8,9]. Interestingly, the histone acetylation status is reversible and can be targeted by drugs [10]. HDACi have the ability to increase the level of protein acetylation in the cancerous cell, restarting the expression of silenced tumor suppressor genes [11]. However, despite their known underlying mechanism, their therapeutic activity is not well-defined. The goal of this review is to highlight the current status of HDACi- and HDAC- targeting radiopharmaceuticals for the imaging and therapy of GB.

2. Role of HDAC in GB Pathology

Epigenetic mechanisms, particularly those involving enzymatic modifications of DNA and the associated histone proteins that regulate gene expression are recognized as a major factor contributing to the pathogenesis of GB [10]. The effects of acetylation on gene expression and tumor phenotype and the antitumor mechanism of HDACi in GB has recently been reviewed [11,12]. In gliomas, epigenetic enzymes, such as HDAC, are aberrantly expressed causing the deregulation of processes, featuring growth arrest, cell differentiation, cytotoxicity and apoptosis induction. RNA-sequencing data from the public TCGA (The Cancer Genome Atlas) showed that HDAC4, HDAC5, HDAC6, HDAC8 and HDAC11 expression was significantly lowered in glioma (WHO grade II–IV) when compared to normal brain tissue [9]. Expression levels of HDAC1-3

and HDAC7 appeared to increase with higher malignancy grades [9,13]. Additionally, HDAC3 and HDAC9 overexpression in GB are both correlated with a poor prognosis. The role of SIRT in GB is currently under debate [13]. *In vitro*, HDAC2 expression is significantly upregulated in GB [14]. The silencing of HDAC4 reactivated p21 (WAF1/Cip1) and inhibited tumor growth in an in vivo human GB model [15]. In addition, HDAC5 is upregulated in U87MG, U251MG, T98G and LN-229 glioma cell lines and promoted their proliferation by the upregulation of Notch 1 [16]. HDAC6 has been shown to promote the proliferation of glioma cells through the primary cilia, MKK7/JNK/c-Jun signaling pathway and attenuating transforming growth factor β (TGFβ) receptor signaling [17–19]. HDAC6 activity also plays a role in temozolomide (TMZ) resistance through the regulation of DNA mismatch repair [20]. HDACi are epigenome-targeting molecules divided into different categories based on their target and chemical structure: short-chain fatty acids (e.g., valproic acid (VPA)), hydroxamic acid derivatives (e.g., trichostatin A (TSA), vorinostat (SAHA), belinostat, panobinostat (LBH-589), pracinostat, quisinostat (JNJ-16241199)), carboxylic acid derivatives, cyclic peptides (romidepsin), and benzamides entinostat (MS-275), tacedinaline (CI- 994) and mocetinostat (MG-0103)). Other categories include electrophilic ketones, hydro- examines, sirtuin inhibitors and miscellaneous [11,21,22]. FDA approval was granted for vorinostat (Zolinza® Rahway, NJ, USA), belinostat (Beleodaq®, PXD101 East Windsor, NJ, USA), panobinostat (Farydak® Barcelona, Spain) and romidepsin (Istodax® Hayes, UK) for the treatment of hematological malignancies, represented by T-cell lymphomas and multiple myeloma (MM). Tucidinostat (Epidaza®, Chedamide, Shenzhen, China) was approved by China's National Medical Products Administration [22]. Combined use of panobinostat with the proteasome inhibitor bortezomib has been approved for the treatment of refractory MM [6,7,21,23]. Advances in the abovementioned malignancies prompted HDACi-based anti-cancer research to expand to solid tumors, although the HDACi mechanisms of action in tumors are still sparsely understood. Figure 1 gives an overview of the confirmed mechanism of actions in GB, as recently reviewed [11,24]. As RT and TMZ therapy are standard in GB, the radiosensitizing and chemosensitizing effects of HDACi are of major interest. Presumably, HDACi promote a more open chromatin formation in tumor cells, thereby permitting DNA alkylating agents (e.g., TMZ) to access genomic DNA. Other mechanisms to reverse TMZ resistance have been suggested, e.g., blocking NF-κB-dependent transcription [13,14,25]. In particular, HDAC6 has been identified as a potential target for the treatment of TMZ-resistant GB [20,26,27]. The radiosensitization mechanism in GB could be induced by multiple mechanisms but eventually leads to a decrease in DNA repair [28–35]. Post-irradiation, HDACi have been shown to induce a prolonged expression of phosphorylated H2AX (γH2AX), a marker for DNA double strand breaks (DSBs) [33]. HDACi have also been shown to induce alterations in DNA replication, causing DNA damage [36,37]. Finally, HDACi may be able to assist in reversing abnormal genetic silencing, therefore leading to enhanced cell-cycle arrest and apoptosis from the action of DNA-damaging agents [13].

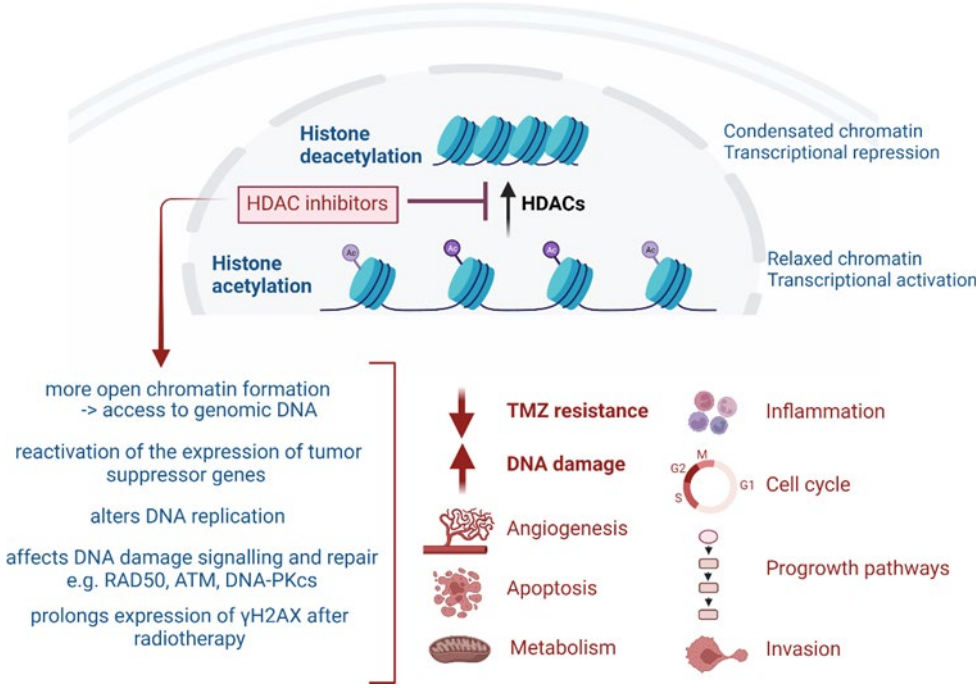

Figure 1. Overview of the broad effects of HDAC inhibitors.

3. Current Status of HDACi for GB Therapy

An overview of the successful clinical trials investigating HDACi in high-grade glioma is given in Table 1. Studies in pediatric glioma patients were excluded. The previous reviews have focused on the mechanisms of HDACi in GB [11,38]. Most research reports on suberoylanilide hydroxamic acid (SAHA, vorinostat), a pan- HDACi, upregulating cancer suppressor genes (p21 (CDKN1A), PTEN, p27) and down- regulating Akt-mTOR signaling, CDK2, CDK4 and cyclin D1/E. SAHA therapy triggered GB cell death and promoted hyper-radiosensitivity in wild-type p53 GB cells [10,34,39]. In GB patients, high doses of SAHA monotherapy appeared to be well-tolerated with modest single-agent activity. SAHA combination regimens with TMZ/RT and/or bevacizumab (BEV) have proven to be tolerable, but no statistical improvement in overall survival (OS) and/or progression-free survival (PFS) was noted [40–45]. Interestingly, phospholipase D1 (PLD1) has been identified as a target of resistance to vorinostat, and combined therapy with a PLD1 inhibitor might improve efficacy [46]. The hydroxymate-based pan-HDACi belinostat (PXD101, Beleodaq®) is structurally similar to SAHA but shows a greater blood brain barrier (BBB) passage [47]. In 2019, the potential of PXD101 was confirmed in an orthotopic rat glioma model. In a pilot study, PXD101 combined with TMZ/RT-delayed GB recurrence [47,48].

Depsipeptide romidepsin (Istodax®, FR901228, FK228) is a stable prodrug isolated from Chromobacterium violaceum and a class I HDACi [49,50]. In a phase I/II clinical trial in recurrent

GB, romidepsin was found to be ineffective as a single agent [49]. Panobinostat (LBH589), a pan-deacetylase inhibitor of class I/II HDAC, is an antineoplastic and antiangiogenic drug that may work synergistically with BEV [51]. However, although this combined treatment strategy was well-tolerated, PFS and OS did not significantly improve compared to BEV monotherapy in recurrent GB [52]. A phase II trial is warranted to assess the combination with fractionated stereotactic re-irradiation therapy [53]. Panobinostat does not cross the BBB, and hence intratumoral or convection-enhanced delivery (CED) administration could be necessary [54]. HDACi valproic acid (valproate, VPA, Depakene), an anticonvulsive drug, has been shown to directly or synergistically exert inhibitory effects on glioma *in vitro* and *in vivo* [55]. VPA combined with TMZ/RT showed improvement in survival, but this might be limited to GB patients with wild-type p53 [56,57]. However, a phase III trial is warranted [58].

Table 1. Overview of clinical trials on HDAC inhibitors (HDACi) in high-grade glioma.

		Regimen	Stage	GB Type	Main Result	Reference
Vorinostat (SAHA, Zolinza, MK0683) *Pan-HDACi*	(+)	/	C(II)		Well-tolerated. Modest single-agent activity. Trials with combination regimens warranted	[40]
		TMZ	NA	rec/prog	MRS imaging may enable quantitative analysis of tumor response	[59] NCT01342757 *
		TMZ	C(I)	HGG	Well-tolerated	[41]
		BEV/Irinotecan	C(I)	rec	(+) Well-tolerated (+) OS and PFS at 400 mg daily or 300 mg twice a day	NCT00762255 *
	(−)	BEV	C(II)	rec	PFS6 or median OS was not improved	[45] NCT01738646 *
		BEV	C(I/II)	rec	Did not improve PFS or OS	[43] NCT01266031 *
		BEV/TMZ	C(I/II)		PFS6 was not statistically improved beyond controls	[44] NCT00939991 *
		BEV/CPT-11	C(I)	rec	Increased toxicities	[60]
		Erlotinib/BEV	C(I/II)	rec	Trial terminated (toxicities)	NCT01110876 *
		Bortezomib	C(II)	rec	Trial closed at interim analysis (0/34 progression-free)	[61] NCT00641706 *
		FSRT	C(I)	rec	Trial terminated	NCT01378481 *
		TMZ/RT	C(I/II)	nd	Acceptable tolerability, but primary efficacy endpoint not met. Sensitivity signatures could facilitate patient selection	[62] NCT00731731 *
	Ongoing	TMZ	C(I)	HGG	Active: not recruiting	NCT00268385 *
		TMZ/Carboplatin/ Isotretinoin	C(I/II)	rec	Active: not recruiting	NCT00555399 *
		Pembrolizumab/ TMZ/RT	C(I)	nd	Active: recruiting	NCT03426891 *

Table 1. *Cont.*

		Regimen	Stage	GB Type	Main Result	Reference
Belinostat (PXD101, Beleodaq) *Pan-HDACi*	Ongoing	TMZ/RT	Pilot study	nd	Active: not recruiting Radiosensitizing effect	[47,48] NCT02137759 *
Romidepsin (Istodax, FK228, FR901228, depsipeptide) *HDAC class I*	(−)		C(I/II)	rec	Ineffective	[49] NCT00085540 *
	Ongoing		C(I)	glioma	Active: not recruiting	NCT01638533 *
Panobinostat (LBH589) *HDAC class I/II*	(+)	FSRT	C(I)	recHGG	Well-tolerated. Phase II trial warranted	[53]
	(−)	BEV	C(II)	recHGG	Did not improve PFS6 compared to BEV monotherapy	[52] NCT00859222 *
			C(II)	recHGG	Trial terminated due to insufficient accrual	NCT00848523 *
			C(II)	rec	Trial withdrawn due to no enrollment	NCT01115036 *
Valproic acid (VPA, valproate, Depakene) *HDAC class I*	(+)		C(II)	HGG	Well-tolerated. May result in improved outcomes. A phase III should follow	[56] NCT00302159 *
				HGG	Delayed hair loss and improvement in survival	[63]
				HGG	Improvement in survival	[64]
				nd	Improvement in PFS and OS confirmed	[58]
				nd	Survival benefit dependent on their p53 gene status	[57]
		Levetiracetam/TMZ/RT	Retro	GB	2-months longer survival	[65]
	(−)	Doxorubicin/TMZ/RT	C(II)	nd	Trials terminated	NCT02758366 *
		Celecoxib	C(II)	Nd		NCT00068770 *
		SRS/Nivolumab	C(I)	Rec		NCT02648633 *
			psa	GB	PFS and OS were comparable to historical controls	[66]
		TMZ	Retro	II/III	VPA was linked to histological progression and decrease in PFS	[67]

Table 1. *Cont.*

	Regimen	Stage	GB Type	Main Result	Reference
Ongoing	Sildenafil/Sorafenib	C(II)	recHGG	Active: not recruiting	NCT01817751 *
	Levetiracetam	C(IV)	glioma	Recruiting: for seizure treatment	NCT03048084 *
	Perampanel	C(IV)	HGG	Recruiting: for seizure treatment	NCT04650204 *
	TMZ	C(III)	HGG	Recruiting	NCT03243461 *

/ = monotherapy. * For current state of clinical trials, visit 'https://clinicaltrials.gov/' (accessed on 1 October 2022) [42]. BEV = bevacizumab; FSRT = fractionated stereotactic re-irradiation therapy; GB = glioblastoma; HGG = high-grade glioma; MRS = magnetic resonance spectroscopy; NA = not applicable; nd = newly diagnosed glioblastoma; OS = overall survival; PFS6 = progression-free survival (6 months); prog = progressive glioblastoma; psa = prospective single-arm study; rec = recurrent glioblastoma; Retro = retrospective; RT = radiotherapy; SRS = stereotactic radiosurgery; TMZ = temozolomide. Note: trials in pediatric glioma patients were not included.

In the last 2 decades, an extensive amount of preclinical research on HDACi and multi- drug combinations in GB has been performed (see Supplementary Table S1) [19,33,68–127]. These studies provided new insights on HDACi-associated signaling processes. HDACi appear to have a vital role in DNA damage response, and a radiosensitizing effect of HDACi (vorinostat, panobinostat, VPA, entinostat, scriptaid) has been shown in GB *in vitro*, with support for vorinostat for GB therapy in combination with heavy ion therapy [31,33,35,128]. HDACi have been shown to inhibit GB cell growth mediated by cell cycle arrest and apoptosis, as highlighted in Supplementary Table S1 [129–135]. The class I/II HDACi trichostatin A (TSA) increased GB apoptosis induction through the p38MAPK- p53 cascade [136]. When combined with the proteasome inhibitor (MG132), 2-deoxy-d- glucose or lomustine (CCNU), synergistic apoptosis induction was shown [137–139]. The GB chemosensitization effects of HDACi therapy have also been noted, such as enhancement of TMZ-induced apoptosis [118,140–143]. However, vorinostat favored the evolution of TMZ resistance through O6-methylguanine DNA methyltransferase (MGMT) overexpression in GB in vivo [144]. HDACi SAHA and MC1568 blocked vascular mimicry in GB, and the inhibiting effects of HDACi on the invasiveness or migration of GB cells have been noted [143,145–149]. Multiple HDACi (vorinostat, romidepsin, MPT0B291, CDK4) have shown to increase the survival time of GB in vivo models [130,131,134,150,151].

Post-HDACi therapy, multiple genes that play a role in complex signaling pathways are up- or down-regulated, as recently summarized [11]. As expected, based on preclinical data, the affected genes are involved in cell cycle progression, apoptosis, invasion and progrowth or include oncogenes and GSC markers [11]. Targeted drug combinations may beneficially affect the outcome of GB therapy, with the possible induction of synthetic lethality. Preclinically, promising combinations include a mix of epigenetic modifiers [152], HDACi combined with imipridones (activation of the mitochondrial ClpP protease) or proteasome inhibitors [153,154], panobinostat combined with a dual PI3K/mTOR inhibitor BEZ235 [155] and combining HDACi with MEK in- hibitors or RTKi [156,157]. A triple combination therapy, involving panobinostat, OTX015 and sorafenib also showed potential in vitro [158]. Interestingly, the R132H mutation in isocitrate dehydrogenase 1 (IDH1R132H), commonly observed and associated with better survival in GB, has been linked to resistance to the anti-cancer effect of HDACi, such as TSA, vorinostat (SAHA) and valproic acid [159].

4. HDAC-Targeting Radiopharmaceuticals

The association of epigenetic dysfunction with disease and the development of di- agnostic or therapeutic agents for treatment are challenging [160]. Most HDACi target a relatively wide spectrum of HDACs that, in turn, inhibits various biological pathways. Their mechanisms of action as tumor suppressors have not yet been fully elucidated [10]. HDAC-targeting radiopharmaceuticals could provide better insights regarding HDAC tissue

expression, HDACi biodistribution and pharmacokinetics and therapeutic efficacy and thereby unravel new insights into the function or behavior of HDACi in vivo [161,162]. Nuclear imaging of HDAC expression in GB may improve the understanding and roleplay of HDAC enzymes within gliomagenesis, identify patients likely to benefit from HDACi- targeted therapy and aid in optimizing therapeutic doses of novel HDACi for glioma treatment [163]. Importantly, there are two main strategies to consider when imaging an epigenetic target in the brain: 1) by direct observation (protein target information indepen- dent of its activity) and 2) functional observation (representative visualization of the impact of a protein or enzyme) [160]. Alternative methods to determine HDAC expression include invasive tumor biopsies and the use of peripheral lymphocytes as surrogate biomarkers for global acetylation after HDACi treatment.

An overview of HDACi-based radiopharmaceuticals is given in Figure 2, and Table 2 summarizes the preclinical development of HDAC radiopharmaceuticals. To visualize or treat GB with radiopharmaceuticals, it is particularly important to only consider those HDACi that sufficiently pass the BBB (even at sub-nanomolar concentration) and are of a small enough structure to allow their penetration into the bulky, heterogeneous tumor tissue [29]. In addition, the cellular location of the targeted HDAC needs to be considered, e.g., HDAC class I proteins are found predominantly in the nucleus, while class II proteins are primarily localized in the cytoplasm but can be shuttled between the cytoplasm and nucleus depending on their phosphorylation status [6].

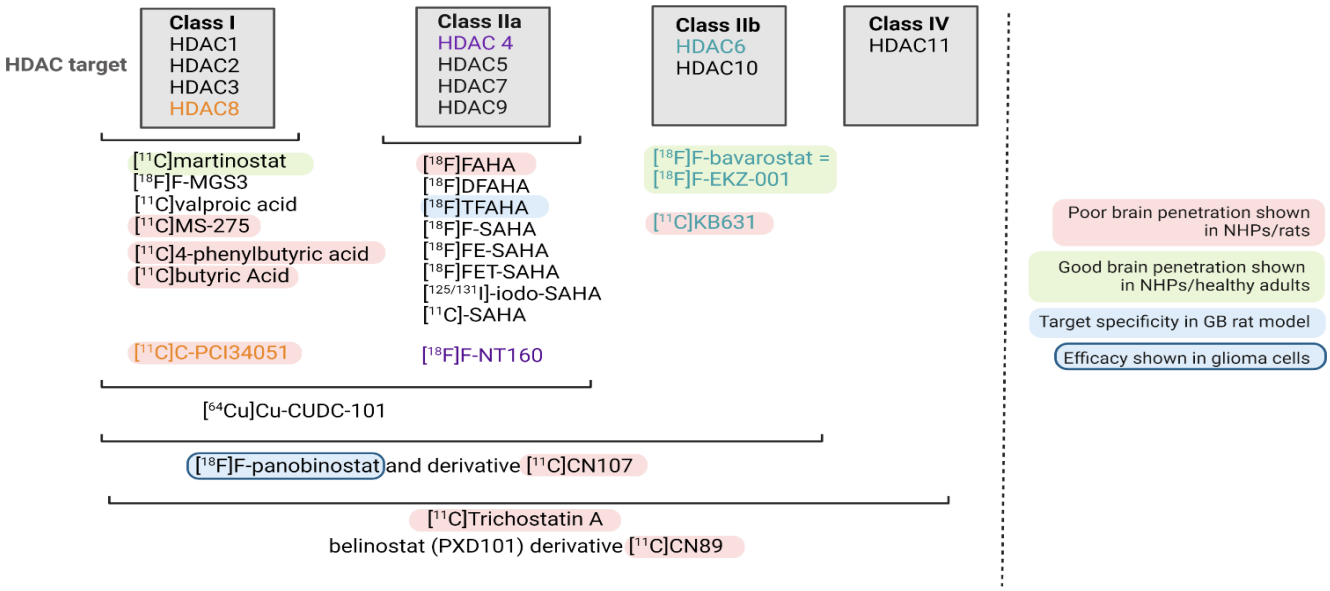

Figure 2. Overview of current radiopharmaceuticals targeting HDAC. The HDAC class targeted is shown. If only one HDAC enzyme is targeted, this is highlighted in color (orange, purple and green).

To our knowledge, the potential of therapeutic HDAC radiopharmaceuticals for targeted radionuclide therapy (TRT) has not yet been explored. Importantly, possible brain toxicity may be a limiting aspect for this kind of application. HDACs play distinct physiological roles in the brain, and HDACi have pleiotropic effects due to their broad targets. This suggests a higher

chance of success for isoform-specific HDACi or the necessity to inject such radioactive agents via CED directly into the GB tumor or its vicinity [164]. Another option is the use of nanovectors with theranostic properties to optimize the tumor delivery of potent HDACi, which could improve their anti-GB properties in vivo [165]. Other criteria to consider for the development of GB TRT agents were recently published by our group [166].

HDAC brain PET has been studied for the potential detection of various neurodegenerative diseases, such as Alzheimer's and Parkinson's disease, and limited studies have investigated their potential for glioma imaging [160,163,164]. Most HDAC radiopharmaceuticals are structurally related to SAHA and include 6-([^{18}F]fluoroacetamido)-1-hexanoicanilide ([^{18}F]FAHA), 6-(di-[^{18}F]fluoroacetamido)-1-hexanoicanilide ([^{18}F]DFAHA), 6-(tri-[^{18}F]fluoroacetamido)-1-hexanoicanilide ([^{18}F]TFAHA), [^{18}F]F-SAHA (Figure 3A), *N*1- (4-(2-fluoroethyl)phenyl)-*N*8-hydroxyoctanediamide ([^{18}F]FE-SAHA), [^{18}F]-fluoro-ethyl-triazole suberohydroxamine acid ([^{18}F]FET-SAHA) (Figure 3B), [^{125}/^{131}I]-iodo-SAHA and two ^{11}C-labeled SAHA-based ligands [162,167–173]. In 2006, the first ^{18}F-labeled SAHA analogue ([^{18}F]FAHA) was radiosynthesized by Mukhopadhyay et al. [168]. Soon thereafter, Nishii et al. confirmed PET in vivo brain uptake in rats of up to 0.44%ID/g between 5 and 60 min [169]. Moreover, blocking studies revealed a specificity similar to that of SAHA, suggesting that [^{18}F]FAHA is a clinically relevant PET tracer capable of targeting HDAC IIa expression [170]. [^{18}F]FAHA has also shown potential to monitor alterations in HDAC activity/expression in a rat model of chemotherapy-induced brain neurotoxicity [174]. Concerns were raised about [^{18}F]fluoroacetate ([^{18}F]FACE), a radiometabolite of the rapidly metabolized [^{18}F]FAHA, that also crosses the BBB and therefore complicates [^{18}F]FAHA quantification [171]. Fortunately, in non-human primates (NHP), the contribution of [^{18}F]FACE to the ^{18}F activity signal was minimal in the first 30 min post-administration [175]. A [^{18}F]FAHA-like sub- strate developed by Seo et al. displayed an insufficient BBB permeability and HDAC specificity [167]. Bonomi et al. modified the structure of [^{18}F]FAHA to add two or three fluorine groups ([^{18}F]DFAHA or [^{18}F]TFAHA, respectively), which increased the lipophilicity and thus BBB permeability [172]. In 2019, [^{18}F]TFAHA was finally studied in GB rat models that confirmed tumor uptake 20 min post-radiotracer administration, which significantly reduced after administration of HDACi MC1568. [^{18}F]TFAHA accumulation was also ob- served in normal brain structures known to overexpress HDAC class IIa: the hippocampus, nucleus accumbens, periaqueductal gray matter and cerebellum [163].

Brain uptake was reported of another radiolabeled SAHA-analogue, [^{18}F]FE-SAHA, but its metabolic instability remains a substantial obstacle (high uptake in the kidneys, liver, bone and small intestines) [176]. Kim et al. developed [^{18}F]FET-SAHA, which showed improved metabolic stability over [^{18}F]FE-SAHA and accumulation in sarcoma tumors [173]. [$^{125/131}$I]-iodo-SAHA maintained a comparable profile (e.g., similar toxicity and pharma- cokinetics) to SAHA. However, in tumor-bearing mice, it showed no preferential tumor accumulation, rapid efflux and unspecific washout. Moreover, accumulation in the liver and kidneys was high [177]. Thus, none of the proposed SAHA-based radiopharmaceuticals have reached a clinical phase. Another group of HDACi-based radiopharmaceuticals, including [^{11}C] trichostatin A, [^{11}C]MS-275, [^{11}C]KB631, [^{11}C]4-phenylbutyric acid, [^{11}C]valproate, [^{11}C]butyric acid, [^{11}C]CN89, [^{11}C]CN107, [^{18}F]F-panobinostat and [^{11}C]PCI34051 demonstrated inadequate BBB penetration, which discourages their application for the HDAC-based imaging of GB, despite possible application in other tumor types [161,167,172,178–181]. [^{18}F]F-panobinostat has bioactivity similar to that of unmodified panobinostat against diffuse intrinsic pontine glioma and U87MG glioma cells (nM efficacy), with low toxicity to healthy astrocytes [180]. [^{18}F]F-panobinostat has also shown potential for PET-guided CED in order to achieve high brain concentrations in healthy mice and a pediatric diffuse midline glioma model, which could be translated to high-grade glioma (Figure 3C,D) [182].

Recently, radiolabeling of trifluoromethyloxadiazole (TFMO)-bearing class-IIa HDACi were explored, and NT160 was identified as a potent inhibitor of class-IIa HDAC4. [^{18}F]F- NT160 was capable of BBB crossing, and binding to class-IIa HDACs was confirmed in mouse brain tissue [183]. In addition, radiometal-nuclide-labeled ligands have also been developed, such as a ^{64}Cu-labeled hydroxamic acid-based radioligand 7-(4-(3-ethynylphenylamino)-7-methoxyquinazolin-6-yloxy)-N-hydroxyheptanamide (CUDC-101). CUDC-101 entered into Phase I clinical trial testing in multiple tumor types (but excluding glioma). [^{64}Cu]Cu- CUDC-101 exhibits the capability to image HDAC expression in triple-negative breast cancer (Figure 3E–G). However, most radioligands conjugated to metal chelators fail to cross an intact BBB [184]. To this end, [^{64}Cu]Cu-CUDC-101 may be a good candidate to explore CED-based administration for GB therapy.

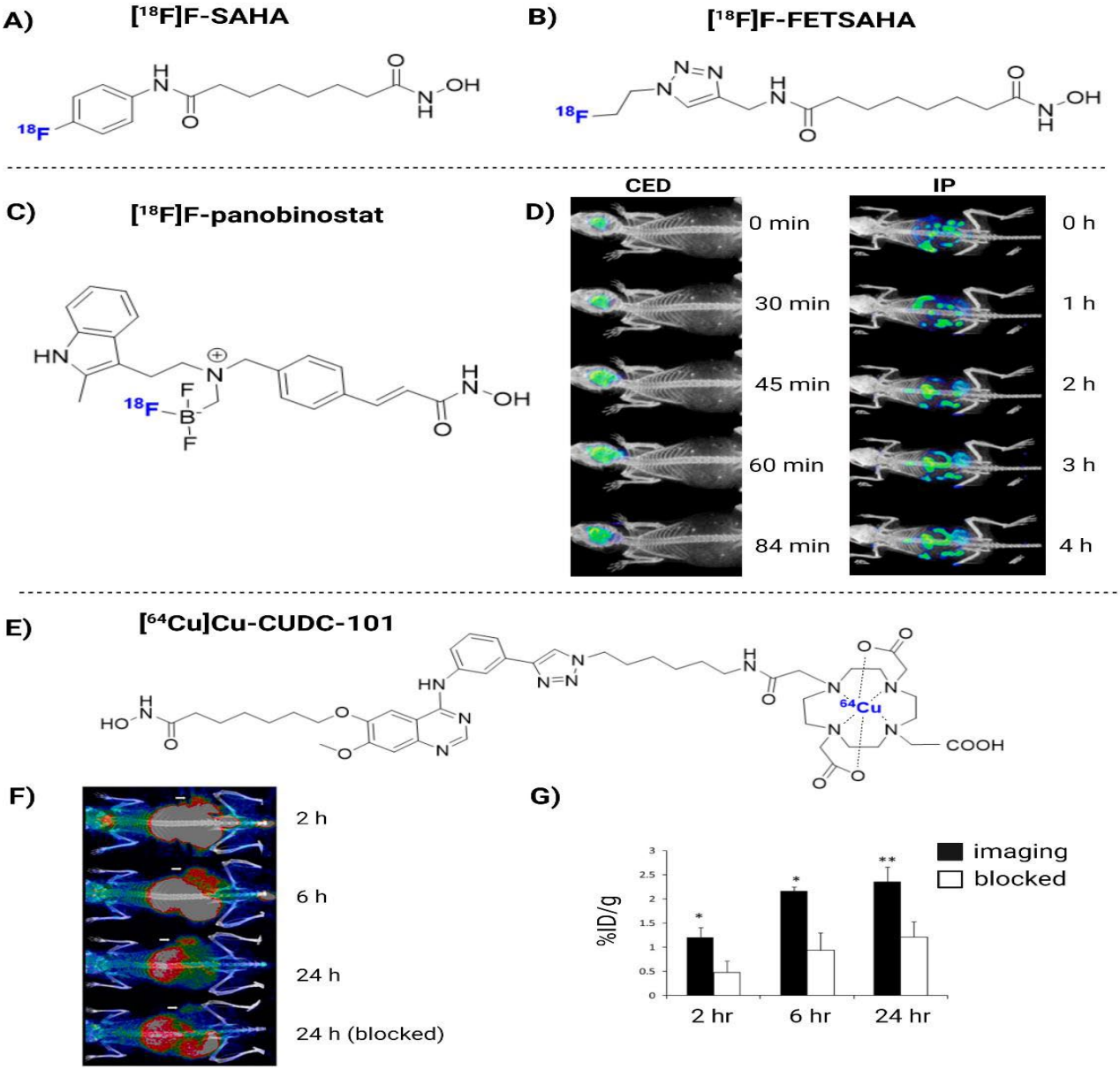

Figure 3. The chemical structure of [^{18}F]F-SAHA (**A**), [^{18}F]FET-SAHA (**B**), [^{18}F]F-panobinostat (**C**) and [^{64}Cu]Cu-CUDC-101 (**E**). [^{18}F]F-panobinostat PET imaging when delivered via convection-enhanced delivery (CED) or intraperitoneal (IP) (**D**). In vivo PET imaging of [^{64}Cu]Cu-CUDC-101 in MDA-MB-231-bearing tumor mice, with or without co-injection of cold CUDC-101 (**F**,**G**). Images reproduced with permission from [180,184]. Copyright 2013 and 2018 American Chemical Society.

As the development of highly brain-penetrant HDACi has been a persistent challenge, research is now shifting from radiolabeling existing HDACi to the development of novel brain-penetrant radiotracers; in particular, adamantane-conjugated radioligands seem promising [164]. The most advanced candidate is (E)-3-(4-((((3r,5r,7r)-adamantan-1-ylmethyl)([^{11}C]methyl)amino)methyl)phenyl)-*N*-hydroxyacrylamide([^{11}C]martinostat), an adamantane-based hydroxamic acid with selective binding to HDAC 1, 2, 3 and 6 with subnanomolar potency and fast-binding kinetics [185]. In vivo, [^{11}C]C-martinostat has shown a selective, reversible and dose-dependent binding, excellent signal-to-noise ratio and desirable safety profiles in rodents, pigs and humans [185–187]. Next, an ^{18}F-labeled derivative of martinostat, [^{18}F]F-MGS3, was developed by Strebl et al. [188]. [^{18}F]F-MGS3 exhibited HDAC-specific binding, as well as comparable brain uptake and regional dis- tribution compared to [^{11}C]martinostat. However, [^{18}F]F-MGS3 warrants more efficient radiosynthesis as poor yields and manual synthesis only allowed for low doses to be administered [188]. Lastly, [^{18}F]F-bavarostat ([^{18}F]F-EKZ-001) appears to be useful for HDAC6 quantification. In NHPs, [^{18}F]F-EKZ-001 displayed rapid and high brain tissue uptake and excellent specific binding which was subsequently confirmed in healthy human adults [189,190].

Table 2. Preclinical development of HDAC radiopharmaceuticals.

Radio-Pharmaceutical	(Pre)clinical Model	Year	Main Outcome and Findings	Ref
[^{18}F]FAHA	Healthy rats	2007	(+) Uptake increased rapidly up to 0.44%ID/g (5–60 min). Target blocking (SAHA) decreased uptake	[169]
	Healthy NHP	2009	(−) Rapidly metabolized to [^{18}F]FACE, which enters the brain	[171]
	Healthy NHP	2013	(-) Lack of BBB permeability and specificity	[167]
	Healthy NHP	2013	(+) BBB crossing. Limited influence of [^{18}F]FACE to brain uptake (first 30 min)	[175]
	NNK-treated A/J mice	2014	(+) Midbrain, cerebellum and brainstem uptake was displaced by SAHA with <10% remaining	[170]
	Healthy mice	2018	(+) Specific uptake consistent with increased HDAC levels	[174]
[^{18}F]DFAHA	Healthy rats	2015	(+) Selectivity for HDAC Class IIa > [^{18}F]FAHA, favorably low unspecific brain accumulation	[172]
[^{18}F]TFAHA	Healthy rats	2015	(+) Selectivity for HDAC class IIa > [^{18}F]DFAHA and [^{18}F]FAHA	[172]
	Intracerebral 9L and U87-MG rat xenografts	2019	(+) Increased accumulation at 20 min post-radiotracer administration (+) Target specificity, i.e., significant reduction uptake in 9L tumors after administration of HDACi MC1568 but not the SIRT1 specific inhibitor EX-527	[163]
	AD mouse model	2021	(+) Potential as an epigenetic radiotracer for AD	[191]
[^{18}F]F-SAHA	A2780 OC mice	2011	(+) Exhibits nM potency. Target binding efficacy can be quantitated within 24 h	[162]
[$^{125/131}$I]-iodo-SAHA	Thyroid, hepatoma, colon carcinoma-bearing mice	2008	(−) Equally toxic as SAHA. Rapid efflux and rapid washout and no preferential tumor accumulation. High (unwanted) accumulation in liver and kidneys	[177]
[^{18}F]FE-SAHA	Mice LNCaP xenografts	2011	(+) Tumor uptake (−) High (unwanted) uptake in small intestines, kidneys, liver and bone (suspected defluorination)	[176]

Table 2. *Cont.*

Radio-Pharmaceutical	(Pre)clinical Model	Year	Main Outcome and Findings	Ref
[^{18}F]FET-SAHA	RR1022 sarcoma rat	2018	(+) Significant accumulation in tumors with rapid blood clearance (gastrointestinal/renal excretion). Tracer accumulation was receptor-specific	[173]
[^{11}C]TSA	Healthy NHP	2013	(−) Lack of BBB permeability and HDAC-specificity	[167]
[^{11}C]MS-275	Healthy mice, rats, NHP	2010	(−) Poor brain penetration and lack of tracer specificity	[178]
[^{11}C]KB631	B16.F10 murine melanoma-bearing mice	2019	(+) Showed HDAC6-selective binding (−) Lack of brain penetrance in rats, possibly due to the hydroxamate moiety	[181]
[^{11}C]CN89	Healthy rats, NHP	2013	(−) Poor BBB penetration	[179]
[^{11}C]CN107				
[^{18}F]F-panobinostat	DIPG IV and XIII + U87MG glioma cells	2018	(+) Retains nM efficacy in glioma cells *in vitro*. Highly selective to glioma, with low toxicity to healthy astrocyte controls. Successful delivery to the murine central nervous system via CED (Figure 3D)	[180]
[^{11}C]-4-phenylbutyric acid	Healthy NHP	2013	(−) Low brain uptake. Showed 15% metabolization after 30 min. High (unwanted) uptake in liver and heart	[161]
[^{11}C]valproic acid	Healthy NHP	2013	(−) Low brain uptake. Showed 2% metabolization after 30 min. Exceptionally high (unwanted) heart uptake possibly due to its involvement in lipid metabolism	[161]
[^{11}C]butyric Acid	Healthy NHP	2013	(−) Low brain uptake. Rapid metabolization (plasma: 80% metabolized after 5 min). Relatively high (unwanted) uptake in spleen and pancreas	[161]
[^{11}C]PCI34051	Healthy rats/NHP	2013	(−) Poor BBB penetration. Low uptake in the brain within 80 min. Pretreatment with 2 mg/kg standard did not improve retention or permeability	[179]
[^{64}Cu]Cu-CUDC-101	MDA-MB-231 xenograft mice	2013	(+) Specific binding to HDACs in vitro (nM). High TBR in vivo (Figure 3F)	[184]
[^{11}C]martinostat	Healthy rats	2014	(+) Can quantify target engagement of structurally distinct, brain-penetrant hydroxamate HDACi in living rat brain	[192]
	Healthy NHP	2014	(+) Highly selective and specific. Testing in humans is warranted	[185]
	Healthy NHP	2015	(+) Allows quantification of brain HDAC expression. Reversible and dose-dependent binding. Slow washout kinetics observed	[193]
	Healthy humans	2016	(+) Selectively binds HDAC1, 2 and 3	[186]
	Healthy pigs	2020	(+) Allowed for accurate in vivo measurement of cerebral HDAC1—3 protein levels. Excellent signal-to-noise ratio	[187]
[^{18}F]F-MGS3	Healthy rats, NHP	2016	(+) Exhibits specific binding/comparable brain uptake and regional distribution to [^{11}C]martinostat	[188]

Table 2. *Cont.*

Radio-Pharmaceutical	(Pre)clinical Model	Year	Main Outcome and Findings	Ref
[^{18}F]F-bavarostat	Healthy rats, NHP	2017	(+) Selective HDAC6 inhibitor. Excellent brain penetrance. Low amount of nonspecific binding observed after pre-treatment with 1 mg/kg unlabeled bavarostat	[194]
	Healthy NHP	2020	(+) Excellent brain penetrance. Good HDAC6 selectivity, enabling quantification	[189]
	Healthy humans	2021	(+) Safe to administer and accurate quantification of HDAC6 expression in the human brain	[190]
[^{18}F]F-NT160	Healthy mice	2022	(+) Can cross the BBB and bind to class-IIa HDACs in vivo in mice brain tissue	[183]

AD = Alzheimer's disease; BBB = blood brain barrier; CED = convection enhanced delivery, CNS = central nervous system; DIPG = diffuse intrinsic pontine glioma; HDAC = histone deacetylase; i.v. = intravenous; LNCaP = lymph node carcinoma of the prostate; NHP = non-human primate; NNK = 4-(methylnitrosamino)-1-(3-pyridyl)-1-butanone; OC = ovarian cancer; PET = positron emission tomography; TBR = tumor-to-background ratio.

5. Challenges and Future Outlook

Although extensive research has been performed on HDACi in glioma with clear radio- and/or chemosensitizing effects, the potential of radiolabeled HDACi has only been confirmed in the field of neurodegenerative diseases and been primarily diagnostic, with the goal of quantifying HDAC expression and/or monitoring treatment response. Their potential for GB imaging and TRT is underexplored. Whilst furthering this field of research should be recommended, one of the major issues that slowed down recent translation to clinics was poor BBB penetration, poor specificity and diverse target locations. Interestingly, adamantane-conjugated radioligands seem promising to increase brain penetrance [164]. Only two radiotracers have been investigated in healthy adults: [^{11}C]martinostat and [^{18}F]F-bavarostat, confirming the ability to quantify HDAC expression [186,190]. Both should be recommended for GB HDAC imaging as they have shown target specificity and reported brain penetrance. [^{18}F]TFAHA is the only radiopharmaceutical that has been evaluated in GB models, with uptake in GB tumors but also in normal brain structures known to overexpress HDAC class IIa [163]. Another recommendable radiopharmaceutical is [^{18}F]F-NT160 featuring potent binding to class-IIa HDACs and BBB crossing in mice [183]. However, future studies are needed to increase its tumor specific uptake while preventing damage to healthy tissues.

The potential for HDACi-based radiopharmaceuticals in GB can currently be formu- lated as (1) biomarkers for HDAC expression, (2) elucidate the roles of HDAC class enzymes and (3) dose optimization of cold HDACi [163]. Cancer resistance and the toxic effects of HDACi are currently an issue to translate radiolabeled HDACi for potential application in TRT. HDACi are often pan-specific towards a specific HDAC class. As their substrates are present all over the human brain, targeting HDACi in GB may cause unwanted effects on healthy tissues too. However, CED could be considered to mitigate any adverse effects and circumvent the BBB. Targeting multiple HDAC proteins could also be advantageous due to the heterogeneous nature of GB. Research should be initiated to confirm this, including optimal combinatorial strategies for HDACi that permit efficacy as well as safety in GB.

Supplementary Materials: The following supporting information can be downloaded at: https:// www.mdpi.com/article/10.3390/ph16020227/s1, Table S1: Representative summary of the preclinical development for candidate HDACi-derived glioma therapy.

Author Contributions: Conceptualization, J.B.; writing—original draft preparation, L.E., J.B. and E.N.S.; writing—review and editing, E.N.S., T.E., I.G. and J.B.; final approval of the version published, L.E., E.N.S., T.E., I.G. and J.B. All authors have read and agreed to the published version of the manuscript.

Funding: This research received no external funding. **Institutional Review Board Statement:** Not applicable. **Informed Consent Statement:** Not applicable.

Data Availability Statement: Not applicable.

Acknowledgments: This review includes data from the thesis of Liesbeth Everix (MSc in Biomedical sciences, Ghent University 2021). BioRender was used for creating images.

Conflicts of Interest: The authors declare no conflict of interest.

References

1. Stupp, R.; Mason, W.P.; van den Bent, M.J.; Weller, M.; Fisher, B.; Taphoorn, M.J.; Belanger, K.; Brandes, A.A.; Marosi, C.; Bogdahn, U.; et al. Radiotherapy plus concomitant and adjuvant temozolomide for glioblastoma. *N. Engl. J. Med.* **2005**, *352*, 987–996. [CrossRef] [PubMed]
2. Jain, K.K. A Critical Overview of Targeted Therapies for Glioblastoma. *Front. Oncol.* **2018**, *8*, 419. [CrossRef] [PubMed]
3. Tan, A.C.; Ashley, D.M.; López, G.Y.; Malinzak, M.; Friedman, H.S.; Khasraw, M. Management of glioblastoma: State of the art and future directions. *CA Cancer J. Clin.* **2020**, *70*, 299–312. [CrossRef]
4. Louis, D.N.; Perry, A.; Wesseling, P.; Brat, D.J.; Cree, I.A.; Figarella-Branger, D.; Hawkins, C.; Ng, H.K.; Pfister, S.M.; Reifenberger, G.; et al. The 2021 WHO Classification of Tumors of the Central Nervous System: A summary. *Neuro-Oncology* **2021**, *23*, 1231–1251. [CrossRef] [PubMed]
5. LoPresti, P. HDAC6 in Diseases of Cognition and of Neurons. *Cells* **2020**, *10*, 12. [CrossRef]
6. Mottamal, M.; Zheng, S.; Huang, T.L.; Wang, G. Histone deacetylase inhibitors in clinical studies as templates for new anticancer agents. *Molecules* **2015**, *20*, 3898–3941. [CrossRef]
7. McClure, J.J.; Li, X.; Chou, C.J. Advances and Challenges of HDAC Inhibitors in Cancer Therapeutics. *Adv. Cancer Res.* **2018**, *138*, 183–211. [CrossRef]
8. Parbin, S.; Kar, S.; Shilpi, A.; Sengupta, D.; Deb, M.; Rath, S.K.; Patra, S.K. Histone deacetylases: A saga of perturbed acetylation homeostasis in cancer. *J. Histochem. Cytochem.* **2014**, *62*, 11–33. [CrossRef]
9. Was, H.; Krol, S.K.; Rotili, D.; Mai, A.; Wojtas, B.; Kaminska, B.; Maleszewska, M. Histone deacetylase inhibitors exert anti-tumor effects on human adherent and stem-like glioma cells. *Clin. Epigenetics* **2019**, *11*, 11. [CrossRef]
10. Bezecny, P. Histone deacetylase inhibitors in glioblastoma: Pre-clinical and clinical experience. *Med. Oncol.* **2014**, *31*, 985. [CrossRef]
11. Chen, R.; Zhang, M.; Zhou, Y.; Guo, W.; Yi, M.; Zhang, Z.; Ding, Y.; Wang, Y. The application of histone deacetylases inhibitors in glioblastoma. *J. Exp. Clin. Cancer Res.* **2020**, *39*, 138. [CrossRef]
12. Singh, A.K.; Bishayee, A.; Pandey, A.K. Targeting Histone Deacetylases with Natural and Synthetic Agents: An Emerging Anticancer Strategy. *Nutrients* **2018**, *10*, 731. [CrossRef]
13. Yelton, C.J.; Ray, S.K. Histone deacetylase enzymes and selective histone deacetylase inhibitors for antitumor effects and enhancement of antitumor immunity in glioblastoma. *Neuroimmunol. Neuroinflamm.* **2018**, *5*, 46. [CrossRef]
14. Zhang, Z.; Wang, Y.; Chen, J.; Tan, Q.; Xie, C.; Li, C.; Zhan, W.; Wang, M. Silencing of histone deacetylase 2 suppresses malignancy for proliferation, migration, and invasion of glioblastoma cells and enhances temozolomide sensitivity. *Cancer Chemother Pharmacol.* **2016**, *78*, 1289–1296. [CrossRef]
15. Mottet, D.; Pirotte, S.; Lamour, V.; Hagedorn, M.; Javerzat, S.; Bikfalvi, A.; Bellahcène, A.; Verdin, E.; Castronovo, V. HDAC4 represses p21(WAF1/Cip1) expression in human cancer cells through a Sp1-dependent, p53-independent mechanism. *Oncogene* **2009**, *28*, 243–256. [CrossRef]
16. Liu, Q.; Zheng, J.M.; Chen, J.K.; Yan, X.L.; Chen, H.M.; Nong, W.X.; Huang, H.Q. Histone deacetylase 5 promotes the proliferation of glioma cells by upregulation of Notch 1. *Mol. Med. Rep.* **2014**, *10*, 2045–2050. [CrossRef]
17. Shi, P.; Hoang-Minh, L.B.; Tian, J.; Cheng, A.; Basrai, R.; Kalaria, N.; Lebowitz, J.J.; Khoshbouei, H.; Deleyrolle, L.P.; Sarkisian, M.R. HDAC6 Signaling at Primary Cilia Promotes Proliferation and Restricts Differentiation of Glioma Cells. *Cancers* **2021**, *13*, 1644. [CrossRef]

18. Li, S.; Liu, X.; Chen, X.; Zhang, L.; Wang, X. Histone deacetylase 6 promotes growth of glioblastoma through inhibition of SMAD2 signaling. *Tumour. Biol.* **2015**, *36*, 9661–9665. [CrossRef]
19. Huang, Z.; Xia, Y.; Hu, K.; Zeng, S.; Wu, L.; Liu, S.; Zhi, C.; Lai, M.; Chen, D.; Xie, L.; et al. Histone deacetylase 6 promotes growth of glioblastoma through the MKK7/JNK/c-Jun signaling pathway. *J. Neurochem.* **2020**, *152*, 221–234. [CrossRef]
20. Kim, G.W.; Lee, D.H.; Yeon, S.K.; Jeon, Y.H.; Yoo, J.; Lee, S.W.; Kwon, S.H. Temozolomide-resistant Glioblastoma Depends on HDAC6 Activity Through Regulation of DNA Mismatch Repair. *Anticancer Res.* **2019**, *39*, 6731–6741. [CrossRef]
21. Chueh, A.C.; Tse, J.W.T.; Dickinson, M.; Ioannidis, P.; Jenkins, L.; Togel, L.; Tan, B.; Luk, I.; Davalos-Salas, M.; Nightingale, R.; et al. ATF3 Repression of BCL-XL Determines Apoptotic Sensitivity to HDAC Inhibitors across Tumor Types. *Clin. Cancer Res.* **2017**, *23*, 5573–5584. [CrossRef] [PubMed]
22. Bondarev, A.D.; Attwood, M.M.; Jonsson, J.; Chubarev, V.N.; Tarasov, V.V.; Schiöth, H.B. Recent developments of HDAC inhibitors: Emerging indications and novel molecules. *Br. J. Clin. Pharmacol.* **2021**, *87*, 4577–4597. [CrossRef] [PubMed]
23. Milazzo, G.; Mercatelli, D.; Di Muzio, G.; Triboli, L.; De Rosa, P.; Perini, G.; Giorgi, F.M. Histone Deacetylases (HDACs): Evolution, Specificity, Role in Transcriptional Complexes, and Pharmacological Actionability. *Genes* **2020**, *11*, 556. [CrossRef] [PubMed]
24. Jenke, R.; Reßing, N.; Hansen, F.K.; Aigner, A.; Büch, T. Anticancer Therapy with HDAC Inhibitors: Mechanism-Based Combina- tion Strategies and Future Perspectives. *Cancers* **2021**, *13*, 634. [CrossRef] [PubMed]
25. Chen, J.C.; Lee, I.N.; Huang, C.; Wu, Y.P.; Chung, C.Y.; Lee, M.H.; Lin, M.H.; Yang, J.T. Valproic acid-induced amphiregulin secretion confers resistance to temozolomide treatment in human glioma cells. *BMC Cancer* **2019**, *19*, 756. [CrossRef]
26. Wang, Z.; Hu, P.; Tang, F.; Lian, H.; Chen, X.; Zhang, Y.; He, X.; Liu, W.; Xie, C. HDAC6 promotes cell proliferation and confers resistance to temozolomide in glioblastoma. *Cancer Lett.* **2016**, *379*, 134–142. [CrossRef]
27. Yang, W.B.; Wu, A.C.; Hsu, T.I.; Liou, J.P.; Lo, W.L.; Chang, K.Y.; Chen, P.Y.; Kikkawa, U.; Yang, S.T.; Kao, T.J.; et al. Histone deacetylase 6 acts upstream of DNA damage response activation to support the survival of glioblastoma cells. *Cell Death Dis.* **2021**, *12*, 884. [CrossRef]
28. Groselj, B.; Sharma, N.L.; Hamdy, F.C.; Kerr, M.; Kiltie, A.E. Histone deacetylase inhibitors as radiosensitisers: Effects on DNA damage signalling and repair. *Br. J. Cancer* **2013**, *108*, 748–754. [CrossRef]
29. Shabason, J.E.; Tofilon, P.J.; Camphausen, K. Grand rounds at the National Institutes of Health: HDAC inhibitors as radiation modifiers, from bench to clinic. *J. Cell Mol. Med.* **2011**, *15*, 2735–2744. [CrossRef]
30. Camphausen, K.; Tofilon, P.J. Inhibition of histone deacetylation: A strategy for tumor radiosensitization. *J. Clin. Oncol.* **2007**, *25*, 4051–4056. [CrossRef]
31. Camphausen, K.; Cerna, D.; Scott, T.; Sproull, M.; Burgan, W.E.; Cerra, M.A.; Fine, H.; Tofilon, P.J. Enhancement of *in vitro* and in vivo tumor cell radiosensitivity by valproic acid. *Int. J. Cancer* **2005**, *114*, 380–386. [CrossRef]
32. Kim, J.H.; Shin, J.H.; Kim, I.H. Susceptibility and radiosensitization of human glioblastoma cells to trichostatin A, a histone deacetylase inhibitor. *Int. J. Radiat. Oncol. Biol. Phys.* **2004**, *59*, 1174–1180. [CrossRef]
33. Camphausen, K.; Burgan, W.; Cerra, M.; Oswald, K.A.; Trepel, J.B.; Lee, M.J.; Tofilon, P.J. Enhanced radiation-induced cell killing and prolongation of gammaH2AX foci expression by the histone deacetylase inhibitor MS-275. *Cancer*

Res. **2004**, *64*, 316–321. [CrossRef]
34. Diss, E.; Nalabothula, N.; Nguyen, D.; Chang, E.; Kwok, Y.; Carrier, F. Vorinostat(SAHA) Promotes Hyper-Radiosensitivity in Wild Type p53 Human Glioblastoma Cells. *J. Clin. Oncol. Res.* **2014**, *2*, 1.
35. Barazzuol, L.; Jeynes, J.C.; Merchant, M.J.; Wéra, A.C.; Barry, M.A.; Kirkby, K.J.; Suzuki, M. Radiosensitization of glioblastoma cells using a histone deacetylase inhibitor (SAHA) comparing carbon ions with X-rays. *Int. J. Radiat. Biol.* **2015**, *91*, 90–98. [CrossRef]
36. Conti, C.; Leo, E.; Eichler, G.S.; Sordet, O.; Martin, M.M.; Fan, A.; Aladjem, M.I.; Pommier, Y. Inhibition of histone deacetylase in cancer cells slows down replication forks, activates dormant origins, and induces DNA damage. *Cancer Res.* **2010**, *70*, 4470–4480. [CrossRef]
37. Namdar, M.; Perez, G.; Ngo, L.; Marks, P.A. Selective inhibition of histone deacetylase 6 (HDAC6) induces DNA damage and sensitizes transformed cells to anticancer agents. *Proc. Natl. Acad. Sci. USA* **2010**, *107*, 20003–20008. [CrossRef]
38. Lee, P.; Murphy, B.; Miller, R.; Menon, V.; Banik, N.L.; Giglio, P.; Lindhorst, S.M.; Varma, A.K.; Vandergrift, W.A., 3rd; Patel, S.J.; et al. Mechanisms and clinical significance of histone deacetylase inhibitors: Epigenetic glioblastoma therapy. *Anticancer Res.* **2015**, *35*, 615–625.
39. Chiao, M.T.; Cheng, W.Y.; Yang, Y.C.; Shen, C.C.; Ko, J.L. Suberoylanilide hydroxamic acid (SAHA) causes tumor growth slowdown and triggers autophagy in glioblastoma stem cells. *Autophagy* **2013**, *9*, 1509–1526. [CrossRef]
40. Galanis, E.; Jaeckle, K.A.; Maurer, M.J.; Reid, J.M.; Ames, M.M.; Hardwick, J.S.; Reilly, J.F.; Loboda, A.; Nebozhyn, M.; Fantin, V.R.; et al. Phase II trial of vorinostat in recurrent glioblastoma multiforme: A north central cancer treatment group study. *J. Clin. Oncol.* **2009**, *27*, 2052–2058. [CrossRef]
41. Lee, E.Q.; Puduvalli, V.K.; Reid, J.M.; Kuhn, J.G.; Lamborn, K.R.; Cloughesy, T.F.; Chang, S.M.; Drappatz, J.; Yung, W.K.; Gilbert, M.R.; et al. Phase I study of vorinostat in combination with temozolomide in patients with high-grade gliomas: North American Brain Tumor Consortium Study 04-03. *Clin. Cancer Res.* **2012**, *18*, 6032–6039. [CrossRef] [PubMed]
42. ClinicalTrials.gov. Available online: https://clinicaltrials.gov/ct2/home (accessed on 5 September 2022).
43. Puduvalli, V.K.; Wu, J.; Yuan, Y.; Armstrong, T.S.; Groves, M.D.; Raizer, J.J.; Giglio, P.; Colman, H.; Peereboom, D.M.; Walbert, T.; et al. Brain Tumor Trials Collaborative Bayesian Adaptive Randomized Phase II trial of bevacizumab plus vorinostat versus bevacizumab alone in adults with recurrent glioblastoma (BTTC-1102). *J. Clin. Oncol.* **2015**, *33*, 2012. [CrossRef]
44. Peters, K.B.; Lipp, E.S.; Miller, E.; Herndon, J.E., 2nd; McSherry, F.; Desjardins, A.; Reardon, D.A.; Friedman, H.S. Phase I/II trial of vorinostat, bevacizumab, and daily temozolomide for recurrent malignant gliomas. *J. Neurooncol.* **2018**, *137*, 349–356. [CrossRef] [PubMed]
45. Ghiaseddin, A.; Reardon, D.; Massey, W.; Mannerino, A.; Lipp, E.S.; Herndon, J.E., 2nd; McSherry, F.; Desjardins, A.; Randazzo, D.; Friedman, H.S.; et al. Phase II Study of Bevacizumab and Vorinostat for Patients with Recurrent World Health Organization Grade 4 Malignant Glioma. *Oncologist* **2018**, *23*, 157-e21. [CrossRef]
46. Kang, D.W.; Hwang, W.C.; Noh, Y.N.; Kang, Y.; Jang, Y.; Kim, J.A.; Min, D.S. Phospholipase D1 is upregulated by vorinostat and confers resistance to vorinostat in glioblastoma. *J. Cell. Physiol.* **2021**, *236*, 549–560. [CrossRef]
47. Gurbani, S.S.; Yoon, Y.; Weinberg, B.D.; Salgado, E.; Press, R.H.; Cordova, J.S.; Ramesh, K.K.; Liang, Z.; Velazquez Vega, J.; Voloschin, A.; et al. Assessing Treatment Response of Glioblastoma to an HDAC Inhibitor Using Whole-Brain Spectroscopic MRI. *Tomography* **2019**, *5*, 53–60. [CrossRef]
48. Xu, K.; Ramesh, K.; Huang, V.; Gurbani, S.S.; Cordova, J.S.; Schreibmann, E.;

Weinberg, B.D.; Sengupta, S.; Voloschin, A.D.; Holdhoff, M.; et al. Final Report on Clinical Outcomes and Tumor Recurrence Patterns of a Pilot Study Assessing Efficacy of Belinostat (PXD-101) with Chemoradiation for Newly Diagnosed Glioblastoma. *Tomography* **2022**, *8*, 688–700. [CrossRef]
49. Iwamoto, F.M.; Lamborn, K.R.; Kuhn, J.G.; Wen, P.Y.; Yung, W.K.; Gilbert, M.R.; Chang, S.M.; Lieberman, F.S.; Prados, M.D.; Fine, H.A. A phase I/II trial of the histone deacetylase inhibitor romidepsin for adults with recurrent malignant glioma: North American Brain Tumor Consortium Study 03-03. *Neuro-Oncology* **2011**, *13*, 509–516. [CrossRef]
50. Furumai, R.; Matsuyama, A.; Kobashi, N.; Lee, K.H.; Nishiyama, M.; Nakajima, H.; Tanaka, A.; Komatsu, Y.; Nishino, N.; Yoshida, M.; et al. FK228 (depsipeptide) as a natural prodrug that inhibits class I histone deacetylases. *Cancer Res.* **2002**, *62*, 4916–4921.
51. Van Veggel, M.; Westerman, E.; Hamberg, P. Clinical Pharmacokinetics and Pharmacodynamics of Panobinostat. *Clin. pharmacokinet.* **2018**, *57*, 21–29. [CrossRef]
52. Lee, E.Q.; Reardon, D.A.; Schiff, D.; Drappatz, J.; Muzikansky, A.; Grimm, S.A.; Norden, A.D.; Nayak, L.; Beroukhim, R.; Rinne, M.L.; et al. Phase II study of panobinostat in combination with bevacizumab for recurrent glioblastoma and anaplastic glioma. *Neuro-Oncology* **2015**, *17*, 862–867. [CrossRef]
53. Shi, W.; Palmer, J.D.; Werner-Wasik, M.; Andrews, D.W.; Evans, J.J.; Glass, J.; Kim, L.; Bar-Ad, V.; Judy, K.; Farrell, C.; et al. Phase I trial of panobinostat and fractionated stereotactic re-irradiation therapy for recurrent high grade gliomas. *J. Neuro-Oncol.* **2016**, *127*, 535–539. [CrossRef]
54. Singleton, W.G.B.; Bienemann, A.S.; Woolley, M.; Johnson, D.; Lewis, O.; Wyatt, M.J.; Damment, S.J.P.; Boulter, L.J.; Killick-Cole, C.L.; Asby, D.J.; et al. The distribution, clearance, and brainstem toxicity of panobinostat administered by convection-enhanced delivery. *J. Neurosurg. Pediatr.* **2018**, *22*, 288–296. [CrossRef]
55. Han, W.; Guan, W. Valproic Acid: A Promising Therapeutic Agent in Glioma Treatment. *Front. Oncol.* **2021**, *11*, 687362. [CrossRef]
56. Krauze, A.V.; Myrehaug, S.D.; Chang, M.G.; Holdford, D.J.; Smith, S.; Shih, J.; Tofilon, P.J.; Fine, H.A.; Camphausen, K. A Phase 2 Study of Concurrent Radiation Therapy, Temozolomide, and the Histone Deacetylase Inhibitor Valproic Acid for Patients With Glioblastoma. *Int. J. Radiat. Oncol. Biol. Phys.* **2015**, *92*, 986–992. [CrossRef]
57. Tsai, H.C.; Wei, K.C.; Chen, P.Y.; Huang, C.Y.; Chen, K.T.; Lin, Y.J.; Cheng, H.W.; Chen, Y.R.; Wang, H.T. Valproic Acid Enhanced Temozolomide-Induced Anticancer Activity in Human Glioma Through the p53-PUMA Apoptosis Pathway. *Front. Oncol.* **2021**, *11*, 722754. [CrossRef]
58. Krauze, A.V.; Megan, M.; Theresa, C.Z.; Peter, M.; Shih, J.H.; Tofilon, P.J.; Rowe, L.; Gilbert, M.; Camphausen, K. The addition of Valproic acid to concurrent radiation therapy and temozolomide improves patient outcome: A Correlative analysis of RTOG 0525, SEER and a Phase II NCI trial. *Cancer Stud. Ther.* **2020**, *5*, 722754. [CrossRef]
59. Shim, H.; Wei, L.; Holder, C.A.; Guo, Y.; Hu, X.P.; Miller, A.H.; Olson, J.J. Use of high-resolution volumetric MR spectroscopic imaging in assessing treatment response of glioblastoma to an HDAC inhibitor. *Am. J. Roentgenol.* **2014**, *203*, W158–W165. [CrossRef]
60. Chinnaiyan, P.; Chowdhary, S.; Potthast, L.; Prabhu, A.; Tsai, Y.Y.; Sarcar, B.; Kahali, S.; Brem, S.; Yu, H.M.; Rojiani, A.; et al. Phase I trial of vorinostat combined with bevacizumab and CPT-11 in recurrent glioblastoma. *Neuro-oncology* **2012**, *14*, 93–100. [CrossRef]
61. Friday, B.B.; Anderson, S.K.; Buckner, J.; Yu, C.; Giannini, C.; Geoffroy, F.;

Schwerkoske, J.; Mazurczak, M.; Gross, H.; Pajon, E.; et al. Phase II trial of vorinostat in combination with bortezomib in recurrent glioblastoma: A north central cancer treatment group study. *Neuro-oncology* **2012**, *14*, 215–221. [CrossRef]
62. Galanis, E.; Anderson, S.K.; Miller, C.R.; Sarkaria, J.N.; Jaeckle, K.; Buckner, J.C.; Ligon, K.L.; Ballman, K.V.; Moore, D.F., Jr.; Nebozhyn, M.; et al. Phase I/II trial of vorinostat combined with temozolomide and radiation therapy for newly diagnosed glioblastoma: Results of Alliance N0874/ABTC 02. *Neuro-oncology* **2018**, *20*, 546–556. [CrossRef] [PubMed]
63. Watanabe, S.; Kuwabara, Y.; Suehiro, S.; Yamashita, D.; Tanaka, M.; Tanaka, A.; Ohue, S.; Araki, H. Valproic acid reduces hair loss and improves survival in patients receiving temozolomide-based radiation therapy for high-grade glioma. *Eur. J. Clin. Pharmacol.* **2017**, *73*, 357–363. [CrossRef] [PubMed]
64. Li, C.; Chen, H.; Tan, Q.; Xie, C.; Zhan, W.; Sharma, A.; Sharma, H.S.; Zhang, Z. The therapeutic and neuroprotective effects of an antiepileptic drug valproic acid in glioma patients. *Prog. Brain Res.* **2020**, *258*, 369–379. [CrossRef] [PubMed]
65. Kerkhof, M.; Dielemans, J.C.; van Breemen, M.S.; Zwinkels, H.; Walchenbach, R.; Taphoorn, M.J.; Vecht, C.J. Effect of valproic acid on seizure control and on survival in patients with glioblastoma multiforme. *Neuro-oncology* **2013**, *15*, 961–967. [CrossRef] [PubMed]
66. Valiyaveettil, D.; Malik, M.; Joseph, D.M.; Ahmed, S.F.; Kothwal, S.A.; Vijayasaradhi, M. Effect of valproic acid on survival in glioblastoma: A prospective single-arm study. *S. Asian J. Cancer* **2018**, *7*, 159–162. [CrossRef]
67. Redjal, N.; Reinshagen, C.; Le, A.; Walcott, B.P.; McDonnell, E.; Dietrich, J.; Nahed, B.V. Valproic acid, compared to other antiepileptic drugs, is associated with improved overall and progression-free survival in glioblastoma but worse outcome in grade II/III gliomas treated with temozolomide. *J. Neuro-Oncol.* **2016**, *127*, 505–514. [CrossRef]
68. Ugur, H.C.; Ramakrishna, N.; Bello, L.; Menon, L.G.; Kim, S.K.; Black, P.M.; Carroll, R.S. Continuous intracranial administration of suberoylanilide hydroxamic acid (SAHA) inhibits tumor growth in an orthotopic glioma model. *J. Neuro-Oncol.* **2007**, *83*, 267–275. [CrossRef]
69. Jane, E.P.; Premkumar, D.R.; Addo-Yobo, S.O.; Pollack, I.F. Abrogation of mitogen-activated protein kinase and Akt signaling by vandetanib synergistically potentiates histone deacetylase inhibitor-induced apoptosis in human glioma cells. *J. Pharmacol. Exp. Ther.* **2009**, *331*, 327–337. [CrossRef]
70. Orzan, F.; Pellegatta, S.; Poliani, P.L.; Pisati, F.; Caldera, V.; Menghi, F.; Kapetis, D.; Marras, C.; Schiffer, D.; Finocchiaro, G. Enhancer of Zeste 2 (EZH2) is up-regulated in malignant gliomas and in glioma stem-like cells. *Neuropathol. Appl. Neurobiol.* **2011**, *37*, 381–394. [CrossRef]
71. Singh, M.M.; Manton, C.A.; Bhat, K.P.; Tsai, W.W.; Aldape, K.; Barton, M.C.; Chandra, J. Inhibition of LSD1 sensitizes glioblastoma cells to histone deacetylase inhibitors. *Neuro-Oncology* **2011**, *13*, 894–903. [CrossRef]
72. Berghauser Pont, L.M.; Spoor, J.K.; Venkatesan, S.; Swagemakers, S.; Kloezeman, J.J.; Dirven, C.M.; van der Spek, P.J.; Lamfers, M.L.; Leenstra, S. The Bcl-2 inhibitor Obatoclax overcomes resistance to histone deacetylase inhibitors SAHA and LBH589 as radiosensitizers in patient-derived glioblastoma stem-like cells. *Genes Cancer* **2014**, *5*, 445–459. [CrossRef]
73. Cornago, M.; Garcia-Alberich, C.; Blasco-Angulo, N.; Vall-Llaura, N.; Nager, M.; Herreros, J.; Comella, J.X.; Sanchis, D.; Llovera, M. Histone deacetylase inhibitors promote glioma cell death by G2 checkpoint abrogation leading to mitotic catastrophe. *Cell Death Dis.* **2014**, *5*, e1435. [CrossRef]
74. Rasmussen, R.D.; Gajjar, M.K.; Jensen, K.E.; Hamerlik, P. Enhanced efficacy of combined HDAC and PARP targeting in glioblastoma. *Mol. Oncol.* **2016**, *10*, 751–

763. [CrossRef]
75. Zhang, C.; Yang, C.; Feldman, M.J.; Wang, H.; Pang, Y.; Maggio, D.M.; Zhu, D.; Nesvick, C.L.; Dmitriev, P.; Bullova, P.; et al. Vorinostat suppresses hypoxia signaling by modulating nuclear translocation of hypoxia inducible factor 1 alpha. *Oncotarget* **2017**, *8*, 56110–56125. [CrossRef]
76. Lohitesh, K.; Saini, H.; Srivastava, A.; Mukherjee, S.; Roy, A.; Chowdhury, R. Autophagy inhibition potentiates SAHA-mediated apoptosis in glioblastoma cells by accumulation of damaged mitochondria. *Oncol. Rep.* **2018**, *39*, 2787–2796. [CrossRef]
77. Gonçalves, R.M.; Agnes, J.P.; Delgobo, M.; de Souza, P.O.; Thomé, M.P.; Heimfarth, L.; Lenz, G.; Moreira, J.C.F.; Zanotto-Filho, A. Late autophagy inhibitor chloroquine improves efficacy of the histone deacetylase inhibitor SAHA and temozolomide in gliomas. *Biochem. Pharmacol.* **2019**, *163*, 440–450. [CrossRef]
78. Khathayer, F.; Taylor, M.A.; Ray, S.K. Synergism of 4HPR and SAHA increases anti-tumor actions in glioblastoma cells. *Apoptosis* **2020**, *25*, 217–232. [CrossRef]
79. Qiu, Y.; Li, Z.; Copland, J.A.; Mehrling, T.; Tun, H.W. Combined alkylation and histone deacetylase inhibition with EDO-S101 has significant therapeutic activity against brain tumors in preclinical models. *Oncotarget* **2018**, *9*, 28155–28164. [CrossRef]
80. Kusaczuk, M.; Kre˛towski, R.; Stypułkowska, A.; Cechowska-Pasko, M. Molecular and cellular effects of a novel hydroxamate- based HDAC inhibitor - belinostat - in glioblastoma cell lines: A preliminary report. *Investig. New Drugs* **2016**, *34*, 552–564. [CrossRef]
81. Berghauser Pont, L.M.; Kleijn, A.; Kloezeman, J.J.; van den Bossche, W.; Kaufmann, J.K.; de Vrij, J.; Leenstra, S.; Dirven, C.M.; Lamfers, M.L. The HDAC Inhibitors Scriptaid and LBH589 Combined with the Oncolytic Virus Delta24-RGD Exert Enhanced Anti-Tumor Efficacy in Patient-Derived Glioblastoma Cells. *PLoS ONE* **2015**, *10*, e0127058. [CrossRef]
82. Meng, W.; Wang, B.; Mao, W.; Wang, J.; Zhao, Y.; Li, Q.; Zhang, C.; Tang, Y.; Ma, J. Enhanced efficacy of histone deacetylase inhibitor combined with bromodomain inhibitor in glioblastoma. *J. Exp. Clin. Cancer Res.* **2018**, *37*, 241. [CrossRef] [PubMed]
83. Nguyen, T.T.T.; Zhang, Y.; Shang, E.; Shu, C.; Torrini, C.; Zhao, J.; Bianchetti, E.; Mela, A.; Humala, N.; Mahajan, A.; et al. HDAC inhibitors elicit metabolic reprogramming by targeting super-enhancers in glioblastoma models. *J. Clin. Investig.* **2020**, *130*, 3699–3716. [CrossRef] [PubMed]
84. De La Rosa, J.; Urdiciain, A.; Zazpe, I.; Zelaya, M.V.; Meléndez, B.; Rey, J.A.; Idoate, M.A.; Castresana, J.S. The synergistic effect of DZ-NEP, panobinostat and temozolomide reduces clonogenicity and induces apoptosis in glioblastoma cells. *Int. J. Oncol.* **2020**, *56*, 283–300. [CrossRef] [PubMed]
85. De La Rosa, J.; Urdiciain, A.; Zelaya, M.V.; Zazpe, I.; Meléndez, B.; Rey, J.A.; Idoate, M.A.; Castresana, J.S. APR-246 combined with 3-deazaneplanocin A, panobinostat or temozolomide reduces clonogenicity and induces apoptosis in glioblastoma cells. *Int. J. Oncol.* **2021**, *58*, 312–330. [CrossRef]
86. Pratap, U.P.; Sareddy, G.R.; Liu, Z.; Venkata, P.P.; Liu, J.; Tang, W.; Altwegg, K.A.; Ebrahimi, B.; Li, X.; Tekmal, R.R.; et al. Histone deacetylase inhibitors enhance estrogen receptor beta expression and augment agonist-mediated tumor suppression in glioblastoma. *Neurooncol. Adv.* **2021**, *3*, vdab099. [CrossRef]
87. Knüpfer, M.M.; Hernáiz-Driever, P.; Poppenborg, H.; Wolff, J.E.; Cinatl, J. Valproic acid inhibits proliferation and changes expression of CD44 and CD56 of malignant glioma cells in vitro. *Anticancer Res.* **1998**, *18*, 3585–3589.
88. Chavez-Blanco, A.; Perez-Plasencia, C.; Perez-Cardenas, E.; Carrasco-Legleu, C.;

Rangel-Lopez, E.; Segura-Pacheco, B.; Taja- Chayeb, L.; Trejo-Becerril, C.; Gonzalez-Fierro, A.; Candelaria, M.; et al. Antineoplastic effects of the DNA methylation inhibitor hydralazine and the histone deacetylase inhibitor valproic acid in cancer cell lines. *Cancer Cell Int.* **2006**, *6*, 2. [CrossRef]Das, C.M.; Aguilera, D.; Vasquez, H.; Prasad, P.; Zhang, M.; Wolff, J.E.; Gopalakrishnan, V. Valproic acid induces p21 and topoisomerase-II (alpha/beta) expression and synergistically enhances etoposide cytotoxicity in human glioblastoma cell lines. *J. Neurooncol.* **2007**, *85*, 159–170. [CrossRef]
89. Papi, A.; Ferreri, A.M.; Rocchi, P.; Guerra, F.; Orlandi, M. Epigenetic modifiers as anticancer drugs: Effectiveness of valproic acid in neural crest-derived tumor cells. *Anticancer Res.* **2010**, *30*, 535–540.
90. Alvarez, A.A.; Field, M.; Bushnev, S.; Longo, M.S.; Sugaya, K. The effects of histone deacetylase inhibitors on glioblastoma-derived stem cells. *J. Mol. Neurosci.* **2015**, *55*, 7–20. [CrossRef]
91. Zhang, C.; Liu, S.; Yuan, X.; Hu, Z.; Li, H.; Wu, M.; Yuan, J.; Zhao, Z.; Su, J.; Wang, X.; et al. Valproic Acid Promotes Human Glioma U87 Cells Apoptosis and Inhibits Glycogen Synthase Kinase-3β Through ERK/Akt Signaling. *Cell Physiol. Biochem.* **2016**, *39*, 2173–2185. [CrossRef]
92. Chang, Y.L.; Huang, L.C.; Chen, Y.C.; Wang, Y.W.; Hueng, D.Y.; Huang, S.M. The synergistic effects of valproic acid and fluvastatin on apoptosis induction in glioblastoma multiforme cell lines. *Int. J. Biochem. Cell Biol.* **2017**, *92*, 155–163. [CrossRef]
93. Tseng, J.H.; Chen, C.Y.; Chen, P.C.; Hsiao, S.H.; Fan, C.C.; Liang, Y.C.; Chen, C.P. Valproic acid inhibits glioblastoma multiforme cell growth via paraoxonase 2 expression. *Oncotarget* **2017**, *8*, 14666–14679. [CrossRef]
94. Garcia, C.G.; Kahn, S.A.; Geraldo, L.H.M.; Romano, I.; Domith, I.; Silva, D.; Dos Santos Assunção, F.; Ferreira, M.J.; Portugal, C.C.; de Souza, J.M.; et al. Combination Therapy with Sulfasalazine and Valproic Acid Promotes Human Glioblastoma Cell Death Through Imbalance of the Intracellular Oxidative Response. *Mol. Neurobiol.* **2018**, *55*, 6816–6833. [CrossRef]
95. Riva, G.; Cilibrasi, C.; Bazzoni, R.; Cadamuro, M.; Negroni, C.; Butta, V.; Strazzabosco, M.; Dalprà, L.; Lavitrano, M.; Bentivegna,
A. Valproic Acid Inhibits Proliferation and Reduces Invasiveness in Glioma Stem Cells Through Wnt/β Catenin Signalling Activation. *Genes* **2018**, *9*, 522. [CrossRef]
96. Berendsen, S.; Frijlink, E.; Kroonen, J.; Spliet, W.G.M.; van Hecke, W.; Seute, T.; Snijders, T.J.; Robe, P.A. Effects of valproic acid on histone deacetylase inhibition *in vitro* and in glioblastoma patient samples. *Neurooncol. Adv.* **2019**, *1*, vdz025. [CrossRef]
97. Sanaei, M.; Kavoosi, F. The effect of valproic acid on intrinsic, extrinsic, and JAK/STAT pathways in neuroblastoma and glioblastoma cell lines. *Res. Pharm. Sci.* **2022**, *17*, 392–409. [CrossRef]
98. Tarasenko, N.; Chekroun-Setti, H.; Nudelman, A.; Rephaeli, A. Comparison of the anticancer properties of a novel valproic acid prodrug to leading histone deacetylase inhibitors. *J. Cell Biochem.* **2018**, *119*, 3417–3428. [CrossRef]
99. Wetzel, M.; Premkumar, D.R.; Arnold, B.; Pollack, I.F. Effect of trichostatin A, a histone deacetylase inhibitor, on glioma proliferation *in vitro* by inducing cell cycle arrest and apoptosis. *J. Neurosurg.* **2005**, *103*, 549–556. [CrossRef]
100. Svechnikova, I.; Almqvist, P.M.; Ekström, T.J. HDAC inhibitors effectively induce cell type-specific differentiation in human glioblastoma cell lines of different origin. *Int. J. Oncol.* **2008**, *32*, 821–827.
101. Gao, J.; Chen, T.; Liu, J.; Liu, W.; Hu, G.; Guo, X.; Yin, B.; Gong, Y.; Zhao, J.; Qiang, B.; et al. Loss of NECL1, a novel tumor suppressor, can be restored in glioma by HDAC inhibitor-Trichostatin A through Sp1 binding site. *Glia* **2009**, *57*, 989–999. [CrossRef] [PubMed]

102. Foltz, G.; Yoon, J.G.; Lee, H.; Ma, L.; Tian, Q.; Hood, L.; Madan, A. Epigenetic regulation of wnt pathway antagonists in human glioblastoma multiforme. *Genes Cancer* **2010**, *1*, 81–90. [CrossRef] [PubMed]
103. Höring, E.; Podlech, O.; Silkenstedt, B.; Rota, I.A.; Adamopoulou, E.; Naumann, U. The histone deacetylase inhibitor trichostatin a promotes apoptosis and antitumor immunity in glioblastoma cells. *Anticancer Res.* **2013**, *33*, 1351–1360. [PubMed]
104. Sassi Fde, A.; Caesar, L.; Jaeger, M.; Nör, C.; Abujamra, A.L.; Schwartsmann, G.; de Farias, C.B.; Brunetto, A.L.; Lopez, P.L.; Roesler, R. Inhibitory activities of trichostatin a in U87 glioblastoma cells and tumorsphere-derived cells. *J. Mol. Neurosci.* **2014**, *54*, 27–40. [CrossRef]
105. Sun, P.; Xia, S.; Lal, B.; Eberhart, C.G.; Quinones-Hinojosa, A.; Maciaczyk, J.; Matsui, W.; Dimeco, F.; Piccirillo, S.M.; Vescovi, A.L.; et al. DNER, an epigenetically modulated gene, regulates glioblastoma-derived neurosphere cell differentiation and tumor propagation. *Stem Cells* **2009**, *27*, 1473–1486. [CrossRef]
106. Carol, H.; Gorlick, R.; Kolb, E.A.; Morton, C.L.; Manesh, D.M.; Keir, S.T.; Reynolds, C.P.; Kang, M.H.; Maris, J.M.; Wozniak, A.; et al. Initial testing (stage 1) of the histone deacetylase inhibitor, quisinostat (JNJ-26481585), by the Pediatric Preclinical Testing Program. *Pediatr. Blood Cancer* **2014**, *61*, 245–252. [CrossRef]
107. Bouché, M.; Dong, Y.C.; Sheikh, S.; Taing, K.; Saxena, D.; Hsu, J.C.; Chen, M.H.; Salinas, R.D.; Song, H.; Burdick, J.A.; et al. Novel Treatment for Glioblastoma Delivered by a Radiation Responsive and Radiopaque Hydrogel. *ACS Biomater. Sci. Eng.* **2021**, *7*, 3209–3220. [CrossRef]
108. Zhang, W.; Lv, S.; Liu, J.; Zang, Z.; Yin, J.; An, N.; Yang, H.; Song, Y. PCI-24781 down-regulates EZH2 expression and then promotes glioma apoptosis by suppressing the PIK3K/Akt/mTOR pathway. *Genet. Mol. Biol.* **2014**, *37*, 716–724. [CrossRef]
109. Asklund, T.; Appelskog, I.B.; Ammerpohl, O.; Ekström, T.J.; Almqvist, P.M. Histone deacetylase inhibitor 4-phenylbutyrate modulates glial fibrillary acidic protein and connexin 43 expression, and enhances gap-junction communication, in human glioblastoma cells. *Eur. J. Cancer* **2004**, *40*, 1073–1081. [CrossRef]
110. Kusaczuk, M.; Kre˛towski, R.; Bartoszewicz, M.; Cechowska-Pasko, M. Phenylbutyrate-a pan-HDAC inhibitor-suppresses proliferation of glioblastoma LN-229 cell line. *Tumour. Biol.* **2016**, *37*, 931–942. [CrossRef]
111. Engelhard, H.H.; Duncan, H.A.; Kim, S.; Criswell, P.S.; Van Eldik, L. Therapeutic effects of sodium butyrate on glioma cells *in vitro* and in the rat C6 glioma model. *Neurosurgery* **2001**, *48*, 616–624. [CrossRef]
112. Nakagawa, H.; Sasagawa, S.; Itoh, K. Sodium butyrate induces senescence and inhibits the invasiveness of glioblastoma cells. *Oncol. Lett.* **2018**, *15*, 1495–1502. [CrossRef]
113. Taylor, M.A.; Khathayer, F.; Ray, S.K. Quercetin and Sodium Butyrate Synergistically Increase Apoptosis in Rat C6 and Human T98G Glioblastoma Cells Through Inhibition of Autophagy. *Neurochem. Res.* **2019**, *44*, 1715–1725. [CrossRef]
114. Majchrzak-Celińska, A.; Kleszcz, R.; Stasiłowicz-Krzemień, A.; Cielecka-Piontek, J. Sodium Butyrate Enhances Curcuminoids Permeability through the Blood-Brain Barrier, Restores Wnt/β-Catenin Pathway Antagonists Gene Expression and Reduces the Viability of Glioblastoma Cells. *Int. J. Mol. Sci.* **2021**, *22*, 11285. [CrossRef]
115. Paja˛k, B.; Siwiak-Niedbalska, E.; Jas´kiewicz, A.; Sołtyka, M.; Zieliński, R.; Domoradzki, T.; Fokt, I.; Skóra, S.; Priebe, W. Synergistic Anticancer Effect of Glycolysis and Histone Deacetylases Inhibitors in a Glioblastoma Model. *Biomedicines* **2021**, *9*, 1749. [CrossRef]
116. Zhang, G.; Gan, Y.H. Synergistic antitumor effects of the combined treatment with

an HDAC6 inhibitor and a COX-2 inhibitor through activation of PTEN. *Oncol. Rep.* **2017**, *38*, 2657–2666. [CrossRef]
117. Urdiciain, A.; Erausquin, E.; Meléndez, B.; Rey, J.A.; Idoate, M.A.; Castresana, J.S. Tubastatin A, an inhibitor of HDAC6, enhances temozolomide-induced apoptosis and reverses the malignant phenotype of glioblastoma cells. *Int. J. Oncol.* **2019**, *54*, 1797–1808. [CrossRef] [PubMed]
118. Auzmendi-Iriarte, J.; Saenz-Antoñanzas, A.; Mikelez-Alonso, I.; Carrasco-Garcia, E.; Tellaetxe-Abete, M.; Lawrie, C.H.; Sampron, N.; Cortajarena, A.L.; Matheu, A. Characterization of a new small-molecule inhibitor of HDAC6 in glioblastoma. *Cell Death Dis.* **2020**, *11*, 417. [CrossRef]
119. Yin, C.; Li, P. Growth Suppression of Glioma Cells Using HDAC6 Inhibitor, Tubacin. *Open Med.* **2018**, *13*, 221–226. [CrossRef]
120. Liffers, K.; Kolbe, K.; Westphal, M.; Lamszus, K.; Schulte, A. Histone Deacetylase Inhibitors Resensitize EGFR/EGFRvIII- Overexpressing, Erlotinib-Resistant Glioblastoma Cells to Tyrosine Kinase Inhibition. *Target Oncol.* **2016**, *11*, 29–40. [CrossRef]
121. Was, H.; Krol, S.K.; Rotili, D.; Mai, A.; Wojtas, B.; Kaminska, B.; Maleszewska, M. Histone deacetylase inhibitors exert anti-tumor effects on human adherent and stem-like glioma cells. *Clin. Epigenetics* **2019**, *11*, 11. [CrossRef] [PubMed]
122. Sharma, V.; Koul, N.; Joseph, C.; Dixit, D.; Ghosh, S.; Sen, E. HDAC inhibitor, scriptaid, induces glioma cell apoptosis through JNK activation and inhibits telomerase activity. *J. Cell. Mol. Med.* **2010**, *14*, 2151–2161. [CrossRef] [PubMed]
123. Balasubramanian, S.; Ramos, J.; Luo, W.; Sirisawad, M.; Verner, E.; Buggy, J.J. A novel histone deacetylase 8 (HDAC8)-specific inhibitor PCI-34051 induces apoptosis in T-cell lymphomas. *Leukemia* **2008**, *22*, 1026–1034. [CrossRef]
124. Angeletti, F.; Fossati, G.; Pattarozzi, A.; Würth, R.; Solari, A.; Daga, A.; Masiello, I.; Barbieri, F.; Florio, T.; Comincini, S. Inhibition of the Autophagy Pathway Synergistically Potentiates the Cytotoxic Activity of Givinostat (ITF2357) on Human Glioblastoma Cancer Stem Cells. *Front. Mol. Neurosci.* **2016**, *9*, 107. [CrossRef]
125. Taiarol, L.; Bigogno, C.; Sesana, S.; Kravicz, M.; Viale, F.; Pozzi, E.; Monza, L.; Carozzi, V.A.; Meregalli, C.; Valtorta, S.; et al. Givinostat-Liposomes: Anti-Tumor Effect on 2D and 3D Glioblastoma Models and Pharmacokinetics. *Cancers* **2022**, *14*, 2978. [CrossRef]
126. Marampon, F.; Leoni, F.; Mancini, A.; Pietrantoni, I.; Codenotti, S.; Ferella, L.; Megiorni, F.; Porro, G.; Galbiati, E.; Pozzi, P.; et al. Correction to: Histone deacetylase inhibitor ITF2357 (givinostat) reverts transformed phenotype and counteracts stemness in *in vitro* and in vivo models of human glioblastoma. *J. Cancer Res. Clin. Oncol.* **2019**, *145*, 2411. [CrossRef]
127. Pont, L.M.; Naipal, K.; Kloezeman, J.J.; Venkatesan, S.; van den Bent, M.; van Gent, D.C.; Dirven, C.M.; Kanaar, R.; Lamfers, M.L.; Leenstra, S. DNA damage response and anti-apoptotic proteins predict radiosensitization efficacy of HDAC inhibitors SAHA and LBH589 in patient-derived glioblastoma cells. *Cancer Lett.* **2015**, *356*, 525–535. [CrossRef]
128. Eyupoglu, I.Y.; Hahnen, E.; Trankle, C.; Savaskan, N.E.; Siebzehnrubl, F.A.; Buslei, R.; Lemke, D.; Wick, W.; Fahlbusch, R.; Blumcke, I. Experimental therapy of malignant gliomas using the inhibitor of histone deacetylase MS-275. *Mol. Cancer Ther.* **2006**, *5*, 1248–1255. [CrossRef]
129. Buyandelger, B.; Bar, E.E.; Hung, K.S.; Chen, R.M.; Chiang, Y.H.; Liou, J.P.; Huang, H.M.; Wang, J.Y. Histone deacetylase inhibitor MPT0B291 suppresses Glioma Growth *in vitro* and in vivo partially through acetylation of p53. *Int. J. Biol. Sci.* **2020**, *16*, 3184–3199. [CrossRef]
130. Choi, S.A.; Kwak, P.A.; Park, C.K.; Wang, K.C.; Phi, J.H.; Lee, J.Y.; Lee, C.S.; Lee, J.H.; Kim, S.K. A novel histone deacetylase inhibitor, CKD5, has potent anti-cancer effects in glioblastoma. *Oncotarget* **2017**, *8*, 9123–9133. [CrossRef]

131. Bacon, C.L.; O'Driscoll, E.; Regan, C.M. Valproic acid suppresses G1 phase-dependent sialylation of a 65 kDa glycoprotein in the C6glioma cell cycle. *Int. J. Dev. Neurosci.* **1998**, *15*, 777–784. [CrossRef] [PubMed]
132. Xu, J.; Sampath, D.; Lang, F.F.; Prabhu, S.; Rao, G.; Fuller, G.N.; Liu, Y.; Puduvalli, V.K. Vorinostat modulates cell cycle regulatory proteins in glioma cells and human glioma slice cultures. *J. Neurooncol.* **2011**, *105*, 241–251. [CrossRef] [PubMed]
133. Sawa, H.; Murakami, H.; Kumagai, M.; Nakasato, M.; Yamauchi, S.; Matsuyama, N.; Tamura, Y.; Satone, A.; Ide, W.; Hashimoto, I.; et al. Histone deacetylase inhibitor, FK228, induces apoptosis and suppresses cell proliferation of human glioblastoma cells *in vitro* and in vivo. *Acta Neuropathol.* **2004**, *107*, 523–531. [CrossRef] [PubMed]
134. Franco-Molina, M.A.; Santana-Krímskaya, S.E.; Madrigal-de-León, L.M.; Coronado-Cerda, E.E.; Zárate-Triviño, D.G.; Hernández- Martínez, S.P.; García-Coronado, P.L.; Rodríguez-Padilla, C. Evaluation of the cytotoxic and immunogenic potential of temozo- lamide, panobinostat, and Lophophora williamsii extract against C6 glioma cells. *Excli. J.* **2021**, *20*, 614–624. [CrossRef]
135. Hsu, Y.F.; Sheu, J.R.; Hsiao, G.; Lin, C.H.; Chang, T.H.; Chiu, P.T.; Wang, C.Y.; Hsu, M.J. p53 in trichostatin A induced C6 glioma cell death. *Biochim. Biophys. Acta* **2011**, *1810*, 504–513. [CrossRef]
136. Staberg, M.; Michaelsen, S.R.; Rasmussen, R.D.; Villingshoj, M.; Poulsen, H.S.; Hamerlik, P. Inhibition of histone deacetylases sensitizes glioblastoma cells to lomustine. *Cell. Oncol.* **2017**, *40*, 21–32. [CrossRef]
137. Egler, V.; Korur, S.; Failly, M.; Boulay, J.L.; Imber, R.; Lino, M.M.; Merlo, A. Histone deacetylase inhibition and blockade of the glycolytic pathway synergistically induce glioblastoma cell death. *Clin. Cancer Res.* **2008**, *14*, 3132–3140. [CrossRef]
138. Yu, C.; Friday, B.B.; Yang, L.; Atadja, P.; Wigle, D.; Sarkaria, J.; Adjei, A.A. Mitochondrial Bax translocation partially mediates synergistic cytotoxicity between histone deacetylase inhibitors and proteasome inhibitors in glioma cells. *Neuro-Oncology* **2008**, *10*, 309–319. [CrossRef]
139. Bangert, A.; Hacker, S.; Cristofanon, S.; Debatin, K.M.; Fulda, S. Chemosensitization of glioblastoma cells by the histone deacetylase inhibitor MS275. *Anticancer Drugs* **2011**, *22*, 494–499. [CrossRef]
140. Vengoji, R.; Atri, P.; Macha, M.A.; Seshacharyulu, P.; Perumal, N.; Mallya, K.; Liu, Y.; Smith, L.M.; Rachagani, S.; Mahapatra, S.; et al. Differential gene expression-based connectivity mapping identified novel drug candidate and improved Temozolomide efficacy for Glioblastoma. *J. Exp. Clin. Cancer Res.* **2021**, *40*, 335. [CrossRef]
141. Li, Z.Y.; Li, Q.Z.; Chen, L.; Chen, B.D.; Wang, B.; Zhang, X.J.; Li, W.P. Histone Deacetylase Inhibitor RGFP109 Overcomes Temozolomide Resistance by Blocking NF-κB-Dependent Transcription in Glioblastoma Cell Lines. *Neurochem. Res.* **2016**, *41*, 3192–3205. [CrossRef]
142. Zhang, I.; Beus, M.; Stochaj, U.; Le, P.U.; Zorc, B.; Rajic, Z.; Petrecca, K.; Maysinger, D. Inhibition of glioblastoma cell proliferation, invasion, and mechanism of action of a novel hydroxamic acid hybrid molecule. *Cell Death Discov.* **2018**, *4*, 41. [CrossRef]
143. Kitange, G.J.; Mladek, A.C.; Carlson, B.L.; Schroeder, M.A.; Pokorny, J.L.; Cen, L.; Decker, P.A.; Wu, W.; Lomberk, G.A.; Gupta, S.K.; et al. Inhibition of histone deacetylation potentiates the evolution of acquired temozolomide resistance linked to MGMT upregulation in glioblastoma xenografts. *Clin. Cancer Res.* **2012**, *18*, 4070–4079. [CrossRef]
144. Pastorino, O.; Gentile, M.T.; Mancini, A.; Del Gaudio, N.; Di Costanzo, A.; Bajetto, A.; Franco, P.; Altucci, L.; Florio, T.; Stoppelli, M.P.; et al. Histone Deacetylase Inhibitors Impair Vasculogenic Mimicry from Glioblastoma Cells. *Cancers* **2019**, *11*, 747. [CrossRef]

145. Yao, Z.G.; Li, W.H.; Hua, F.; Cheng, H.X.; Zhao, M.Q.; Sun, X.C.; Qin, Y.J.; Li, J.M. LBH589 Inhibits Glioblastoma Growth and Angiogenesis Through Suppression of HIF-1α Expression. *J. Neuropathol. Exp. Neurol.* **2017**, *76*, 1000–1007. [CrossRef]
146. An, Z.; Gluck, C.B.; Choy, M.L.; Kaufman, L.J. Suberoylanilide hydroxamic acid limits migration and invasion of glioma cells in two and three dimensional culture. *Cancer Lett.* **2010**, *292*, 215–227. [CrossRef]
147. Perez, T.; Bergès, R.; Maccario, H.; Oddoux, S.; Honoré, S. Low concentrations of vorinostat decrease EB1 expression in GBM cells and affect microtubule dynamics, cell survival and migration. *Oncotarget* **2021**, *12*, 304–315. [CrossRef]
148. Rampazzo, E.; Manfreda, L.; Bresolin, S.; Cani, A.; Mariotto, E.; Bortolozzi, R.; Della Puppa, A.; Viola, G.; Persano, L. Histone Deacetylase Inhibitors Impair Glioblastoma Cell Motility and Proliferation. *Cancers* **2022**, *14*, 1897. [CrossRef]
149. Eyupoglu, I.Y.; Hahnen, E.; Buslei, R.; Siebzehnrubl, F.A.; Savaskan, N.E.; Luders, M.; Trankle, C.; Wick, W.; Weller, M.; Fahlbusch, R.; et al. Suberoylanilide hydroxamic acid (SAHA) has potent anti-glioma properties *in vitro*, ex vivo and in vivo. *J. Neurochem.* **2005**, *93*, 992–999. [CrossRef]
150. Yin, D.; Ong, J.M.; Hu, J.; Desmond, J.C.; Kawamata, N.; Konda, B.M.; Black, K.L.; Koeffler, H.P. Suberoylanilide hydroxamic acid, a histone deacetylase inhibitor: Effects on gene expression and growth of glioma cells *in vitro* and in vivo. *Clin. Cancer Res.* **2007**, *13*, 1045–1052. [CrossRef]
151. Alexanian, A.R.; Brannon, A. Unique combinations of epigenetic modifiers synergistically impair the viability of the U87 glioblastoma cell line while exhibiting minor or moderate effects on normal stem cell growth. *Med. Oncol.* **2022**, *39*, 86. [CrossRef] [PubMed]
152. Nguyen, T.T.T.; Shang, E.; Schiffgens, S.; Torrini, C.; Shu, C.; Akman, H.O.; Prabhu, V.V.; Allen, J.E.; Westhoff, M.A.; Karpel-Massler, G.; et al. Induction of Synthetic Lethality by Activation of Mitochondrial ClpP and Inhibition of HDAC1/2 in Glioblastoma. *Clin. Cancer Res.* **2022**, *28*, 1881–1895. [CrossRef] [PubMed]
153. Premkumar, D.R.; Jane, E.P.; Agostino, N.R.; DiDomenico, J.D.; Pollack, I.F. Bortezomib-induced sensitization of malignant human glioma cells to vorinostat-induced apoptosis depends on reactive oxygen species production, mitochondrial dysfunction, Noxa upregulation, Mcl-1 cleavage, and DNA damage. *Mol. Carcinog.* **2013**, *52*, 118–133. [CrossRef] [PubMed]
154. Meng, W.; Wang, B.; Mao, W.; Wang, J.; Zhao, Y.; Li, Q.; Zhang, C.; Ma, J. Enhanced efficacy of histone deacetylase inhibitor panobinostat combined with dual PI3K/mTOR inhibitor BEZ235 against glioblastoma. *Nagoya J. Med. Sci.* **2019**, *81*, 93–102. [CrossRef]
155. Essien, E.I.; Hofer, T.P.; Atkinson, M.J.; Anastasov, N. Combining HDAC and MEK Inhibitors with Radiation against Glioblastoma- Derived Spheres. *Cells* **2022**, *11*, 775. [CrossRef]
156. Marino, A.M.; Sofiadis, A.; Baryawno, N.; Johnsen, J.I.; Larsson, C.; Vukojevic, V.; Ekstrom, T.J. Enhanced effects by 4- phenylbutyrate in combination with RTK inhibitors on proliferation in brain tumor cell models. *Biochem. Biophys. Res. Commun.* **2011**, *411*, 208–212. [CrossRef]
157. Zhang, Y.; Ishida, C.T.; Ishida, W.; Lo, S.L.; Zhao, J.; Shu, C.; Bianchetti, E.; Kleiner, G.; Sanchez-Quintero, M.J.; Quinzii, C.M.; et al. Combined HDAC and Bromodomain Protein Inhibition Reprograms Tumor Cell Metabolism and Elicits Synthetic Lethality in Glioblastoma. *Clin. Cancer Res.* **2018**, *24*, 3941–3954. [CrossRef]
158. Kim, G.H.; Choi, S.Y.; Oh, T.I.; Kan, S.Y.; Kang, H.; Lee, S.; Oh, T.; Ko, H.M.; Lim, J.H. IDH1(R132H) Causes Resistance to HDAC Inhibitors by Increasing NANOG in Glioblastoma Cells. *Int. J. Mol. Sci.* **2019**, *20*, 2679. [CrossRef]
159. Wang, C.; Schroeder, F.A.; Hooker, J.M. Visualizing epigenetics: Current advances and advantages in HDAC PET imaging techniques. *Neuroscience* **2014**, *264*, 186–

197. [CrossRef]
160. Kim, S.W.; Hooker, J.M.; Otto, N.; Win, K.; Muench, L.; Shea, C.; Carter, P.; King, P.; Reid, A.E.; Volkow, N.D.; et al. Whole-body pharmacokinetics of HDAC inhibitor drugs, butyric acid, valproic acid and 4-phenylbutyric acid measured with carbon-11 labeled analogs by PET. *J. Nucl. Med.* **2013**, *40*, 912–918. [CrossRef]
161. Hendricks, J.A.; Keliher, E.J.; Marinelli, B.; Reiner, T.; Weissleder, R.; Mazitschek, R. In vivo PET imaging of histone deacetylases by 18F-suberoylanilide hydroxamic acid (18F-SAHA). *J. Med. Chem.* **2011**, *54*, 5576–5582. [CrossRef]
162. Laws, M.T.; Bonomi, R.E.; Kamal, S.; Gelovani, D.J.; Llaniguez, J.; Potukutchi, S.; Lu, X.; Mangner, T.; Gelovani, J.G. Molec- ular imaging HDACs class IIa expression-activity and pharmacologic inhibition in intracerebral glioma models in rats using PET/CT/(MRI) with [(18)F]TFAHA. *Sci. Rep.* **2019**, *9*, 3595. [CrossRef]
163. Tago, T.; Toyohara, J. Advances in the Development of PET Ligands Targeting Histone Deacetylases for the Assessment of Neurodegenerative Diseases. *Molecules* **2018**, *23*, 300. [CrossRef]
164. El Bahhaj, F.; Denis, I.; Pichavant, L.; Delatouche, R.; Collette, F.; Linot, C.; Pouliquen, D.; Grégoire, M.; Héroguez, V.; Blanquart, C.; et al. Histone Deacetylase Inhibitors Delivery using Nanoparticles with Intrinsic Passive Tumor Targeting Properties for Tumor Therapy. *Theranostics* **2016**, *6*, 795–807. [CrossRef]
165. Bolcaen, J.; Kleynhans, J.; Nair, S.; Verhoeven, J.; Goethals, I.; Sathekge, M.; Vandevoorde, C.; Ebenhan, T. A perspective on the radiopharmaceutical requirements for imaging and therapy of glioblastoma. *Theranostics* **2021**, *11*, 7911–7947. [CrossRef]
166. Seo, Y.J.; Muench, L.; Reid, A.; Chen, J.; Kang, Y.; Hooker, J.M.; Volkow, N.D.; Fowler, J.S.; Kim, S.W. Radionuclide labeling and evaluation of candidate radioligands for PET imaging of histone deacetylase in the brain. *Bioorg. Med. Chem. Lett.* **2013**, *23*, 6700–6705. [CrossRef]
167. Mukhopadhyay, U.; Tong, W.P.; Gelovani, J.G.; Alauddin, M.M. Radiosynthesis of 6-([18F]fluoroacetamido)-1-hexanoicanilide ([18F]FAHA) for PET imaging of histone deacetylase (HDAC). *J. Label Compd. Radiopharm.* **2006**, *49*, 997–1006. [CrossRef]
168. Nishii, R.; Mukhopadhyay, U.; Yeh, H.; Soghomonyan, S.; Volgin, A.; Alauddin, M.; Tong, W.; Gelovani, J. PET imaging of histone deacetylase activity in a rat brain using 6-([18F]-fluoroacetamide)-1-hexanoicanilide ([18F]-FAHA). *J. Nucl. Med.* **2007**, *48*, 336P.
169. Tang, W.; Kuruvilla, S.A.; Galitovskiy, V.; Pan, M.L.; Grando, S.A.; Mukherjee, J. Targeting histone deacetylase in lung cancer for early diagnosis: (18)F-FAHA PET/CT imaging of NNK-treated A/J mice model. *Am. J. Nucl. Med. Mol. Imaging* **2014**, *4*, 324–332.
170. Reid, A.E.; Hooker, J.; Shumay, E.; Logan, J.; Shea, C.; Kim, S.W.; Collins, S.; Xu, Y.; Volkow, N.; Fowler, J.S. Evaluation of 6-([(18)F]fluoroacetamido)-1-hexanoicanilide for PET imaging of histone deacetylase in the baboon brain. *J. Nucl. Med.* **2009**, *36*, 247–258. [CrossRef]
171. Bonomi, R.; Mukhopadhyay, U.; Shavrin, A.; Yeh, H.H.; Majhi, A.; Dewage, S.W.; Najjar, A.; Lu, X.; Cisneros, G.A.; Tong, W.P.; et al. Novel Histone Deacetylase Class IIa Selective Substrate Radiotracers for PET Imaging of Epigenetic Regulation in the Brain. *PLoS ONE* **2015**, *10*, e0133512. [CrossRef] [PubMed]
172. Kim, I.S.; Kim, H.S.; Kim, M.; Kwon, J.; Kim, E.M.; Hwang, H.; Oh, P.S.; Lim, S.T.; Sohn, M.H.; Kim, D.H.; et al. Synthesis and Evaluation of 2-[(18)F]Fluoroethyltriazolesuberohydroxamine Acid for Histone Deacetylase in a Tumor Model as a Positron Emission Tomography Radiotracer. *Cancer Biother Radiopharm* **2018**, *33*, 52–59. [CrossRef] [PubMed]
173. Fukumitsu, N.; Yeh, S.H.; Flores Ii, L.G.; Mukhopadhyay, U.; Young, D.; Ogawa, K.;

Jeong, H.J.; Tong, W.; Gelovani, J.G. In Vivo 6-([(18)F]Fluoroacetamido)-1-hexanoicanilide PET Imaging of Altered Histone Deacetylase Activity in Chemotherapy-Induced Neurotoxicity. *Contrast Media Mol. Imaging* **2018**, *2018*, 3612027. [CrossRef] [PubMed]
174. Yeh, H.H.; Tian, M.; Hinz, R.; Young, D.; Shavrin, A.; Mukhapadhyay, U.; Flores, L.G.; Balatoni, J.; Soghomonyan, S.; Jeong, H.J.; et al. Imaging epigenetic regulation by histone deacetylases in the brain using PET/MRI with (1)(8)F-FAHA. *Neuroimage* **2013**, *64*, 630–639. [CrossRef]
175. Zeglis, B.M.; Pillarsetty, N.; Divilov, V.; Blasberg, R.A.; Lewis, J.S. The synthesis and evaluation of N1-(4-(2-[18F]- fluoroethyl)phenyl)-N8-hydroxyoctanediamide ([18F]-FESAHA), a PET radiotracer designed for the delineation of histone deacetylase expression in cancer. *J. Nucl. Med.* **2011**, *38*, 683–696. [CrossRef]
176. Haberkorn, U.; Beijer, B.; Altmann, A.; Gelovani, J.; Strauss, L.; Dimitrakopoulou-Strauss, A.; Eisenhut, M.; Mier, W. Uptake and biodistribution of the histone deacetylase inhibitor SAHA in tumor bearing animals. *J. Nucl. Med.* **2008**, *49*, 332P.
177. Hooker, J.M.; Kim, S.W.; Alexoff, D.; Xu, Y.; Shea, C.; Reid, A.; Volkow, N.; Fowler, J.S. Histone deacetylase inhibitor, MS-275, exhibits poor brain penetration: PK studies of [C]MS-275 using Positron Emission Tomography. *ACS Chem. Neurosci.* **2010**, *1*, 65–73. [CrossRef]
178. Wang, W.J.; Long, L.M.; Yang, N.; Zhang, Q.Q.; Ji, W.J.; Zhao, J.H.; Qin, Z.H.; Wang, Z.; Chen, G.; Liang, Z.Q. NVP-BEZ235, a
novel dual PI3K/mTOR inhibitor, enhances the radiosensitivity of human glioma stem cells *in vitro*. *Acta Pharmacol. Sin.* **2013**, *34*, 681–690. [CrossRef]
179. Kommidi, H.; Tosi, U.; Maachani, U.B.; Guo, H.; Marnell, C.S.; Law, B.; Souweidane, M.M.; Ting, R. (18)F-Radiolabeled Panobinostat Allows for Positron Emission Tomography Guided Delivery of a Histone Deacetylase Inhibitor. *ACS Med. Chem. Lett.* **2018**, *9*, 114–119. [CrossRef]
180. Vermeulen, K.; Ahamed, M.; Luyten, K.; Bormans, G. Evaluation of [(11)C]KB631 as a PET tracer for in vivo visualisation of HDAC6 in B16.F10 melanoma. *J. Nucl. Med.* **2019**, *74-75*, 1–11. [CrossRef]
181. Tosi, U.; Kommidi, H.; Adeuyan, O.; Guo, H.; Maachani, U.B.; Chen, N.; Su, T.; Zhang, G.; Pisapia, D.J.; Dahmane, N.; et al. PET, image-guided HDAC inhibition of pediatric diffuse midline glioma improves survival in murine models. *Sci. Adv.* **2020**, *6*, eabb4105. [CrossRef]
182. Turkman, N.; Liu, D.; Pirola, I. Design, synthesis, biochemical evaluation, radiolabeling and in vivo imaging with high affinity class-IIa histone deacetylase inhibitor for molecular imaging and targeted therapy. *Eur. J. Med. Chem.* **2022**, *228*, 114011. [CrossRef]
183. Meng, Q.; Li, F.; Jiang, S.; Li, Z. Novel (64)Cu-Labeled CUDC-101 for in Vivo PET Imaging of Histone Deacetylases. *ACS Med. Chem. Lett.* **2013**, *4*, 858–862. [CrossRef]
184. Wang, C.; Schroeder, F.A.; Wey, H.Y.; Borra, R.; Wagner, F.F.; Reis, S.; Kim, S.W.; Holson, E.B.; Haggarty, S.J.; Hooker, J.M. In vivo imaging of histone deacetylases (HDACs) in the central nervous system and major peripheral organs. *J. Med. Chem.* **2014**, *57*, 7999–8009. [CrossRef]
185. Wey, H.Y.; Gilbert, T.M.; Zurcher, N.R.; She, A.; Bhanot, A.; Taillon, B.D.; Schroeder, F.A.; Wang, C.; Haggarty, S.J.; Hooker, J.M. Insights into neuroepigenetics through human histone deacetylase PET imaging. *Sci. Transl. Med.* **2016**, *8*, 351ra106. [CrossRef]
186. Donovan, L.L.; Magnussen, J.H.; Dyssegaard, A.; Lehel, S.; Hooker, J.M.; Knudsen, G.M.; Hansen, H.D. Imaging HDACs In Vivo: Cross-Validation of the [(11)C]Martinostat Radioligand in the Pig Brain. *Mol. Imaging Biol.* **2020**, *22*, 569–577. [CrossRef]
187. Strebl, M.G.; Wang, C.; Schroeder, F.A.; Placzek, M.S.; Wey, H.Y.; Van de Bittner, G.C.;

Neelamegam, R.; Hooker, J.M. Development of a Fluorinated Class-I HDAC Radiotracer Reveals Key Chemical Determinants of Brain Penetrance. *ACS Chem. Neurosci.* **2016**, *7*, 528–533. [CrossRef]
188. Fang, X.T.; Zheng, M.Q.; Holden, D.; Fowles, K.; Tamagnan, G.; Hooker, J.; Huang, Y.Y.; Carson, R. Assessment of HDAC6 PET radiotracer F-18-Bavarostat. *J. Nucl. Med.* **2020**, *61*, 1021.
189. Koole, M.; Van Weehaeghe, D.; Serdons, K.; Herbots, M.; Cawthorne, C.; Celen, S.; Schroeder, F.A.; Hooker, J.M.; Bormans, G.; de Hoon, J.; et al. Clinical validation of the novel HDAC6 radiotracer [(18)F]EKZ-001 in the human brain. *Eur. J. Nucl. Med. Mol. Imaging* **2021**, *48*, 596–611. [CrossRef]
190. Chen, Y.A.; Lu, C.H.; Ke, C.C.; Chiu, S.J.; Chang, C.W.; Yang, B.H.; Gelovani, J.G.; Liu, R.S. Evaluation of Class IIa Histone Deacetylases Expression and In Vivo Epigenetic Imaging in a Transgenic Mouse Model of Alzheimer's Disease. *Int. J. Mol. Sci.* **2021**, *22*, 8633. [CrossRef]
191. Schroeder, F.A.; Wang, C.; Van de Bittner, G.C.; Neelamegam, R.; Takakura, W.R.; Karunakaran, A.; Wey, H.Y.; Reis, S.A.; Gale, J.; Zhang, Y.L.; et al. PET imaging demonstrates histone deacetylase target engagement and clarifies brain penetrance of known and novel small molecule inhibitors in rat. *ACS Chem. Neurosci.* **2014**, *5*, 1055–1062. [CrossRef] [PubMed]
192. Wey, H.Y.; Wang, C.; Schroeder, F.A.; Logan, J.; Price, J.C.; Hooker, J.M. Kinetic Analysis and Quantification of [(1)(1)C]Martinostat for in Vivo HDAC Imaging of the Brain. *ACS Chem. Neurosci.* **2015**, *6*, 708–715. [CrossRef] [PubMed]
193. Strebl, M.G.; Campbell, A.J.; Zhao, W.N.; Schroeder, F.A.; Riley, M.M.; Chindavong, P.S.; Morin, T.M.; Haggarty, S.J.; Wagner, F.F.; Ritter, T.; et al. HDAC6 Brain Mapping with [(18)F]Bavarostat Enabled by a Ru-Mediated Deoxyfluorination. *ACS Cent. Sci.* **2017**, *3*, 1006–1014. [CrossRef] [PubMed]

CHAPTER 3: RESULTS

Published Article:

Seane, E.N.; Nair, S.; Vandevoorde, C.; Bisio, A.; Joubert, A. Multi-Target Inhibitor CUDC-101 Impairs DNA Damage Repair and Enhances Radiation Response in Triple-Negative Breast Cell Line. Pharmaceuticals 2024, 17, 1467. https://doi.org/10.3390/ph17111467

The results were presented at:

1. 59th South African Association of Physicists in Medicine and Biology (SAAPMB) Congress
   01-04 May 2023
   Sun City, North-West Province

2. Boron Nuclear capture Therapy (BNCT) webinars, organised by the German Society of Boron Neutron capture Therapy (DGBNCT)
   24 February 2024

3. International Society of Radiographers and Radiological Technologist (ISRRT) World Congress (**Annexure C**)
   06-09 June 2024
   Hong Kong, China

Bridging Text:

The study included the use of two radiation types (protons and X-rays), two HDACi (SAHA and CUDC-101) and five assays, some of which included different timepoints. Due to the large volume of data collected, the results were divided into three manuscripts. The manuscript presented in this Chapter presents the results from the colony survival (objective 1), γ-H2AX foci, apoptosis, as well as cell cycle analysis assays (objectives 2-4) which were conducted using HDACi CUDC-101.

pharmaceuticals

MDPI

Article

Multi-Target Inhibitor CUDC-101 Impairs DNA Damage Repair and Enhances Radiation Response in Triple-Negative Breast Cell Line

Elsie Neo Seane [1,2,3,*], Shankari Nair [3], Charlot Vandevoorde [4], Alessandra Bisio [5] and Anna Joubert [6]

[1] Department of Radiography, School of Health Care Sciences, Faculty of Health Sciences, University of Pretoria, Pretoria 0028, South Africa
[2] Department of Medical Imaging and Therapeutic Sciences, Faculty of Health and Wellness, Cape Peninsula University of Technology, Bellville 7535, South Africa
[3] Separate Sector Cyclotron (SSC) Laboratory, Radiation Biophysics Division, iThemba LABS, Cape Town 7530, South Africa; s.nair@ilabs.nrf.ac.za
[4] Department of Biophysics, GSI Helmholtzzentrum für Schwerionenforschung, 64291 Darmstadt, Germany; c.vandevoorde@gsi.de
[5] Department of Cellular, Computational and Integrative Biology, Via Sommarive, 9, Povo, 38123 Trento, Italy; alessandra.bisio@unitn.it
[6] Department of Physiology, School of Medicine, Faculty of Health Sciences, University of Pretoria, Pretoria 0028, South Africa; annie.joubert@up.ac.za
* Correspondence: seanee@cput.ac.za

Abstract: Background: Since the discovery that Histone deacetylase inhibitors (HDCAi) could enhance radiation response, a number of HDACi, mainly pan-HDAC inhibitors, have been studied either as monotherapy or in combination with X-ray irradiation or chemotherapeutic drugs in the management of breast cancer. However, studies on the combination of HDACi and proton radiation remain limited. CUDC-101 is a multitarget inhibitor of Histone deacetylases (HDACs), epidermal growth factor receptor (EGFR), and human epidermal growth factor receptor 2 (HER-2). In this paper, the effectiveness of CUDC-101 in enhancing radiation response to both proton and X-ray irradiation was studied. Methods: MCF-7, MDA-MB-231, and MCF-10A cell lines were pre-treated with CUDC-101 and exposed to 148 MeV protons, and X-rays were used as reference radiation. Colony survival, γ-H2AX foci, apoptosis, and cell cycle analysis assays were performed. Results: γ-H2AX foci assays showed increased sensitivity to CUDC-101 in the MDA-MB-231 cell line compared to the MCF-7 cell line. In both cell lines, induction of apoptosis was enhanced in CUDC-101 pre-treated cells compared to radiation (protons or X-rays) alone. Increased apoptosis was also noted in CUDC-101 pre-treated cells in the MCF-10A cell line. Cell cycle analysis showed increased G2/M arrest by CUDC-101 mono-treatment as well as combination of CUDC-101 and X-ray irradiation in the MDA-MB-231 cell line. Conclusions: CUDC-101 effectively enhances response to both proton and X-ray irradiation, in the triple-negative MDA-MB-231 cell line. This enhancement was most notable when CUDC-101 was combined with proton irradiation. This study highlights that CUDC-101 holds potential in the management of triple-negative breast cancer as monotherapy or in combination with protons or X-ray irradiation.

Keywords: Histone deacetylase inhibitors; CUDC-101; proton therapy; proton irradiation

Citation: Seane, E.N.; Nair, S.; Vandevoorde, C.; Bisio, A.; Joubert, A. Multi-Target Inhibitor CUDC-101 Impairs DNA Damage Repair and Enhances Radiation Response in Triple-Negative Breast Cell Line. *Pharmaceuticals* **2024**, *17*, 1467. https://doi.org/10.3390/ph17111467

Academic Editor: Yoshikatsu Koga

Received: 4 October 2024
Revised: 23 October 2024
Accepted: 24 October 2024
Published: 1 November 2024

1. Introduction

Megavoltage (MV) X-ray-based radiation therapy is commonly indicated as adjuvant therapy to reduce the risk of loco-regional recurrence of breast cancer and to improve disease-free survival [1]. Recent advances in treatment planning and delivery techniques such as intensity modulated radiotherapy (IMRT) and volumetric modulated arc therapy (VMAT)have improved dose distribution and sparing of healthy tissues; however, associated late side-effects such as secondary malignancies and cardiopulmonary toxicities are still observed in breast cancer survivors [2–5]. While X-ray-based therapy is widely available, the number of proton therapy centres across the globe is on the rise, and this has improved access for breast cancer patients. In general, the number of cancer patients treated with proton therapy is increasing rapidly with an estimated 190,000 in 2018, and an expected increase to over 300,000 in 2030 [6]. Furthermore, the superior dose distribution of protons makes it also a suitable modality for re-irradiation in a number of tumour types [7]. The physical aspects of proton therapy are well understood, but the biological aspects remain under-explored for protons alone as well as in combination therapies with drugs and concomitant therapies [5,8,9]. In recent years, combination therapies of Histone deacetylase inhibitors (HDACi) and photon irradiation have been a focus of many studies [10–16]. However, combination therapies with particle type of radiation and HDACi remain limited.

Histone deacetylase inhibitors (HDACi) are epigenetic drugs that can sensitise cancer cells to ionising radiation with little effect on healthy cells [17,18]. To date, five HDACi SAHA (generic name vorinostat), belinostat, panabinostat, chidamide, and romidepsin have been approved by the Food and Drug Administration (FDA) for cancer therapy [19,20]. More than 20 different HDACi are in different phases of clinical trials as monotherapy or in combination with other DNA damaging agents [21]. HDACi are classified into several classes according to their chemical structure: benzamides (e.g., chidamide, entinostat), hydroxamic acids (e.g., SAHA, belinostat, panabinostat, CUDC-101), cyclic tetrapeptides (e.g., romidepsin), and aliphatic acids (e.g., butyrate, valproic acid) [16,22]. Of these classes, hydroxamic acids is the main class that has been used and is continuously being applied in most studies [23]. This class is also preferred as they inhibit a broad range of HDACs (HDACs1–11), and they have been shown to cause cellular effects at low (nM) concentrations [21].

Evidence from pre-clinical studies has revealed that the combination of photon radiation

and HDACi results in increased cell death in a number of cell lines including lung, melanoma, prostate, glioma, colon, non-small cell lung cancer (NSCLC), osteosarcoma, and breast to name a few [10–16,24–27]. Reports on combination of HDACi with proton irradiation and particle radiation in general remain limited [28–32]. For treatment of breast cancer, several studies have explored the use of pan-HDACi SAHA or Panobinostat in combination with chemotherapeutic drugs, but studies on CUDC-101 are lacking [33–36]. CUDC-101 is a hydroxamic acid that inhibits HDACs, epidermal growth factor receptor (EGFR), and human epidermal growth factor receptor 2 (HER-2) [37]. EGFR and HER-2 have been recognized as biomarkers for resistance in tumours. EGFR is reported to be expressed in all molecular sub-types of breast cancer and over-expressed in triple-negative breast cancers [38,39]. Therefore, the dual targeting of EGFR and HER-2 may be beneficial for EGFR over-expressing triple-negative breast cancer [40], for which CUDC-1010 would be an appealing HDACi candidate. To the best of our knowledge, only one *in vitro* study has been conducted on the effect of CUDC-101 and X-ray irradiation in the triple-negative breast cancer cell line MDA-MB-231 [14]. Considering the growing interest in using proton therapy for breast cancer patients, we aimed to quantify and compare the efficacy of CUDC-101 in combination proton and X-ray radiation, in MCF-7, MCF-10A, and MDA-MB-231 cell lines. The results of this *in vitro* study serve to highlight the potential of CUDC101 in the treatment of breast cancer, to motivate further in vivo preclinical work and to guide future clinical trials.

2. Results

2.1. ***Determination of IC_{50} and Timepoint of Irradiation in Relation to the Drug***

To determine the half maximal inhibitory concentration (IC_{50}) of HDACi, MCF-7, MDA-MB-231, and MCF-10A cells were pre-treated with CUDC-101 at concentrations that ranged from 0.16 µM to 20 µM. Cell proliferation was assesed 72 h post-treatment using 3-(4,5-dimethylthiazol-2-yl)-2,5-diphenyl-2H-tetrazolium bromide (MTT) cell viability assays. The determined half-maximal inhibitory concentration (IC_{50}) values are presented in Table 1.

Table 1. Half maximal inhibitory concentration (IC_{50}) values for the different cell lines.

Cell Line	CUDC-101 (µM)
MCF-7	0.31
MDA-MB-231	0.60
MCF-10A	2.70

To determine the optimal sequence of administration of HDACi and radiation, cells were irradiated with X-rays (2 Gy) at 8 h, 16 h, and 24 h before treatment with CUDC-101 as well as immediately, at 8 h, 16 h, and 24 h post-treatment with CUDC-101. Cell proliferation was determined at 72 h post-irradiation using MTT assays. Pre-treatment with HDACi 24 h before irradiation resulted in the least cell survival for all three cell lines and was subsequently used for all experiments (Figure 1).

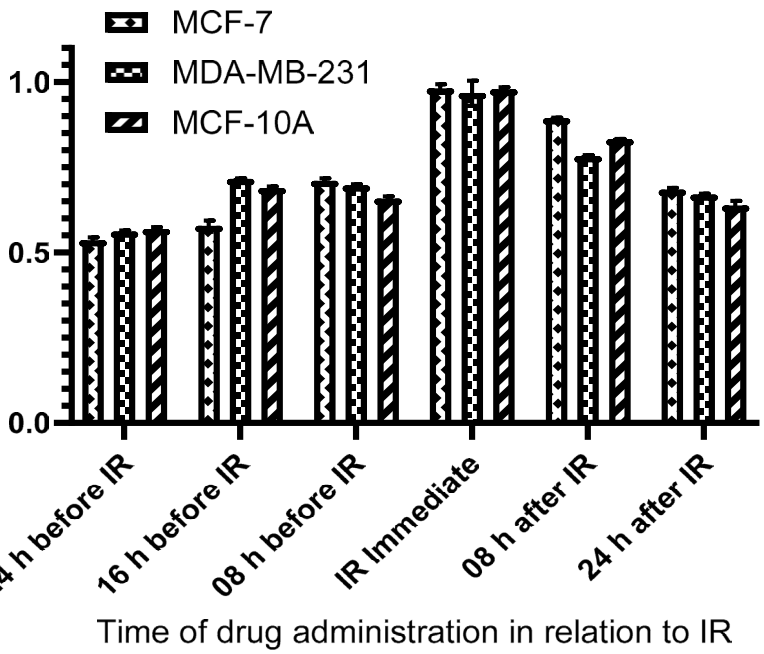

Figure 1. Pre-treatment with CUDC-101 at 24 h before 250 kVp X-ray irradiation offered maximal sensitization. Cells were pre-treated with 0.3 μM, 0.6 μM, and 2.7 μM CUDC-101 in MCF-7, MDA- MB-231, and MCF-10A cell lines. Cell proliferation was evaluated at 24, 16, 8 h before irradiation, immediately, and at 8 and 24 h after irradiation, as depicted on the *x*-axis. Cell proliferation was assessed with MTT assay at 72 h post irradiation.

2.2. Effect of CUDC-101 in Enhancing Radiation Response in Breast Cell Lines

Colony survival assays were performed to determine the effect of CUDC-101 in enhancing radiation-mediated cell killing (or inhibition of cell proliferation). For all three cell lines, comparison of survival curves showed an increased cell killing after proton irradiation compared to X-ray irradiated cells (Figure 2a–f). This resulted in relative biologic effectiveness at 10% survival (RBE10) values of 1.51, 1.31, and 1.20, in MCF-7, MDA-MB-231, and MCF-10A cell lines, respectively. All observed RBE values are close to the RBE

value of 1.1, which is used in clinical practice. The proton RBE was further enhanced by pre-treatment with CUDC-101, from 1.15 to 1.34 in the MCF-7 cell line and from 1.2 to 1.34 in MCF-10A cell line (Table 2). In the case of the MDA-MB-231 cell line, combination treatment of 2 Gy protons and CUDC-101 and 2 Gy X-rays and CUDC-101 yielded similar values, as shown in Figure 2d, which inferred that the differential effect of two radiation types might be obscured by the effect of CUDC-101. Accordingly, the sensitization enhancement ratio (SER) after X-ray irradiation was higher (2.09) than the proton SER (1.77), which suggested that in the MDA-MB-231 cell line, an increased biologic effect can be anticipated after CUDC-101 and X-rays compared to combination therapy of protons and CUDC-101. The MDA-MB-231 cell line also exhibited a higher RBE compared to the other two cell lines, suggesting increased sensitivity to proton irradiation. The SER values observed for the MCF-7 and MCF-10A cell lines were higher for protons compared to X-rays, which indicates increased sensitisation after proton irradiation compared to X-ray irradiation. The proton SER for MCF-7 was higher (1.50) than that determined in MCF-10A cell line (1.23), and the X-ray SER values of the cell lines were comparable (1.16 and 1.10 in MCF-7 and MCF-10A cell lines, respectively).

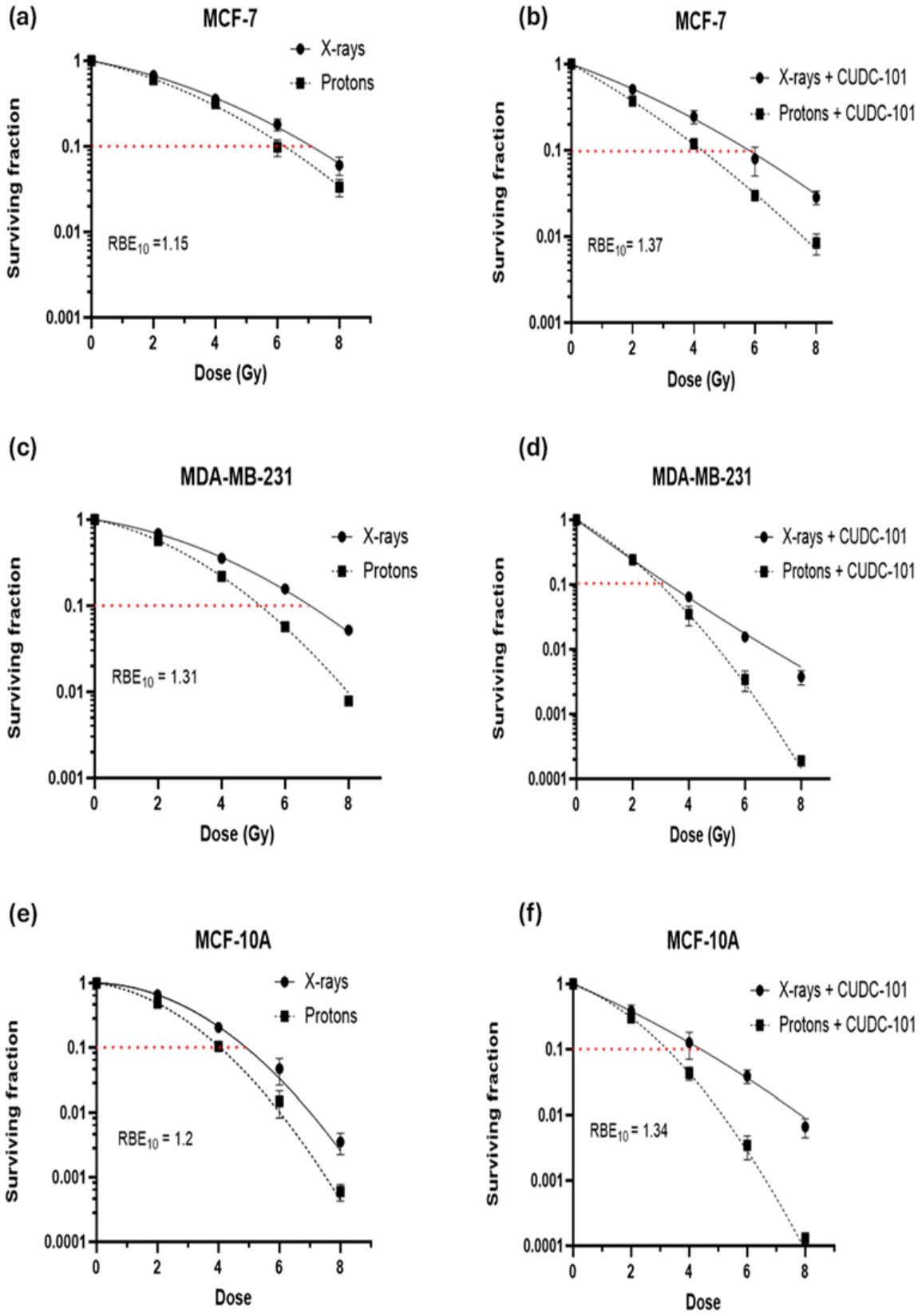

Figure 2. Colony survival curves and associated RBE calculations. CUDC-101 sensitises MCF-7 (**a,b**), MDA-MB-231 (**c,d**), and MCF-10A (**e,f**) cells to proton and X-ray irradiation. Data are expressed as the mean ± SD of three independent experiments.

Table 2. Radiation response parameters of MCF-7, MDA-MB-231, and MCF-10A cell lines.

Cell Line	RBE10	HDACi-Mediated RBE	SER10 (Protons)	SER10 (X-Rays)
MCF-7	1.15 ± 0.03	1.37 ± 0.00	1.50 ± 0.01	1.16 ± 0.03
MDA-MB-231	1.31 ± 0.01	-	1.77 ± 0.03	2.09 ± 0.02
MCF-10A	1.20 ± 0.01	1.34 ± 0.02	1.23 ± 0.04	1.10 ± 0.01

Data represent the mean ± SD. RBE: relative biologic effectiveness; SER: the sensitisation enhancement ratio.

2.3. Effect of CUDC-101 on Radiation-Induced DNA DSB Formation and Repair

To assess DNA damage induction and repair after combination treatment with CUDC- 101 and irradiation, γ-H2AX foci assays were performed as molecular markers of DNA double strand break (DSB) and repair. Cells were pre-treated with IC_{50} concentrations of HDACi for 24 h and irradiated with protons or X-rays. γ-H2AX foci assays were performed at 1 h and 24 h post-irradiation with 2 Gy 148 MeV mid-spread-out Bragg peak (SOBP) protons or 250 kVp X-rays. Overall, an increased number of γ-H2AX foci were noted post-irradiation with protons compared to X-irradiation in all three cell lines (Figure 3a–f). Further, in comparison to X-ray irradiated cells, an increased number of persisting γ-H2AX foci at 24 h post-proton irradiated cells was observed, which suggested that the type of damage induced by protons is complex in nature and more difficult to repair (Figure 3a–f).

In the MCF-7 cell line, at 24 h post irradiation, a significant reduction in the number of γ-H2AX foci was noted after irradiation protons ($p < 0.0047$) or X-rays ($p < 0.0009$) as well as in CUDC-101 pre-treated cells ($p < 0.0001$), which suggests that addition of the CUDC-101 did not impair the repair of the DNA DSB (Figure 3a,b). Comparison of the combination treatment (CUDC-101 and 2Gy) and irradiation alone (2 Gy protons), resulted in a non-significant result with p values of 0.1580 and 0.1319 at 1 h and 24 h post irradiation, respectively. Comparison of combination treatment of 2 Gy and X-irradiation and X-rays also yielded a non-significant result with p values of 0.0718 and 0.3018 at 1 h and 24 h post irradiation, respectively. Although not statistically significant, it was noted that proton irradiation alone yielded a higher number of γ-H2AX foci as compared to combination treatment of proton and CUDC-101 at 1 h post irradiation in this cell line (Figure 3a). This was not observed after irradiation with X-rays (Figure 3b).

In the MDA-MB-231 cell line, the number of γ-H2AX foci induced by radiation alone (protons or X-rays) and those induced by combination of radiation and CUDC-101 were

not statistically significant (p = 0.7672) at 1 h post irradiation (Figure 3c,d). A significantly reduced (p = 0.0003) but notable number of retained γ-H2AX foci was observed after combination therapy with proton and CUDC-101 as well as proton irradiation alone (Figure 3c). For X-ray irradiation, the number of retained γ-H2AX foci at 24 h after combined treatment remained high and the decrease in the number of γ-H2AX foci was not statistically significant (p = 0.4262) compared to the 1 h time point (Figure 3d). Taken together, the findings suggest repair impairment in the MDA-MB-231 cell line and a high sensitivity to CUDC-101, which is also observable in the unirradiated CUDC-101 control samples. This is reflected as an increase in the number of γ-H2AX foci induced by CUDC-101 monotherapy at 24 h as compared to 1 h (Figure 3c,d).

In the MCF-10A cell line, the only non-malignant cell line included in the study, an overall reduced number of γ-H2AX foci were noticed compared to the other two cell lines. A statistically significant (p = 0.008) higher number of remaining γ-H2AX foci at 24 h was noted with 2 Gy protons and CUDC-101 compared to proton irradiation alone (Figure 3e). Almost complete repair was noted after proton and X-ray irradiation alone and in the combination treatment of X-rays and CUDC-101 at 24 h (Figure 3f). Representative immunohistochemistry images of MCF-7 and MDA-MB-231 cell lines are shown in Figures 3g and 3h, respectively.

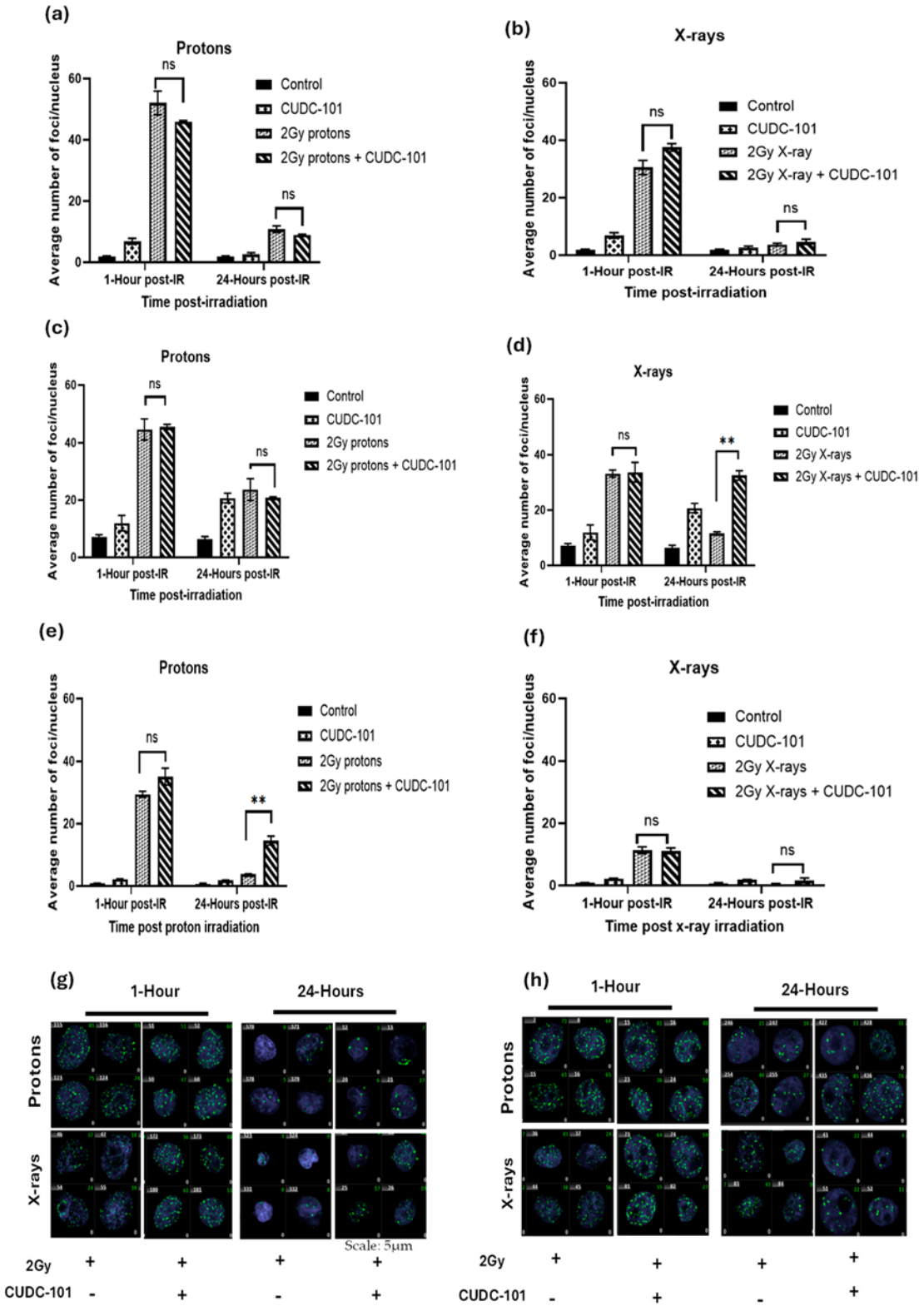

Figure 3. Effect of CUDC-101 combined with protons or X-rays in MCF-7 (**a**,**b**), MDA-MB-231 (**c**,**d**), and MCF-10A (**e**,**f**) cell lines. Histograms show the mean ± SD of three independent experiments (n = 3) ** p = 0.0037 in MDA-MB-231 and ** p = 0.0088 in MCF-10A cell lines. Representative images of γ-H2AX foci at 1 h and 24 h post-irradiation in MCF-7 (**g**) and MDA-MB-231 cell lines (**h**). Images are obtained at 40× magnification using a Metafer 4 scanning system. Analysis was performed using unpaired two-tailed Student's t test, ** p (<0.002).

2.4. Impact of CUDC-101 and Radiation on Apoptosis in Breast Cell Lines

To investigate the induction of apoptosis after treatment with CUDC-101, radiation (protons or X-rays), or combination therapy of CUDC-101 and radiation, the Annexin V/PI apoptosis assay was performed. Apoptosis and necrosis were assessed at 48 h post- irradiation with 2 Gy and 6 Gy protons or X-rays, as well as after combination of CUDC-101 and radiation (proton or X-rays). In all three cell lines, increased apoptosis levels were observed post proton-irradiations as compared to X-ray irradiations (Figure 4a-c). Pre- treatment with CUDC-101 significantly increased the level of proton-induced apoptosis after 2 Gy (p = 0.0020) and after 6 Gy (p = 0.0011) in MCF-7 cell line (Figure 4a). Similarly, in the MDA-MB-231 cell line, a significant increase was observed in CUDC-101 pre-treated samples after 2 Gy (p = 0.0219) and 6 Gy (p = 0.0216) (Figure 4b). In the spontaneously immortalised MCF-10A cell samples, increased apoptotic fractions were observed in the CUDC-101 treated MCF-10A cells (Figure 4c). Further, treatment with 1 µM of apoptosis inducer staurosporine induced apoptosis in MCF-7 and MCF-10A cell lines, whereas necrosis was induced in the MDA-MB-231 cell line at 24 h after treatment (Figure 4d).

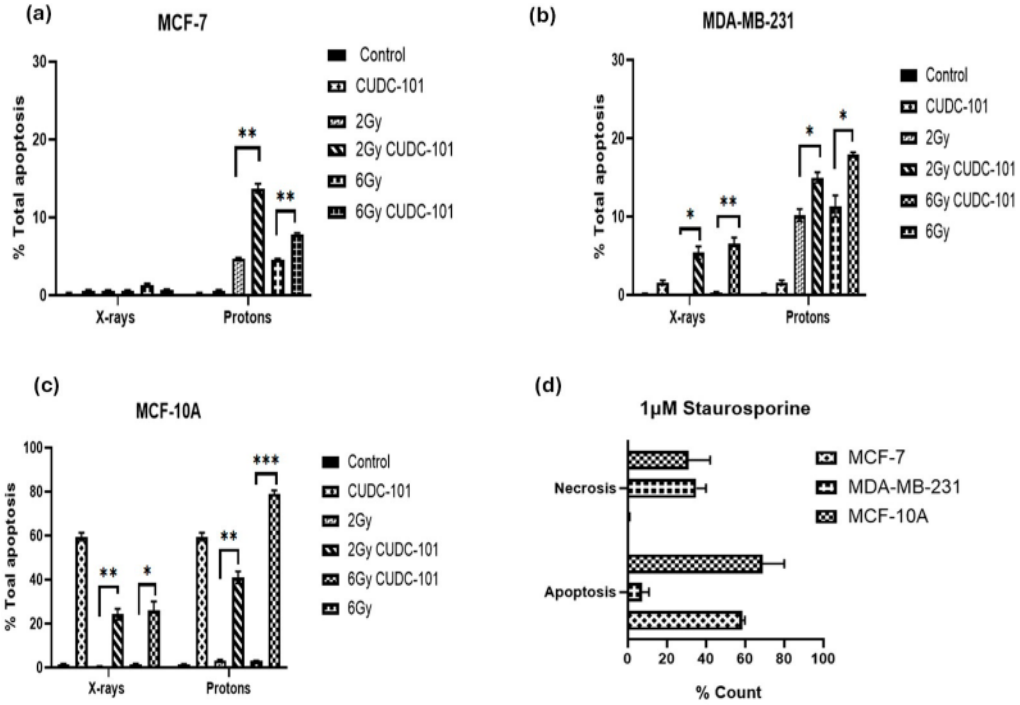

Figure 4. Induction of apoptosis and necrosis at 48 h post treatment with CUDC-101 combined with protons or X-rays in MCF-7 (**a**), MDA-MB-231 (**b**), and MCF-10A (**c**) cell lines. Induction of apoptosis and necrosis at 24 h after treatment with 1 µM staurosporine in the three cell lines (**d**). Histograms show the mean ± SD of three independent experiments (n = 3). Comparisons were conducted using unpaired two-tailed Student's *t* test, *** p (<0.0003) ** p (<0.002), * p (<0.05).

In addition, in the MCF-7 cell line, increased necrosis was noted after proton irradiations compared to X-ray irradiations (p = 0.0063). Pre-treatment with CUDC-101 further increased levels of necrosis after X-ray irradiation in this cell line (p = 0.0051) (Figure 5a,b). A different observation was made in the MDA-MB-231 cell line, pre-treatment with CUDC-101 reduced levels of necrosis after proton irradiation (p = 0.0136) and X-rays (p = 0.3647). Comparison of levels of necrosis between the two cell lines showed increased amounts of necrotic cell populations in the MCF-7 cell line compared to the MDA-MB-231 cell line after protons (p = 0.0174) and protons and CUDC-101 (p = 0.0095) (Figure 5g). Representative images of apoptosis profiles are included in Supplementary Material (Figure S1).

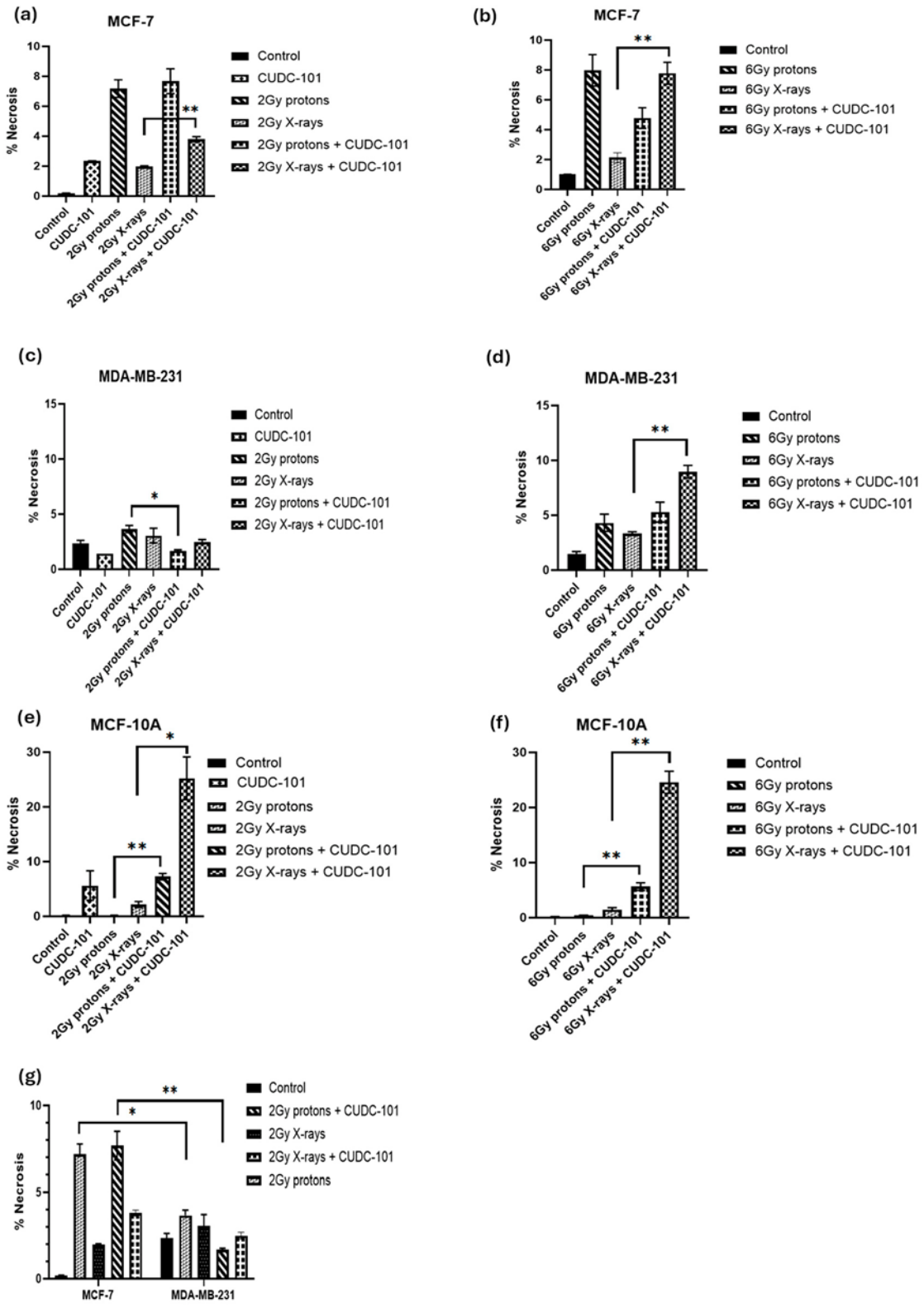

Figure 5. Induction of necrosis at 48 h post treatment with CUDC-101 combined with protons or X-rays in MCF-7 (**a,b**), MDA-MB-231 (**c,d**), and MCF-10A (**e,f**) cell lines. Increased amounts of necrosis after treatment with 2 Gy protons and 2 Gy protons and CUDC-101 in MCF-7 cell line compared to MDA-MB-231 cell line (**g**). Histograms show the mean ± SD of three independent experiments (n = 3). Comparisons were conducted using unpaired two-tailed Student's *t* test, ** *p* (<0.002), * *p* (<0.05).

2.5. Effect of CUDC-101 and Radiation on Cell Cycle Progression

Cell cycle progression after treatment with CUDC-101 and radiation was assessed using propidium iodide with RNase staining. For all cell lines, an increased fraction of cells was observed in the G2/M phase of the cell cycle at 24 h post-irradiation with 6 Gy protons or X-rays, indicating a G2/M cell cycle arrest (Figure 6a–f). Also, in all three cell lines, mono-treatment with CUDC-101 induced G2/M cell cycle arrest at 24 h, which persisted at 48 h (Figure 6a-f). In the MCF-7 and MDA-MB-231 cell lines, an increase in fraction of G2/M cells was also observed at 48 h in X-ray irradiated cells compared to proton-irradiated cells at doses of 2 Gy ($p = 0.0012$) and at 6 Gy ($p = 0.0007$). This increase was more evident in the MDA-MB-231 cell line compared to the MCF-7 cell line (Figure 6g,h). Furthermore, compared to radiation treatment alone, pre-treatment with CUDC-101 had a minimal effect on the cell cycle progression in MCF-7 cells at neither 24 h ($p = 0.4929$ for 2 Gy and $p = 0.0532$ for 6 Gy) nor 48 h ($p = 0.6985$ for 2 Gy and $p = 0.3118$ for 6 Gy) post proton-irradiation as evidenced by comparable G2/M fractions at these timepoints (Figure 5g). However, in the MDA-MB-231 cell line, pre-treatment with CUDC-101 increased the G2/M fraction after exposure to both 2 Gy $p = 0.0030$) and 6 Gy ($p = 0.0027$) X-rays which was maintained at 48 h post irradiation (Figure 6h). It seems sensible to associate the increased fraction of G2/M cells after X-ray irradiations to the reduced levels of apoptosis and necrosis that were seen in the MCF-7 and MDA-MB-231 cell lines at 48 h post irradiation. In this instance, the increased G2/M could be an indicator of mitotic catastrophe as a mode of cell death after x-irradiations. Similarly, in the MCF-10A cells, increased G2/M fractions were noted in CUDC-101 pre-treated compared to radiation alone. Cell cycle profiles are included in the Supplementary Material (Figure S2).

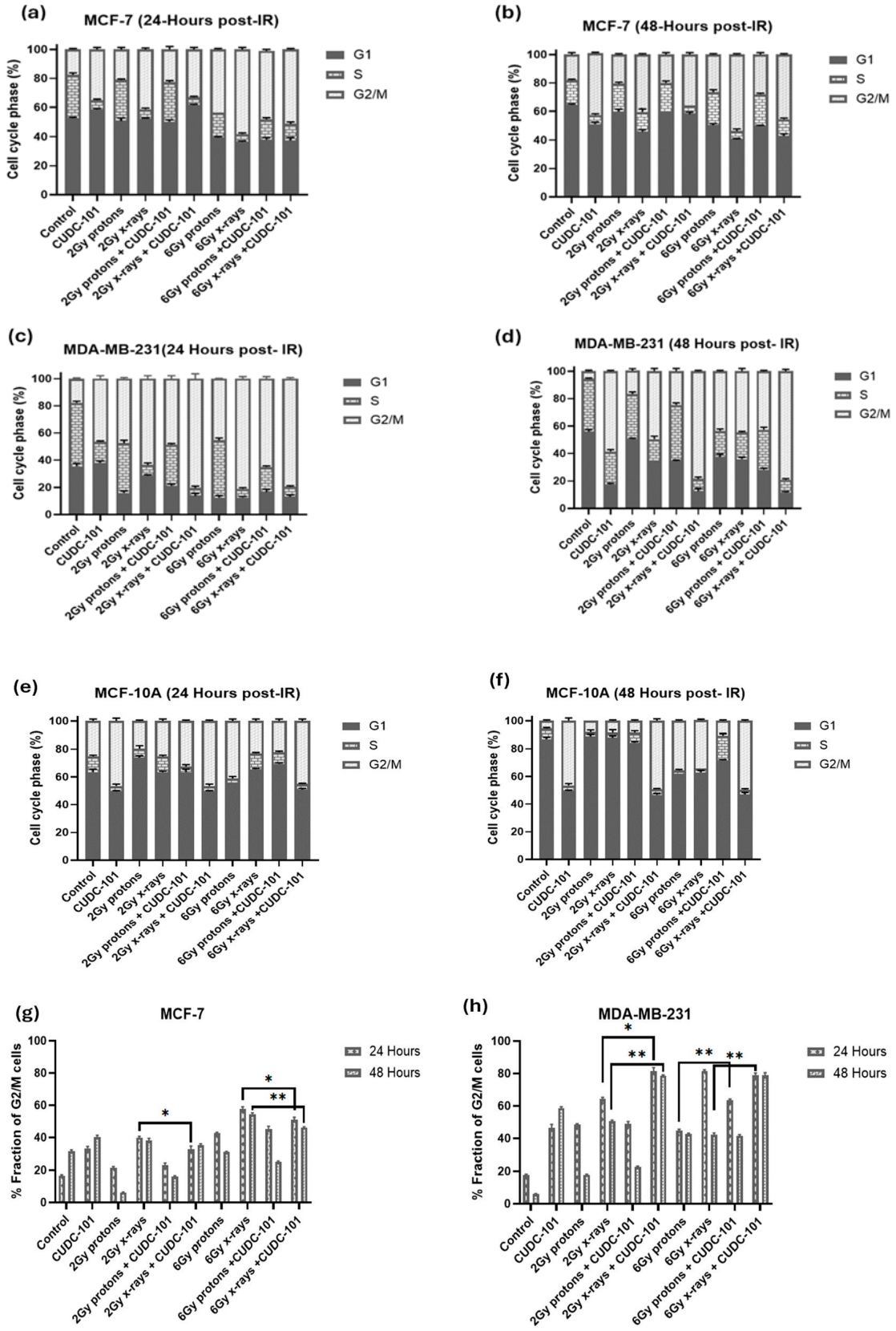

Figure 6. Quantification of the effect of CUDC-101 alone and in combination with X-rays and protons on cell cycle progression in MCF-7 (**a,b,g**) MDA-MB-231 (**c,d,h**); and MCF-10A (**e**,**f**) cell lines. Data represent the mean ± SD of three independent experiments (n = 3). Comparisons were conducted using two-tailed Student's *t* test, * $p < 0.05$, ** $p < 0.008$.

3. Discussion

3.1. CUDC-101 Increases Sensitivity of MCF-7, MDA-MB-231 and MCF-10A Cell Lines to Proton and X-Ray Irradiation

Our data show that the multi-target inhibitor CUDC-101 enhances the response to both protons and X-rays in MCF-7 and MCF-10A breast cell lines. The enhancement was most notable after proton irradiation, with proton SER values of 1.50 and 1.23 and X-ray SER values of 1.16 and 1.10 in MCF-7 and MCF-10A cell lines, respectively. Similarly, in hepatocellular carcinoma (HCC) cell lines, Choi et al. reported higher proton SER values of 1.25 and 1.21 compared to X-ray SER values of 1.15 and 1.11, using Panobinostat in Huh7 and Hep3B cells, respectively. Yu et al. also reported Valproic acid (VPA)-mediated RBE_{10} value of 1.17 compared to RBE_{10} value of 1.08 without VPA in Hep3B cells after treatment with 6 MV photons [31]. In another study, Gerelchuluun et al. reported an RBE_{10} value of 1.24 and proton SER values of 1.31 and 1.16 compared to γ-ray SER values of 1.43 and 1.08 in lung carcinoma (A549) and normal fibroblast (AG1522) cell lines, respectively, following treatment with 2 μM of SAHA [29]. Although different HDACi and different cell lines were used in the mentioned studies, the findings are consistent with those of the current study, where higher RBE and SER values were reported for proton compared to X-rays. The enhanced radiation response in the MCF-7 cell line indicate a potential benefit of using CUDC-101 and protons in treatment of breast tumours with oestrogen, progesterone, and her-2 positive molecular sub-types. Previous studies have asserted that HDACs are not overexpressed in normal tissues, which leads to minimal effect of HDACi on normal tissues [17,41,42]. While our study indicates SER of 1.10 and 1.23 in the normal breast cell line (MCF-10A) following pre-treatment with CUDC-101, these values were lower than the ones observed in the malignant cell lines. It should be noted that the former studies used SAHA, which inhibits HDACs only, whereas in the current study CUDC-101, which inhibits HDACs, EGFR and HER-2, was used. Therefore, the effect of CUDC-101 observed in the normal cell line can be attributed to inhibition of EGFR, which is important for growth and maintenance of MCF-10A cells [43].

A different effect was seen in the MDA-MB-231 cell line in the current study, with a higher X-ray SER value of 2.09 compared to proton SER value of 1.77, which implies that in this cell line, CUDC-101 is best combined with X-rays for maximal therapeutic benefit of the combination treatment. It is yet to be determined if a similar result will be seen using other triple-negative breast cell lines. In addition, the RBE_{10} value of 1.31 for the MDA-MB-231 cell line indicates that protons are more effective than X-rays to inhibit the proliferation capacity, at a higher rate than the RBE_{10} values observed in the MCF-7 and MCF-10A cell

lines. Previous studies have associated higher RBE values to DNA damage repair capacity of the cell line. In other words, cell lines with higher RBE values reported to be deficient in DNA repair capacity [44,45].

3.2. Proton Irradiation Induces Increased DNA Damage That Is Not Easily Repaired in Breast Cell Lines

The complexity of DNA damage induction and repair after proton therapy remains a subject of discussion [46]. Contrary to X-rays that have no mass and no charge, protons are charged particles with a larger mass, which can create more direct and complex DNA damage. Previous studies reported an increased number of γ-H2AX foci that are larger in size after proton irradiation as compared to X-rays in different cell lines [47–53]. Other studies reported that SOBP protons induced increased γ-H2AX foci, which were larger in size and reached maximum point at 1 h post irradiation, whereas maximal γ-H2AX foci count was reached at 30 min post irradiation with X-rays and plateau protons, which were also smaller in size and were resolved at 6 h post irradiation [47,50,54]. Gerelchuulun et al. reported a 1.2–1.6-fold increase in γ-H2AX foci in ONS76 medulloblastoma and MOLT4 leukaemia cells after proton irradiation compared to 10 MV X-rays [51]. In another study, irradiation with SOBP protons induced more clustered DNA damage, whereas entrance plateau protons induced mixed-type damage that consisted of clustered and non- clustered DNA damage [50]. Consistent with these studies, a significantly increased number (1.4–1.5-fold) of γ-H2AX foci was observed at 1 h post-irradiation with 2 Gy SOBP protons compared to 2 Gy X-rays in all three cell lines (Figure 3a–h). The fact that persisting γ-H2AX foci at 24 h post irradiation were observed mainly after proton irradiation (Figure 3b,c), suggests that the type of DNA damage induced by protons is difficult to repair, supporting the assertions of complex DNA damage [47,50,51,53,55–57].

Of relevance is also the ongoing discussions about differential requirement of DNA DSB repair pathways following protons and X-rays [47,55]. Previous studies reported that post proton irradiation, the error free homologous repair (HR) is preferred, and non-homologous end joining (NHEJ) is preferred after irradiation with X-rays [53,55]. Latter reports indicated that HR is required post proton irradiation due to the complex nature of the DNA damage, but NHEJ is also indispensable for repair of proton-induced DSB [45,47,57]. Further evidence pointed out that irrespective of the type of radiation, the initial fast repair is conducted by NHEJ, and HR occurs at a later stage [53,58,59]. In a recent report by Lohberger et al., mismatch repair (MMR) and nucleotide excision repair (NER) repair pathways together with HR and NHEJ pathways were found to be activated mainly post-

proton irradiation in chondrosarcoma cells [52]. These studies bear relevance to the observed prolonged appearance of γ-H2AX foci after proton irradiation as compared to x-irradiated cells, particularly in the MDA-MB-231 cell line in the current study. Consistent with the notion that cell lines with higher RBE values have defective repair pathways, Lee et al. reported that MDA-MB-231 cells are deficient in HR, base excision, and nucleotide excision repair (NER) [60]. This would explain the increased retention of γ-H2AX foci in MDA-MB-231 cell line and increased sensitivity to proton irradiation (RBE_{10} of 1.31) compared to the MCF-7 cell line (RBE_{10} of 1.15). As previously mentioned, the HDACi-mediated RBE was, however, lower than the proton RBE due to the compounding effect of DNA damage that has been induced by CUDC-101 in the MDA-MB-231 cell line, which was not observed in the other cell lines. Several studies also reported having observed increased sensitivity to proton irradiation in cells that are deficient in HR machinery [47,53,55,56,61].

Limited studies have been conducted on combination therapy of HDACi and proton irradiation with respect to DNA DSB induction and repair. A 3 h pre-treatment with 1 mM HDACi Valproic acid (VPA) and mid-SOBP protons prolonged appearance of γ-H2AX foci in Hep3B and Huh7 hepatocellular carcinoma cell lines [31]. Pre-treatment with 5 nM Panobinostat increased the γ-H2AX foci yield at 24 h post irradiation with 6 Gy mid-SOBP protons in Huh7 and Hep3B hepatocellular carcinoma cell lines [28]. In NFF28 normal fibroblast cells, Johnson et al. reported resolution of γ-H2AX foci to near background levels at 24 h post-treatment with 10 μM SAHA and irradiation with 200 MeV protons [30]. The results of these earlier studies are consistent with the observation in the current study, since the retention of γ-H2AX foci was in general higher after proton irradiation in malignant cell lines compared to the MCF-10A cell line. It is also worth noting that in the study by Johnson et al., 200 MeV entrance plateau protons were used, whereas 148 MeV mid-SOBP protons were used in the current study. Persisting γ-H2AX foci were detected at 24 h post treatment with 2 Gy protons and CUDC-101 in the MCF-10A cell line, which could be an indication of increased normal tissue effect.

Treatment with CUDC-101 alone resulted in an induction of γ-H2AX foci at 1 h, which increased at 24 h post treatment in MDA-MB-231 cell line (Figure 3c–e), but not in theMCF-7 and MCF-10A cell lines. Similarly, in the MDA-MB-231 cell line, an increased G2/M phase fraction in comparison to the untreated control was seen at 24 h (p = 0.003) and at 48 h (p = 0.0002). The increase in the number of γ-H2AX foci at 24 h suggests that additional γ-H2AX foci might have been induced by cell death mechanisms. Induction of DNA damage by sole treatment with HDACi has previously been reported mainly in leukaemia cells

[62,63], which would explain the success of HDACi monotherapies in treating haematological malignancies with poor performance in solid tumours. In a study by Choi et al., Panobinostat alone did not induce γ-H2AX foci in hepatocellular carcinoma cell lines [28]. Further investigation is required to confirm the observations of CUDC-101-induced DNA DSB formation in the current study.

3.3. CUDC-101 Enhances Protons-Induced Apoptosis

The type of cell death after irradiation is mainly determined by the cell type and type of radiation. Apoptosis was formerly reported to be the main mode of cell death in haematological cancer cells whereas mitotic catastrophe was reported to be the main mode of cell death in solid tumours after irradiation [64]. Further, several studies asserted that apoptosis would be the main mode of cell death in solid tumours, through either the intrinsic or extrinsic apoptotic pathways, whereas the main mode of cell death post X-ray irradiation would be mitotic catastrophe [51,64–70]. Consistent with these assertions made in these reports, increased apoptosis was observed post proton irradiations, whereas minimal levels of apoptosis were noted after X-ray irradiation in all three cell lines (Figure 4a–c). Apoptosis was most notable in the MDA-MB-231 cell line at 2 Gy and 6 Gy proton irradiations, as well as after combination therapy of proton irradiation (2 Gy and 6 Gy) and CUDC-101. Although a marked number of unresolved DSB was noted at 24 h after treatment with CUDC-101 monotherapy in this cell line, minimal levels of apoptosis were noted, suggesting a different type of cell death. Indeed, cell cycle analysis in both MCF-7 and MDA-MB-231 cell lines showed increased G2/M arrest at 48 h after CUDC-101 monotherapies, as well as after combination treatments of CUDC-101 and X-ray irradiation (Figure 5a–d), which suggested induction of mitotic catastrophe. Similar observations were made by Schlaff et al. who reported induction of mitotic catastrophe in glioblastoma cell line after CUDC-101 treatment [14]. Keeping with the argument that CUDC-101 and X-ray monotherapies induces mitotic catastrophe, the combination therapy of X-rays and CUDC-101 was expected to result in higher levels of mitotic catastrophe (G2/M) compared to proton irradiations and CUDC-101. Certainly, Figure 5d,e show an even higher proportion of G2/M cells after combination therapy of 2 Gy X-rays and CUDC-101 compared to monotherapies with either X-rays or CUDC-101 in the MDA-MB-231 cell line.

In the MCF-7 cell line, the levels of apoptosis and necrosis were comparable at the lower dose of 2 Gy (Figure 4a,b). The levels of necrosis exceeded that of apoptosis at doses of 6 Gy, as shown in Figure 4c. Several reports have asserted that MCF-7 cells are deficient in caspase 3 and therefore lack the morphological features associated with apoptosis [71,72].

Natarajan et al. reported that MCF-7 cells can switch to a necroptosis pathway after treatment with HDACi SAHA [73]. Necroptosis is a caspase-independent mechanism of programmed cell death that is activated when apoptosis is blocked and it bears mechanistic similarity to apoptosis and morphological similarity to necrosis [74]. Treatment with 1 μM of apoptosis inducer staurosporine, induced more apoptosis in the MCF-7 cell line compared to the MDA-MB-231 cell line at 24 h post treatment (Figure 6d). In earlier studies, staurosporine, at a concentration of 1 μM, was reported to induce apoptosis in MCF-7 cells through partial activation of caspase-6 [71]. The authors also noted that apoptosis occurred earlier (16 h), with the absence of typical apoptotic morphology and absence of apoptotic bodies in the MCF-7 cell line compared to T47D cells [71]. To the contrary, Poliseno et al. reported that at 5 h post treatment with staurisporine at 1 μM induced necrosis in MCF-7 cell lines expressing low anti-apoptotic Bcl-2 protein [75]. Taken together, these studies imply that necrosis is induced earlier, and apoptosis is only detectable at a later stage in MCF-7 cells. In view of the mentioned overlapping similarities between necroptosis, necrosis, and partial apoptosis in this cell line, it seems reasonable to assume that what was reported in previous literature, as well as in the current study, might have been necroptosis. In view of the fact that very little apoptosis was observed in all three cell lines, it is advisable that other modes of cell death such as mitotic catastrophe, autophagy, and necroptosis be investigated in follow-up *in vitro* work, particularly in the MCF-7 cell line, which is caspase 3-deficient [76].

The increased apoptosis seen in CUDC-101-treated cells in the MCF-10A cell line is thought to be due to inhibition of EGFR (Figure 4c). Increased apoptosis was seen mainly after treatment with protons and CUDC-101 compared to X-ray irradiated cells (Figure 4c). Further, lower levels of apoptosis were seen after treatment with 2 Gy X-rays and CUDC-101 compared to 6 Gy X-rays and CUDC-101. These findings imply that, if CUDC-101 is considered for use in triple-negative breast cancer, it might be better to combine it with X-rays to reduce normal tissue reactions. Notwithstanding, in a Phase 1 study of 275 mg/m2 CUDC-101 in combination with cisplatin and X-ray radiation in squamous cell head and neck cancers, out of the 12 patients that enrolled for the study, 5 patients discontinued CUDC-101 due to adverse side effects. CUDC-101 was administered three times a week for one week before starting with radiation and cisplatin and was concurrently administered with cisplatin and radiation in a fractionated regime up to a total dose of 70 Gy. The authors suggested alternate scheduling of CUDC-101 and using different routes of administration to minimize adverse effects [76]. Subsequently, in another Phase I trial in advanced solid tumours, Schlaff et al. reported that intravenous administration of CUDC-101 for 1 h for 5 consecutive days every 2 weeks were well tolerated. The authors recommended a dose of

275 mg/m2 to be used [77]. A Phase I study (NCT01702285) to assess safety and tolerability of orally administered CUDC-101 was terminated for unknown reasons.

3.4. CUDC-101 Induces G2/M Cell Cycle Arrest and Enhances X-Irradiation-Induced G2/M Cell Cycle Arrest

Previous studies highlighted the important role that HDACs play in cell cycle progression. In particular, HDAC 3 and HDAC 10 have been implicated in mediating progression through the G2/M phase of the cell cycle [78–80]. HDACs 2, 3, 5, and SIRT2 have also been implicated in facilitating exit from mitosis stage [78,81–83]. HDACi, therefore, induces CDK-inhibitor p21, to induce cell cycle arrest [78]. Monotherapy with 5 nM of HDACi panobinostat induced G2/M arrest from 24.3% to 51.4% at 24 h post-treatment in Huh7 HCC cell lines. Pre-treatment with 5 nM panobinostat also increased G2/M proportions of cells after 6 Gy X-ray or proton irradiation [28]. The amounts of G2/M cells seen after single panobinostat treatment and after combination therapy of panobinostat and proton- or X-ray irradiation were not statistically signinficant [28]. In another study, 6 Gy photons or 6 Gy protons increased proportions of G2/M cells to 71% and 70%, respectively in Hep3 HCC cell line [31]. Pre-treatment with 1 mM of HDACi VPA before radiation further increased G2/M fraction from 73.4% to 80.1% at 24 h and from 59.9% to 58.6% at 72 h [31]. In the current study, similar to the mentioned studies, 6 Gy protons and 6 Gy X-rays increased G2/M cells at 24 h compared to the untreated control. Also, similar to Choi et al., treatment with CUDC-101 monotherapy increased G2/M cell cycle arrest in all three breast cell lines at 24 h. The increase was most notable in the MDA-MB-231 and MCF-10A cell lines, indicating increased toxicity of CUDC-101 in these cell lines. Contrary to the studies mentioned, increased G2/M was seen in X-ray-irradiated cells compared to the proton-irradiated cells, with or without HDACi pre-treatment in the current study. As previously mentioned, this differential increase in G2/M fraction after X-rays suggested mitotic catastrophe as a mode of cell death. The summary of the cellular effects of CUDC-101 is presented in Figure 7.

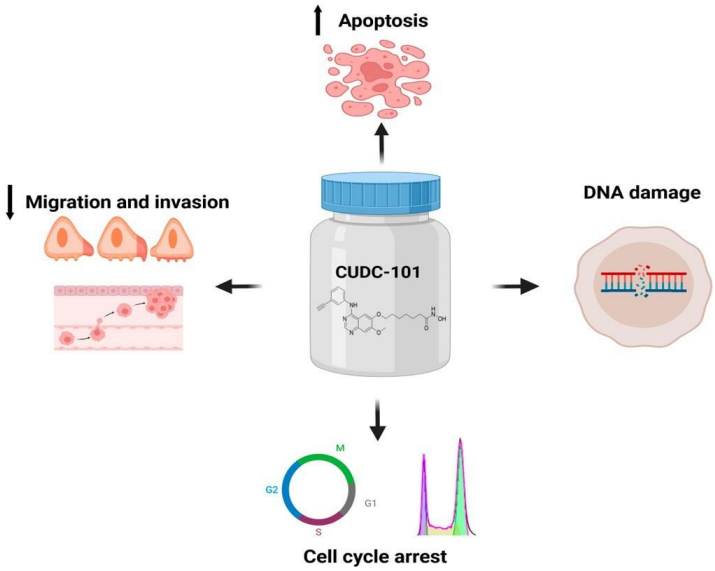

Figure 7. Summary illustration of the cellular effects of CUDC-101.

4. Materials and Methods

4.1. Cell Cultures

MCF-7 and MCF-10A (gifted by the Physiology Department, University of Pretoria) cells were cultured in Dulbecco's Modified Eagle's Medium F-12 (DMEM-F12; GibcoTM, Thermo Fisher Scientific, Sandton, South Africa) and Ham's F-12 (GibcoTM, Thermo Fisher Scientific, Sandton, South Africa) supplemented with 10% foetal bovine serum (FBS) (GibcoTM, Thermo Fisher Scientific, Sandton, South Africa), 100 µg/mL penicillin (GibcoTM, Thermo Fisher Scientific, Sandton, South Africa), and 100 µg/mL streptomycin for bacterial contamination. MCF-10A medium was further supplemented with epidermal growth factor (EGF) (20 ng/mL final concentration) (GibcoTM, Thermo Fisher Scientific, Sandton, South Africa) and hydrocortisone (0.5 mg/mL final concentration) (Sigma-Aldrich, St. Louis, MO, USA).

MDA-MB-231 cells (gifted by the Department of Natural Sciences, University of Western Cape) were cultured in Roswell Park Memorial Institute (RPMI) 1640 (GibcoTM, Thermo Fisher Scientific, Sandton, South Africa) supplemented with 10% FBS, 100 µg/L penicillin and 100 µg/mL streptomycin (Sigma-Aldrich, St. Louis, MO, USA).

All cell lines were cultured in T275 or T75 cell culture flasks (Thermo Fisher Scientific, Sandton, South Africa) under standard conditions in a humidified incubator at 37 ◦C, 5% CO_2 (Forma series 3 water jacketed incubator, Thermo Fisher Scientific, Waltham, MA,

USA). Cell growth was assessed over 24 h intervals and sub-cultured once 80% confluence was reached.

4.2. Histone Deacetylase Inhibitor

CUDC-101 (molecular weight of 434.49) (Figure 8) was purchased from Sigma Aldrich (Sigma-Aldrich, St. Louis, MO, USA) and 1 mM stock solution was prepared according to the manufacturer's instructions (5 mg of CUDC-101 was resolved in 11.5077 mL dimethyl-sulfide (DMSO) (Biotechnology Hub, Johannesburg, South Africa) and stored at −20°C for short term storage and at −80°C for long term storage.

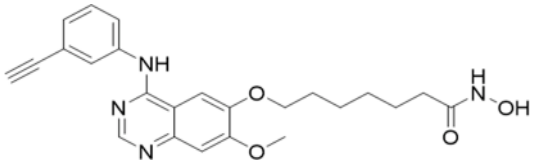

Figure 8. Molecular structure of CUDC-101.

4.3. Irradiations

Photon irradiations were performed using the 250 kVp X-Rad 320 unit (Precision X-ray, Madison, WI, USA) at a mean dose rate of 0.69 Gy/min at a Source Surface Distance (SSD) of 50 cm. Calibrations of the unit were performed according to the Technical Report Series-398 (TRS-398) protocol, with a Farmer 117 chamber for which a chamber calibration factor has been obtained from the National Metrology Institute of South Africa (NMISA).

Proton irradiations were performed at the Trento Institute for Fundamental Physics and Application (TIFPA). An SOBP beam of 2.5 cm has been produced, as detailed in Tommasino et al. through a 2D rang modulator applied to a beam with initial energy of 148 MeV/u and enlarged with a dual ring system to a lateral profile maintaining a 98% dose uniformity across a 6 cm diameter. The beam was calibrated with EBT gafchromic film and Markus chamber measurements. The cells were exposed after 11 cm of solid water slabs, corresponding to 11.45 cm of water [84]. For both X-ray and proton irradiations, cells were irradiated in 5 mL media in T25 flasks.

4.4. Cell Proliferation Assays

Cell proliferation assays were conducted using the thiazolyl blue tetrazolium bromide (MTT) cell viability assay kit. Cells were seeded at a pre-determined density of 3000 cells/well in 96-well plates and allowed to attach. Cells were treated with different concentrations of the HDACi (SAHA or CUDC-101) ranging from 0 μM to 20 μM and incubated for a further 72 h. A 20 μL of a 5 mg/mL stock solution of MTT (Sigma-Aldrich, St. Louis, MO, USA) was added

to each well and incubated for a further 4 h to allow formazan formation. MTT-containing media was carefully removed and 100 µL of DMSO was added to each well. The formation of formazan in the viable cells was monitored by measuring absorbance at wavelengths of 595 nm on a spectrophotometer to determine the half-maximal inhibitory concentrations (IC_{50}) values for HDACi SAHA for the different cell lines.

4.5. Colony Survival Assays (CSA) and RBE Analysis

Cells (250–1500) were seeded in 6-well plates (Whitehead Scientific, Cape Town, South Africa) and allowed to attach overnight. Cells were treated with CUDC-101 at a concentration of 0.6 µM, 2.7 µM, and 0.3 µM for MCF-7, MCF-10A, and MDA-MB-231, respectively, for 24 h and irradiated with 0, 2, 4, 6, and 8 Gy of 250 KeV X-rays or 148 MeV SOBP protons. The cells were returned for incubation for a further 8–14 days to allow for colony development. Once colonies of approximately 50 cells were formed, they were fixed with methanol and stained with 2% crystal violet dissolved in methanol and left to dry overnight. Colonies were manually counted, and the size was validated by microscopic inspection. Plating efficiency was calculated under untreated conditions using the equation:

$$Plating\ efficiency(PE) = \frac{number\ of\ colonies\ counted}{number\ of\ cells\ seeded} X\ 100\%$$

Plating efficiency was used to normalise the surviving fractions for HDACi and radiation-induced cell death. The surviving fraction of cells was calculated using the equation:

$$Surviving\ Fraction = \frac{number\ of\ colonies\ formed\ after\ treatment}{number\ of\ cells\ seeded} x\ platting\ efficiency$$

Survival curves were plotted and analysed using GraphPad Prism Software Version10.00 for Windows (GraphPad Software, San Diego, CA, USA). The RBE of the different treatment conditions was calculated at a survival fraction of 10%:

$$RBE = \frac{Dose\ of\ photon\ radiation}{Dose\ of\ proton\ radiation}\ that\ reduce\ fraction\ of\ surviving\ cells\ to\ 10\%$$

The sensitisation enhancement ratio (SER) was calculated using the equation [28,29]:

$$SER = \frac{Dose\ of\ Radiation\ that\ reduces\ cell\ survival\ to\ 10\%\ without\ CUDC-101}{Dose\ of\ radiation\ that\ reduces\ cell\ survival\ to\ 10\%\ with\ CUDC-101}$$

4.6. Annexin V-FITC/Propidium Iodide Apoptosis and Cell Cycle Analysis Assays

Apoptosis and cell cycle progression were analysed using flow cytometry. For the apoptosis assays, at 48 h post-irradiation, the media in which the cells were incubated was retained and combined with harvested cells before centrifugation. The cell pellet was resuspended in 100 µL 1× annexin-binding buffer and stained with with 2.5 µL Annexin V FITC and 2.5 µL propidium iodide (PI) (catalogue number 13242, Invitrogen, Thermo Fisher Scientific, Sandton, South Africa) according to the manufacturer's instructions. Cells were incubated at room temperature (25 ◦C) for 15 min in the dark. An additional annexin- binding buffer was added after incubation, and the samples were analysed using the BD AccuriTM C6 Plus (BD Biosciences, Johannesburg, South Africa) with 15,000–20,000 cells per measurement.

For analysis of the cell cycle, cells were harvested at 24 h and 48 h post treatments, and the cell pellet was resuspended in a solution of 100 µL propidium iodide and RNase (FxCycleTM PI/RNase, Invitrogen, Waltham, MA, USA). Propidium iodide stains for both DNA and RNA, therefore the ribonuclease (RNase) digests and removes RNA to ensure that only DNA content is analysed [85]. The samples were analysed using FACSort (Beckton Dickinson, San Jose, CA, USA), with 15,000–20,000 events per measurement. Fluorescence measurements were done at 495 nm and 519 nm (peak emission) at fluorescein isothio- cyanate (FITC) channel for Annexin V FITC; 536 nm and 616 nm (peak emission) at FL2 or FL3 channels for propidium iodide for all flow cytometry assays.

4.7. Gamma-H2AX Foci Assay

Treated cells were harvested 1 h and at 24 h post irradiation and a suspension of approximately 120,000 cells/0.25 mL was centrifuged onto coated slides (X-tra adhesive slides, Leica Biosystems, Buffalo Grove, IL, USA). Three slides were prepared for each treatment condition. The slides were fixed in freshly prepared 4% paraformaldehyde (PFA) for 20 min and washed in PBS for 5 min. Cells were then permeabilised with PBS-triton X-100 solution (GibcoTM, Thermo Fisher Scientific, Sandton, South Africa) for 10 min and blocking of no-specific antibody binding by washing 3 times in 1% bovine serum albumin (BSA) solution (Roche, Sigma-Aldrich/Merck, St. Louis, MO, USA) for 10 min per wash. Cells were incubated with phospho-histone H2A.X (Ser139) Monoclonal Antibody (3F2) antibody (Invitrogen, Biocom Africa (Pty) Ltd., Centurion, South Africa) for 1 h at room temperature, followed by washing 3 times in 1% bovine serum albumin (BSA) (Roche, Sigma-Aldrich/Merck, St. Louis, MO, USA) to remove any unbound primary antibody. Cells were then incubated for a further 1 h in the dark with rabbit anti-mouse IgG (H + L) FITC Secondary Antibody, secondary antibody (Invitrogen, Thermo Fisher Scientific, Sandton,

South Africa) in a humidified chamber. Nuclear counterstaining was performed with Prolong diamond anti-fade with DAPI (Thermo Fisher Scientific, Sandton, South Africa). Slides were stored at room temperature for a minimum of 24 h and scanned automatically using the MetaCyte software module of the Metafer 4 scanning system with a 40× objective. For each slide, a minimum of 1000 cells were captured, and the average number of γ-H2AX foci per scanned slide was derived from the MetaCyte software, version 4.3.

4.8. Statistical Analysis

Statistical analysis was performed using Graphpad Prism version 10.2. All data was expressed as the mean ± SD of three independent experiments (n = 3). Statistical significance was determined using two-tailed Student's *t*-test, and $p < 0.05$ was considered statistically significant.

5. Conclusions

Positive EGFR status has long been recognised as a negative prognostic factor in breast cancer, and evidence has pointed out that EGFR is overexpressed in triple-negative cancer [40]. The marked response seen in the MDA-MB-231 and MCF-10A cell lines in this study can be attributed to inhibition of EGFR by CUDC-101. The radiation-enhancing capacity of CUDC-101 was more pronounced when combined with X-rays (SER values of 2.09 and 1.77, for X-rays and protons, respectively). The current results draw attention to the potential benefit of CUDC-101 in the management of triple-negative breast cancers as monotherapy or when combined with X-ray irradiation or proton irradiation. However, the increased toxicity of CUDC-101 on normal cells (MCF-10A) particularly when combined with protons cannot be ignored. Data from a Phase I studies have shown that CUDC-101 in combination with X-rays can be tolerated [76,84]. For these reasons, it is advisable that CUDC-101 in combination with X-rays, rather than with protons, be considered. Although the results show that CUDC-101 has potential to enhance treatment efficacy in combination treatment with radiation, future preclinical *in vivo* research and clinical trials are warranted to confirm these *in vitro* findings.

Supplementary Materials: The following supporting information can be downloaded at: https://www.mdpi.com/article/10.3390/ph17111467/s1, Figure S1: Representative images for apoptosis profiles; Figure S2: Representative images of the cell cycle profile after different treatment conditions.

Author Contributions: Conceptualization, E.N.S., S.N., C.V., and A.J.; methodology, E.N.S., S.N., C.V., and A.J.; formal analysis, E.N.S., S.N., C.V., and A.J.; investigation, E.N.S., S.N., C.V., A.B., A.J., and S.N.; writing—original draft preparation, E.N.S.; writing—review and editing, E.N.S., S.N., C.V., and A.J.; supervision, S.N., C.V., and A.J.; funding acquisition, E.N.S., S.N., C.V., A.B., and A.J. All authors have read and agreed to the published version of the manuscript.

Funding: This research was funded by NRF iThemba Laboratories and Department of Higher Education and Training, South Africa. The APC was funded by the University of Pretoria, Cape Peninsula University of Technology, NRF iThemba Laboratories and GSI Helmholtzzentrum für Schwerionenforschung.

Institutional Review Board Statement: This study was conducted in accordance with the Declaration of Helsinki and approved by the Institutional Ethics Committee of University of Pretoria (Ethics number: 689/2021).

Informed Consent Statement: Not applicable.

Data Availability Statement: The original contributions presented in the study are included in the article/Supplementary Materials, further inquiries can be directed to the corresponding author.

Acknowledgments: We acknowledge the Radiation biology team in the Biophysics Division at iThemba NRF Laboratories, South Africa for assistance with proton data collection. We also acknowledge the Trento Institute of Fundamental Physics (TIFPA) for provision of the proton beam, and the Cellular, Computational, and Integrative Biology (CIBIO) Laboratories where the proton experiments were conducted.

Conflicts of Interest: The authors declare no conflicts of interest.

Ethics Number: 689/2021

References

1. Zhao, X.; Tang, Y.; Wang, S.; Yang, Y.; Fang, H.; Wang, J.; Jing, H.; Zhang, J.; Sun, G.; Chen, S.; et al. Locoregional recurrence patterns in women with breast cancer who have not undergone post-mastectomy radiotherapy. *Radiat. Oncol.* **2020**, *15*, 212. [CrossRef] [PubMed]
2. Kowalchuk, R.O.; Corbin, K.S.; Jimenez, R.B. Particle Therapy for Breast Cancer. *Cancers* **2022**, *14*, 1066. [CrossRef] [PubMed]
3. Corbin, K.S.; Mutter, R.W. Proton therapy for breast cancer: Progress & pitfalls. *Breast Cancer Manag.* **2018**, *7*, BMT06. [CrossRef]
4. Chowdhary, M.; Lee, A.; Gao, S.; Wang, D.; Barry, P.N.; Diaz, R.; Bagadiya, N.R.; Park, H.S.; Yu, J.B.; Wilson, L.D.; et al. Is Proton Therapy a "Pro" for Breast Cancer? A Comparison of Proton vs. Non-proton Radiotherapy Using the National Cancer Database. *Front. Oncol.* **2018**, *8*, 678. [CrossRef] [PubMed]
5. Mutter, R.W.; Choi, J.I.; Jimenez, R.B.; Kirova, Y.M.; Fagundes, M.; Haffty, B.G.; Amos, R.A.; Bradley, J.A.; Chen, P.Y.; Ding, X.; et al. Proton Therapy for Breast Cancer: A Consensus Statement from the Particle Therapy Cooperative Group Breast Cancer Subcommittee. *Int. J. Radiat. Oncol. Biol. Phys.* **2021**, *111*, 337–359. [CrossRef]
6. Luo, W.; Ali, Y.F.; Liu, C.; Wang, Y.; Liu, C.; Jin, X.; Zhou, G.; Liu, N.-A. Particle Therapy for Breast Cancer: Benefits and Challenges. *Front. Oncol.* **2021**, *11*, 662826. [CrossRef]
7. Verma, V.; Rwigema, J.M.; Malyapa, R.S.; Regine, W.F.; Simone, C.B., 2nd. Systematic assessment of clinical outcomes and toxicities of proton radiotherapy for reirradiation. *Radiother. Oncol.* **2017**, *125*, 21–30. [CrossRef]
8. Lühr, A.; von Neubeck, C.; Pawelke, J.; Seidlitz, A.; Peitzsch, C.; Bentzen, S.M.; Bortfeld, T.; Debus, J.; Deutsch, E.; Langendijk, J.A.; et al. "Radiobiology of Proton Therapy": Results of an international expert workshop. *Radiother. Oncol.* **2018**, *128*, 56–67. [CrossRef]
9. Ahmad, R.; Barcellini, A.; Baumann, K.; Benje, M.; Bender, T.; Bragado, P.; Charalampopoulou, A.; Chowdhury, R.; Davis, A.J.; Ebner, D.K.; et al. Particle Beam Radiobiology Status and Challenges: A PTCOG Radiobiology Subcommittee Report. *Int. J. Part. Ther.* **2024**, *13*, 100626. [CrossRef]
10. Baschnagel, A.; Russo, A.; Burgan, W.E.; Carter, D.; Beam, K.; Palmieri, D.; Steeg, P.S.; Tofilon, P.; Camphausen, K. Vorinostat enhances the radiosensitivity of a breast cancer brain metastatic cell line grown *in vitro* and as intracranial xenografts. *Mol. Cancer Ther.* **2009**, *8*, 1589–1595. [CrossRef]

11. Camphausen, K.; Scott, T.; Sproull, M.; Tofilon, P.J. Enhancement of xenograft tumor radiosensitivity by the histone deacetylase inhibitor MS-275 and correlation with histone hyperacetylation. *Clin. Cancer Res.* **2004**, *10*, 6066–6071. [CrossRef] [PubMed]
12. Camphausen, K.; Tofilon, P.J. Inhibition of Histone Deacetylation: A Strategy for Tumor Radiosensitization. *J. Clin. Oncol.* **2007**, *25*, 4051–4056. [CrossRef]
13. Chinnaiyan, P.; Cerna, D.; Burgan, W.E.; Beam, K.; Williams, E.S.; Camphausen, K.; Tofilon, P.J. Postradiation sensitization of the histone deacetylase inhibitor valproic acid. *Clin. Cancer Res.* **2008**, *14*, 5410–5415. [CrossRef] [PubMed]
14. Schlaff, C.D.; Arscott, W.T.; Gordon, I.; Tandle, A.; Tofilon, P.; Camphausen, K. Radiosensitization Effects of Novel Triple-Inhibitor CUDC-101 in Glioblastoma Multiforme and Breast Cancer Cells *In Vitro*. *Int. J. Radiat. Oncol. Biol. Phys.* **2013**, *87*, S650. [CrossRef]
15. Groselj, B.; Sharma, N.L.; Hamdy, F.C.; Kerr, M.; Kiltie, A.E. Histone deacetylase inhibitors as radiosensitisers: Effects on DNA damage signalling and repair. *Br. J. Cancer* **2013**, *108*, 748–754. [CrossRef]
16. Damaskos, C.; Garmpis, N.; Valsami, S.; Kontos, M.; Spartalis, E.; Kalampokas, T.; Kalampokas, E.; Athanasiou, A.; Moris, D.; Daskalopoulou, A.; et al. Histone Deacetylase Inhibitors: An Attractive Therapeutic Strategy Against Breast Cancer. *Anticancer Res.* **2017**, *37*, 35–46. [CrossRef]
17. Lee, J.H.; Choy, M.L.; Ngo, L.; Foster, S.S.; Marks, P.A. Histone deacetylase inhibitor induces DNA damage, which normal but not transformed cells can repair. *Proc. Natl. Acad. Sci. USA* **2010**, *107*, 14639–14644. [CrossRef] [PubMed]
18. Armeanu, S.; Pathil, A.; Venturelli, S.; Mascagni, P.; Weiss, T.S.; Göttlicher, M.; Gregor, M.; Lauer, U.M.; Bitzer, M. Apoptosis on hepatoma cells but not on primary hepatocytes by histone deacetylase inhibitors valproate and ITF2357. *J. Hepatol.* **2005**, *42*, 210–217. [CrossRef]
19. Li, Y.; Seto, E. HDACs and HDAC Inhibitors in Cancer Development and Therapy. *Cold Spring Harb. Perspect. Med.* **2016**, *6*, a026831. [CrossRef]
20. Jenke, R.; Ressing, N.; Hansen, F.K.; Aigner, A.; Buch, T. Anticancer Therapy with HDAC Inhibitors: Mechanism-Based Combination Strategies and Future Perspectives. *Cancers* **2021**, *13*, 634. [CrossRef]
21. Smalley, J.P.; Cowley, S.M.; Hodgkinson, J.T. Bifunctional HDAC Therapeutics: One Drug to Rule Them All? *Molecules* **2020**, *25*, 4394. [CrossRef] [PubMed]
22. Dokmanovic, M.; Clarke, C.; Marks, P.A. Histone deacetylase inhibitors: Overview

and perspectives. *Mol. Cancer Res.* **2007**, *5*, 981–989. [CrossRef] [PubMed]

23. Rajak, H.; Singh, A.; Raghuwanshi, K.; Kumar, R.; Dewangan, P.K.; Veerasamy, R.; Sharma, P.C.; Dixit, A.; Mishra, P. A structural insight into hydroxamic acid based histone deacetylase inhibitors for the presence of anticancer activity. *Curr. Med. Chem.* **2014**, *21*, 2642–2664. [CrossRef] [PubMed]
24. Chiu, H.W.; Yeh, Y.L.; Wang, Y.C.; Huang, W.J.; Chen, Y.A.; Chiou, Y.S.; Ho, S.Y.; Lin, P.; Wang, Y.J. Suberoylanilide hydroxamic acid, an inhibitor of histone deacetylase, enhances radiosensitivity and suppresses lung metastasis in breast cancer *in vitro* and in vivo. *PLoS ONE* **2013**, *8*, e76340. [CrossRef]
25. Chen, X.; Wong, P.; Radany, E.; Wong, J.Y. HDAC inhibitor, valproic acid, induces p53-dependent radiosensitization of colon cancer cells. *Cancer Biother. Radiopharm.* **2009**, *24*, 689–699. [CrossRef]
26. Munshi, A.; Kurland, J.F.; Nishikawa, T.; Tanaka, T.; Hobbs, M.L.; Tucker, S.L.; Ismail, S.; Stevens, C.; Meyn, R.E. Histone deacetylase inhibitors radiosensitize human melanoma cells by suppressing DNA repair activity. *Clin. Cancer Res.* **2005**, *11*, 4912–4922. [CrossRef]
27. Munshi, A.; Tanaka, T.; Hobbs, M.L.; Tucker, S.L.; Richon, V.M.; Meyn, R.E. Vorinostat, a histone deacetylase inhibitor, enhances the response of human tumor cells to ionizing radiation through prolongation of gamma-H2AX foci. *Mol. Cancer Ther.* **2006**, *5*, 1967–1974. [CrossRef]
28. Choi, C.; Lee, G.H.; Son, A.; Yoo, G.S.; Yu, J.I.; Park, H.C. Downregulation of Mcl-1 by Panobinostat Potentiates Proton Beam Therapy in Hepatocellular Carcinoma Cells. *Cells* **2021**, *10*, 554. [CrossRef]
29. Gerelchuluun, A.; Maeda, J.; Manabe, E.; Brents, C.A.; Sakae, T.; Fujimori, A.; Chen, D.J.; Tsuboi, K.; Kato, T.A. Histone Deacetylase Inhibitor Induced Radiation Sensitization Effects on Human Cancer Cells after Photon and Hadron Radiation Exposure. *Int. J. Mol. Sci.* **2018**, *19*, 496. [CrossRef]
30. Johnson, A.M.; Bennett, P.V.; Sanidad, K.Z.; Hoang, A.; Jardine, J.H.; Keszenman, D.J.; Wilson, P.F. Evaluation of Histone Deacetylase Inhibitors as Radiosensitizers for Proton and Light Ion Radiotherapy. *Front. Oncol.* **2021**, *11*, 735940. [CrossRef]
31. Yu, J.I.; Choi, C.; Shin, S.-W.; Son, A.; Lee, G.-H.; Kim, S.-Y.; Park, H.C. Valproic Acid Sensitizes Hepatocellular Carcinoma Cells to Proton Therapy by Suppressing NRF2 Activation. *Sci. Rep.* **2017**, *7*, 14986. [CrossRef]
32. Antrobus, J.; Parsons, J.L. Histone Deacetylases and Their Potential as Targets to Enhance Tumour Radiosensitisation. *Radiation* **2022**, *2*, 149–167. [CrossRef]
33. Abdel-Ghany, S.; Raslan, S.; Tombuloglu, H.; Shamseddin, A.; Cevik, E.; Said, O.A.; Madyan, E.F.; Senel, M.; Bozkurt, A.; Rehman, S.; et al. Vorinostat-loaded titanium

oxide nanoparticles (anatase) induce G2/M cell cycle arrest in breast cancer cells via PALB2 upregulation. *3 Biotech* **2020**, *10*, 407. [CrossRef] [PubMed]

34. Lyu, H.; Hou, D.; Liu, H.; Ruan, S.; Tan, C.; Wu, J.; Hicks, C.; Liu, B. HER3 targeting augments the efficacy of panobinostat in claudin-low triple-negative breast cancer cells. *npj Precis. Oncol.* **2023**, *7*, 72. [CrossRef]
35. Nouriemamzaden, F.; Word, B.; Cotton, E.; Hawkins, A.; Littlejohn, K.; Moore, R.; Miranda-Carbon, G.; Orish, C.N.; Lyn-Cook, B. Modulation of Estrogen α and Progesterone Receptors in Triple Negative Breast Cancer Cell Lines: The Effects of Vorinostat and Indole-3-Carbinol *In Vitro*. *Anticancer Res.* **2020**, *40*, 3669–3683. [CrossRef] [PubMed]
36. Wawruszak, A.; Luszczki, J.J.; Grabarska, A.; Gumbarewicz, E.; Dmoszynska-Graniczka, M.; Polberg, K.; Stepulak, A. Assessment of Interactions between Cisplatin and Two Histone Deacetylase Inhibitors in MCF7, T47D and MDA-MB-231 Human Breast Cancer Cell Lines—An Isobolographic Analysis. *PLoS ONE* **2015**, *10*, e0143013. [CrossRef] [PubMed]
37. Lai, C.-J.; Bao, R.; Tao, X.; Wang, J.; Atoyan, R.; Qu, H.; Wang, D.-G.; Yin, L.; Samson, M.; Forrester, J.; et al. CUDC-101, a Multitargeted Inhibitor of Histone Deacetylase, Epidermal Growth Factor Receptor, and Human Epidermal Growth Factor Receptor 2, Exerts Potent Anticancer Activity. *Cancer Res.* **2010**, *70*, 3647–3656. [CrossRef]
38. Masuda, H.; Zhang, D.; Bartholomeusz, C.; Doihara, H.; Hortobagyi, G.N.; Ueno, N.T. Role of epidermal growth factor receptor in breast cancer. *Breast Cancer Res. Treat.* **2012**, *136*, 331–345. [CrossRef]
39. Hossein-Nejad-Ariani, H.; Althagafi, E.; Kaur, K. Small Peptide Ligands for Targeting EGFR in Triple Negative Breast Cancer Cells. *Sci. Rep.* **2019**, *9*, 2723. [CrossRef]
40. O'Donovan, N.; Crown, J. EGFR and HER-2 antagonists in breast cancer. *Anticancer Res.* **2007**, *27*, 1285–1294.
41. Qiu, L.; Burgess, A.; Fairlie, D.P.; Leonard, H.; Parsons, P.G.; Gabrielli, B.G. Histone deacetylase inhibitors trigger a G2 checkpoint in normal cells that is defective in tumor cells. *Mol. Biol. Cell* **2000**, *11*, 2069–2083. [CrossRef] [PubMed]
42. Kim, H.J.; Bae, S.C. Histone deacetylase inhibitors: Molecular mechanisms of action and clinical trials as anti-cancer drugs. *Am. J. Transl. Res.* **2011**, *3*, 166–179. [PubMed]
43. Bessette, D.C.; Tilch, E.; Seidens, T.; Quinn, M.C.; Wiegmans, A.P.; Shi, W.; Cocciardi, S.; McCart-Reed, A.; Saunus, J.M.; Simpson, P.T.; et al. Using the MCF10A/MCF10CA1a Breast Cancer Progression Cell Line Model to Investigate the Effect of Active, Mutant Forms of EGFR in Breast Cancer Development and

Treatment Using Gefitinib. *PLoS ONE* **2015**, *10*, e0125232. [CrossRef] [PubMed]

44. Choi, C.; Son, A.; Lee, G.H.; Shin, S.W.; Park, S.; Ahn, S.H.; Chung, Y.; Yu, J.I.; Park, H.C. Targeting DNA-dependent protein kinase sensitizes hepatocellular carcinoma cells to proton beam irradiation through apoptosis induction. *PLoS ONE* **2019**, *14*, e0218049. [CrossRef]
45. Bright, S.J.; Flint, D.B.; Chakraborty, S.; McFadden, C.H.; Yoon, D.S.; Bronk, L.; Titt, U.; Mohan, R.; Grosshans, D.R.; Sumazin, P.; et al. Nonhomologous End Joining Is More Important Than Proton Linear Energy Transfer in Dictating Cell Death. *Int. J. Radiat. Oncol. Biol. Phys.* **2019**, *105*, 1119–1125. [CrossRef]
46. Vitti, E.T.; Parsons, J.L. The Radiobiological Effects of Proton Beam Therapy: Impact on DNA Damage and Repair. *Cancers* **2019**, *11*, 946. [CrossRef]
47. Szymonowicz, K.; Krysztofiak, A.; Linden, J.V.; Kern, A.; Deycmar, S.; Oeck, S.; Squire, A.; Koska, B.; Hlouschek, J.; Vüllings, M.; et al. Proton Irradiation Increases the Necessity for Homologous Recombination Repair Along with the Indispensability of Non-Homologous End Joining. *Cells* **2020**, *9*, 889. [CrossRef]
48. Costes, S.V.; Boissière, A.; Ravani, S.; Romano, R.; Parvin, B.; Barcellos-Hoff, M.H. Imaging features that discriminate between foci induced by high- and low-LET radiation in human fibroblasts. *Radiat. Res.* **2006**, *165*, 505–515. [CrossRef]
49. Leatherbarrow, E.L.; Harper, J.V.; Cucinotta, F.A.; O'Neill, P. Induction and quantification of gamma-H2AX foci following low and high LET-irradiation. *Int. J. Radiat. Biol.* **2006**, *82*, 111–118. [CrossRef]
50. Oeck, S.; Szymonowicz, K.; Wiel, G.; Krysztofiak, A.; Lambert, J.; Koska, B.; Iliakis, G.; Timmermann, B.; Jendrossek, V. Relating Linear Energy Transfer to the Formation and Resolution of DNA Repair Foci After Irradiation with Equal Doses of X-ray Photons, Plateau, or Bragg-Peak Protons. *Int. J. Mol. Sci.* **2018**, *19*, 3779. [CrossRef]
51. Gerelchuluun, A.; Hong, Z.; Sun, L.; Suzuki, K.; Terunuma, T.; Yasuoka, K.; Sakae, T.; Moritake, T.; Tsuboi, K. Induction of in situ DNA double-strand breaks and apoptosis by 200 MeV protons and 10 MV X-rays in human tumour cell lines. *Int. J. Radiat. Biol.* **2011**, *87*, 57–70. [CrossRef]
52. Bracalente, C.; Ibañez, I.L.; Molinari, B.; Palmieri, M.; Kreiner, A.; Valda, A.; Davidson, J.; Durán, H. Induction and persistence of large γH2AX foci by high linear energy transfer radiation in DNA-dependent protein kinase-deficient cells. *Int. J. Radiat. Oncol. Biol. Phys.* **2013**, *87*, 785–794. [CrossRef] [PubMed]
53. Grosse, N.; Fontana, A.O.; Hug, E.B.; Lomax, A.; Coray, A.; Augsburger, M.; Paganetti, H.; Sartori, A.A.; Pruschy, M. Deficiency in homologous recombination

renders Mammalian cells more sensitive to proton versus photon irradiation. *Int. J. Radiat. Oncol. Biol. Phys.* **2014**, *88*, 175–181. [CrossRef]

54. Hojo, H.; Dohmae, T.; Hotta, K.; Kohno, R.; Motegi, A.; Yagishita, A.; Makinoshima, H.; Tsuchihara, K.; Akimoto, T. Difference in the relative biological effectiveness and DNA damage repair processes in response to proton beam therapy according to the positions of the spread out Bragg peak. *Radiat. Oncol.* **2017**, *12*, 111. [CrossRef] [PubMed]
55. Fontana, A.O.; Augsburger, M.A.; Grosse, N.; Guckenberger, M.; Lomax, A.J.; Sartori, A.A.; Pruschy, M.N. Differential DNA repair pathway choice in cancer cells after proton- and photon-irradiation. *Radiother. Oncol.* **2015**, *116*, 374–380. [CrossRef] [PubMed]
56. Liu, Q.; Ghosh, P.; Magpayo, N.; Testa, M.; Tang, S.; Gheorghiu, L.; Biggs, P.; Paganetti, H.; Efstathiou, J.A.; Lu, H.M.; et al. Lung cancer cell line screen links fanconi anemia/BRCA pathway defects to increased relative biological effectiveness of proton radiation. *Int. J. Radiat. Oncol. Biol. Phys.* **2015**, *91*, 1081–1089. [CrossRef] [PubMed]
57. Gerelchuluun, A.; Manabe, E.; Ishikawa, T.; Sun, L.; Itoh, K.; Sakae, T.; Suzuki, K.; Hirayama, R.; Asaithamby, A.; Chen, D.J.; et al. The major DNA repair pathway after both proton and carbon-ion radiation is NHEJ, but the HR pathway is more relevant in carbon ions. *Radiat. Res.* **2015**, *183*, 345–356. [CrossRef] [PubMed]
58. Mao, Z.; Bozzella, M.; Seluanov, A.; Gorbunova, V. DNA repair by nonhomologous end joining and homologous recombination during cell cycle in human cells. *Cell Cycle* **2008**, *7*, 2902–2906. [CrossRef]
59. Mladenov, E.; Kalev, P.; Anachkova, B. The Complexity of Double-Strand Break Ends is a Factor in the Repair Pathway Choice. *Radiat. Res.* **2009**, *171*, 397–404. [CrossRef] [PubMed]
60. Lee, K.J.; Mann, E.; Wright, G.; Piett, C.G.; Nagel, Z.D.; Gassman, N.R. Exploiting DNA repair defects in triple negative breast cancer to improve cell killing. *Ther. Adv. Med. Oncol.* **2020**, *12*, 1758835920958354. [CrossRef]
61. Rostek, C.; Turner, E.L.; Robbins, M.; Rightnar, S.; Xiao, W.; Obenaus, A.; Harkness, T.A. Involvement of homologous recombina- tion repair after proton-induced DNA damage. *Mutagenesis* **2008**, *23*, 119–129. [CrossRef] [PubMed]
62. Gaymes, T.J.; Padua, R.A.; Pla, M.; Orr, S.; Omidvar, N.; Chomienne, C.; Mufti, G.J.; Rassool, F.V. Histone deacetylase inhibitors (HDI) cause DNA damage in leukemia cells: A mechanism for leukemia-specific HDI-dependent apoptosis? *Mol. Cancer Res.* **2006**, *4*, 563–573. [CrossRef] [PubMed]
63. Petruccelli, L.A.; Dupéré-Richer, D.; Pettersson, F.; Retrouvey, H.; Skoulikas, S.;

Miller, W.H., Jr. Vorinostat induces reactive oxygen species and DNA damage in acute myeloid leukemia cells. *PLoS ONE* **2011**, *6*, e20987. [CrossRef] [PubMed]

64. Vanderwaeren, L.; Dok, R.; Verstrepen, K.; Nuyts, S. Clinical Progress in Proton Radiotherapy: Biological Unknowns. *Cancers* **2021**, *13*, 604. [CrossRef]
65. Di Pietro, C.; Piro, S.; Tabbì, G.; Ragusa, M.; Di Pietro, V.; Zimmitti, V.; Cuda, F.; Anello, M.; Consoli, U.; Salinaro, E.T.; et al. Cellular and molecular effects of protons: Apoptosis induction and potential implications for cancer therapy. *Apoptosis* **2006**, *11*, 57–66. [CrossRef]
66. Lee, K.B.; Lee, J.S.; Park, J.W.; Huh, T.L.; Lee, Y.M. Low energy proton beam induces tumor cell apoptosis through reactive oxygen species and activation of caspases. *Exp. Mol. Med.* **2008**, *40*, 118–129. [CrossRef]
67. Alan Mitteer, R.; Wang, Y.; Shah, J.; Gordon, S.; Fager, M.; Butter, P.P.; Jun Kim, H.; Guardiola-Salmeron, C.; Carabe-Fernandez, A.; Fan, Y. Proton beam radiation induces DNA damage and cell apoptosis in glioma stem cells through reactive oxygen species. *Sci. Rep.* **2015**, *5*, 13961. [CrossRef]
68. Zhang, X.; Lin, S.H.; Fang, B.; Gillin, M.; Mohan, R.; Chang, J.Y. Therapy-resistant cancer stem cells have differing sensitivity to photon versus proton beam radiation. *J. Thorac. Oncol.* **2013**, *8*, 1484–1491. [CrossRef]
69. Finnberg, N.; Wambi, C.; Ware, J.H.; Kennedy, A.R.; El-Deiry, W.S. Gamma-radiation (GR) triggers a unique gene expression profile associated with cell death compared to proton radiation (PR) in mice in vivo. *Cancer Biol. Ther.* **2008**, *7*, 2023–2033. [CrossRef]
70. Ristic-Fira, A.M.; Todorovic, D.V.; Koricanac, L.B.; Petrovic, I.M.; Valastro, L.M.; Cirrone, P.G.; Raffaele, L.; Cuttone, G. Response of a human melanoma cell line to low and high ionizing radiation. *Ann. N. Y. Acad. Sci.* **2007**, *1095*, 165–174. [CrossRef]
71. Mooney, L.M.; Al-Sakkaf, K.A.; Brown, B.L.; Dobson, P.R. Apoptotic mechanisms in T47D and MCF-7 human breast cancer cells. *Br. J. Cancer* **2002**, *87*, 909–917. [CrossRef] [PubMed]
72. Jänicke, R.U. MCF-7 breast carcinoma cells do not express caspase-3. *Breast Cancer Res. Treat.* **2009**, *117*, 219–221. [CrossRef] [PubMed]
73. Natarajan, U.; Venkatesan, T.; Radhakrishnan, V.; Samuel, S.; Rathinavelu, A. Differential Mechanisms of Cell Death Induced by HDAC Inhibitor SAHA and MDM2 Inhibitor RG7388 in MCF-7 Cells. *Cells* **2018**, *8*, 8. [CrossRef] [PubMed]
74. Escobar, M.L.; Echeverría, O.M.; Vázquez-Nin, G.H. Necrosis as Programmed Cell Death. In *Cell Death*; Tobias, M.N., Ed.; IntechOpen: Rijeka, Croatia, 2015;

Chapter 19.
75. Poliseno, L.; Bianchi, L.; Citti, L.; Liberatori, S.; Mariani, L.; Salvetti, A.; Evangelista, M.; Bini, L.; Pallini, V.; Rainaldi, G. Bcl2-low-expressing MCF7 cells undergo necrosis rather than apoptosis upon staurosporine treatment. *Biochem. J.* **2004**, *379*, 823–832. [CrossRef] [PubMed]
76. Galloway, T.J.; Wirth, L.J.; Colevas, A.D.; Gilbert, J.; Bauman, J.E.; Saba, N.F.; Raben, D.; Mehra, R.; Ma, A.W.; Atoyan, R.; et al. A Phase I Study of CUDC-101, a Multitarget Inhibitor of HDACs, EGFR, and HER2, in Combination with Chemoradiation in Patients with Head and Neck Squamous Cell Carcinoma. *Clin. Cancer Res.* **2015**, *21*, 1566–1573. [CrossRef]
77. Schlaff, C.; Arscott, W.; Gordon, I.; Camphausen, K.; Tandle, A. Human EGFR-2, EGFR and HDAC triple-inhibitor CUDC-101 enhances radiosensitivity of GBM cells. *Biomed. Res. J.* **2015**, *2*, 105. [CrossRef]
78. Li, G.; Tian, Y.; Zhu, W.-G. The Roles of Histone Deacetylases and Their Inhibitors in Cancer Therapy. *Front. Cell Dev. Biol.* **2020**, *8*, 576946. [CrossRef]
79. Bhaskara, S.; Chyla, B.J.; Amann, J.M.; Knutson, S.K.; Cortez, D.; Sun, Z.W.; Hiebert, S.W. Deletion of histone deacetylase 3 reveals critical roles in S phase progression and DNA damage control. *Mol. Cell* **2008**, *30*, 61–72. [CrossRef]
80. Bhaskara, S.; Knutson, S.K.; Jiang, G.; Chandrasekharan, M.B.; Wilson, A.J.; Zheng, S.; Yenamandra, A.; Locke, K.; Yuan, J.L.; Bonine-Summers, A.R.; et al. Hdac3 is essential for the maintenance of chromatin structure and genome stability. *Cancer Cell* **2010**, *18*, 436–447. [CrossRef]
81. Park, S.H.; Ozden, O.; Liu, G.; Song, H.Y.; Zhu, Y.; Yan, Y.; Zou, X.; Kang, H.J.; Jiang, H.; Principe, D.R.; et al. SIRT2-Mediated Deacetylation and Tetramerization of Pyruvate Kinase Directs Glycolysis and Tumor Growth. *Cancer Res.* **2016**, *76*, 3802–3812. [CrossRef]
82. Dryden, S.C.; Nahhas, F.A.; Nowak, J.E.; Goustin, A.S.; Tainsky, M.A. Role for human SIRT2 NAD-dependent deacetylase activity in control of mitotic exit in the cell cycle. *Mol. Cell Biol.* **2003**, *23*, 3173–3185. [CrossRef] [PubMed]
83. Sun, Y.; Liu, P.Y.; Scarlett, C.J.; Malyukova, A.; Liu, B.; Marshall, G.M.; MacKenzie, K.L.; Biankin, A.V.; Liu, T. Histone deacetylase 5 blocks neuroblastoma cell differentiation by interacting with N-Myc. *Oncogene* **2014**, *33*, 2987–2994. [CrossRef] [PubMed]
84. Tommasino, F.; Rovituso, M.; Bortoli, E.; La Tessa, C.; Petringa, G.; Lorentini, S.; Verroi, E.; Simeonov, Y.; Weber, U.; Cirrone, P.; et al. A new facility for proton radiobiology at the Trento proton therapy centre: Design and implementation. *Phys.*

Med. **2019**, *58*, 99–106. [CrossRef] [PubMed]
85. Coms¸a, S; Cîmpean, A.M.; Raica, M. The Story of MCF-7 Breast Cancer Cell Line: 40 years of Experience in Research. *Anticancer Res.* **2015**, *35*, 3147–3154.

Critical discussion to the Chapter

The management of breast cancer has improved over the years and the life expectancy of breast cancer survivors has also improved. Enhancing the effectiveness of radiation therapy and sparing normal tissues has therefore become important. The findings of this study chapter highlighted the potential use of CUDC-101 to enhance the response, not only to X-irradiation which is most commonly used in clinical practice, but to proton irradiation as well as evidenced by increased sensitization enhancement ratios following proton therapy, particularly in the triple negative MDA-MB-231 cell line. Triple negative breast cancer, which is characterized by an aggressive phenotype and resistance to common therapies, remains a challenge. Further, irradiation with proton therapy, which is advantageous in sparing normal tissues due to its superior physical dose distribution, has increased in use as evidenced by the exponential increase in the number of proton therapy units across the world. However, the relative biological effectiveness of protons is similar to that of X-rays, the use of a radiosensitizer would therefore improve the therapeutic ratio. Impaired DNA double strand break following the combination treatment of CUDC-101 and proton irradiation were identified as the underlying mechanisms of radiosensitisation. To date, limited studies have been conducted on combination therapy of HDACi and proton irradiation with respect to DNA DSB induction and repair. The findings of the study chapter therefore contribute new knowledge which highlights the potential use of CUDC-101 as radiosensitising agent when combined with either X-rays or protons. The effect of CUDC-101 was more pronounced when combined with protons in the triple negative cell line. As mentioned in the paper, to my knowledge the paper is the first to report on the effect of CUDC-101 in breast cell lines.

Personal contribution to Paper 4:

Seane, E.N.; Nair, S.; Vandevoorde, C.; Bisio, A.; Joubert, A. Multi-Target Inhibitor CUDC-101 Impairs DNA Damage Repair and Enhances Radiation Response in Triple-Negative Breast Cell Line. Pharmaceuticals 2024, 17, Article 1467. https://doi.org/10.3390/ph17111467; Impact factor 4.3.

This manuscript was based on original and novel ideas by the Candidate in the field of triple negative, breast cancer (TNBC) and treatment employing cutting-edge research combination techniques in cancer therapy. The research was done in collaboration with four other researchers, some of whom are experts in the field. The study was based on the idea and conception thought out by the candidate about various strategies and future research

knowledge, understanding and scope for the best way forward in treating breast cancer which kills more women globally. This work was done in the Radiation biology section of

iThemba Laboratory for Accelerators Based Sciences (LABS), Faure, Cape Town, South Africa (SA). Proton beam was generated at Trento Institute of Fundamental Physics and Applications (TIFPA), Azienda Provinciale per i Servizi Sanitari, Trento, Italy. All the proton experiments were conducted at the Department of Cellular, Computational and Integrative Biology (CIBIO) Laboratories, Via Sommarive, 9, Povo, 38123 Trento, Italy. The work was done under the guidance of Professor Annie Joubert, Department of Physiology, University of Pretoria. The Candidate was the main contributor, and she was involved in designing and doing the experiments, collection of data, formulating and writing the manuscript. Her contribution was about 80% while the other authors assisted in analysis and reviewing the manuscript prior to publication. This article is well cited in the field of breast cancer treatment.

CHAPTER 4: RESULTS

Submitted Article(in press):

Seane, E.; Nair, S.; Vandevoorde, C.; Bisio, A.; Joubert, A. CUDC-101 and Proton Irradiation Reduces Migration and Invasion Capacity of Triple Negative Breast Cell Line. *Preprints* **2024**, 2024110513. https://doi.org/10.20944/preprints202411.0513.v1

Proof of manuscript submission is included as **Annexure D**

This Chapter was also presented at:
60th South African Association of Physicists in Medicine and Biology (SAAPMB) Congress
16-20 September 2024
Bloemfontein

Bridging text:

The manuscript presented in this chapter presents the results of objective 5, i.e. migration and invasion assays. The manuscript includes data from both HDACi SAHA and CUDC-101.

Article

CUDC-101 and Proton Irradiation Reduces Migration and Invasion Capacity of Triple Negative Breast Cell Line

Elsie Neo Seane [1,2,3,*], Shankari Nair [4], Charlot Vandevoorde [5], Alessandra Bisio [6] and Anna Joubert [7]

[1] Department of Radiography, School of Health Care Sciences, Faculty of Health Sciences, University of Pretoria, Pretoria 0028, South Africa
[2] Department of Medical Imaging and Therapeutic Sciences, Faculty of Health and Wellness, Cape Peninsula University of Technology, Bellville 7535, South Africa
[3] Separate Sector Cyclotron (SSC) laboratory, Radiation Biophysics Division, iThemba LABS, Cape Town, South Africa
[4] Bayer AG, Research and Development, Pharmaceuticals, 13342 Berlin, Germany
[5] Department of Biophysics, GSI Helmholtzzentrum für Schwerionenforschung, 64291 Darmstadt, Germany
[6] Department of Cellular, Computational and Integrative Biology, Via Sommarive, 9, Povo, 38123 Trento, Italy
[7] Department of Physiology, School of Medicine, Faculty of Health Sciences, University of Pretoria, Pretoria, South Africa
* Correspondence: seanee@cput.ac.za

Simple Summary: Cases of metastatic breast cancer are estimated to have increased by 54.8% in 2030 compared to 2015. Triple negative breast cancer, which is more aggressive and has high metastatic potential is more common in young African American and in Sub-Saharan African populations. The aim of our study was to assess the effectiveness of histone deacetylase inhibitors SAHA and CUDC-101 in reducing metastatic potential in breast cell lines. We assessed migration and invasion of the three breast cell lines under different treatment conditions and determined that proton irradiation alone or in combination with CUDC-101 can reduce metastasis.

Abstract: Background: Radiation therapy remains to be one of the main treatment modalities for the management of breast cancer. Several reports have asserted that low dose photon irradiation, which is the most available radiation modality, can promote migration and invasion of malignant cells. Also, some approved chemotherapy drugs used in the management of breast cancer are implicated in promoting metastasis. Therefore, it has become critical to unravel novel therapies that are effective on tumour cells and can reduce the metastatic potential. **Methods**: Malignant (MCF-7), triple-negative (MDA-MB-231) and spontaneously immortalized MCF-10A human breast cancer cell lines were pre-treated with pan-HDACi SAHA or multi-target inhibitor CUDC-101 and exposed to 2Gy and 6Gy 148 MeV mid-SOBP protons or 250KeV X-rays. Wound healing and trans-well invasion assays were performed. Imaging was done at 4-hour intervals for wound healing assays, and at 24-hours post-irradiation for trans-well migration assays. **Results**: Significant reduction in migration was observed after treatment with proton alone at lower doses (2Gy) and at higher (6Gy) doses in the MCF-7 cell line. In the triple negative cell line MDA-MB-231 cell line, reduction in migration was evident at higher doses(6Gy) protons. Combination therapy of CUDC-101 or SAHA and protons also inhibited migration and invasion in the MDA-MB-231 cell line. Treatment with CUDC-101 monotherapy showed benefit in reducing migration and invasion in the MDA-MB-231 cell line. Treatment with SAHA, either as monotherapy or in combination with X-rays, promoted migration in the MCF-7 cell line. **Conclusions**: CUDC-101 or proton monotherapies, as well as combination therapy with radiation, inhibits migration as monotherapy particularly in the MDA-MB-231 which has high metastatic potential.

Keywords: metastasis; cell migration and invasion; histone deacetylase inhibitor; triple negative breast cancer

1. Introduction

Cancer metastases remain to be a major cause of death in cancer patients and a significant challenge to public health worldwide [1,2]. Metastasis is a multi-step process which includes local tumor cell invasion, entry into the vasculature followed by the exit of carcinoma cells from the circulation and colonization at the distal sites [3]. Migration and invasion capacity of breast cancer cells has been linked to the reversible process of epithelial-to-mesenchymal transition (EMT), where the epithelial phenotype is lost and mesenchymal phenotype is gained, leading to metastasis [4]. During EMT, epithelial cadherin (E-cadherin), which regulates cell adhesion is lost and mesenchymal cadherin (M-cadherin) is induced. Loss of E-cadherin has been associated with increased resistance to epidermal growth factor receptor (EGFR) inhibitors, resistance to radiotherapy and increased circulating tumour cells [5–8]. Class 1 histone deacetylase (HDACs) (HDAC 1,2,3 and 8) play an important role in regulating E-cadherin. Expression of E-cadherin has been reported to be suppressed by HDACs [9–11]. Therefore, inhibition of HDACs by HDACi is, in theory, expected to reverse the repression of E-cadherin. But controversy remains around the mechanisms through which HDACi affect the EMT. Several studies have reported reversal of EMT while others have observed induction of EMT in different types of solid tumours including cholangiocarcinoma, prostate, lung, ductal pancreatic and breast, to name a few, using different classes of HDACi [6,12–16]. Similarly, in breast cancer, conflicting reports exist on the effect of the different HDACi, including SAHA, on migration and invasion [17–19]. Taken together, it is tempting to conclude that the role of EMT is dependent on the type of cell and the class of HDACi used. Nevertheless, the role EMT in breast cancer metastasis has been brought under question and remains a matter of discussion [20].

Another point of ongoing discussions is the fact that radiation promotes metastasis. Ample evidence has supported that non-curative doses of photon radiation induce migration [21–31]. However, more recent reports suggest that the clinical significance of this process is small when curative doses of radiation are given but can be significant after non-curative doses of photon radiation and in irradiated normal tissues [32]. The suggested mechanisms of radiation-induced migration include vascular damage, presence of hypoxia, epithelial-mesenchymal transition, cytokine expression and modulation of matrix-degrading enzymes [22,33–37]. Treatment with carbon ion beams was subsequently suggested as one of the strategies to counteract malignant cell migration and invasion after radiotherapy treatment [22]. Both carbon ion and proton therapies have a superior dose distribution compared to X-rays that allows most of the dose to be delivered at the Bragg peak, but carbon ions have an exit dose due to nuclear fragmentation [38]. Also, treatment centers that offer carbon ion

are very limited compared to proton treatment centers. Existing reports on the effect of proton therapy on migration and invasion suggest that it is cell line dependent. For example, proton irradiation induced migration and invasion in human glioma cells, but inhibited migration and invasion in melanoma cells and HT1080 human fibrosarcoma cells [39–41]. All considered, the study set out to determine the effectiveness of pan-HDAC inhibitor SAHA and multi-target inhibitor CUDC-101 in reducing migration and invasion of MCF-7, MDA-MB-231 and MCF-10A breast cell lines.

2. Materials and Methods

2.1. Cell Cultures

MCF-7 and MCF-10A (gifted by the Physiology Department, University of Pretoria) cells were cultured in Dulbecco's Modified Eagle's Medium F-12 (DMEM-F12; GibcoTM, Thermo Fisher Scientific, Sandton, South Africa) and Ham's F-12 (GibcoTM, Thermo Fisher Scientific, Sandton, South Africa) supplemented with 10% foetal bovine serum (FBS) (GibcoTM, Thermo Fisher Scientific, Sandton, South Africa), 100 µg/mL penicillin (GibcoTM, Thermo Fisher Scientific, Sandton, South Africa), and 100 µg/mL streptomycin for bacterial contamination. MCF-10A medium was further supplemented with epidermal growth factor (EGF) (20 ng/mL final concentration) (GibcoTM, Thermo Fisher Scientific, Sandton, South Africa) and hydrocortisone (0.5 mg/mL final concentration) (Sigma- Aldrich, St. Louis, MO, USA).

MDA-MB-231 cells (gifted by the Department of Natural Sciences, University of Western Cape) were cultured in Roswell Park Memorial Institute (RPMI) 1640 (GibcoTM, Thermo Fisher Scientific, Sandton, South Africa) supplemented with 10% FBS, 100 µg/L penicillin and 100 µg/mL streptomycin (Sigma-Aldrich, St. Louis, MO, USA).

All cell lines were cultured in T275 or T75 cell culture flasks (Thermo Fisher Scientific, Sandton, South Africa) under standard conditions in a humidified incubator at 37 °C, 5% CO_2 (Forma series 3 water jacketed incubator, Thermo Fisher Scientific, Waltham, MA, USA). Cell growth was assessed over 24 h intervals and sub-cultured once 80% confluence was reached.

2.2. Histone Deacetylase Inhibitors

SAHA (molecular weight of 264.32) and CUDC-101 (molecular weight of 434.49) Figure 1, were purchased from Sigma Aldrich (Sigma-Aldrich, Missouri, USA) and 1 mM stock solution was prepared according to the manufacturer's instructions (5 mg of CUDC-101 was resolved in 11.5077 mL dimethylsulfide (DMSO), and 5mg of SAHA was resolved in

18.9165 mL DMSO) (Biotechnology Hub, Johannesburg, South Africa) and stored at-20° for short term storage and at -80° for long term storage.

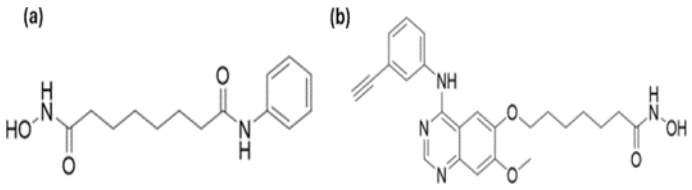

Figure 1. Molecular structures of SAHA (**a**) and CUDC-101 (**b**).

2.3. Irradiations

Photon irradiations were performed using the 250 kVp X-Rad 320 unit (Precision X-ray, Madison, WI, USA) at a mean dose rate of 0.69 Gy/min at a Source Surface Distance (SSD) of 50 cm. Calibrations of the unit were performed according to the Technical Report Series-398 (TRS-398) protocol, with a Farmer 117 chamber for which a chamber calibration factor has been obtained from the National Metrology Institute of South Africa (NMISA).

Proton irradiations were performed at the Trento Institute for Fundamental Physics and Application (TIFPA). An SOBP beam of 2.5 cm has been produced, as detailed in Tommasino et al. through a 2D rang modulator applied to a beam with initial energy of 148 MeV/u and enlarged with a dual ring system to a lateral profile maintaining a 98% dose uniformity across a 6 cm diameter. The beam was calibrated with EBT gafchromic film and Markus chamber measurements. The cells were exposed after 11 cm of solid water slabs, corresponding to 11.45 cm of water [42]. For both X-ray and proton irradiations, cells were irradiated in 5 mL media in T25 flasks.

2.4. Wound Healing Assays

Wound healing assays were performed using the 2 well cell culture-Insert (ibidi, Gräfelfing, Germany). Cells were harvested and seeded in each well of the inserts and allowed to attach and reach 80% confluency. Cells were treated with IC50 concentrations of the HDACi for 24 hours and irradiated with protons or X-rays. Immediately after irradiation, the inserts were removed and imaging using CytoSMART^{TM} 2 live imaging system (Whitehead scientific, Cape Town, South Africa) was done at 0hrs (immediately) and every 4 hours for 24 hours. Images were analysed using the ImageJ processing software (Version 1.54i, National Institutes of Health, Bethesda, MD, United States of America.

2.5. Trans-Well Invasion Assays

Cell invasion was assessed using 8µm pore trans-well inserts in 24 well plates (Greiner bio-one®, North Carolina, United States of America). Geltrex basement matrix (Gibco, Thermo Fisher Scientific, South Africa) was removed from freezer and thawed in ice in the fridge at 4-8°C. Geltrex (50µl) was carefully added to the upper chamber of the insert using pre-cooled pipette tips and the plates were incubated at 37°C for 30 minutes to allow the Geltrex to solidify. Cells were harvested using serum free media and 5000 cells were seeded in the upper chamber of the insert. Complete media (600µl) with 10% fetal bovine serum (FBS) were added at the bottom of the bottom wells of the 24 well plate and the trans-well insert was placed in the media containing plate. The plates were incubated for a further 24 hours at 37°C to allow cell invasion. After 24 hours, trans-well inserts were washed in PBS and cells were fixed with 4% paraformaldehyde (Merck Life Sciences, Johannesburg, South Africa) and stained using 2% crystal violet (Inqaba Biotechnical Industries, Pretoria, South Africa). Cells that did not invade were carefully removed from the upper chamber using a wet cotton swab and the inserts were allowed to dry for a minimum of 24 hours. Four quadrants of the inserts were imaged at 10X magnification using the CytoSMART^{TM} 2 live imaging system (Whitehead Scientific, Cape Town, South Africa).

2.6. Statistical Analysis

Statistical analysis was performed using Graphpad Prism version 10.2. All data was expressed as the mean ± SD of three independent experiments (n=3). Statistical significance was determined using two-tailed Student's test, and $p < 0.05$ was considered statistically significant.

3. Results

Wound healing (migration) and trans-well invasion assays were performed to assess the effect of HDACi SAHA and CUDC-101 on the migration and invasion capacity of MCF-7, MDA-MB-231 and spontaneously immortalised MCF-10A cell lines. Cells were treated with half maximal inhibitory concentration (IC_{50}) concentrations of SAHA or CUDC-101 and 24 hours after drug treatment; cells were irradiated with either 2Gy or 6Gy X-rays or protons. In the MCF-7 cell line at 16 hours post treatment, significantly increased migration was seen after treatment with SAHA monotherapy compared to the untreated control ($p = 0.0008$). Significantly increased migration was also evident in SAHA pre-treated cells after 2Gy ($p = 0.0016$) and 6Gy ($p = 0.0018$) protons, as well as after 2Gy ($p = 0.0005$) and 6Gy ($p = 0.0341$) X-rays (Figures 1 a and b). Similarly, from the results of the trans-well invasion assays, compared to X-ray alone, a significantly increased number of invaded cells were

seen in SAHA pre-treated cells after 2Gy (p = 0.0091) and 6Gy (p = 0.0088) respectively. A non- significant difference in the number of invaded cells was observed in cells treated with SAHA and 2Gy proton (p = 0.24) or 6Gy protons (p = 0.2979) (Figures 1 c-d). Taken together, the results suggest that SAHA increases migration and invasion in the MCF-7 cell line. Treatment with protons alone statistically significantly reduced migration compared to combination treatment of protons and CUDC-101 with p = 0.0054 and p = 0.0018 after 2Gy and 6Gy protons respectively. Treatment with protons also statistically significantly reduced migration compared to X-rays with p = 0.0014 and p = 0. 0017 after 2Gy and 6Gy respectively. A similar pattern of results was seen after combination treatments where significant reduction in migration was seen in CUDC-101 pre-treated cells after treatment with 2Gy protons compared to 2Gy X-rays (p = 0.0115, as well as after 6Gy protons compared to 6Gy X-rays (p = 0.0454). Reduction in migration in the proton-irradiated cells was still evident at 24 hours post treatment (Figures 1a-b). The latter result suggests that proton irradiation alone reduces migration and invasion to a greater degree compared to the combination treatment of protons and CUDC-101 in the MCF-7 cell lines. Representative images are shown in Figures 1(e)-(f).

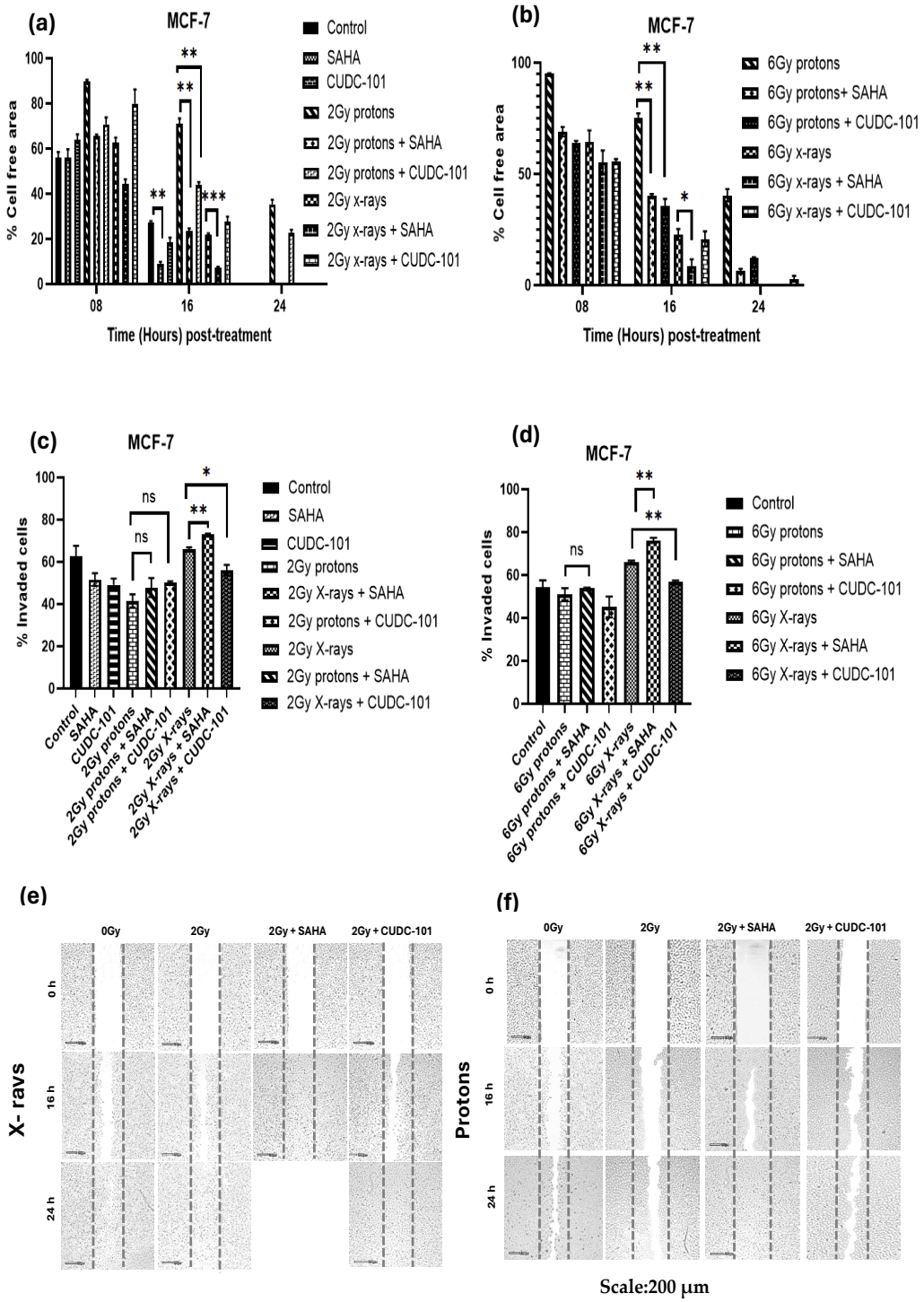

Figure 2. Effect of SAHA and CUDC-101 on migration (**a**)-(**b**) and invasion (**c**)-(**d**) of MCF-7 cells. Representative images are shown in (**e**) and (**f**). Samples were treated with SAHA (1.2μM) and CUDC-101 (0.3μM) and irradiated with either protons or X-rays. Histograms show the mean ± SD of three independent experiments, (n=3). Comparisons were conducted using unpaired two-tailed Student t test, $p < 0.05$ was considered significant.

In the MDA-MB-231 cell line, significantly reduced migration was observed after treatment with CUDC-101 monotherapy compared to either proton irradiation (p = 0.0056) or X-rays (p = 0.0072). Compared to radiation alone, significantly reduced migration was seen after combination treatment of CUDC-101 and 2Gy protons (p = 0.0183) or 6Gy protons (p = 0.0095), as well as after 2Gy X-rays (p = 0.0015) and 6Gy X-rays (p = 0.0115 (Figures 2a-b). Contrary to the observations made in the MCF-7 cell line, proton irradiation (2Gy or 6Gy) alone did not reduce migration (Figure 2 a-b). Comparison of migration after 2Gy protons and combination treatment of SAHA and 2Gy protons yielded a non- significant result (p = 0.571). However, a significant reduction in migration was seen when SAHA was combined with 2Gy X-rays (p = 0.0022), 6Gy X-rays (p = 0.004) and 6Gy protons (p = 0.0066). Taken together, the results highlight the effect of CUDC-101 in reducing migration as monotherapy or in combination with X-rays. Also, the results suggest that SAHA augments the effect of X-rays in reducing migration but does not augment the effect of protons. Reduction in migration was evident at 24 hours after treatment with CUDC-101 alone, 2Gy X-rays and CUDC-101 as well as with 2Gy X- rays and SAHA (Figures 2 a-b). These observations were, however, not supported by the results of the trans-well invasion assay. Nevertheless, a significant difference in the number of invaded cells was seen after treatment with SAHA and 6Gy protons compared to protons alone (p=0.0294).

In the MCF-10A cell line, treatment with CUDC-101 alone significantly reduced migration compared to the control (p = 0.0032). This observation was supported by the results of the trans-well invasion assays which shown significantly reduced number of invaded cells after treatment with CUDC-101 compared with the control (p = 0.0373). Proton irradiation alone also significantly reduced migration compared to X-rays, p = 0.0002 and p = 0.0005 after 2Gy and 6Gy, respectively. However, the results of the trans-well invasion assay showed a non-significant difference between protons and X-rays, p = 0.3629 after 2Gy and p = 0.1400 after 6Gy protons. Compared to radiation alone, combination treatment of both HDACi and proton irradiation (2Gy or 6Gy) yielded a non-significant result, p = 0.2598 and p = 0.0.0712 in SAHA and CUDC-101 pre-treated cells, respectively, suggesting that addition of both HDACi did not enhance the effect of protons in reducing migration. A significant difference in the number of invaded cells was observed after combination treatment of both HDACi and X-irradiation, p = 0.0295 and p = 0.0012 in SAHA and CUDC-101 pre-treated cells respectively. Similarly, at higher doses (6Gy), pre-treatment with both HDACi significantly reduced migration when combined with X-rays, p = 0.0064 and p = 0.0027 in SAHA and CUDC-101 pre-treated cells, respectively.

MCF-7 and MCF-10A were co-cultured, pre-treated with SAHA or CUDC-101 and irradiated with 2Gy or 6Gy X-rays. Wound healing assays were performed 24 hours after drug treatment. Comparison of the untreated controls at 16 hours showed increased migration (wound closure) when MCF-7 and MCF-10A cells were co-cultured compared to the untreated control of MCF-7 cells (p = 0.0134). Comparison of the untreated co-culture control to the untreated control of the MCF-10A yielded a non-significant result (p = 0.3858). The result implies that the increased migration observed with the co-seeding might be due to increased migration of the MCF-10A rather than the MCF-7 cells. Compared to 2Gy X-rays alone, decreased migration was seen in HDACi pre-treated cells with p = 0. 0013 and p = 0.0099 in SAHA and CUDC-101 respectively. Increased migration was seen after 6Gy doses compared to lower doses (2Gy); complete wound closure occurred before 16hrs (Figure 4 a-b). At 8 hours post irradiation with 6Gy X-rays, significantly reduced migration was observed compared to combination treatment of 6Gy X-rays and SAHA (p = 0.0439). However, treatment with 6Gy X-rays and CUDC-101 showed significant reduction in migration compared to 6Gy X-rays (p = 0.0259). The former result suggests that increased migration might be from SAHA treated MCF-7 cells. The reduced migration seen after CUDC-101 might be due to the effect of CUDC-101 on MCF-10A cells (Figure 4a-b).

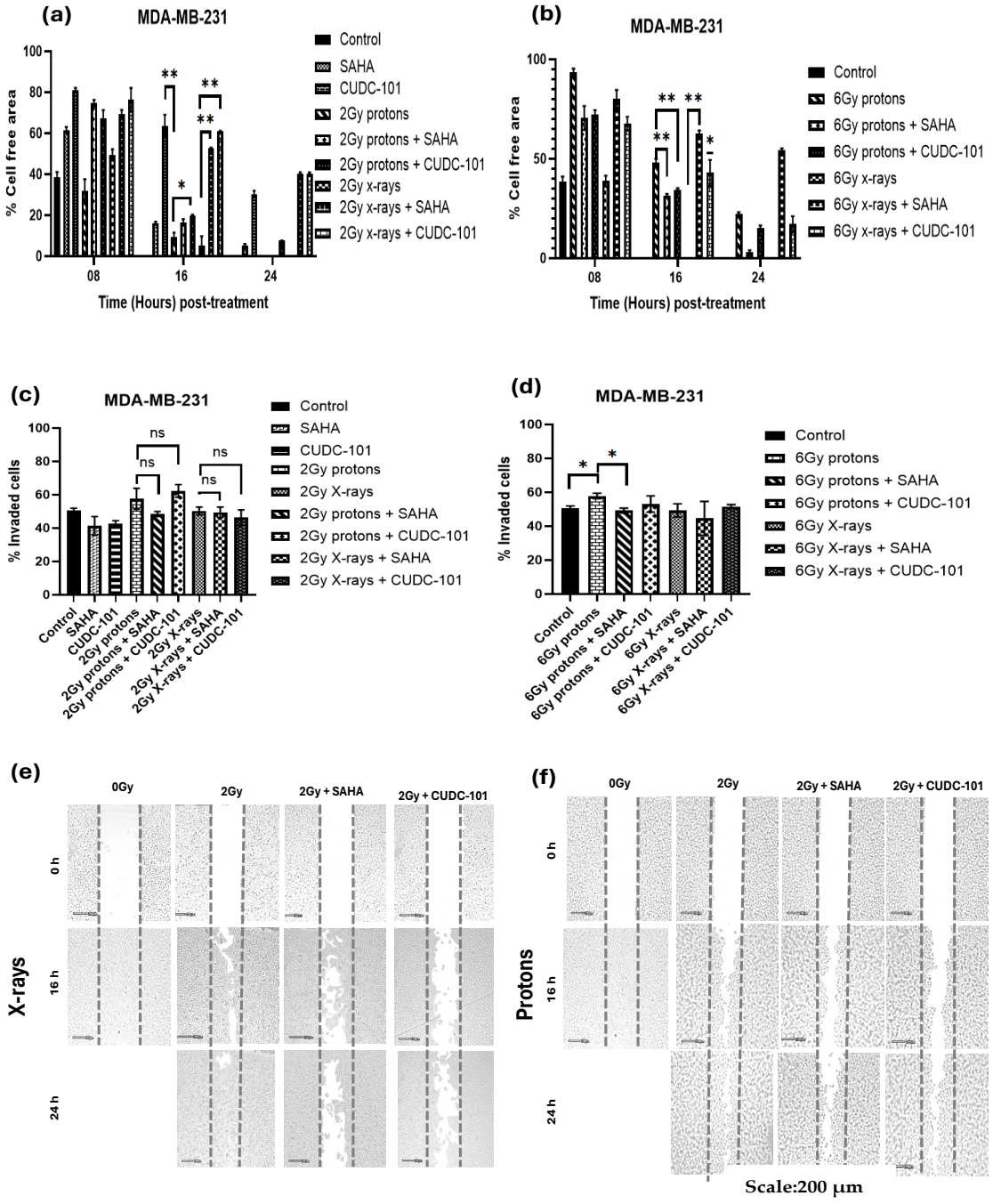

Figure 3. Effect of SAHA and CUDC-101 on migration (**a**)-(**b**) and invasion potential (**c**)-(**d**) of MDA- MB-231 cells. Representative images are shown in (**e**) and (**f**). Samples were treated with SAHA (2μM) and CUDC-101 (0.6μM) and irradiated with either protons or X-rays. Histograms show the mean ± SD of three independent experiments (n=3). Comparisons were conducted using unpaired two-tailed Student *t* test where $p < 0.05$ was considered significant.

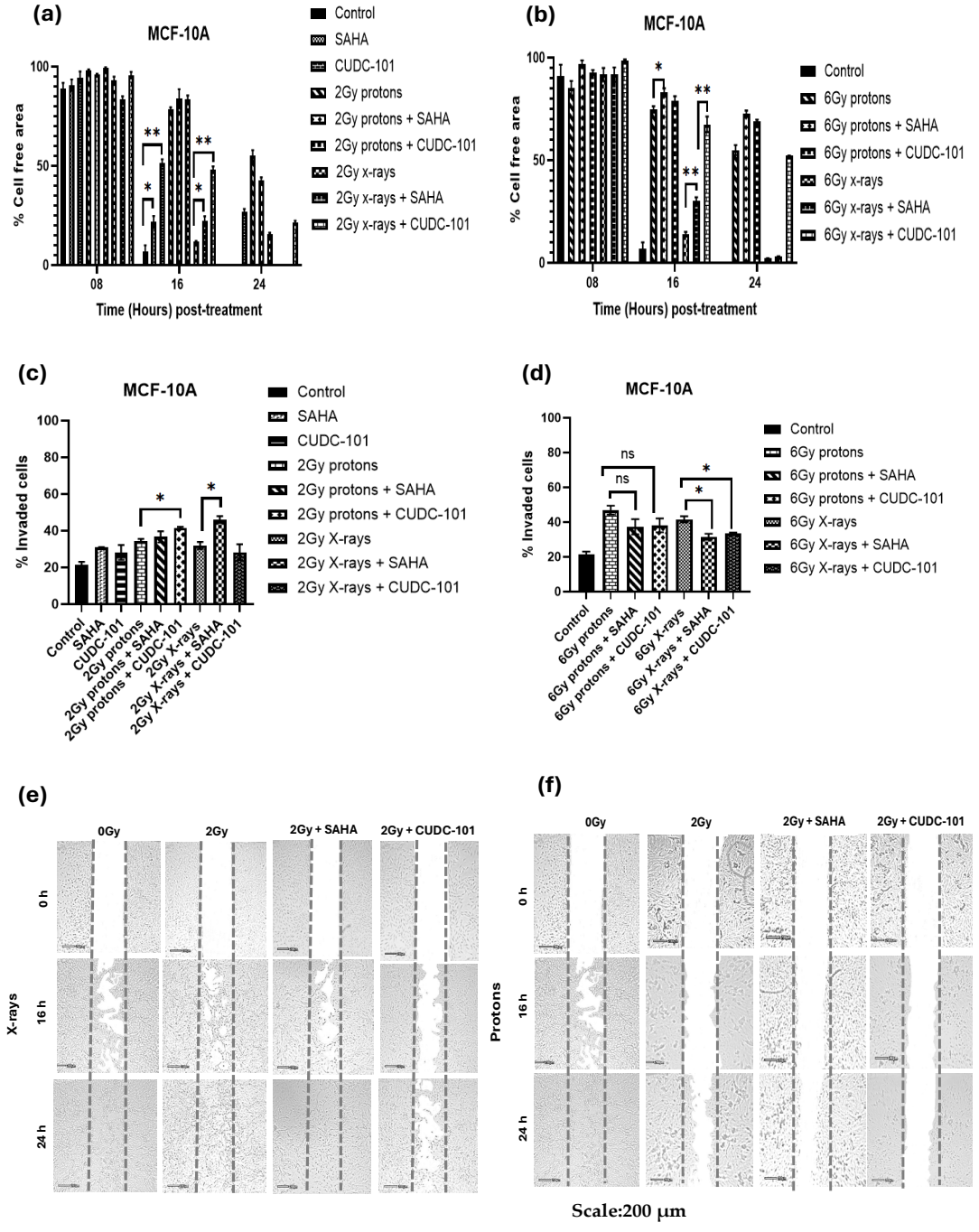

Figure 4. Effect of SAHA and CUDC-101 on migration (**a**)-(**b**) and invasion potential (**c**)-(**d**) of MCF- 10A cells. Representative images are shown in (**e**) and (**f**). Samples were treated with SAHA (6.3μM) and CUDC-101 (2.7μM) and irradiated with either protons or X-rays. Histograms show the mean ± SD of three independent experiments, (n=3). Comparisons were conducted using unpaired two-tailed Student's *t* test, $p < 0.05$ was considered significant.

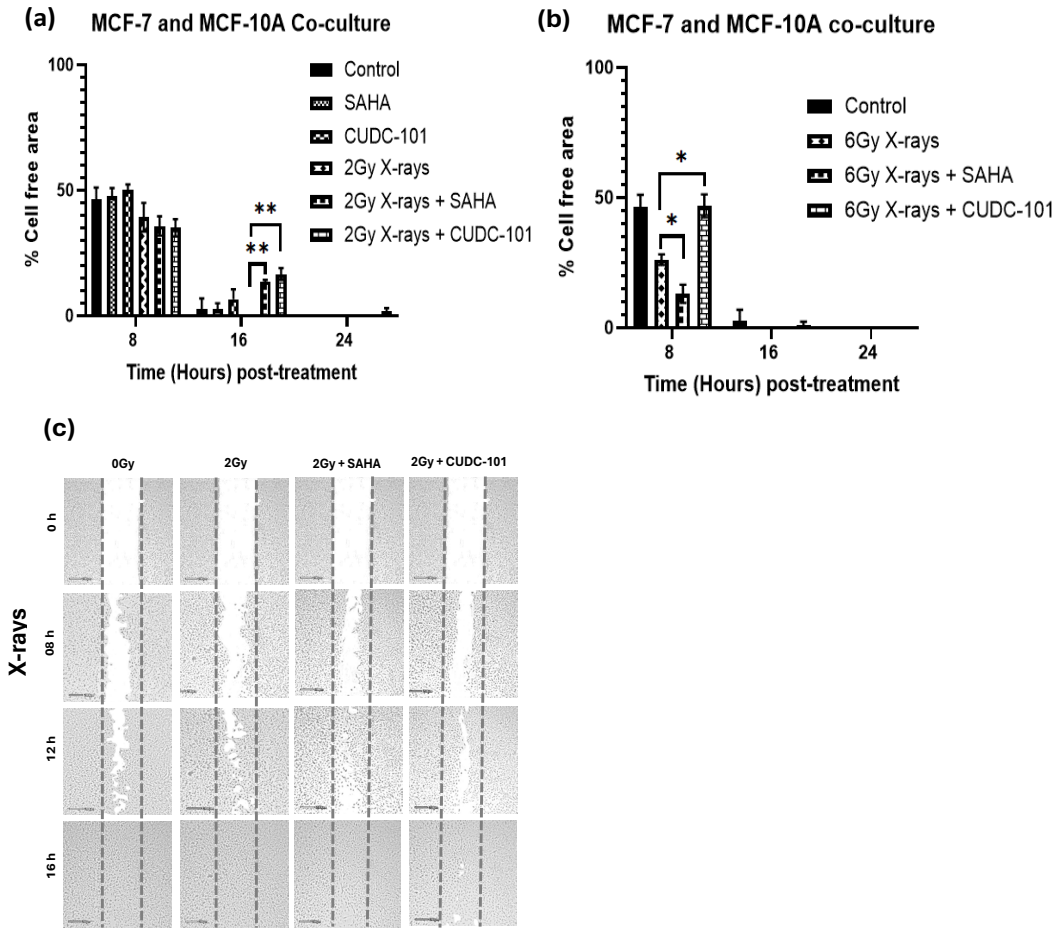

Figure 5. Effect of SAHA and CUDC-101 on migration and invasion potential of co-cultured MCF7 and MCF-10A cells (**a**)-(**b**). Representative images are shown in (c). Samples were treated with SAHA (2μM) or CUDC-101 (0.6μM) and irradiated with 2 Gy or 6 Gy X-rays. Histograms show the mean ± SD of three independent experiments (n=3). Comparisons were conducted using unpaired two-tailed Student's *t* test, $p < 0.05$ was considered significant.

4. Discussion

Migration of tumour cells is required for invasion and metastasis [43]. Migration is facilitated by the dynamic process of epithelial mesenchymal transition (EMT). The effect of HDACi on EMT in different solid tumours, remains a matter of discussion. Several reports supported the notion that HDACi inhibits migration and invasion in human breast cell lines including MCF-7, MDA-MB-231, BT549 and rat breast cell lines (MT-450 [44,45]. Chiu et al. also reported inhibition of migration in 4T1 breast cancer cells after treatment with 600nM SAHA [46]. In another study, SAHA was observed to significantly inhibit leptin stimulated migration in MCF-7 and MDA-MB-231 cell lines [47]. To the contrary, Wu et al. observed that SAHA induced EMT via HDAC8/FOXA1 and promoted migration in MDA-MB-231 and

BT549 breast cells [18]. In a recent study by Hu et al. treatment with 2.5 and 5 μM SAHA and LBH589 were reported to promote migration in BT549 and MDA-MB-231 breast cell lines by elevating the pro-metastasis gene NEDD9 [19]. The authors concluded that monotherapy with pan-HDACi should be avoided in breast cancer [19]. Further, in a phase II trial, SAHA monotherapy failed to show success in 14 patients with metastatic breast cancer [48]. The results of this Phase II trial are congruent with the findings of the later studies. To that effect, in the current study, SAHA was combined with proton or X-radiation. Treatment with 1.2μM SAHA was observed to increase migration and invasion in the MCF-7 cell line when used as monotherapy, but not in the MDA-MB-231 cell lines as reported by Hu et al. [19]. The migration promoting effect of SAHA was also evident when SAHA was combined with X-rays but was repressed when SAHA was combined with protons (Figures 1a-d). Further, in the MCF-7 cell line, proton irradiation alone (2Gy and 6Gy) inhibited migration more effectively than combination therapy with either SAHA ($p=0.0016$) or CUDC-101 ($p= 0.0053$) after 2Gy and $p= 0.0018$ and $p=0.0044$ after 6Gy. Indeed, the migration inhibiting capacity of protons was previously reported in the MCF-7 and MDA-MB-231 cell lines [40,41,49].

Contrary to the observations made in the MCF-7 cell line, at lower doses (2Gy, protons irradiation alone did not reduce migration in the MDA-MB-231 cell line, Figure 2a. However, significant reduction was seen after 6Gy protons. This result agrees with previous studies that reported a dose-dependent inhibition of migration by protons in the MDA-MB-231 cell line [49,50]. In opposition to the observations of Wu et al. and Hu et al. that reported increased migration after SAHA treatment, in the MDA-MB-231 cell line, SAHA modestly inhibited migration when used as monotherapy and when combined with X-rays (Figures 2 a-d). This observation is in line with the observations from our previous paper where we reported increased γ-H2AX foci retention at 24 hours post irradiation after treatment with 2Gy X-rays and SAHA [51]. The MDA-MB-231 cell line possesses a mesenchymal phenotype and expresses low levels of E-cadherin [5]. Consistent with this, Wang et al. reported a slight increase in E-cadherin that indicates reversal of EMT in SAHA-treated MDA-MB-231[5]. Furthermore, Shah et al. also reported reversal of EMT through reversal of repression of E-cadherin in the MDA-MB-231 cell line [17]. Taken together, the latter studies also support the modest inhibition in migration that was observed in the current study. Notwithstanding, in the triple negative cell line MDA-MB-468, although SAHA inhibited migration, mesenchymal marker N-cadherin was observed to be overexpressed [6]. This brings into question whether EMT markers alone can provide a reliable measure of migration and invasion capacity [52]. This could also explain the conflicting reports when

SAHA is used in triple negative breast cell lines. In both the MCF-7 and MDA-MB-231 repression of migration by protons has been associated with reduction in cyclooxygenase-2 (COX-2) and matrix metalloproteinase-9 (MMP-9 [49,53]. Indeed, molecular profiling of MCF-7 cells after proton irradiation revealed increased sensitivity of this cell line to proton irradiation compared to MDA-MB-231 and MCF-10A cell lines [54]. This is in line with the observed sensitivity to 2Gy protons as well as 6Gy in the current study, Figure 1a. COX-2 has been found to be overexpressed in a number of tumour types including breast tumour [49,55–57]. In the MCF-10A cell line, significant reduction in migration was seen after proton irradiation alone (Figures 3 a-d). Although previous reports indicated that HDACi have little effect on normal cells due to active G2 checkpoint which is defective in malignant cells, modest reduction in migration was seen when SAHA was combined with X-rays in the current study (Figures 3 a-d) [13,58–61].

CUDC-101 is a multi-target inhibitor of HDACs, EGFR and human epidermal growth factor receptor 2 (HER2). Data on CUDC-101 in breast cancer is very limited. Schlaff et al. reported inhibition of HER2, EGFR and HDAC in MDA-MB-231 cells after treatment with 0.5μM CUDC-101 [62]. In the current study, reduction in migration and invasion were observed after 2Gy protons combined with CUDC-101 in the MCF-7 cell line. In the MDA-MB-231 cell line, significantly reduced migration was observed after monotherapy with CUDC-101 and 2Gy X-rays combined with CUDC- 101 (Figure 2 a-d). The reduction in migration after treatment with CUDC-101 in the MDA-MB-231 is thought to be due to inhibition of EGFR [63,64]. In support, Wang et al. also observed a significant increase in E-cadherin after treatment with CUDC-101 compared to treatment with SAHA in MDA- MB-231 cell line [5]. In the MCF-10A cell line, reduced migration was observed after CUDC-101 monotherapy, as well as after combination therapies in CUDC-101 pre-treated cells. (Figure 3a, b). Previous studies had alluded that HDACi has little effect on healthy cells. Most of these studies were conducted with SAHA which is a pan-HDACi. The effect of CUDC-101 in the MCF-10A cell line could also be attributed to inhibition of EGFR, which is crucial for maintenance of MCF-10A cell line [65]. The reduced migration in MCF-10A cell line implies increased side effects in clinical practice.

Previous reports have indicated that the migration capacity of malignant cells is influenced by the presence of normal cells [66]. To that effect, MCF-7 and MCF-10A cells were co-cultured and treated with HDACi or X-rays as well as combination treatment of HDACi and X-rays. In general, increased migration was observed compared to when the MCF-7 or MCF-10A cells were cultured individually (Figures 4 a-b) The MCF-10A showed increased

migration speed towards the MCF- 7(Figure 3 a-b). The observed differences in migration speed between the MCF-7 and MCF-10A cells could be explained by the facts that MCF-7 has lower metastatic potential, and low migration speed. Also, the differences in basal adenosine triphosphate (ATP) between these cell lines are different. Normal cells have higher levels of ATP, which is needed for migration, whereas in malignant cells, ATP production is reduced due to the Warburg effect [66].

5. Conclusions

Metastasis is a complex multi-step process, and despite extensive research, efficacious therapies are yet to be found. The focus of most studies on HDACi has been placed on their ability to enhance radiation response, as well as in unraveling the mechanisms that underlie their radiation enhancing effect. The current study explored the systematic effects of HDACi when combined not only with X- rays but also with protons. The results highlighted that although pan-HDACi SAHA was previously proved to enhance radiation response, the observed *in vitro* migration promoting effects in the MCF- 7 cell line, nullifies the previously reported benefits. The observed migration and invasion reducing capacity of proton irradiation alone in both malignant MCF-7 and MDA-MB-231 cell lines at 2Gy dose, which is commonly used in clinical, is encouraging in light of the increasing number of protons centers around the world. Also, the migration inhibiting effects protons higher doses (6Gy), bears relevance to the hypofractionation schedule, which is increasing in use in the treatment of breast cancers. Of note is also the significant reduction in migration seen in the normal MCF-10A, which infers slower wound healing in normal tissues. The results also highlighted the potential of CUDC- 101 either as monotherapy or in combination with radiation, as a therapeutic strategy in reducing metastasis in triple negative breast cancers. The results of this *in vitro* study needs to be validated in *in vivo* studies.

Supplementary Materials: The following supporting information can be downloaded at the website of this paper posted on Preprints.org, Figure S1: Representative images for apoptosis profiles; Figure S2: Representative images of the cell cycle profile after different treatment conditions.

Author Contributions: Conceptualization, E.N.S, S.N., C.V. and A.J.; methodology, E.N.S, S.N., C.V. and A.J.; formal analysis, E.N.S, S.N., C.V. and A.J.; investigation, E.N.,S.N., C.V.,A.B.,A.J.,S.; data curation, E.N.S.; writing—original draft preparation, E.N.S; writing—review and editing, E.N.S, S.N., C.V.,A.B. and A.J.; supervision, S.N., C.V. and A.J.; funding acquisition, E.N.S, S.N., C.V.,A.B.,A.J. All authors have read and agreed to the published version of the manuscript.". Authorship must be limited to those who have contributed substantially to the work reported.

Funding: This research was funded by NRF iThemba Laboratories and Department of Higher Education and Training, South Africa. The APC was funded by the University of

Pretoria, Cape Peninsula University of Technology, NRF iThemba Laboratories and GSI Helmholtzzentrum für Schwerionenforschung.

Conflicts of Interest: The authors Elsie Neo Seane, Charlot Vandevoorde, Alessandra Bisio and Anna Joubert declare no conflicts of interest. Author Shankari Nair is currently employed by the company Bayer AG. The authors confirm that no financial contribution was received from BAYER AG and the company was not involved in any way in the study. The funders had no role in the design of the study; in the collection, analyses, or interpretation of data; in the writing of the manuscript; or in the decision to publish the results.
Ethics Number: 689/2021

References

1. Liu, Z.; Chen, J.; Ren, Y.; Liu, S.; Ba, Y.; Zuo, A.; Luo, P.; Cheng, Q.; Xu, H.; Han, X. Multi-stage mechanisms of tumor metastasis and therapeutic strategies. *Signal Transduction and Targeted Therapy* **2024**, *9*, 270, doi:10.1038/s41392-024-01955-5.
2. Fares, J.; Fares, M.Y.; Khachfe, H.H.; Salhab, H.A.; Fares, Y. Molecular principles of metastasis: a hallmark of cancer revisited. *Signal Transduction and Targeted Therapy* **2020**, *5*, 28, doi:10.1038/s41392-020-0134-x.
3. van Zijl, F.; Krupitza, G.; Mikulits, W. Initial steps of metastasis: cell invasion and endothelial transmigration. *Mutat Res* **2011**, *728*, 23-34, doi:10.1016/j.mrrev.2011.05.002.
4. Liu, X.; Chen, Y.; Li, Y.; Shen, Y.; Dong, S.; Tan, J. A Novel Class I HDAC Inhibitor, AW01178, Inhibits Epithelial-Mesenchymal Transition and Metastasis of Breast Cancer. *Int J Mol Sci* **2024**, *25*, doi:10.3390/ijms25137234.
5. Wang, J.; Pursell, N.W.; Samson, M.E.S.; Atoyan, R.; Ma, A.W.; Selmi, A.; Xu, W.; Cai, X.; Voi, M.; Savagner, P.; et al. Potential advantages of CUDC-101, a multitargeted HDAC, EGFR, and HER2 inhibitor, in treating drug resistance and preventing cancer cell migration and invasion. *Molecular Cancer Therapeutics* **2013**, *12*, 925-936, doi:10.1158/1535-7163.MCT-12-1045.
6. Wawruszak, A.; Gumbarewicz, E.; Okon, E.; Jeleniewicz, W.; Czapinski, J.; Halasa, M.; Okla, K.; Smok- Kalwat, J.; Bocian, A.; Rivero-Muller, A.; et al. Histone deacetylase inhibitors reinforce the phenotypical markers of breast epithelial or mesenchymal cancer cells but inhibit their migratory properties. *Cancer Manag Res* **2019**, *11*, 8345-8358, doi:10.2147/cmar.S210029.
7. Lamouille, S.; Xu, J.; Derynck, R. Molecular mechanisms of epithelial-mesenchymal transition. *Nat Rev Mol Cell Biol* **2014**, *15*, 178-196, doi:10.1038/nrm3758.
8. Francart, M.E.; Lambert, J.; Vanwynsberghe, A.M.; Thompson, E.W.; Bourcy, M.; Polette, M.; Gilles, C. Epithelial-mesenchymal plasticity and circulating tumor cells: Travel companions to metastases. *Dev Dyn* **2018**, *247*, 432-450, doi:10.1002/dvdy.24506.
9. Aghdassi, A.; Sendler, M.; Guenther, A.; Mayerle, J.; Behn, C.O.; Heidecke, C.D.; Friess, H.; Büchler, M.; Evert, M.; Lerch, M.M.; et al. Recruitment of histone deacetylases HDAC1 and HDAC2 by the transcriptional repressor ZEB1 downregulates E-cadherin expression in pancreatic cancer. *Gut* **2012**, *61*, 439-448, doi:10.1136/gutjnl-2011-300060.
10. Serrano-Gomez, S.J.; Maziveyi, M.; Alahari, S.K. Regulation of epithelial-

mesenchymal transition through epigenetic and post-translational modifications. *Molecular Cancer* **2016**, *15*, 18, doi:10.1186/s12943-016-0502.

11. Choi, S.Y.; Kee, H.J.; Kurz, T.; Hansen, F.K.; Ryu, Y.; Kim, G.R.; Lin, M.Q.; Jin, L.; Piao, Z.H.; Jeong, M.H.Class I HDACs specifically regulate E-cadherin expression in human renal epithelial cells. *J Cell Mol Med* **2016**, *20*, 2289-2298, doi:10.1111/jcmm.12919.
12. Wang, J.H.; Lee, E.J.; Ji, M.; Park, S.M. HDAC inhibitors, trichostatin A and valproic acid, increase E- cadherin and vimentin expression but inhibit migration and invasion of cholangiocarcinoma cells. *Oncol Rep* **2018**, *40*, 346-354, doi:10.3892/or.2018.6441.
13. Kim, N.H.; Kim, S.N.; Kim, Y.K. Involvement of HDAC1 in E-cadherin expression in prostate cancer cells; its implication for cell motility and invasion. *Biochemical and Biophysical Research Communications* **2011**, *404*, 915-921, doi:https://doi.org/10.1016/j.bbrc.2010.12.081.
14. Kakihana, M.; Ohira, T.; Chan, D.; Webster, R.B.; Kato, H.; Drabkin, H.A.; Gemmill, R.M. Induction of E- Cadherin in Lung Cancer and Interaction with Growth Suppression by Histone Deacetylase Inhibition. *Journal of Thoracic Oncology* **2009**, *4*, 1455-1465, doi:https://doi.org/10.1097/JTO.0b013e3181bc9419.
15. Schiedlauske, K.; Deipenbrock, A.; Pflieger, M.; Hamacher, A.; Hänsel, J.; Kassack, M.U.; Kurz, T.; Teusch,N.E. Novel Histone Deacetylase (HDAC) Inhibitor Induces Apoptosis and Suppresses Invasion via E- Cadherin Upregulation in Pancreatic Ductal Adenocarcinoma (PDAC). *Pharmaceuticals* **2024**, *17*, 752.
16. Law, M.; Corsino, P.; Jahn, S.; Davis, B.; Chen, S.; Patel, B.; Pham, K.; Lu, J.; Sheppard, B.; Norgaard, P.; et al. Glucocorticoids and histone deacetylase inhibitors cooperate to block the invasiveness of basal-like breast cancer cells through novel mechanisms. *Oncogene* **2012**, *32*, doi:10.1038/onc.2012.138.
17. Shah, P.; Gau, Y.; Sabnis, G. Histone deacetylase inhibitor entinostat reverses epithelial to mesenchymal transition of breast cancer cells by reversing the repression of E-cadherin. *Breast Cancer Res Treat* **2014**, *143*, 99-111, doi:10.1007/s10549-013-2784-7.
18. Wu, S.; Luo, Z.; Yu, P.J.; Xie, H.; He, Y.W. Suberoylanilide hydroxamic acid (SAHA) promotes the epithelial mesenchymal transition of triple negative breast cancer cells via HDAC8/FOXA1 signals. *Biol Chem* **2016**, *397*, 75-83, doi:10.1515/hsz-2015-0215.
19. Hu, Z.; Wei, F.; Su, Y.; Wang, Y.; Shen, Y.; Fang, Y.; Ding, J.; Chen, Y. Histone deacetylase inhibitors promote breast cancer metastasis by elevating NEDD9

expression. *Signal Transduct Target Ther* **2023**, *8*, 11, doi:10.1038/s41392-022-01221-6.

20. Bill, R.; Christofori, G. The relevance of EMT in breast cancer metastasis: Correlation or causality? *FEBS Letters* **2015**, *589*, 1577-1587, doi:https://doi.org/10.1016/j.febslet.2015.05.002.
21. Vilalta, M.; Rafat, M.; Graves, E.E. Effects of radiation on metastasis and tumor cell migration. *Cell Mol Life Sci* **2016**, *73*, 2999-3007, doi:10.1007/s00018-016-2210-5.
22. Moncharmont, C.; Levy, A.; Guy, J.B.; Falk, A.T.; Guilbert, M.; Trone, J.C.; Alphonse, G.; Gilormini, M.; Ardail, D.; Toillon, R.A.; et al. Radiation-enhanced cell migration/invasion process: a review. *Crit Rev Oncol Hematol* **2014**, *92*, 133-142, doi:10.1016/j.critrevonc.2014.05.006.
23. Zhou, Y.-C.; Liu, J.-Y.; Li, J.; Zhang, J.; Xu, Y.-Q.; Zhang, H.-W.; Qiu, L.-B.; Ding, G.-R.; Su, X.-M.; Mei, S.; et al. Ionizing Radiation Promotes Migration and Invasion of Cancer Cells Through Transforming Growth Factor-Beta–Mediated Epithelial–Mesenchymal Transition. *International Journal of Radiation Oncology, Biology, Physics* **2011**, *81*, 1530-1537, doi:10.1016/j.ijrobp.2011.06.1956.
24. Li, J.; Wu, D.M.; Han, R.; Yu, Y.; Deng, S.H.; Liu, T.; Zhang, T.; Xu, Y. Low-Dose Radiation Promotes Invasion and Migration of A549 Cells by Activating the CXCL1/NF-κB Signaling Pathway. *Onco Targets Ther* **2020**, *13*, 3619-3629, doi:10.2147/ott.S243914.
25. De Bacco, F.; Luraghi, P.; Medico, E.; Reato, G.; Girolami, F.; Perera, T.; Gabriele, P.; Comoglio, P.M.; Boccaccio, C. Induction of MET by ionizing radiation and its role in radioresistance and invasive growth of cancer. *JNCI: Journal of the National Cancer Institute* **2011**, *103*, 645-661.
26. Kaplan, H.S.; Murphy, E.D. The effect of local roentgen irradiation on the biological behavior of a transplantable mouse carcinoma; increased frequency of pulmonary metastasis. *J Natl Cancer Inst* **1949**, *9*, 407-413.
27. Anderson, P.; Dische, S. Local tumor control and the subsequent incidence of distant metastatic disease. *International Journal of Radiation Oncology*Biology*Physics* **1981**, *7*, 1645-1648, doi:https://doi.org/10.1016/0360-3016(81)90186-3.
28. Fagundes, H.; Perez, C.A.; Grigsby, P.W.; Lockett, M.A. Distant metastases after irradiation alone in carcinoma of the uterine cervix. *Int J Radiat Oncol Biol Phys* **1992**, *24*, 197-204, doi:10.1016/0360- 3016(92)90671-4.
29. Wild-Bode, C.; Weller, M.; Rimner, A.; Dichgans, J.; Wick, W. Sublethal irradiation promotes migration and invasiveness of glioma cells: implications for radiotherapy of human glioblastoma. *Cancer Res* **2001**, *61*, 2744-2750.

30. Sheldon, P.W.; Fowler, J.F. The effect of low-dose pre-operative X-irradiation of implanted mouse mammary carcinomas on local recurrence and metastasis. *Br J Cancer* **1976**, *34*, 401-407, doi:10.1038/bjc.1976.183.
31. Strong, M.S.; Vaughan, C.W.; Kayne, H.L.; Aral, I.M.; Ucmakli, A.; Feldman, M.; Healy, G.B. A randomized trial of preoperative radiotherapy in cancer of the oropharynx and hypopharynx. *Am J Surg* **1978**, *136*, 494- 500, doi:10.1016/0002-9610(78)90268-4.
32. von Essen, C.F. Radiation enhancement of metastasis: a review. *Clin Exp Metastasis* **1991**, *9*, 77-104, doi:10.1007/bf01756381.
33. Jung, J.W.; Hwang, S.Y.; Hwang, J.S.; Oh, E.S.; Park, S.; Han, I.O. Ionising radiation induces changes associated with epithelial-mesenchymal transdifferentiation and increased cell motility of A549 lung epithelial cells. *Eur J Cancer* **2007**, *43*, 1214-1224, doi:10.1016/j.ejca.2007.01.034.
34. López-Novoa, J.M.; Nieto, M.A. Inflammation and EMT: an alliance towards organ fibrosis and cancer progression. *EMBO Mol Med* **2009**, *1*, 303-314, doi:10.1002/emmm.200900043.
35. Moeller, B.J.; Cao, Y.; Li, C.Y.; Dewhirst, M.W. Radiation activates HIF-1 to regulate vascular radiosensitivity in tumors: role of reoxygenation, free radicals, and stress granules. *Cancer Cell* **2004**, *5*, 429- 441, doi:10.1016/s1535-6108(04)00115-1.
36. Moeller, B.J.; Dreher, M.R.; Rabbani, Z.N.; Schroeder, T.; Cao, Y.; Li, C.Y.; Dewhirst, M.W. Pleiotropic effects of HIF-1 blockade on tumor radiosensitivity. *Cancer Cell* **2005**, *8*, 99-110, doi:10.1016/j.ccr.2005.06.016.
37. Derer, A.; Frey, B.; Fietkau, R.; Gaipl, U.S. Immune-modulating properties of ionizing radiation: rationale for the treatment of cancer by combination radiotherapy and immune checkpoint inhibitors. *Cancer Immunol Immunother* **2016**, *65*, 779-786, doi:10.1007/s00262-015-1771-8.
38. Ioakeim-Ioannidou, M.; Rose, M.; Chen, Y.-L.; MacDonald, S.M. The Use of Proton and Carbon Ion Radiation Therapy for Sarcomas. *Seminars in Radiation Oncology* **2024**, *34*, 207-217, doi:https://doi.org/10.1016/j.semradonc.2024.02.003.
39. Zaboronok, A.; Isobe, T.; Yamamoto, T.; Sato, E.; Takada, K.; Sakae, T.; Tsurushima, H.; Matsumura, A. Proton beam irradiation stimulates migration and invasion of human U87 malignant glioma cells. *J Radiat Res* **2014**, *55*, 283-287, doi:10.1093/jrr/rrt119.
40. Jasińska-Konior, K.; Pochylczuk, K.; Czajka, E.; Michalik, M.; Romanowska-Dixon, B.; Swakoń, J.; Urbańska, K.; Elas, M. Proton beam irradiation inhibits the migration of melanoma cells. *PLOS ONE* **2017**, *12*, e0186002, doi:

10.1371/journal.pone.0186002.

41. Ogata, T.; Teshima, T.; Kagawa, K.; Hishikawa, Y.; Takahashi, Y.; Kawaguchi, A.; Suzumoto, Y.; Nojima, K.; Furusawa, Y.; Matsuura, N. Particle irradiation suppresses metastatic potential of cancer cells. *Cancer Res* **2005**, *65*, 113-120.
42. Tommasino, F.; Rovituso, M.; Bortoli, E.; La Tessa, C.; Petringa, G.; Lorentini, S.; Verroi, E.; Simeonov, Y.; Weber, U.; Cirrone, P.; et al. A new facility for proton radiobiology at the Trento proton therapy centre: Design and implementation. *Phys Med* **2019**, *58*, 99-106, doi:10.1016/j.ejmp.2019.02.001.
43. Entschladen, F.; Drell, T.L.t.; Lang, K.; Joseph, J.; Zaenker, K.S. Tumour-cell migration, invasion, and metastasis: navigation by neurotransmitters. *Lancet Oncol* **2004**, *5*, 254-258, doi:10.1016/s1470- 2045(04)01431-7.
44. Rhodes, L.V.; Tate, C.R.; Segar, H.C.; Burks, H.E.; Phamduy, T.B.; Hoang, V.; Elliott, S.; Gilliam, D.; Pounder, F.N.; Anbalagan, M.; et al. Suppression of triple-negative breast cancer metastasis by pan-DAC inhibitor panobinostat via inhibition of ZEB family of EMT master regulators. *Breast Cancer Res Treat* **2014**, *145*, 593-604, doi:10.1007/s10549-014-2979-6.
45. Göttlicher, M.; Minucci, S.; Zhu, P.; Krämer, O.H.; Schimpf, A.; Giavara, S.; Sleeman, J.P.; Lo Coco, F.; Nervi, C.; Pelicci, P.G.; et al. Valproic acid defines a novel class of HDAC inhibitors inducing differentiation of transformed cells. *Embo j* **2001**, *20*, 6969-6978, doi:10.1093/emboj/20.24.6969.
46. Chiu, H.W.; Yeh, Y.L.; Wang, Y.C.; Huang, W.J.; Chen, Y.A.; Chiou, Y.S.; Ho, S.Y.; Lin, P.; Wang, Y.J. Suberoylanilide hydroxamic acid, an inhibitor of histone deacetylase, enhances radiosensitivity and suppresses lung metastasis in breast cancer in vitro and in vivo. *PLoS One* **2013**, *8*, e76340, doi:10.1371/journal.pone.0076340.
47. Feng, X.; Han, H.; Zou, D.; Zhou, J.; Zhou, W. Suberoylanilide hydroxamic acid-induced specific epigenetic regulation controls Leptin-induced proliferation of breast cancer cell lines. *Oncotarget* **2017**, *8*, 3364-3379, doi:10.18632/oncotarget.13764.
48. Luu, T.H.; Morgan, R.J.; Leong, L.; Lim, D.; McNamara, M.; Portnow, J.; Frankel, P.; Smith, D.D.; Doroshow, J.H.; Wong, C.; et al. A phase II trial of vorinostat (suberoylanilide hydroxamic acid) in metastatic breast cancer: a California Cancer Consortium study. *Clin Cancer Res* **2008**, *14*, 7138-7142, doi:10.1158/1078-0432.Ccr-08-0122.
49. Kyu-Shik, L.; Jin-Young, M.; Kyung-Soo, N.; Yun-Hee, S. Inhibition of Metastatic Activities in Human Breast Cancer Cells Irradiated by a Proton Beam. *Journal of The Korean Physical Society J. Korean Phys. Soc.* **2011**, *59*,

doi:10.3938/jkps.59.653.

50. Kwon, Y.-S.; Lee, K.-S.; Chun, S.-Y.; Jang, T.J.; Nam, K.-S. Suppressive effects of a proton beam on tumor growth and lung metastasis through the inhibition of metastatic gene expression in 4T1 orthotopic breast cancer model. *Int J Oncol* **2016**, *49*, 336-342, doi:10.3892/ijo.2016.3520.
51. Seane, E.N.; Nair, S.; Vandevoorde, C.; Bisio, A.; Joubert, A. Multi-Target Inhibitor CUDC-101 Impairs DNA Damage Repair and Enhances Radiation Response in Triple-Negative Breast Cell Line. *Pharmaceuticals* **2024**, *17*, 1467.
52. Wawruszak, A.; Borkiewicz, L.; Okon, E.; Kukula-Koch, W.; Afshan, S.; Halasa, M. Vorinostat (SAHA) and Breast Cancer: An Overview. *Cancers (Basel)* **2021**, *13*, doi:10.3390/cancers13184700.
53. Lee, K.S.; Lee, D.H.; Chun, S.Y.; Nam, K.S. Metastatic potential in MDA-MB-231 human breast cancer cells is inhibited by proton beam irradiation via the Akt/nuclear factor-κB signaling pathway. *Mol Med Rep* **2014**, *10*, 1007-1012, doi:10.3892/mmr.2014.2259.
54. Bravatà, V.; Cammarata, F.P.; Minafra, L.; Pisciotta, P.; Scazzone, C.; Manti, L.; Savoca, G.; Petringa, G.; Cirrone, G.A.P.; Cuttone, G.; et al. Proton-irradiated breast cells: molecular points of view. *J Radiat Res* **2019**, *60*, 451-465, doi:10.1093/jrr/rrz032.
55. Atula, T.; Hedström, J.; Ristimäki, A.; Finne, P.; Leivo, I.; Markkanen-Leppänen, M.; Haglund, C. Cyclooxygenase-2 expression in squamous cell carcinoma of the oral cavity and pharynx: association to p53 and clinical outcome. *Oncol Rep* **2006**, *16*, 485-490.
56. Tucker, O.N.; Dannenberg, A.J.; Yang, E.K.; Zhang, F.; Teng, L.; Daly, J.M.; Soslow, R.A.; Masferrer, J.L.; Woerner, B.M.; Koki, A.T.; et al. Cyclooxygenase-2 expression is up-regulated in human pancreatic cancer. *Cancer Res* **1999**, *59*, 987-990.
57. Kang, J.H.; Song, K.H.; Jeong, K.C.; Kim, S.; Choi, C.; Lee, C.H.; Oh, S.H. Involvement of Cox-2 in the metastatic potential of chemotherapy-resistant breast cancer cells. *BMC Cancer* **2011**, *11*, 334, doi:10.1186/1471-2407-11-334.
58. Lee, J.H.; Choy, M.L.; Ngo, L.; Foster, S.S.; Marks, P.A. Histone deacetylase inhibitor induces DNA damage, which normal but not transformed cells can repair. *Proc Natl Acad Sci U S A* **2010**, *107*, 14639-14644, doi:10.1073/pnas.1008522107.
59. Namdar, M.; Perez, G.; Ngo, L.; Marks, P.A. Selective inhibition of histone deacetylase 6 (HDAC6) induces DNA damage and sensitizes transformed cells to anticancer agents. *Proceedings of the National Academy of Sciences* **2010**, *107*, 20003-20008, doi:doi:10.1073/pnas.1013754107.

60. Qiu, L.; Burgess, A.; Fairlie, D.P.; Leonard, H.; Parsons, P.G.; Gabrielli, B.G. Histone deacetylase inhibitors trigger a G2 checkpoint in normal cells that is defective in tumor cells. *Mol Biol Cell* **2000**, *11*, 2069-2083, doi:10.1091/mbc.11.6.2069.
61. Huang, L.; Pardee, A.B. Suberoylanilide Hydroxamic Acid as a Potential Therapeutic Agent for Human Breast Cancer Treatment. *Molecular Medicine* **2000**, *6*, 849-866, doi:10.1007/BF03401823.
62. Schlaff, C.; Arscott, W.; Gordon, I.; Camphausen, K.; Tandle, A. Human EGFR-2, EGFR and HDAC triple- inhibitor CUDC-101 enhances radiosensitivity of GBM cells. *Biomedical Research Journal* **2015**, *2*, 105, doi:10.4103/2349-3666.240616.
63. Masuda, K.; Horinouchi, H.; Tanaka, M.; Higashiyama, R.; Shinno, Y.; Sato, J.; Matsumoto, Y.; Okuma, Y.; Yoshida, T.; Goto, Y.; et al. Efficacy of anti-PD-1 antibodies in NSCLC patients with an EGFR mutation and high PD-L1 expression. *J Cancer Res Clin Oncol* **2021**, *147*, 245-251, doi:10.1007/s00432-020-03329-0.
64. Hossein-Nejad-Ariani, H.; Althagafi, E.; Kaur, K. Small Peptide Ligands for Targeting EGFR in Triple Negative Breast Cancer Cells. *Scientific Reports* **2019**, *9*, 2723, doi:10.1038/s41598-019-38574-y.
65. Tang, Wai Ying Y.; Beckett, Alison J.; Prior, Ian A.; Coulson, Judy M.; Urbé, S.; Clague, Michael J. Plasticity of Mammary Cell Boundaries Governed by EGF and Actin Remodeling. *Cell Reports* **2014**, *8*, 1722-1730, doi:https://doi.org/10.1016/j.celrep.2014.08.026.
66. Kim, B.; Lopez, A.T.; Thevarajan, I.; Osuna, M.F.; Mallavarapu, M.; Gao, B.; Osborne, J.K. Unexpected Differences in the Speed of Non-Malignant versus Malignant Cell Migration Reveal Differential Basal Intracellular ATP Levels. *Cancers (Basel)* **2023**, *15*, doi:10.3390/cancers15235519.

Critical discussion to the Chapter

In South Africa, it has been reported that patients are more likely to present with late-stage (stage III or IV) breast cancer and the incidence of advanced stage breast cancer is estimated between 50% and 57%. Similarly in Sub Saharan Africa, 64.9% of breast cancer cases are identified as stage III and IV at diagnosis. This statistic highlights the need for unravel effective management for metastatic breast cancer, particularly for the triple negative breast cancer which has high metastatic potential. Significant inhibition in migration and invasion was seen in the MCF-7 and MDA-MB-231 cell lines after irradiation with 6Gy protons, as well as after 2Gy protons in the MCF-7 cell line. The observed metastasis inhibiting effect of proton monotherapy is encouraging in view of the increased use of proton irradiation in the treatment of breast cancer around the world. The observed migration promoting effect of pan-HDACi SAHA in the MCF-7 cell line, discourages its potential use in the luminal A molecular sub-type (MCF-7). Further, reduced metastasis after combination treatments of HDACi SAHA and CUDC-101 and X-radiation, as well as CUDC-101 monotherapy treatments in the MDA-MB-231 cell line, highlights the potential of these therapies in the management of triple negative breast cancers.

Personal contribution to Paper 4:

Submitted Article(in press):

Seane, E.; Nair, S.; Vandevoorde, C.; Bisio, A.; Joubert, A. CUDC-101 and Proton Irradiation Reduces Migration and Invasion Capacity of Triple Negative Breast Cell Line. *Preprints* **2024**, 2024110513. https://doi.org/10.20944/preprints202411.0513.v1; Impact factor 4.9.

This manuscript was based on original and novel ideas by the candidate to investigate the effect of HDACi SAHA and CUDC-101 on migration and invasion capacity of malignant MCF-7 and MDA-MB-231 breast cell lines as well the effect on normal MCF-10A cell line. The research was done in collaboration with four other researchers, some of whom are experts in the field. The study was based on the idea and conception thought out by the candidate about various strategies and future research knowledge, understanding and scope for the best way forward in managing breast cancer metastasis which kills more women globally. This work was done in the Radiation biology section of iThemba Laboratory for Accelerators Based Sciences (LABS), Faure, Cape Town, South Africa (SA). Proton beam was generated at Trento Institute of Fundamental Physics and Applications (TIFPA),

Azienda Provinciale per i Servizi Sanitari, Trento, Italy. All the proton experiments were conducted at the Department of Cellular, Computational and Integrative Biology (CIBIO) Laboratories, Via Sommarive, 9, Povo, 38123 Trento, Italy. The work was done under the guidance of Professor Annie Joubert, Department of Physiology, University of Pretoria. The Candidate was the main contributor, and she was involved in designing and doing the experiments, collection of data, formulating and writing the manuscript. Her contribution was about 80% while the other authors assisted in analysis and reviewing the manuscript prior to publication.

CHAPTER 5: RESULTS

Draft Article:

Title: Radiosensitising capacity of SAHA in human breast cell lines

Seane, E.; Nair, S.; Vandevoorde, C.; Bisio, A.; Joubert, A.

Bridging Text:

Chapter 3 presented the results of objectives 1-4 performed using histone deacetylation inhibitor CUDC-101. This draft manuscript included results of objectives 1-4 performed using SAHA. This draft is included to indicate that the results have been analysed and have been incorporated in the final conclusions of the study. The draft manuscript is being finalised and will be submitted for publication.

Article

Radiosensitising capacity of SAHA in human breast cell lines

Elsie Neo Seane [1,2,3,*], Shankari Nair [3], Charlot Vandevoorde [4], Alessandra Bisio [5] and Anna Joubert [6]

[1] Department of Radiography, School of Health Care Sciences, Faculty of Health Sciences, University of Pretoria, Pretoria 0028, South Africa
[2] Department of Medical Imaging and Therapeutic Sciences, Faculty of Health and Wellness, Cape Peninsula University of Technology, Bellville 7535, South Africa
[3] Separate Sector Cyclotron (SSC) Laboratory, Radiation Biophysics Division, iThemba LABS, Cape Town, South Africa; s.nair@ilabs.nrf.ac.za
[4] Department of Biophysics, GSI Helmholtzzentrum für Schwerionenforschung, 64291 Darmstadt, Germany; c.vandevoorde@gsi.de
[5] Department of Cellular, Computational and Integrative Biology, Via Sommarive, 9, Povo, 38123 Trento, Italy; alessandra.bisio@unitn.it
[6] Department of Physiology, School of Medicine, Faculty of Health Sciences, University of Pretoria, Pretoria, South Africa; annie.joubert@up.ac.za
* Correspondence: seanee@cput.ac.za

Abstract: Significant opportunities remain for pharmacologically enhancing the clinical effectiveness of proton and carbon ion-based radiotherapies to achieve both tumor cell radiosensitization and normal tissue radioprotection. We investigated whether pre-treatment with the hydroxamate-based histone deacetylase inhibitors SAHA impacts radiation-induced DNA double-strand break (DSB) induction and repair, cell killing and cell cycle progression. The results indicated that SAHA enhances the response of MCF-7 and MDA-MB-231 cell lines to both protons and X-rays. The results also showed different mechanisms of cell death following protons and X-rays. Post proton irradiation, apoptosis predominated and mitotic catastrophe was mostly seen after exposure to X-rays.

Keywords: Histone deacetylase inhibitor, colony survival assay, proton irradiation

1. Introduction

Suberoylanilide hydroxamic acid (SAHA) was the first histone deacetylase inhibitor (HDACi) to be licensed by the food and drug administration (FDA) in 2006 for cutaneous T cell lymphoma treatment.[1] Several studies have reported radiosensitisation effects of SAHA through DNA double strand break repair inhibition[2-4] The DNA double strand repair pathways that were implicated to be attenuated by SAHA was the homologous recombination repair and non-homologous end joining repair through Ku70 and 86. [5-9] Of interest is also the selective toxicity of SAHA in malignant cells, but not in healthy cells.[4] This protective effect was attributed to sup-pression of oncogenes, radiation-induced inflammatory cytokines.[10,11] Since cytotoxicity and radiation sensitivity often share the same mechanisms, SAHA's radiosensitisation effect may also be cell line dependent. This would explain the different results reported in the different studies when SAHA was used in the different cell lines. As an example, in our previous study, SAHA was observed to promote migration and invasion of MCF-7 cells, but SAHA was observed to repress migration in other cell lines.

A number of studies have investigated SAHA in combination with X-rays, but studies on HDACi, including SAHA and proton therapy are limited. Moreover, the radiobiology of protons is also still a matter of ongoing research.[12] Despite the improved dose distributions and increased relative biological effectiveness (RBE) afforded by proton therapy, significant opportunities remain for enhancing their clinical effectiveness through pharmacological means to achieve tumor cell radio-sensitization.[13] In our previous study, proton irradiation alone was observed to also reduce migration and invasion of MCF-7 cells. Identifying effective radiosensitisers that synergistically enhance charged particle-induced tumor cell killing would allow for lower doses per fraction to be used, thereby reducing normal tissue exposures. Taken together, it would be expected that the combination treatment of SAHA and proton therapy would not only improve local tumour control, but overall survival after treatment.

2. Results

2.1. Determination of IC_{50} and Timepoint of Irradiation in Relation to the Drug

The half maximal inhibitory concentration (IC50) of SAHA was determined using 3-(4,5-dimethylthiazol-2-yl)-2,5-diphenyl-2H-tetrazolium bromide (MTT) cell proliferation assays. MCF-7, MDA-MB-231, and MCF-10A cells were pre-treated with SAHA at concentrations that ranged from 0.16 μM to 20 μM and cell proliferation was assessed at 72 h post-treatment. The determined half-maximal inhibitory concentration (IC50) values are presented in Table 1.

Table 1. Half maximal inhibitory concentration (IC_{50}) values for the different cell lines.

Cell Line	SAHA (μM)
MCF-7	1.2
MDA-MB-231	2
MCF-10A	6.7

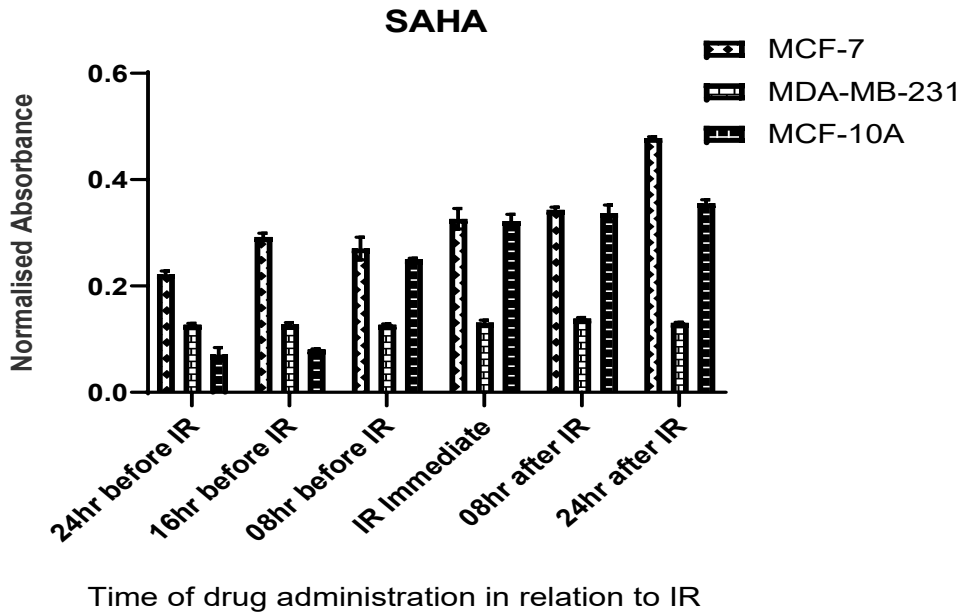

Figure 1. Pre-treatment with SAHA at 24 h before 250 kVp X-ray irradiation offered maximal sensitization. Cells were pre-treated with 1.2 μM, 2 μM, and 6.7 μM SAHA in MCF-7, MDA-MB-231, and MCF-10A cell lines. Cell proliferation was evaluated at 24, 16, 8 h before irradiation, immediately, and at 8 and 24 h after irradiation, as depicted on the x-axis. Cell proliferation was assessed with MTT assay at 72 h post irradiation

To determine the cell killing effect of SAHA in combination with radiation on the cell survival, colony survival assays were performed. For all three cell lines, comparison of survival curves showed an increased cell killing after proton irradiation compared to X-ray irradiated cells (Figure 2a–f). This resulted in relative biologic effectiveness at 10% survival (RBE_{10}) values of 1.51, 1.31, and 1.20, in MCF-7, MDA-MB-231, and MCF-10A cell lines, respectively. All observed RBE values are close to the RBE value of 1.1, which is used in clinical practice. Pre-treatment with SAHA further enhanced the proton RBE, the determined RBE values. In all three cell lines, sensitization enhancement values (SER) of protons were higher than the X-ray irradiation SER, which suggested that an increased biologic effect can be anticipated after SAHA and protons compared to combination therapy of X-rays and SAHA. The MDA-MB-231

cell line also exhibited a higher RBE compared to the other two cell lines, suggesting increased sensitivity to proton irradiation. Lower SER values were observed in the MCF-10A cell line, which supports the reduced effect of SAHA on normal cells. The determined SER values are presented in Table 2.

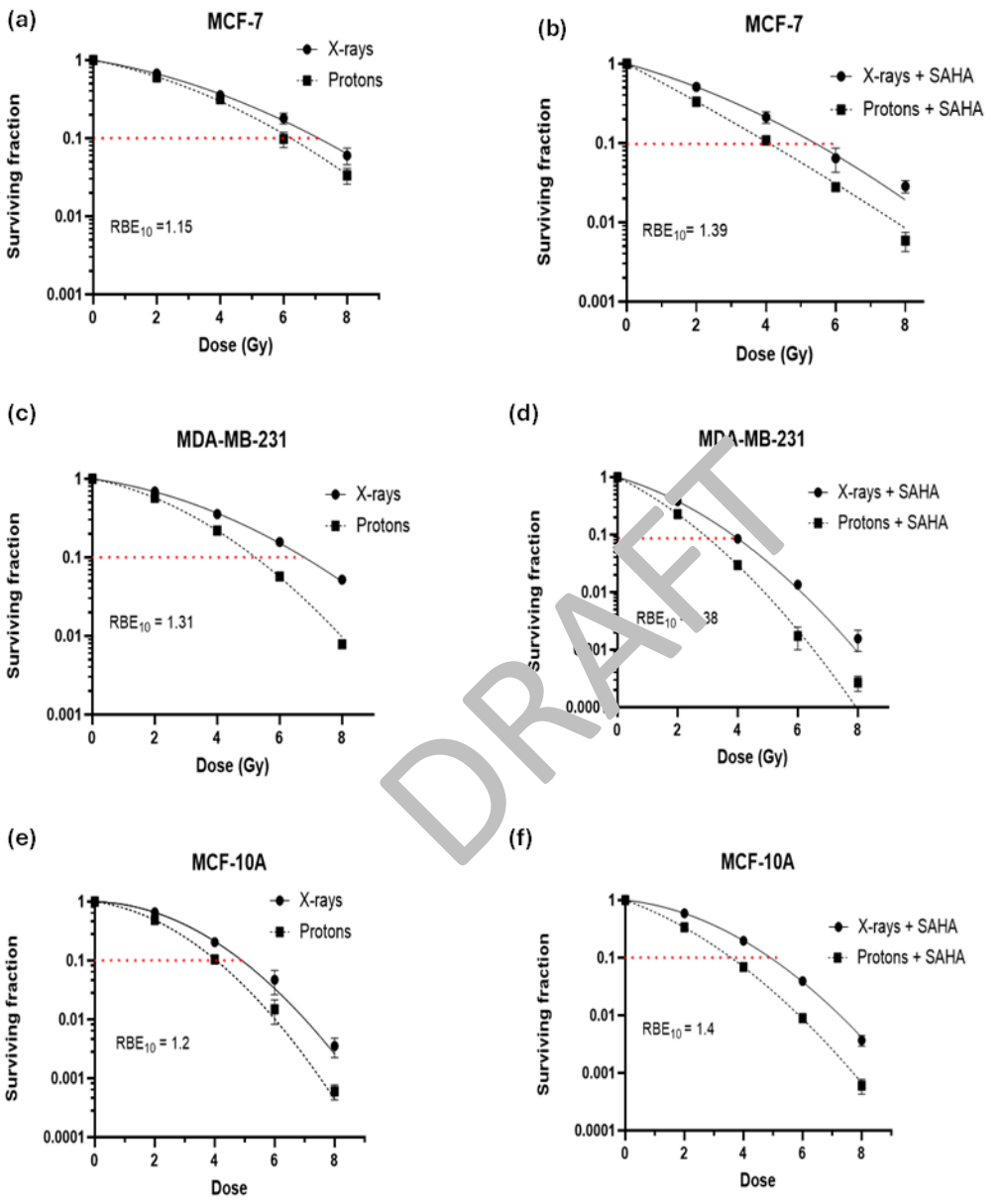

Figure 2. Colony survival curves and associated RBE calculations. SAHA sensitises MCF-7 (**a,b**), MDA-MB-231 (**c,d**), and MCF-10A (**e,f**) cells to proton and X-ray irradiation. Data are expressed as the mean ± SD of three independent experiments.

Table 2. Radiation response parameters of MCF-7, MDA-MB-231, and MCF-10A cell lines.

Cell Line	RBE_{10}	SAHA-Mediated RBE	SER_{10} (Protons)	SER_{10} (X-Rays)
MCF-7	1.15 ± 0.03	1.39 ± 0.01	1.40 ± 0.03	1.31 ± 0.02
MDA-MB-231	1.31 ± 0.01	1.38 ± 0.01	1.71 ± 0.03	1.68 ± 0.01
MCF-10A	1.20 ± 0.01	1.40 ± 0.03	1.20 ± 0.02	0.94 ± 0.03

2.2. Effect of SAHA on Radiation-Induced DNA DSB Formation and Repair

To assess DNA damage induction and repair after combination treatment with SAHA and radiation, γ-H2AX foci assays were performed as molecular biomarkers of DNA double strand break (DSB) and repair. Cells were pre-treated with IC_{50} concentrations of SAHA for 24 h and irradiated with protons or X-rays. γ-H2AX foci assays were performed at 1 h and 24 h post-irradiation with 2 Gy 148 MeV mid-spread-out Bragg peak (SOBP) protons or 250 kVp X-rays. Overall, an increased number of γ-H2AX foci were noted post-irradiation with protons compared to X-irradiation in all three cell lines (Figure 3a–f). Further, in comparison to X-ray irradiated cells, an increased number of persisting γ-H2AX foci at 24 h post-proton irradiated cells was observed, which suggested that the type of damage induced by protons is complex in nature and more difficult to repair (Figure 3a–f).

In the MCF-7 cell line, at 24 h post irradiation, a significant reduction in the number of γ-H2AX foci was noted after irradiation protons or X-rays as well as in SAHA pre-treated cells which suggests that addition of the SAHA minimally impaired the repair of the DNA DSB (Figure 3a,b). Comparison of the combination treatment (SAHA and 2Gy) and irradiation alone (2 Gy protons), resulted in a non-significant result at 1 h and 24 h post irradiation, respectively. Comparison of combination treatment of 2 Gy and X-irradiation and X-rays also yielded a non-significant result at 24 h post irradiation. Although not statistically significant, it was noted that proton irradiation alone yielded a higher number of γ-H2AX foci as compared to combination treatment of proton and SAHA at 1 h post irradiation in this cell line (Figure 3a). This was not observed after irradiation with X-rays (Figure 3b).

In the MDA-MB-231 cell line, the number of γ-H2AX foci induced by radiation alone (protons or X-rays) and those induced by combination of radiation and SAHA were not statistically significant at 1 h post irradiation (Figure 3c, d). A notable number of retained γ-H2AX foci was observed after combination therapy with proton and SAHA, after SAHA alone, as well as proton irradiation alone (Figure 3c). For X-ray irradiation, the number of retained γ-H2AX foci at 24 h after combined treatment remained high and the decrease in the number of γ-H2AX foci compared to the 1 h time point (Figure 3d). Taken together, the findings suggest repair

impairment in the MDA-MB-231 cell line and a sensitivity to SAHA, which is also observable in the unirradiated SAHA control samples. This is reflected as an increase in the number of γ-H2AX foci induced by SAHA monotherapy at 24 h as compared to 1 h (Figure 3c, d).

In the MCF-10A cell line, the only non-malignant cell line included in the study, an overall reduced number of γ-H2AX foci were noticed compared to the other two cell lines. A statistically significant higher number of remaining γ-H2AX foci at 24 h was noted with 2 Gy protons and SAHA compared to proton irradiation alone (Figure 3e). Almost complete repair was noted after proton and X-ray irradiation alone and in the combination treatment of X-rays and SAHA at 24 h (Figure 3f).

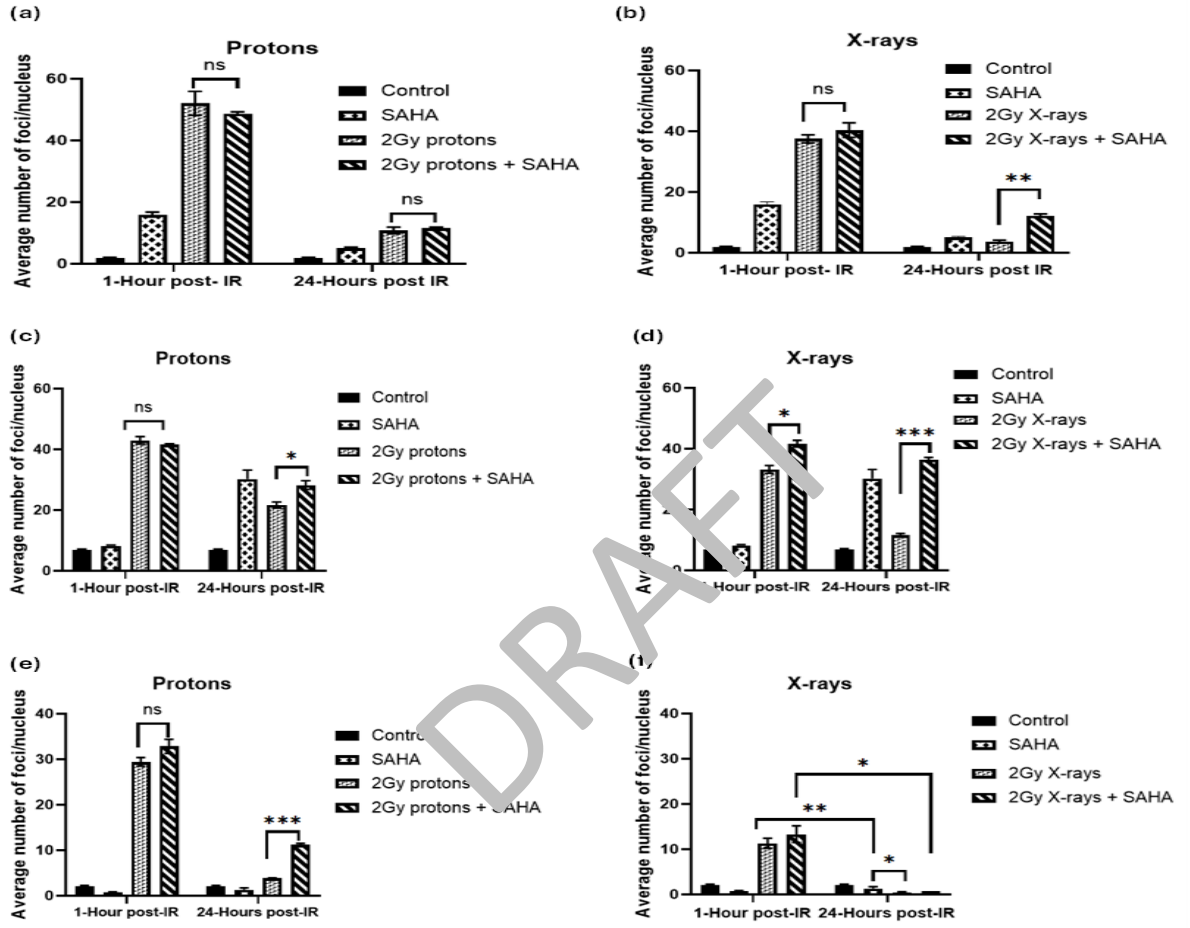

Figure 3. Effect of SAHA combined with protons or X-rays in MCF-7 (**a,b**), MDA-MB-231 (**c,d**), and MCF-10A (**e,f**) cell lines. Histograms show the mean ± SD of three independent experiments (n = 3). Analysis was performed using unpaired two-tailed Student's t test, $p < 0.05$ was significant.

2.3. Impact of SAHA and Radiation on Apoptosis in Breast Cell Lines

To investigate the induction of apoptosis after treatment with SAHA, radiation (protons or X-rays), or combination therapy of SAHA and radiation, the Annexin V/PI apoptosis assay was performed. Apoptosis and necrosis were assessed at 48 h post- irradiation with 2 Gy and 6 Gy protons or X-rays, as well as after combination of SAHA and radiation (proton or X-rays). In all three cell lines, increased apoptosis levels were observed post proton-irradiations as compared to X-ray irradiations (Figure 4a–c). Pre- treatment with SAHA significantly increased the level of proton-induced apoptosis after 2 Gy ($p = 0.0020$) and after 6 Gy in the MCF-7 cell line (Figure 4a). Similarly, in the MDA-MB-231 cell line, a significant increase was observed in SAHA pre-treated samples after 2 Gy and 6 Gy (Figure 4b). In the spontaneously immortalised MCF-10A cell samples, minimal apoptotic fractions were observed after SAHA treatment (Figure 4c). Further, treatment with 1 µM of apoptosis inducer staurosporine induced apoptosis in MCF-7 and MCF-10A cell lines, whereas necrosis was induced in the MDA-MB-231 cell line at 24 h after treatment (Figure 4d).

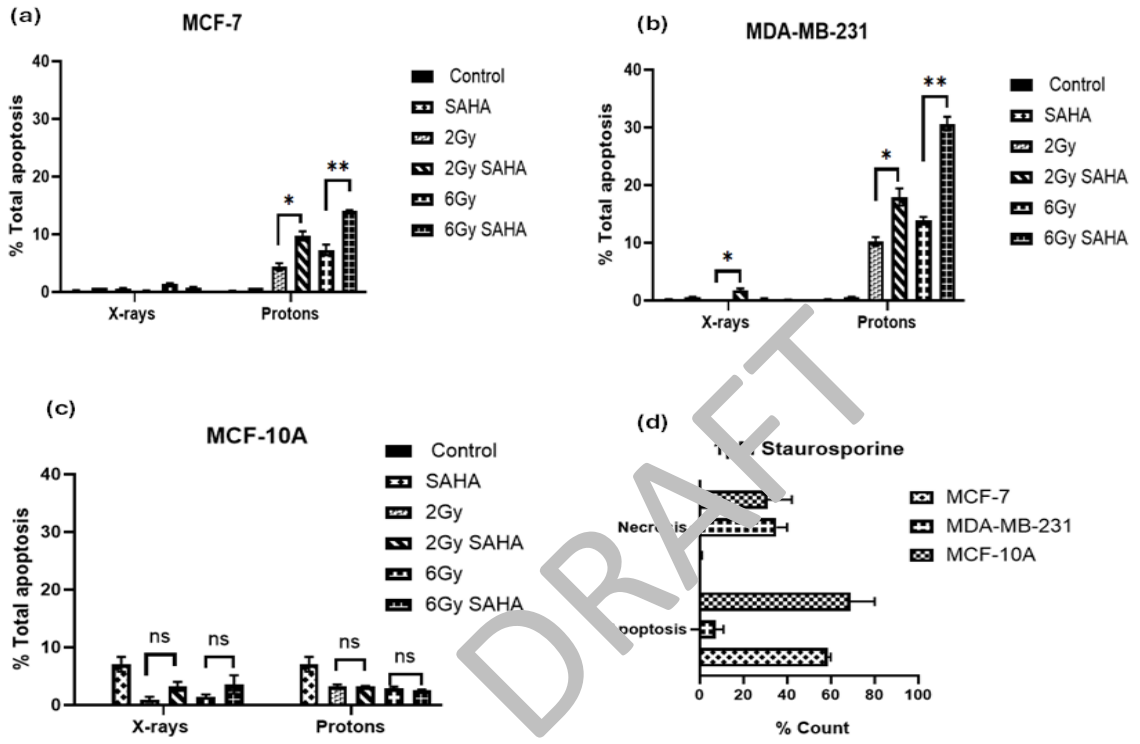

Figure 4. Induction of apoptosis at 48 h post treatment with SAHA combined with protons or X-rays in MCF-7 (**a**), MDA-MB-231 (**b**), and MCF-10A (**c**) cell lines. Induction of apoptosis and necrosis at 24 h after treatment with 1 µM staurosporine in the three cell lines (d). Histograms show the mean ± SD of three independent experiments (n = 3). Comparisons were conducted using unpaired two-tailed Student's t test, $p < 0.05$ was considered to be statistically significant.

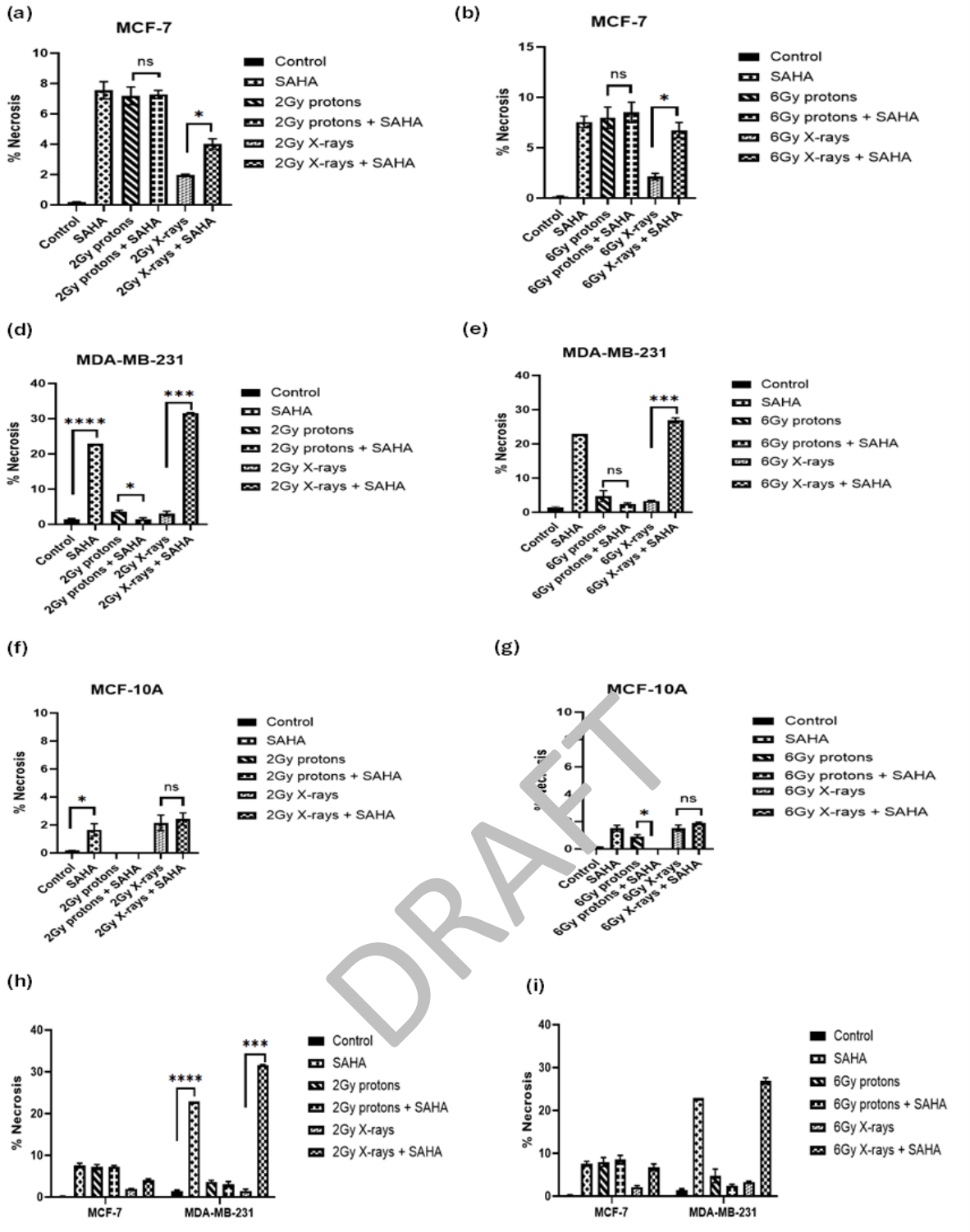

Figure 5. Induction of necrosis at 48 h post treatment with SAHA combined with protons or X-rays in MCF-7 (**a,b**), MDA-MB-231 (**c,d**), and MCF-10A (**e,f**) cell lines. Increased amounts of necrosis after treatment with 2 Gy protons and 2 Gy protons and SAHA in MCF-7 cell line compared to MDA-MB-231 cell line (**g**). Histograms show the mean ± SD of three independent experiments (n = 3). Comparisons were conducted using unpaired two-tailed Student's t test, $p < 0.05$ was considered to be statistically significant.

2.4. Effect of SAHA and Radiation on Cell Cycle Progression

Cell cycle progression after treatment with SAHA and radiation was assessed using propidium iodide with RNase staining. For all cell lines, an increased fraction of cells was observed in the G2/M phase of the cell cycle at 24 h post-irradiation with 6 Gy protons or X-rays, indicating a G2/M cell cycle arrest (Figure 6a–f). Also, in the MDA-MB-231 cell line, monotreatment with SAHA induced G2/M cell cycle arrest at 48 h (Figure 6d). In the MCF-7 and MDA-MB-231 cell lines, an increase in fraction of G2/M cells was also observed at 48 h in X-ray irradiated cells compared to proton-irradiated cells at doses of 2 Gy and at 6 Gy. This increase was more evident in the MDA-MB-231 cell line compared to the MCF-7 cell line (Figure 6a-d). Furthermore, compared to radiation treatment alone, pre-treatment with SAHA had a minimal effect on the cell cycle progression in MCF-7 cells at neither 24 h nor 48 h for 2 Gy post proton-irradiation as evidenced by comparable G2/M fractions at these timepoints (Figure 6a-b). However, in the MDA-MB-231 cell line, pre-treatment with SAHA increased the G2/M fraction after exposure to both 2 Gy and 6 Gy X-rays which was maintained at 48 h post irradiation (Figure 6b-c). It seems sensible to associate the increased fraction of G2/M cells after X-ray irradiations to the reduced levels of apoptosis and necrosis that were seen in the MCF-7 and MDA-MB-231 cell lines at 48 h post irradiation. In this instance, the increased G2/M could be an indicator of mitotic catastrophe as a mode of cell death after x-irradiations.

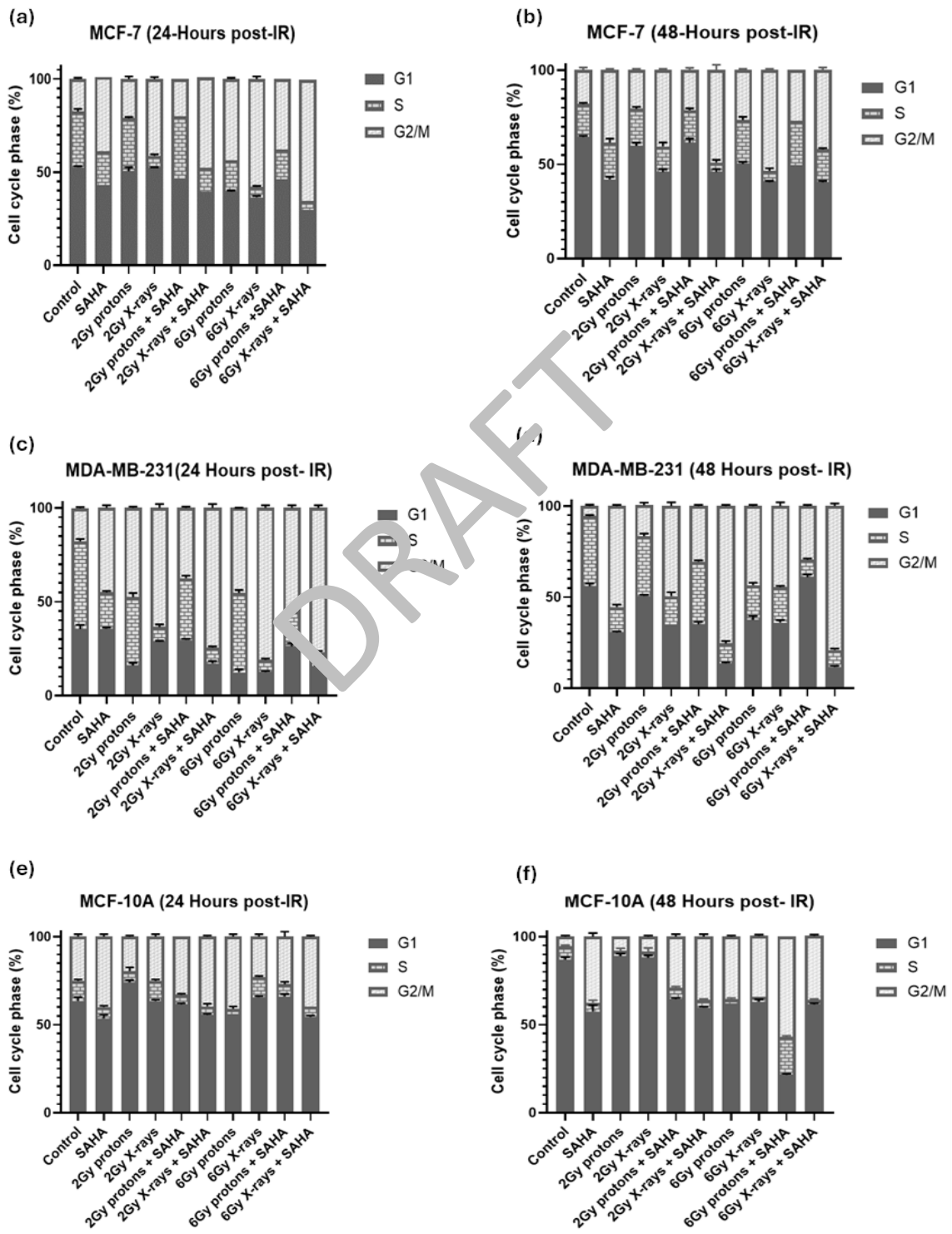

Figure 6. Quantification of the effect of SAHA alone and in combination with X-rays and protons on cell cycle progression in MCF-7 (a,b) MDA-MB-231 (c,d); and MCF-10A (e,f) cell lines. Data represent the mean ± SD of three independent experiments (n = 3). Comparisons were conducted using two-tailed Student's t test, $p < 0.05$ was statistically significant.

3. Discussion

SAHA is a pan-inhibitor of class I (HDAC ,2,3 and 8) and class II HDACs (HDAC 4,5,6,7 and 9.[14] Our data show that SAHA enhances the response to both protons and X-rays in MCF-7 and MDA-MB-231 breast cell lines. The enhancement was most notable after proton irradiation compared to X-rays. Similarly, in hepatocellular carcinoma (HCC) cell lines, Choi et al. reported higher proton SER values of 1.25 and 1.21 compared to X-ray SER values of 1.15 and 1.11, using Panobinostat in Huh7 and Hep3B cells, respectively. Yu et al. also reported Valproic acid (VPA)-mediated RBE10 value of 1.17 compared to RBE10 value of 1.08 without VPA in Hep3B cells after treatment with 6 MV photons [15]. In another study, Gerelchuluun et al. reported an RBE10 value of 1.24 and proton SER values of 1.31 and 1.16 compared to γ-ray SER values of 1.43 and 1.08 in lung carcinoma (A549) and normal fibroblast (AG1522) cell lines, respectively, following treatment with 2 μM of SAHA [16]. Although different HDACi and different cell lines were used in the mentioned studies, the findings are consistent with those of the current study, where higher RBE and SER values were reported for protons compared to X-rays. Similar pattern of results was also reported in our previous study.[17] Previous studies have asserted that HDACs are not overexpressed in normal tissues, which leads to minimal effect of HDACi on normal tissues [4,18,19]. In the normal breast cell line (MCF-10A) following pre-treatment with SAHA, SER values were lower than the ones observed in the malignant cell lines indicating the reduced effect of SAHA in this cell line, which is in agreement with previous studies.

Previous studies reported an increased number of γ-H2AX foci that are larger in size after proton irradiation as compared to X-rays in different cell lines [20-26]. Gerelchuulun et al. reported a 1.2–1.6-fold increase in γ-H2AX foci in ONS76 medulloblastoma and MOLT4 leukaemia cells after proton irradiation compared to 10 MV X-rays [24]. In another study, irradiation with SOBP protons induced more clustered DNA damage, whereas entrance plateau protons induced mixed-type damage that consisted of clustered and non-clustered DNA damage.[23] Consistent with these studies, a significantly increased number (1.4–1.5-fold) of γ-H2AX foci was observed at 1 h post-irradiation with 2 Gy SOBP protons compared to 2 Gy X-rays in all three cell lines. Limited studies have been conducted on combination therapy of HDACi and proton irradiation with respect to DNA DSB induction and repair. A 3 h pre-treatment with 1 mM HDACi Valproic acid (VPA) and mid-SOBP protons prolonged appearance of γ-H2AX foci in Hep3B and Huh7 hepatocellular carcinoma cell lines [15]. Pre-treatment with 5 nM Panobinostat increased the γ-H2AX foci yield at 24 h post irradiation with 6 Gy mid-SOBP protons in Huh7 and Hep3B hepatocellular carcinoma cell lines [27]. In NFF28 normal fibroblast cells, Johnson et al. reported resolution of γ-H2AX foci to near background levels at 24 h post-treatment with 10 μM SAHA and irradiation with 200 MeV protons [13]. The

results of these earlier studies are consistent with the observation in the current study, since the retention of γ-H2AX foci was in general higher after proton irradiation in malignant cell lines compared to the MCF-10A cell line.

In terms of the mode of cell death induced by SAHA or combination of SAHA with radiation, our study revealed increased apoptosis post proton irradiations, whereas minimal levels of apoptosis were noted after X-ray irradiation in all three cell lines (Figure 4a–c). Rather, after X-rays, increased proportions of cells in G2/M phase were observed, indicating mitotic catastrophe. The results of our study are therefore consistent with previous reports that highlighted increased apoptosis after protons and mitotic catastrophe after X-rays.

4. Materials and Methods

4.1 Cell Cultures

MCF-7 and MCF-10A (gifted by the Physiology Department, University of Pretoria) cells were cultured in Dulbecco's Modified Eagle's Medium F-12 (DMEM-F12; Gibco™, Thermo Fisher Scientific, Sandton, SA) and Ham's F-12 (Gibco™, Thermo Fisher Scientific, Sandton, SA) supplemented with 10% fetal bovine serum (FBS) (Gibco™, Thermo Fisher Scientific, Sandton, SA), 100 µg/mL penicillin (Gibco™, Thermo Fisher Scientific, Sandton, SA) and 100 µg/mL streptomycin for bacterial contamination. MCF-10A medium was further supplemented with epidermal growth factor (EGF) (20 ng/mL final concentration) (Gibco™, Thermo Fisher Scientific, Sandton, SA) and hydrocortisone (0.5 mg/mL final concentration) (Sigma-Aldrich, Missouri, USA).

MDA-MB-231 cells (gifted by the Department of Natural Sciences, University of Western Cape) were cultured in Roswell Park Memorial Institute (RPMI) 1640 (Gibco™, Thermo Fisher Scientific, Sandton, SA) supplemented with 10% FBS, 100 µg/L penicillin and 100 µg/mL streptomycin (Sigma-Aldrich, Missouri, USA).

All cell lines were cultured in T275 or T75 cell culture flasks (Corning® T-75 flasks (ATCC catalogue #430641, USA) under standard conditions in a humidified incubator at 37ºC, 5% CO2 (Forma series 3 water jacketed incubator, Thermo Fisher Scientific, Waltham, Massachusetts, USA). Cell growth was assessed over 24-hour intervals and sub-cultured once 80% confluence was reached.

4.2 Histone Deacetylase Inhibitor

SAHA (molecular weight of 264.32) was purchased from Sigma Aldrich (Sigma-Aldrich, Missouri, USA) and 1mM stock solution was prepared according to manufacturer's instructions

(5 mg of SAHA was resolved in 18.9165mL dimethyl sulfoxide (DMSO) (Biotechnology Hub, Johannesburg, S.A) and stored at-20°C for short term storage and at -80°C for long term storage.

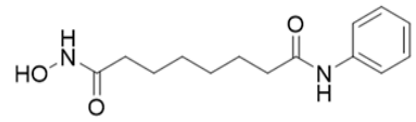

Figure 8. Molecular structure of SAHA. (Created with ChemDraw Professional 15.0.)

4.3 Irradiations

Photon irradiations were performed using the 250 kVp X-Rad 320 unit (Precision X-ray, Madison, US) at a mean dose rate of 0.69 Gy/min at a Source Surface Distance (SSD) of 50 cm. Calibrations of the unit were performed according to the Technical report series-398 (TRS-398) protocol, with a Farmer 117 chamber for which a chamber calibration factor has been obtained from the National Metrology Institute of South Africa (NMISA).

Proton irradiations were performed at the Trento Institute for fundamental Physics and Application (TIFPA). An SOBP beam of 2.5 cm has been produced, as detailed in Tommasino et al. through a 2D rang modulator applied to a beam with initial energy of 148 MeV/u and enlarged with a dual ring system to a lateral profile maintaining a 98% dose uniformity across a 6 cm diameter. The beam was calibrated with EBT gafchromic film and Markus chamber measurements. The cells were exposed after 11 cm of solid water slabs, corresponding to 11.45 cm of water[55]. For both X-ray and proton irradiations, cells were irradiated in 5 ml media in T25 flasks.

4.4 Cell proliferation assays

Cell proliferation assays were conducted using the thiazolyl blue tetrazolium-bromide (MTT) cell viability assay kit. Cells were seeded at a pre-determined density of 3000 cells/well in 96-well plates and allowed to attach. Cells were treated with different concentrations of the HDACi (SAHA) ranging from 0 µM to 20µM and incubated for a further 72 hours. A 20 µl of a 5 mg/mL stock solution of MTT (Sigma-Aldrich, Missouri, USA) was added to each well and incubated for a further 4 hours to allow formazan formation. MTT containing media was carefully removed and 100 µL of DMSO was added to each well. The formation of formazan in the viable cells was monitored by measuring absorbance at wavelengths of 595 nm on a spectrophotometer to determine the half-maximal inhibitory concentrations (IC_{50}) values for HDACi SAHA for the different cell lines.

4.5 Colony survival assays (CSA) and RBE analysis

Cells (250-1500) were seeded in 6-well plates (Whitehead Scientific, Cape Town, SA) and allowed to attach overnight. Cells were treated with SAHA at a concentration of 0.6μM, 2.7 μM and 0.3 μM for MCF-7, MCF-10A and MDA-MB-231 respectively for 24 hours and irradiated with 0, 2, 4 ,6 and 8 Gy of 250 KeV X-rays or 148 MeV SOBP protons. The cells were returned for incubation for a further 8-14 days to allow for colony development. Once colonies of approximately 50 cells were formed, they were fixed with methanol and stained with 2% crystal violet dissolved in methanol and left to dry overnight. Colonies were manually counted and the size was validated by microscopic inspection. Plating efficiency was calculated under untreated conditions using the equation:

$$Plating\ efficiency\ (PE) = \frac{number\ of\ colonies\ counted}{number\ of\ cells\ seeded} X\ 100\%$$

Plating efficiency was used to normalise the surviving fractions for HDACi and radiation induced cell death. Surviving fraction of cells was calculated using the equation:

$$Surviving\ Fraction = \frac{number\ of\ colonies\ formed\ after\ treatment}{number\ of\ cells\ seeded\ x\ PE}$$

Survival curves were plotted and analysed using Graphpad Prism Software Version 10.00 for Windows (GraphPad Software, San Diego, CA, USA). The RBE of the different treatment conditions was calculated at a survival fraction of 10%:

$$RBE = \frac{Dose\ of\ photon\ radiation\ inducing\ 10\%\ SF}{Dose\ of\ proton\ radiation\ inducing\ 10\%\ SF}$$

The sensitisation enhancement ratio (SER) was calculated using the equation [16,27]:

$$SER = \frac{Radiaton\ dose\ to\ inducing\ 10\%\ SF\ without\ SAHA}{Radiation\ dose\ inducing\ 10\%\ SF\ with\ SAHA}$$

4.6 Annexin V-FITC/propidium iodide apoptosis and cell cycle analysis assays

Apoptosis and cell cycle progression were analysed using flow cytometry. For the apoptosis assays, at 48 hours post-irradiation, the media in which the cells were incubated was retained and combined with harvested cells before centrifugation. The cell pellet was resuspended in

100µl 1X annexin-binding buffer and stained with 2.5µlAnnexin V FITC and 2.5µl propidium iodide (PI) (catalogue number 13242, Invitrogen, Thermo Fisher Scientific, Sandton, S.A) according to the manufacturer's instructions. Cells were incubated at room temperature (25ºC) for 15 minutes in the dark. An additional annexin-binding buffer was added after incubation and the samples analysed using the BD Accuri™ C6 Plus (*BD Biosciences, SA*) with 15 000-20 000 cells per measurement.

For analysis of the cell cycle, cells were harvested at 24 hours and 48 hours post treatments and the cell pellet was resuspended in a solution of 100µl propidium iodide and RNase (FxCycle™ PI/RNase, Invitrogen, Massachusetts, USA). Propidium iodide stains for both DNA and RNA, therefore the ribonuclease (RNase) digests and removes RNA to ensure that only DNA content is analysed [56]. The samples were analysed using FACSort (Beckton Dickinson, San Jose, CA, USA), with 15 000-20 000 events per measurement. Fluorescence measurements were done at 495 nm and 519 nm (peak emission) at fluorescein isothiocyanate (FITC) channel for Annexin V FITC; 536 nm and 616 nm (peak emmision) at FL2 or FL3 channels for propidium iodide for all flow cytometry assays.

4.7 Gamma-H2AX foci assay

Treated cells were harvested 1 hour and at 24 hours post-irradiation and a suspension of approximately 120000 cells/0.25 mL were centrifuged onto coated slides (X-tra adhesive slides, Leica Biosystems, Buffalo Grove, IL, USA). Three slides were prepared for each treatment condition. The slides were fixed in freshly prepared 4% paraformaldehyde (PFA) for 20 min and washed in PBS for 5 minutes. Cells were then permeabilised with PBS-triton X-100 solution (GibcoTM, Thermo Fisher Scientific, Sandton, SA) for 10 minutes and blocking of no-specific antibody binding by washing 3 times in 1% bovine serum albumin (BSA) solution (Roche, Sigma-Aldrich/Merck, St. Louis, Missouri, USA) for 10 minutes per wash. Cells were incubated with phospho-histone H2A.X (Ser139) Monoclonal Antibody (3F2**)** antibody (Invitrogen, Biocom Africa (Pty) Ltd., Centurion, South Africa) for 1 hour at room temperature, followed by washing 3 times in 1% bovine serum albumin (BSA) (Roche, Sigma-Aldrich/Merck, St. Louis, Missouri, USA) to remove any unbound primary antibody. Cells were then incubated for a further 1-hour in the dark with Rabbit anti-Mouse IgG (H+L) FITC Secondary Antibody, secondary antibody (Invitrogen, Thermo Fisher Scientific, Sandton, SA) in a humidified chamber. Nuclear counterstaining was done with Prolong diamond anti-fade with DAPI (Thermo Fisher Scientific, Sandton, SA). Slides were stored at room temperature for a minimum of 24 hours and scanned automatically using the MetaCyte software module of the Metafer 4 scanning system with a 40X objective. For each slide, a minimum of 1000 cells were

captured, and the average number of γ-H2AX foci per scanned slide was derived from the MetaCyte software.

4.8 Statistical analysis

Statistical analysis was performed using Graphpad Prism version 10.2. All data was expressed as the mean ± SD of three independent experiments (n=3). Statistical significance was determined using two-tailed Student's t-test, and $p<0.05$ was considered statistically significant.

5. Conclusion

The results of the study supported previous studies that alluded that SAHA as a potential radiosensitiser in breast cell lines. Also, SAHA was observed to have minimal effect on normal cells (MCF-10A). However, in our previous study, we observed increased cellular migration and invasion in SAHA treated MCF-7 cells. This observation nullifies the observed benefit of radiosensitisation. Notwithstanding, SAHA showed benefit in the triple negative breast cell line. Although the results shows that SAHA has potential to enhance treatment efficacy in combination treatment with radiation in the triple negative breast cell line, future preclinical in vivo research and clinical trials are warranted to confirm these *in vitro* findings.

Author Contributions: Conceptualization, E.N.S., S.N., C.V., and A.J.; methodology, E.N.S., S.N., C.V., and A.J.; formal analysis, E.N.S., S.N., C.V., and A.J.; investigation, E.N.S., S.N., C.V., A.B., A.J., and S.N.; writing—original draft preparation, E.N.S.; writing—review and editing, E.N.S., S.N., C.V., and A.J.; supervision, S.N., C.V., and A.J.; funding acquisition, E.N.S., S.N., C.V., A.B., and A.J. All authors have read and agreed to the published version of the manuscript.

Funding: This research was funded by NRF iThemba Laboratories and Department of Higher Education and Training, South Africa. The APC was funded by the University of Pretoria, Cape Peninsula University of Technology, NRF iThemba Laboratories and GSI Helmholtzzentrum für Schwerionenforschung.

Institutional Review Board Statement: This study was conducted in accordance with the Declaration of Helsinki and approved by the Institutional Ethics Committee of University of Pretoria (Ethics number: 689/2021).

Acknowledgments: We acknowledge the Radiation biology team in the Biophysics Division at iThemba NRF Laboratories, South Africa for assistance with proton data collection. We also acknowledge the Trento Institute of Fundamental Physics (TIFPA) for provision of the proton beam, and the Cellular, Computational, and Integrative Biology (CIBIO) Laboratories where the proton experiments were conducted.

References

1. Schaefer, E.W.; Loaiza-Bonilla, A.; Juckett, M.; DiPersio, J.F.; Roy, V.; Slack, J.; Wu, W.; Laumann, K.; Espinoza-Delgado, I.; Gore, S.D. A phase 2 study of vorinostat in acute myeloid leukemia. *Haematologica* **2009**, *94*, 1375-1382, doi:10.3324/haematol.2009.009217.
2. Frame, F.M.; Pellacani, D.; Collins, A.T.; Simms, M.S.; Mann, V.M.; Jones, G.D.; Meuth, M.; Bristow, R.G.; Maitland, N.J. HDAC inhibitor confers radiosensitivity to prostate stem-like cells. *Br J Cancer* **2013**, *109*, 3023-3033, doi:10.1038/bjc.2013.691.
3. Munshi, A.; Tanaka, T.; Hobbs, M.L.; Tucker, S.L.; Richon, V.M.; Meyn, R.E. Vorinostat, a histone deacetylase inhibitor, enhances the response of human tumor cells to ionizing radiation through prolongation of γ-H2AX foci. *Molecular Cancer Therapeutics* **2006**, *5*, 1967-1974, doi:10.1158/1535-7163.Mct-06-0022.
4. Lee, J.H.; Choy, M.L.; Ngo, L.; Foster, S.S.; Marks, P.A. Histone deacetylase inhibitor induces DNA damage, which normal but not transformed cells can repair. *Proc Natl Acad Sci U S A* **2010**, *107*, 14639-14644, doi:10.1073/pnas.1008522107.
5. Chen, X.; Wong, P.; Radany, E.H.; Stark, J.M.; Laulier, C.; Wong, J.Y. Suberoylanilide hydroxamic acid as a radiosensitizer through modulation of RAD51 protein and inhibition of homology-directed repair in multiple myeloma. *Mol Cancer Res* **2012**, *10*, 1052-1064, doi:10.1158/1541-7786.Mcr-11-05[illegible].
6. Chiu, H.W.; Yeh, Y.L.; Wang, Y.C.; Huang, W.J.; Chen, Y.A.; Chiou, Y.S.; Ho, S.Y.; Lin, P.; Wang, Y.J. Suberoylanilide hydroxamic acid, an inhibitor of histone deacetylase, enhances radiosensitivity and suppresses lung metastasis in breast cancer *in vitro* and in vivo. *PLoS One* **2013**, *8*, e76340, doi:10.1371/journal.pone.007[illegible].
7. Adimoolam, S.; Sirisawad, M.; Chen, J.; Thiemann, P.; Ford, J.M.; Buggy, J.J. HDAC inhibitor PCI-24781 decreases RAD51 expression and inhibits homologous recombination. *Proc Natl Acad Sci U S A* **2007**, *104*, 19482-19487, doi:10.1073/pnas.0707828104.
8. Ladd, B.; Ackroyd, J.J.; Hicks, J.K.; Canman, C.E.; Flanagan, S.A.; Shewach, D.S. Inhibition of homologous recombination with vorinostat synergistically enhances ganciclovir cytotoxicity. *DNA Repair (Amst)* **2013**, *12*, 1114-1121, doi:10.1016/j.dnarep.2013.10.008.
9. Subramanian, C.; Hada, M.; Opipari, A.W., Jr.; Castle, V.P.; Kwok, R.P. CREB-binding protein regulates Ku70 acetylation in response to ionization radiation in neuroblastoma. *Mol Cancer Res* **2013**, *11*, 173-181, doi:10.1158/1541-7786.Mcr-12-0065.

10. Chung, Y.L.; Wang, A.J.; Yao, L.F. Antitumor histone deacetylase inhibitors suppress cutaneous radiation syndrome: Implications for increasing therapeutic gain in cancer radiotherapy. *Mol Cancer Ther* **2004**, *3*, 317-325.
11. Blattmann, C.; Oertel, S.; Thiemann, M.; Weber, K.J.; Schmezer, P.; Zelezny, O.; Lopez Perez, R.; Kulozik, A.E.; Debus, J.; Ehemann, V. Suberoylanilide hydroxamic acid affects γH2AX expression in osteosarcoma, atypical teratoid rhabdoid tumor and normal tissue cell lines after irradiation. *Strahlenther Onkol* **2012**, *188*, 168-176, doi:10.1007/s00066-011-0028-5.
12. Vanderwaeren, L.; Dok, R.; Verstrepen, K.; Nuyts, S. Clinical Progress in Proton Radiotherapy: Biological Unknowns. *Cancers (Basel)* **2021**, *13*, doi:10.3390/cancers13040604.
13. Johnson, A.M.; Bennett, P.V.; Sanidad, K.Z.; Hoang, A.; Jardine, J.H.; Keszenman, D.J.; Wilson, P.F. Evaluation of Histone Deacetylase Inhibitors as Radiosensitizers for Proton and Light Ion Radiotherapy. *Front Oncol* **2021**, *11*, 735940, doi:10.3389/fonc.2021.735940.
14. Park, S.-Y.; Kim, J.-S. A short guide to histone deacetylases including recent progress on class II enzymes. *Experimental & Molecular Medicine* **2020**, *52*, 204-212, doi:10.1038/s12276-020-0382-4.
15. Yu, J.I.; Choi, C.; Shin, S.-W.; Son, A.; Lee, G.-H.; Kim, [illegible]; Park, H.C. Valproic Acid Sensitizes Hepatocellular Carcinoma Cells to Proton Therapy by Suppressing NRF2 Activation. *Scientific Reports* **2017**, *7*, 14986, doi:10.1038/s41598-017-15165-3.
16. Gerelchuluun, A.; Maeda, J.; Manabe, E.; Brents, C.; Sakae, T.; Fujimori, A.; Chen, D.J.; Tsuboi, K.; Kato, T.A. Histone Deacetylase Inhibitor Induced Radiation Sensitization Effects on Human Cancer Cells after Photon and Hadron Radiation Exposure. *Int J Mol Sci* **2018**, *19*, 496, doi:10.3390/ijms19020496.
17. Seane, E.; Nair, S.; Vandevoorde, C.; Bisio, A.; Joubert, A. Multi-Target Inhibitor CUDC-101 Impairs DNA Damage Repair and Enhances Radiation Response in Triple-Negative Breast Cell Line. *Pharmaceuticals* **2024**, *17*, 1467, doi:10.3390/ph17111467.
18. Qiu, L.; Burgess, A.; Fairlie, D.P.; Leonard, H.; Parsons, P.G.; Gabrielli, B.G. Histone deacetylase inhibitors trigger a G2 checkpoint in normal cells that is defective in tumor cells. *Mol Biol Cell* **2000**, *11*, 2069-2083, doi:10.1091/mbc.11.6.2069.
19. Kim, H.J.; Bae, S.C. Histone deacetylase inhibitors: molecular mechanisms of action and clinical trials as anti-cancer drugs. *Am J Transl Res* **2011**, *3*, 166-179.
20. Szymonowicz, K.; Krysztofiak, A.; Linden, J.V.; Kern, A.; Deycmar, S.; Oeck, S.; Squire, A.; Koska, B.; Hlouschek, J.; Vüllings, M.; et al. Proton Irradiation Increases the Necessity for Homologous Recombination Repair Along with the Indispensability of Non-Homologous End Joining. *Cells* **2020**, *9*, doi:10.3390/cells9040889.

21. Costes, S.V.; Boissière, A.; Ravani, S.; Romano, R.; Parvin, B.; Barcellos-Hoff, M.H. Imaging features that discriminate between foci induced by high- and low-LET radiation in human fibroblasts. *Radiat Res* **2006**, *165*, 505-515, doi:10.1667/rr3538.1.
22. Leatherbarrow, E.L.; Harper, J.V.; Cucinotta, F.A.; O'Neill, P. Induction and quantification of gamma-H2AX foci following low and high LET-irradiation. *Int J Radiat Biol* **2006**, *82*, 111-118, doi:10.1080/09553000600599783.
23. Oeck, S.; Szymonowicz, K.; Wiel, G.; Krysztofiak, A.; Lambert, J.; Koska, B.; Iliakis, G.; Timmermann, B.; Jendrossek, V. Relating Linear Energy Transfer to the Formation and Resolution of DNA Repair Foci After Irradiation with Equal Doses of X-ray Photons, Plateau, or Bragg-Peak Protons. *Int J Mol Sci* **2018**, *19*, doi:10.3390/ijms19123779.
24. Gerelchuluun, A.; Hong, Z.; Sun, L.; Suzuki, K.; Terunuma, T.; Yasuoka, K.; Sakae, T.; Moritake, T.; Tsuboi, K. Induction of in situ DNA double-strand breaks and apoptosis by 200 MeV protons and 10 MV X-rays in human tumour cell lines. *Int J Radiat Biol* **2011**, *87*, 57-70, doi:10.3109/09553002.2010.518201.
25. Bracalente, C.; Ibañez, I.L.; Molinari, B.; Palmieri, M.; Kreiner, A.; Valda, A.; Davidson, J.; Durán, H. Induction and persistence of large γH2AX foci by high linear energy transfer radiation in DNA-dependent protein kinase-deficient cells. *Int J Radiat Oncol Biol Phys* **2013**, *87*, 785-794, doi:10.1016/j.ijrobp.2013.07.014.
26. Grosse, N.; Fontana, A.O.; Hug, E.B.; Lomax, A.; Coray, A.; Augsburger, M.; Paganetti, H.; Sartori, A.A.; Pruschy, M. Deficiency in homologous recombination renders Mammalian cells more sensitive to proton versus photon irradiation. *Int J Radiat Oncol Biol Phys* **2014**, *88*, 175-181, doi:10.1016/j.ijrobp.2013.09.041.
27. Choi, C.; Lee, G.H.; Son, A.; Yoo, G.S.; Yu, J.I.; Park, H.C. Downregulation of Mcl-1 by Panobinostat Potentiates Proton Beam Therapy in Hepatocellular Carcinoma Cells. *Cells* **2021**, *10*, doi:10.3390/cells10030554.
28. Tommasino, F.; Rovituso, M.; Bortoli, E.; La Tessa, C.; Petringa, G.; Lorentini, S.; Verroi, E.; Simeonov, Y.; Weber, U.; Cirrone, P.; et al. A new facility for proton radiobiology at the Trento proton therapy centre: Design and implementation. *Phys Med* **2019**, *58*, 99-106, doi:10.1016/j.ejmp.2019.02.001.
29. Comşa, Ş.; Cîmpean, A.M.; Raica, M. The Story of MCF-7 Breast Cancer Cell Line: 40 years of Experience in Research. *Anticancer Res* **2015**, *35*, 3147-3154.

Critical discussion to the Chapter

Most of the studies that explored combination treatments of HDACi and radiation focused on local effects, i.e. radiosensitisation of cells in the tumour bulk, and very little has been reported about the systematic effects. The current study filled a significant gap in knowledge by assessing the effect of the two HDACi inhibitors on the migration and invasion capacity of the MCF-7 and MDA-MB-231 cell lines. This was particularly crucial in light of numerous reports that highlighted the metastasis-promoting effects of radiation.

Personal contribution to the Chapter

The draft article was prepared by the candidate, 100% contribution, and is yet to be reviewed by the other collaborators.

CHAPTER 6: GENERAL DISCUSSIONS AND CONCLUSION

6.1 Introduction of the Chapter

This chapter brings together the results of the study presented in the published and in the draft manuscripts. The discussion is aligned with the five objectives of the study, in objective (i) radiosensitising capacities of CUDC-101 and SAHA was assessed by quantifying relative cell survival and proliferation post treatment with HDACi (SAHA or CUDC-101), in combination with proton and X-radiation. The mechanisms of radiosensitisation were then investigated in objectives (ii) - (v) by quantifying the proportion of cells in G1, S and G2/M phases of the cell cycle, gamma-H2AX foci formation and retention, (iv) the fraction of apoptotic and necrotic cells, and assessing the cell migratory and invasion capacity, post treatment with HDACi (CUDC-101 or SAHA) in combination with proton and photon irradiations. The limitations of the study are highlighted and recommendations for future studies are made.

6.2 Radiosensitising efficacy of CUDC-101 and SAHA in breast cell lines

The study set out to assess the efficacy of the two HDACi CUDC-101 and SAHA as potential radiosensitisers in two breast cancer cell lines. The aim of radiotherapy treatments is to eradicate malignant cells with little effect on normal cells. Therefore, it was imperative that the effect of this combination treatments on normal breast cell line is also assessed. Since combination therapy was used, it was crucial to first determine the best sequencing protocol for the administration of radiation and the HDACi. From previous studies discussed in Chapter 2, different sequencing protocols had been used, where in some cases HDACi was given before radiation and in some studies HDACi was given after radiation. In the current study, administering HDACi 24 hours before irradiation was determined to yield the most radiosensitisation and was subsequently used for all experiments. Mechanistically, administering the HDACi before radiation allows time for inhibition of HDACs leading to opening of chromatin and increased yield of DNA double strand break, which are the lethal to the cell.[57] [58]

The results of the study revealed that both HDACi, SAHA and CUDC-101 are able to enhance the radiation-induced cytoxicity in the two breast cancer cell lines when combined with either X-rays or protons, Chapters 3 and 5. In the study, sensitisation by HDACi was expressed in terms of sensitisation enhancement ratio (SER). Of the two HDACi, CUDC-101, proved to be a more potent radiosensitiser with higher proton SER values (1.50 and 1.77) than SAHA (SER

values of 1.40 and 1.71) for MCF-7 and MDA-MB-231, respectively. Similarly, after treatment with X-rays, CUDC-101 (SER of 2.09) was determined to be a more effective radiosensitizer than SAHA (SER of 1.68) in the MDA-MB-231 cell line. These results point out that the most radiation enhancement was observed in the triple negative MDA-MB-231 cell line. In this cell line, modest CUDC-101 induced radiosensitisation was observed after protons (SER value of 1.77) compared to X-rays (SER value 2.09). A similar observation was made by Johnson et al. in glioma cell lines. The authors also observed modest levels of radiosensitisation after treatment with 200MeV protons compared to γ-ray irradiation.[59] The increased sensitising effect of CUDC-101 is attributed to inhibition of multiple targets, i.e. HDACs, EGFR and HER-2, compared to SAHA that inhibits only HDACs. In pancreatic cell lines (MIA PaCa-2, Su.86.86 and T3M-4), Moertl et al. also reported increased sensitization by CUDC-101 compared to SAHA. [36] Likewise, Schlaff et al. reported inhibition of HDACs, EGFR and HER-2 in the MDA-MB-231 cell line.[19] Similar to breast cancer, over expression of EGFR and HER-2 has been reported in pancreatic tumours, hence dual targeting of EGFR and HER-2 in these cancers has showed some benefit.[37, 60]. A number of studies have investigated combination therapies of HDACi and X-rays in different cell lines. The current study was the first to investigate the efficacy of SAHA and CUDC-101 in combination with proton therapy in breast cell lines. Combination therapy of HDACi Panobinostat and valproic acid, which are also hydroxamic acid, with protons was previously assessed in HCC cell lines.[11, 12] In view of the fact that the effect of HDACi is cell line specific, the results of these studies could not be extrapolated to breast cell lines, which motivated for the current study to be conducted.

Of relevance is also the HDACi-induced sensitization which was observed in the spontaneously immortalised normal MCF-10A cell line, particularly in CUDC-101 (SER of 1.23 and 1.10) pre-treated cells compared to SAHA (1.20 and 0.94) for protons and X-rays, respectively. Clinically, this would translate into increased normal tissue side effects. As discussed in Chapter 1, due to the superior dose distribution of proton beam, little dose is deposited in normal tissues, which is advantageous for normal tissue sparing. Therefore, the superior dose distribution of proton therapy would, in principle, negate the increased local side effects as suggested by the observed increased SER values after proton irradiation. However, the system side effects such nausea, fatigue, vomiting, dyspnea, pyrexia, and dry skin were observed after CUDC-101 treatment combined either chemotherapy and X-radiation in Phase 1 clinical trials, could be managed by optimal scheduling of the drug and radiotherapy treatment as well as by finding the other routes of administration other than oral administration.[61] These systemic side effects were reported to last for a short period and were reversible upon stopping the drug treatment.[61, 62]

The results of this *in vitro* study provide significant contribution to the pursuit of effective treatment strategies for triple negative breast cancers. Triple negative breast cancer is characterised by an aggressive phenotype and increased metastatic potential, and prognosis is poor.[64] Further, current treatment strategies such as hormonal therapy and trastuzumab-based treatments have proved to be ineffective in patients with triple negative breast cancer.[65] Increased incidences of triple negative breast cancer and increased rates of mortality has been reported to occur mainly in young (less than 55 years) females of black ethnicity, most of whom are situated in Sub-Saharan Africa.[66-69] The results of the study therefore hold relevance in attaining effective treatment strategy for the breast cancer molecular subtype that is most prevalent in Sub-Saharan populations.

6.3 Mechanisms of radiosensitisation

The radiosensitising effect of HDACi can be explained in two ways: 1) effect on the chromatin structure, and 2) effect on DNA damage repair (DDR) proteins. Over-expression of HDACs which leads to compact chromatin structure and repression of gene expression, has been reported in many tumours including breast cancer.[70-73] As discussed in Chapter 2, ample evidence exists to support that compact chromatin has radioprotective effects. Treatment with HDACi therefore represses the effect of HDACs, opening the chromatin, which allows increased DSB induction upon irradiation.[57, 58] In the study, DNA DSB induction was assessed by detection of γ-H2AX foci, which is widely accepted as a reliable biomarker for double strand break.[74] The ability of HDACi to impair DNA DSB repair was assessed by retention of γ-H2AX foci at 24 hours post irradiation. Of the two malignant breast cell lines, increased DNA DSB induction and retention following treatment with CUDC-101 or SAHA monotherapy and in combination treatments with 2Gy protons or X-rays, was seen mainly in the triple negative MDA-MB-231 cell line, which supports the observed increased radiosensitisation in this cell line. In clinical practice, conventional fractionation of 2Gy is often used in the radiotherapy treatment of most tumours including breast tumours. The increased DNA DSB formation after 2Gy X-rays and CUDC-101 that was observed in the triple negative breast cell line therefore bears clinical relevance.

Previous studies had reported that the main mechanisms of radiosensitisation by HDACi is through repression of DSB damage repair proteins such as MRE11/Rad50/NBS1 (MRN) complex and Rad51 involved in HR and repression of ku70, ku80, DNA-PK's involved in NHEJ.[23, 35, 50, 75]. In the current study, persisting γ-H2AX foci at 24 hours post irradiation was interpreted to indicate repression of DNA damage repair proteins. Although γ-H2AX foci is accepted as a reliable marker of DSB, it is acknowledged that it does not provide information about the levels of the repair proteins. In a previous study, Moertl *et al.* did not observe

persistence of γ-H2AX foci after combination therapy of HDACi and radiation in pancreatic cell lines, but the levels of DNA repair protein PARP-1 were found to be reduced.[36] This highlights the need to assess the levels of DNA repair proteins in conjunction with the γ-H2AX foci results. The failure to assess the DNA repair proteins in the current study is therefore acknowledged as a shortcoming of this study.

The mechanisms of radiosensitisation were further probed by assessing the modes of cell death following combination therapy of HDACi and radiation. Although previous studies had reported increased apoptosis after proton irradiation[76-78], in the current study the total apoptosis in the malignant cell lines (MCF-7 and MDA-MB-231) averaged below 20% after proton irradiation or HDACi and proton irradiation. Induction of necrosis was notable in the MCF-7 cell line, but also averaged below 10% for the two malignant cell lines. This finding indicated that apoptosis, which was previously reported as the main mode of cell death by HDACi, is not necessarily the main modes of cell death for the HDACi (SAHA or CUDC101) and for the cell lines (MCF-7, MDA-MB-231), used in the study. Another mode of cell death, mitotic catastrophe, was previously reported to be the main mode of cell death after X-radiation.[79] In the current study, mitotic catastrophe was not assessed but persisting G2/M cell cycle arrest at 48 hours post irradiation was interpreted as an indicator of mitotic catastrophe. In line with previous reports, persisting G2/M arrest was seen after X-irradiation in the triple negative cell line, which indicated mitotic catastrophe. Autophagy, which has also been flagged in some studies as another mode of cell death following treatments with HDACi, was not assessed, which is another limitation of the study.

Most of the studies that explored combination treatments of HDACi and radiation focused on local effects, i.e. radiosensitisation of cells in the tumour bulk, and very little has been reported about the systematic effects. The current study filled a significant gap in knowledge by assessing the effect of the two HDACi inhibitors on the migration and invasion capacity of the MCF-7 and MDA-MB-231 cell lines. This was particularly crucial in light of numerous reports that highlighted the metastasis-promoting effects of radiation.[80-83] MCF-7 cell have little metastatic potential, whereas the MDA-MB-231 cell line have increased migration and invasion potential.[49, 84, 85] In the current study, both SAHA and CUDC-101 reduced migration and invasion in the triple negative MDA-MB-231 cell. The two HDACi also reduced migration and invasion when used as monotherapy. An unexpected finding in the study was the increase in migration and invasion after SAHA treatment in the MCF-7 cell line, which is in contradiction to most of the previous studies.[20, 86] This finding provides significant contribution in explaining the disappointing results that were seen after SAHA treatment in clinical trials in solid tumours.[31]

6.4 Conclusions and recommendations

The results of this *in vitro* study highlighted the potential benefit of CUDC-101 in enhancing the effect of radiation which can improve tumour control mainly in the triple negative breast cell line. Migration and invasion, which are the requirements for metastasis, were also observed to be reduced by CUDC-101 in the triple negative cell line. The observed metastasis promoting potential of SAHA in the breast luminal, ER, PR positive and HER-2 negative molecular sub-type (MCF-7), nullifies the observed benefit of radiosensitisation. Although CUDC-101, showed potential benefit as a radiosensitiser as well in reducing metastatic potential of the triple negative MDA-MB-231 cell line (adenocarcinoma), it is recommended that other types of triple-negative breast cell lines with different histological profiles such as MDA-MB-157 (Medullary carcinoma), MDA-MB-453 (Carcinoma), or BT-549 (Ductal carcinoma), be conducted. Given the *in vitro* nature of the study, in vivo studies are also recommended to validate the observed results. Also, to fully understand the mechanisms, future *in vitro* studies should investigate other modes of cell death such as autophagy.

LIST OF REFERENCES

1. Cancer in South Africa National Institute for Communicable Diseases, Service NHL; 2017.

2. Sung H, Ferlay J, Siegel RL, Laversanne M, Soerjomataram I, Jemal A, et al. Global Cancer Statistics 2020: GLOBOCAN Estimates of Incidence and Mortality Worldwide for 36 Cancers in 185 Countries. CA Cancer J Clin. 2021; 71(3):209-49. doi:10.3322/caac.21660

3. O'Neil DS, Chen WC, Ayeni O, Nietz S, Buccimazza I, Singh U, et al. Breast Cancer Care Quality in South Africa's Public Health System: An Evaluation Using American Society of Clinical Oncology/National Quality Forum Measures. J Glob Oncol. 2019; 5:1-16. doi:10.1200/JGO.19.00171

4. Corbin KS, Mutter RW. Proton therapy for breast cancer: progress & pitfalls. Breast Cancer Management. 2018; 7(1): BMT06. doi:10.2217/bmt-2018-0001

5. Dillekås H, Rogers MS, Straume O. Are 90% of deaths from cancer caused by metastases? Cancer Med. 2019; 8(12):5574-6. doi:10.1002/cam4.2474

6. Lambert M, Mendenhall E, Kim AW, Cubasch H, Joffe M, Norris SA. Health system experiences of breast cancer survivors in urban South Africa. Womens Health (Lond). 2020; 16:1745506520949419. doi:10.1177/1745506520949419

7. Gray M, Turnbull AK, Ward C, Meehan J, Martinez-Perez C, Bonello M, et al. Development and characterisation of acquired radioresistant breast cancer cell lines. Radiat Oncol. 2019; 14(1):64. doi:10.1186/s13014-019-1268-2

8. Chowdhary M, Lee A, Gao S, Wang D, Barry PN, Diaz R, et al. Is Proton Therapy a "Pro" for Breast Cancer? A Comparison of Proton vs. Non-proton Radiotherapy Using the National Cancer Database. Front Oncol. 2018; 8:678. doi:10.3389/fonc.2018.00678

9. Leeman JE, Romesser PB, Zhou Y, McBride S, Riaz N, Sherman E, et al. Proton therapy for head and neck cancer: expanding the therapeutic window. The Lancet Oncology. 2017; 18(5):e254-e65. doi:10.1016/S1470-2045(17)30179-1

10. Alonso-González C, González A, Menéndez-Menéndez J, Martínez-Campa C, Cos S. Melatonin as a Radio-Sensitizer in Cancer. Biomedicines. 2020; 8(8):247. doi:10.3390/biomedicines8080247

11. Choi C, Lee GH, Son A, Yoo GS, Yu JI, Park HC. Downregulation of Mcl-1 by Panobinostat Potentiates Proton Beam Therapy in Hepatocellular Carcinoma Cells. Cells. 2021; 10(3) doi:10.3390/cells10030554

12. Yu JI, Choi C, Shin S-W, Son A, Lee G-H, Kim S-Y, et al. Valproic Acid Sensitizes Hepatocellular Carcinoma Cells to Proton Therapy by Suppressing NRF2 Activation. Scientific Reports. 2017; 7(1):14986. doi:10.1038/s41598-017-15165-3

13. Choi C, Son A, Lee GH, Shin SW, Park S, Ahn SH, et al. Targeting DNA-dependent protein kinase sensitizes hepatocellular carcinoma cells to proton beam irradiation through apoptosis induction. PLoS One. 2019; 14(6):e0218049. doi:10.1371/journal.pone.0218049

14. Camphausen K, Scott T, Sproull M, Tofilon PJ. Enhancement of xenograft tumor radiosensitivity by the histone deacetylase inhibitor MS-275 and correlation with histone hyperacetylation. Clin Cancer Res. 2004; 10(18 Pt 1):6066-71. doi:10.1158/1078-0432.Ccr-04-0537

15. Camphausen K, Tofilon PJ. Inhibition of histone deacetylation: a strategy for tumor radiosensitization. J Clin Oncol. 2007; 25(26):4051-6. doi:10.1200/JCO.2007.11.6202

16. Groselj B, Sharma NL, Hamdy FC, Kerr M, Kiltie AE. Histone deacetylase inhibitors as radiosensitisers: effects on DNA damage signalling and repair. Br J Cancer. 2013; 108(4):748-54. doi:10.1038/bjc.2013.21

17. Damaskos C, Garmpis N, Valsami S, Kontos M, Spartalis E, Kalampokas T, et al. Histone Deacetylase Inhibitors: An Attractive Therapeutic Strategy Against Breast Cancer. Anticancer Res. 2017; 37(1):35-46. doi:10.21873/anticanres.11286

18. Chinnaiyan P, Cerna D, Burgan WE, Beam K, Williams ES, Camphausen K, et al. Postradiation sensitization of the histone deacetylase inhibitor valproic acid. Clin Cancer Res. 2008; 14(17):5410-5. doi:10.1158/1078-0432.CCR-08-0643

19. Schlaff CD, Arscott WT, Gordon I, Tandle A, Tofilon P, Camphausen K. Radiosensitization Effects of Novel Triple-Inhibitor CUDC-101 in Glioblastoma Multiforme and Breast Cancer Cells *In Vitro*. International Journal of Radiation Oncology*Biology*Physics. 2013; 87(2) doi:10.1016/j.ijrobp.2013.06.1722

20. Chiu HW, Yeh YL, Wang YC, Huang WJ, Chen YA, Chiou YS, et al. Suberoylanilide hydroxamic acid, an inhibitor of histone deacetylase, enhances radiosensitivity and

suppresses lung metastasis in breast cancer in vitro and in vivo. PLoS One. 2013; 8(10):e76340. doi:10.1371/journal.pone.0076340

21. Baschnagel A, Russo A, Burgan WE, Carter D, Beam K, Palmieri D, et al. Vorinostat enhances the radiosensitivity of a breast cancer brain metastatic cell line grown *in vitro* and as intracranial xenografts. Mol Cancer Ther. 2009; 8(6):1589-95. doi:10.1158/1535-7163.MCT-09-0038

22. Chen X, Wong P, Radany E, Wong JY. HDAC inhibitor, valproic acid, induces p53-dependent radiosensitization of colon cancer cells. Cancer Biother Radiopharm. 2009; 24(6):689-99. doi:10.1089/cbr.2009.0629

23. Munshi A, Kurland JF, Nishikawa T, Tanaka T, Hobbs ML, Tucker SL, et al. Histone deacetylase inhibitors radiosensitize human melanoma cells by suppressing DNA repair activity. Clin Cancer Res. 2005; 11(13):4912-22. doi:10.1158/1078-0432.Ccr-04-2088

24. Munshi A, Tanaka T, Hobbs ML, Tucker SL, Richon VM, Meyn RE. Vorinostat, a histone deacetylase inhibitor, enhances the response of human tumor cells to ionizing radiation through prolongation of γ-H2AX foci. Molecular Cancer Therapeutics. 2006; 5(8):1967-74. doi:10.1158/1535-7163.Mct-06-0022

25. Li Y, Seto E. HDACs and HDAC Inhibitors in Cancer Development and Therapy. Cold Spring Harb Perspect Med. 2016; 6(10) doi:10.1101/cshperspect.a026831

26. Jenke R, Ressing N, Hansen FK, Aigner A, Buch T. Anticancer Therapy with HDAC Inhibitors: Mechanism-Based Combination Strategies and Future Perspectives. Cancers (Basel). 2021; 13(4) doi:10.3390/cancers13040634

27. Smalley JP, Cowley SM, Hodgkinson JT. Bifunctional HDAC Therapeutics: One Drug to Rule Them All? Molecules. 2020; 25(19) doi:10.3390/molecules25194394

28. Dokmanovic M, Clarke C, Marks PA. Histone Deacetylase Inhibitors: Overview and Perspectives. Molecular Cancer Research. 2007; 5(10):981-9. doi:10.1158/1541-7786.Mcr-07-0324

29. Rajak H, Singh A, Raghuwanshi K, Kumar R, Dewangan PK, Veerasamy R, et al. A structural insight into hydroxamic acid based histone deacetylase inhibitors for the presence of anticancer activity. Curr Med Chem. 2014; 21(23):2642-64. doi:10.2174/0929867313209990191

30. Ediriweera MK, Tennekoon KH, Samarakoon SR. Emerging role of histone deacetylase inhibitors as anti-breast-cancer agents. Drug Discov Today. 2019; 24(3):685-702. doi:10.1016/j.drudis.2019.02.003

31. Luu TH, Morgan RJ, Leong L, Lim D, McNamara M, Portnow J, et al. A phase II trial of vorinostat (suberoylanilide hydroxamic acid) in metastatic breast cancer: a California Cancer Consortium study. Clin Cancer Res. 2008; 14(21):7138-42. doi:10.1158/1078-0432.CCR-08-0122

32. Camphausen K, Cerna D, Scott T, Sproull M, Burgan WE, Cerra MA, et al. Enhancement of in vitro and in vivo tumor cell radiosensitivity by valproic acid. Int J Cancer. 2005; 114(3):380-6. doi:10.1002/ijc.20774

33. Cerna D, Camphausen K, Tofilon PJ. Histone deacetylation as a target for radiosensitization. Curr Top Dev Biol. 2006; 73:173-204. doi:10.1016/s0070-2153(05)73006-4

34. Suraweera A, O'Byrne KJ, Richard DJ. Combination Therapy With Histone Deacetylase Inhibitors (HDACi) for the Treatment of Cancer: Achieving the Full Therapeutic Potential of HDACi. Front Oncol. 2018; 8:92. doi:10.3389/fonc.2018.00092

35. Shabason JE, Tofilon PJ, Camphausen K. Grand rounds at the National Institutes of Health: HDAC inhibitors as radiation modifiers, from bench to clinic. J Cell Mol Med. 2011; 15(12):2735-44. doi:10.1111/j.1582-4934.2011.01296.x

36. Moertl S, Payer S, Kell R, Winkler K, Anastasov N, Atkinson MJ. Comparison of Radiosensitization by HDAC Inhibitors CUDC-101 and SAHA in Pancreatic Cancer Cells. Int J Mol Sci. 2019; 20(13) doi:10.3390/ijms20133259

37. Grapa CM, Mocan T, Gonciar D, Zdrehus C, Mosteanu O, Pop T, et al. Epidermal Growth Factor Receptor and Its Role in Pancreatic Cancer Treatment Mediated by Nanoparticles. Int J Nanomedicine. 2019; 14:9693-706. doi:10.2147/IJN.S226628

38. Cody D. Schlaff WTA, Ira Gordon , Kevin A. Camphausen Anita Tandle. Human EGFR-2, EGFR and HDAC Triple-Inhibitor CUDC-101 Enhances Radiosensitivity of GBM Cells. Biomed Res J. 2015; 2(1):105-19.

39. Shi W, Lawrence YR, Choy H, Werner-Wasik M, Andrews DW, Evans JJ, et al. Vorinostat as a radiosensitizer for brain metastasis: a phase I clinical trial. J Neurooncol. 2014; 118(2):313-9. doi:10.1007/s11060-014-1433-2

40. Ree AH, Dueland S, Folkvord S, Hole KH, Seierstad T, Johansen M, et al. Vorinostat, a histone deacetylase inhibitor, combined with pelvic palliative radiotherapy for gastrointestinal carcinoma: the Pelvic Radiation and Vorinostat (PRAVO) phase 1 study. The Lancet Oncology. 2010; 11(5):459-64. doi:10.1016/s1470-2045(10)70058-9

41. A Phase I Study of LBH589 (Panobinostat) in Combination with External Beam Radiotherapy for the Treatment of Prostate Cancer, Esophageal Cancer and Head and Neck Cancer.NCT00670553.Last updated 2017-05-17. Accessed: 2024-10-23

42. DuBois SG, Groshen S, Park JR, Haas-Kogan DA, Yang X, Geier E, et al. Phase I Study of Vorinostat as a Radiation Sensitizer with 131I-Metaiodobenzylguanidine (131I-MIBG) for Patients with Relapsed or Refractory Neuroblastoma. Clin Cancer Res. 2015; 21(12):2715-21. doi:10.1158/1078-0432.Ccr-14-3240

43. Traynor AM, Dubey S, Eickhoff JC, Kolesar JM, Schell K, Huie MS, Groteluschen DL, Marcotte SM, Hallahan CM, Weeks HR, Wilding G, Espinoza-Delgado I, Schiller JH. Vorinostat (NSC# 701852) in patients with relapsed non-small cell lung cancer: a Wisconsin Oncology Network phase II study. J Thorac Oncol. 2009;4(4):522-6. doi: 10.1097/jto.0b013e3181952478. PMID: 19347984; PMCID: PMC3050710.

44. Krauze AV, Myrehaug SD, Chang MG, Holdford DJ, Smith S, Shih J, et al. A Phase 2 Study of Concurrent Radiation Therapy, Temozolomide, and the Histone Deacetylase Inhibitor Valproic Acid for Patients With Glioblastoma. Int J Radiat Oncol Biol Phys. 2015; 92(5):986-92. doi:10.1016/j.ijrobp.2015.04.038

45. Barazzuol L, Jeynes JC, Merchant MJ, Wéra AC, Barry MA, Kirkby KJ, et al. Radiosensitization of glioblastoma cells using a histone deacetylase inhibitor (SAHA) comparing carbon ions with X-rays. Int J Radiat Biol. 2015; 91(1):90-8. doi:10.3109/09553002.2014.946111

46. Gerelchuluun A, Maeda J, Manabe E, Brents CA, Sakae T, Fujimori A, et al. Histone Deacetylase Inhibitor Induced Radiation Sensitization Effects on Human Cancer Cells after Photon and Hadron Radiation Exposure. Int J Mol Sci. 2018; 19(2):496. doi:10.3390/ijms19020496

47. Fontana AO, Augsburger MA, Grosse N, Guckenberger M, Lomax AJ, Sartori AA, et al. Differential DNA repair pathway choice in cancer cells after proton- and photon-irradiation. Radiother Oncol. 2015; 116(3):374-80. doi:10.1016/j.radonc.2015.08.014

48. Girdhani S, Sachs R, Hlatky L. Biological effects of proton radiation: what we know and don't know. Radiat Res. 2013; 179(3):257-72. doi:10.1667/rr2839.1

49. Vanderwaeren L, Dok R, Verstrepen K, Nuyts S. Clinical Progress in Proton Radiotherapy: Biological Unknowns. Cancers (Basel). 2021; 13(4) doi:10.3390/cancers13040604

50. Groselj B, Kerr M, Kiltie AE. Radiosensitisation of bladder cancer cells by panobinostat is modulated by Ku80 expression. Radiother Oncol. 2013; 108(3):429-33. doi:10.1016/j.radonc.2013.06.021

51. Gong L, Zhang Y, Liu C, Zhang M, Han S. Application of Radiosensitizers in Cancer Radiotherapy. Int J Nanomedicine. 2021; 16:1083-102. doi:10.2147/IJN.S290438

52. Yung-Chi C, Prusoff WH. Relationship between the inhibition constant (KI) and the concentration of inhibitor which causes 50 per cent inhibition (I50) of an enzymatic reaction. Biochemical Pharmacology. 1973; 22(23):3099-108. doi:https://doi.org/10.1016/0006-2952(73)90196-2

53. Baumann BC, Mitra N, Harton JG, Xiao Y, Wojcieszynski AP, Gabriel PE, et al. Comparative Effectiveness of Proton vs Photon Therapy as Part of Concurrent Chemoradiotherapy for Locally Advanced Cancer. JAMA Oncology. 2020; 6(2):237. doi:10.1001/jamaoncol.2019.4889

54. Franken NA, Rodermond HM, Stap J, Haveman J, van Bree C. Clonogenic assay of cells *in vitro*. Nat Protoc. 2006; 1(5):2315-9. doi:10.1038/nprot.2006.339

55. Tommasino F, Rovituso M, Bortoli E, La Tessa C, Petringa G, Lorentini S, et al. A new facility for proton radiobiology at the Trento proton therapy centre: Design and implementation. Phys Med. 2019; 58:99-106. doi:10.1016/j.ejmp.2019.02.001

56. Comşa Ş, Cîmpean AM, Raica M. The Story of MCF-7 Breast Cancer Cell Line: 40 years of Experience in Research. Anticancer Res. 2015; 35(6):3147-54.

57. Takata H, Hanafusa T, Mori T, Shimura M, Iida Y, Ishikawa K, et al. Chromatin compaction protects genomic DNA from radiation damage. PLoS One. 2013; 8(10):e75622. doi:10.1371/journal.pone.0075622

58. Venkatesh P, Panyutin IV, Remeeva E, Neumann RD, Panyutin IG. Effect of Chromatin Structure on the Extent and Distribution of DNA Double Strand Breaks Produced by Ionizing

Radiation; Comparative Study of hESC and Differentiated Cells Lines. Int J Mol Sci. 2016; 17(1) doi:10.3390/ijms17010058

59. Johnson, A.M.; Bennett, P.V.; Sanidad, K.Z.; Hoang, A.; Jardine, J.H.; Keszenman, D.J.; Wilson, P.F. Evaluation of Histone Deacetylase Inhibitors as Radiosensitizers for Proton and Light Ion Radiotherapy. *Front Oncol* **2021**, *11*, 735940, doi:10.3389/fonc.2021.735940.

60. Larbouret C, Gaborit N, Chardès T, Coelho M, Campigna E, Bascoul-Mollevi C, et al. In pancreatic carcinoma, dual EGFR/HER2 targeting with cetuximab/trastuzumab is more effective than treatment with trastuzumab/erlotinib or lapatinib alone: implication of receptors' down-regulation and dimers' disruption. Neoplasia. 2012; 14(2):121-30. doi:10.1593/neo.111602

61. Galloway TJ, Wirth LJ, Colevas AD, Gilbert J, Bauman JE, Saba NF, et al. A Phase I Study of CUDC-101, a Multitarget Inhibitor of HDACs, EGFR, and HER2, in Combination with Chemoradiation in Patients with Head and Neck Squamous Cell Carcinoma. Clin Cancer Res. 2015; 21(7):1566-73. doi:10.1158/1078-0432.Ccr-14-2820

62. Shimizu T, LoRusso PM, Papadopoulos KP, Patnaik A, Beeram M, Smith LS, et al. Phase I first-in-human study of CUDC-101, a multitargeted inhibitor of HDACs, EGFR, and HER2 in patients with advanced solid tumors. Clin Cancer Res. 2014; 20(19):5032-40. doi:10.1158/1078-0432.Ccr-14-0570

63. Paganetti H, Beltran C, Both S, Dong L, Flanz J, Furutani K, et al. Roadmap: proton therapy physics and biology. Phys Med Biol. 2021; 66(5) doi:10.1088/1361-6560/abcd16

64. O'Reilly D, Sendi MA, Kelly CM. Overview of recent advances in metastatic triple negative breast cancer. World J Clin Oncol. 2021; 12(3):164-82. doi:10.5306/wjco.v12.i3.164

65. Maqbool M, Bekele F, Fekadu G. Treatment Strategies Against Triple-Negative Breast Cancer: An Updated Review. Breast Cancer (Dove Med Press). 2022; 14:15-24. doi:10.2147/bctt.S348060

66. Siddharth S, Sharma D. Racial Disparity and Triple-Negative Breast Cancer in African-American Women: A Multifaceted Affair between Obesity, Biology, and Socioeconomic Determinants. Cancers (Basel). 2018; 10(12) doi:10.3390/cancers10120514

67. Huo D, Ikpatt F, Khramtsov A, Dangou JM, Nanda R, Dignam J, et al. Population differences in breast cancer: survey in indigenous African women reveals over-representation of triple-negative breast cancer. J Clin Oncol. 2009; 27(27):4515-21. doi:10.1200/jco.2008.19.6873

68. Ly M, Antoine M, Dembélé AK, Levy P, Rodenas A, Touré BA, et al. High incidence of triple-negative tumors in sub-saharan Africa: a prospective study of breast cancer characteristics and risk factors in Malian women seen in a Bamako university hospital. Oncology. 2012; 83(5):257-63. doi:10.1159/000341541

69. Siegel SD, Brooks MM, Lynch SM, Sims-Mourtada J, Schug ZT, Curriero FC. Racial disparities in triple negative breast cancer: toward a causal architecture approach. Breast Cancer Research. 2022; 24(1):37. doi:10.1186/s13058-022-01533-z

70. Wilson AJ, Byun DS, Popova N, Murray LB, L'Italien K, Sowa Y, et al. Histone deacetylase 3 (HDAC3) and other class I HDACs regulate colon cell maturation and p21 expression and are deregulated in human colon cancer. J Biol Chem. 2006; 281(19):13548-58. doi:10.1074/jbc.M510023200

71. Huang BH, Laban M, Leung CH, Lee L, Lee CK, Salto-Tellez M, et al. Inhibition of histone deacetylase 2 increases apoptosis and p21Cip1/WAF1 expression, independent of histone deacetylase 1. Cell Death Differ. 2005; 12(4):395-404. doi:10.1038/sj.cdd.4401567

72. Zhu P, Huber E, Kiefer F, Göttlicher M. Specific and redundant functions of histone deacetylases in regulation of cell cycle and apoptosis. Cell Cycle. 2004; 3(10):1240-2. doi:10.4161/cc.3.10.1195

73. Ishihama K, Yamakawa M, Semba S, Takeda H, Kawata S, Kimura S, et al. Expression of HDAC1 and CBP/p300 in human colorectal carcinomas. J Clin Pathol. 2007; 60(11):1205-10. doi:10.1136/jcp.2005.029165

74. Nair S, Engelbrecht M, Miles X, Ndimba R, Fisher R, du Plessis P, et al. The Impact of Dose Rate on DNA Double-Strand Break Formation and Repair in Human Lymphocytes Exposed to Fast Neutron Irradiation. Int J Mol Sci. 2019; 20(21) doi:10.3390/ijms20215350

75. Kachhap SK, Rosmus N, Collis SJ, Kortenhorst MS, Wissing MD, Hedayati M, et al. Downregulation of homologous recombination DNA repair genes by HDAC inhibition in prostate cancer is mediated through the E2F1 transcription factor. PLoS One. 2010; 5(6):e11208. doi:10.1371/journal.pone.0011208

76. Miszczyk J, Rawojć K, Panek A, Borkowska A, Prasanna PGS, Ahmed MM, et al. Do protons and X-rays induce cell-killing in human peripheral blood lymphocytes by different mechanisms? Clin Transl Radiat Oncol. 2018; 9:23-9. doi:10.1016/j.ctro.2018.01.004

77. Ghita - Raileanu M, Straticiuc M, Decebal I, Andrei R-F, Radu M, Bacalum M. Proton irradiation induced reactive oxygen species promote morphological and functional changes in HepG2 cells. Journal of Structural Biology. 2022; 214:107919. doi:10.1016/j.jsb.2022.107919

78. Alan Mitteer R, Wang Y, Shah J, Gordon S, Fager M, Butter P-P, et al. Proton beam radiation induces DNA damage and cell apoptosis in glioma stem cells through reactive oxygen species. Scientific Reports. 2015; 5(1):13961. doi:10.1038/srep13961

79. Gerelchuluun A, Hong Z, Sun L, Suzuki K, Terunuma T, Yasuoka K, et al. Induction of in situ DNA double-strand breaks and apoptosis by 200 MeV protons and 10 MV X-rays in human tumour cell lines. Int J Radiat Biol. 2011; 87(1):57-70. doi:10.3109/09553002.2010.518201

80. Vilalta M, Rafat M, Graves EE. Effects of radiation on metastasis and tumor cell migration. Cell Mol Life Sci. 2016; 73(16):2999-3007. doi:10.1007/s00018-016-2210-5

81. Moncharmont C, Levy A, Guy JB, Falk AT, Guilbert M, Trone JC, et al. Radiation-enhanced cell migration/invasion process: a review. Crit Rev Oncol Hematol. 2014; 92(2):133-42. doi:10.1016/j.critrevonc.2014.05.006

82. Zhou YC, Liu JY, Li J, Zhang J, Xu YQ, Zhang HW, et al. Ionizing radiation promotes migration and invasion of cancer cells through transforming growth factor-beta-mediated epithelial-mesenchymal transition. Int J Radiat Oncol Biol Phys. 2011; 81(5):1530-7. doi:10.1016/j.ijrobp.2011.06.1956

83. Li J, Wu DM, Han R, Yu Y, Deng SH, Liu T, et al. Low-Dose Radiation Promotes Invasion and Migration of A549 Cells by Activating the CXCL1/NF-κB Signaling Pathway. Onco Targets Ther. 2020; 13:3619-29. doi:10.2147/ott.S243914

84. Chen W, Park S, Patel C, Bai Y, Henary K, Raha A, et al. The migration of metastatic breast cancer cells is regulated by matrix stiffness via YAP signalling. Heliyon. 2021; 7(2):e06252. doi:10.1016/j.heliyon.2021.e06252

85. Di Pietro C, Piro S, Tabbì G, Ragusa M, Di Pietro V, Zimmitti V, et al. Cellular and molecular effects of protons: apoptosis induction and potential implications for cancer therapy. Apoptosis. 2006; 11(1):57-66. doi:10.1007/s10495-005-3346-1

86. Feng X, Han H, Zou D, Zhou J, Zhou W. Suberoylanilide hydroxamic acid-induced specific epigenetic regulation controls Leptin-induced proliferation of breast cancer cell lines. Oncotarget. 2017; 8(2):3364-79. doi:10.18632/oncotarget.13764

ANNEXURES

ANNEXURE A: Ethical clearance for 2022- 2024

UNIVERSITEIT VAN PRETORIA
UNIVERSITY OF PRETORIA
YUNIBESITHI YA PRETORIA

Faculty of Health Sciences

Institution: The Research Ethics Committee, Faculty Health Sciences, University of Pretoria complies with ICH-GCP guidelines and has US Federal wide Assurance.

- FWA 00002567, Approved dd 22 May 2002 and Expires 03/20/2022.
- IORG #: IORG0001762 OMB No. 0990-0279 Approved for use through February 28, 2022 and Expires: 03/04/2023.

Faculty of Health Sciences **Research Ethics Committee**

19 January 2022

Approval Certificate
New Application

Dear Ms EN Seane

Ethics Reference No.: 689/2021
Title: Radiosensitising efficacy of histone deacetylase inhibitors CUDC-101 and SAHA in breast cell lines

The **New Application** as supported by documents received between 2022-01-03 and 2022-01-19 for your research, was approved by the Faculty of Health Sciences Research Ethics Committee on 2022-01-19 as resolved by its quorate meeting.

Please note the following about your ethics approval:

- Ethics Approval is valid for 1 year and needs to be renewed annually by 2023-01-19.
- Please remember to use your protocol number (689/2021) on any documents or correspondence with the Research Ethics Committee regarding your research.
- Please note that the Research Ethics Committee may ask further questions, seek additional information, require further modification, monitor the conduct of your research, or suspend or withdraw ethics approval.

Ethics approval is subject to the following:

- The ethics approval is conditional on the research being conducted as stipulated by the details of all documents submitted to the Committee. In the event that a further need arises to change who the investigators are, the methods or any other aspect, such changes must be submitted as an Amendment for approval by the Committee.

We wish you the best with your research.

Yours sincerely

On behalf of the FHS REC, Dr R Sommers
MBChB, MMed (Int), MPharmMed, PhD
Deputy Chairperson *of the Faculty of Health Sciences Research Ethics Committee, University of Pretoria*

The Faculty of Health Sciences Research Ethics Committee complies with the SA National Act 61 of 2003 as it pertains to health research and the United States Code of Federal Regulations Title 45 and 46. This committee abides by the ethical norms and principles for research, established by the Declaration of Helsinki, the South African Medical Research Council Guidelines as well as the Guidelines for Ethical Research: Principles Structures and Processes, Second Edition 2015 (Department of Health)

UNIVERSITEIT VAN PRETORIA
UNIVERSITY OF PRETORIA
YUNIBESITHI YA PRETORIA

Faculty of Health Sciences

Institution: The Research Ethics Committee, Faculty Health Sciences, University of Pretoria complies with ICH-GCP guidelines and has US Federal wide Assurance.

- FWA 00002567, Approved dd 18 March 2022 and Expires 18 March 2027.
- IORG #: IORG0001762 OMB No. 0990-0278 Approved for use through August 31, 2023.

Faculty of Health Sciences **Research Ethics Committee**

19 January 2023

Approval Certificate
Annual Renewal

Dear Ms EN Seane,

Ethics Reference No.: 689/2021 – Line 1
Title: Radiosensitising efficacy of histone deacetylase inhibitors CUDC-101 and SAHA in breast cell lines

The **Annual Renewal** as supported by documents received between 2022-12-05 and 2023-01-18 for your research, was approved by the Faculty of Health Sciences Research Ethics Committee on 2023-01-18 as resolved by its quorate meeting.

Please note the following about your ethics approval:

- Renewal of ethics approval is valid for 1 year, subsequent annual renewal will become due on 2024-01-19.
- Please remember to use your protocol number (689/2021) on any documents or correspondence with the Research Ethics Committee regarding your research.
- Please note that the Research Ethics Committee may ask further questions, seek additional information, require further modification, monitor the conduct of your research, or suspend or withdraw ethics approval.

Ethics approval is subject to the following:

- The ethics approval is conditional on the research being conducted as stipulated by the details of all documents submitted to the Committee. In the event that a further need arises to change who the investigators are, the methods or any other aspect, such changes must be submitted as an Amendment for approval by the Committee.

We wish you the best with your research.

Yours sincerely

On behalf of the FHS REC, Dr R Sommers
MBChB, MMed (Int), MPharmMed, PhD
Deputy Chairperson *of the Faculty of Health Sciences Research Ethics Committee, University of Pretoria*

The Faculty of Health Sciences Research Ethics Committee complies with the SA National Act 61 of 2003 as it pertains to health research and the United States Code of Federal Regulations Title 45 and 46. This committee abides by the ethical norms and principles for research, established by the Declaration of Helsinki, the South African Medical Research Council Guidelines as well as the Guidelines for Ethical Research: Principles Structures and Processes, Second Edition 2015 (Department of Health)

UNIVERSITEIT VAN PRETORIA
UNIVERSITY OF PRETORIA
YUNIBESITHI YA PRETORIA

Faculty of Health Sciences

Institution: The Research Ethics Committee, Faculty Health Sciences, University of Pretoria complies with ICH-GCP guidelines and has US Federal wide Assurance.
- FWA 00002567, Approved dd 18 March 2022 and Expires 18 March 2027.
- IORG #: IORG0001762 OMB No. 0990-0279 Approved for use through June 30, 2025 and Expires 07/28/2026.

Faculty of Health Sciences **Research Ethics Committee**

18 January 2024

Approval Certificate
Annual Renewal

Dear Ms EN Seane,

Ethics Reference No.: 689/2021 – Line 2
Title: Radiosensitising efficacy of histone deacetylase inhibitors CUDC-101 and SAHA in breast cell lines

The **Annual Renewal** as supported by documents received between 2023-12-01 and 2024-01-17 for your research, was approved by the Faculty of Health Sciences Research Ethics Committee on 2024-01-17 as resolved by its quorate meeting.

Please note the following about your ethics approval:

- Renewal of ethics approval is valid for 1 year, subsequent annual renewal will become due on 2025-01-18.
- The Research Ethics Committee (REC) must monitor your research continuously. To this end, you must submit as may be applicable for your kind of research:
  a) annual reports;
  b) reports requested *ad hoc* by the REC;
  c) all visitation and audit reports by a regulatory body (e.g. the HPCSA, FDA, SAHPRA) within 10 days of receiving one;
  d) all routine monitoring reports compiled by the Clinical Research Associate or Site Manager within 10 days of receiving one.
- The REC may select your research study for an audit or a site visitation by the REC.
- The REC may require that you make amendments and take corrective actions.
- The REC may suspend or withdraw approval.
- Please remember to use your protocol number (689/2021) on any documents or correspondence with the Research Ethics Committee regarding your research.

Ethics approval is subject to the following:

- The ethics approval is conditional on the research being conducted as stipulated by the details of all documents submitted to the Committee. In the event that a further need arises to change who the investigators are, the methods or any other aspect, such changes must be submitted as an Amendment for approval by the Committee.

We wish you the best with your research.

Yours sincerely

On behalf of the FHS REC, Dr R Sommers
MBChB, MMed (Int), MPharmMed, PhD
Deputy Chairperson *of the Faculty of Health Sciences Research Ethics Committee, University of Pretoria*

The Faculty of Health Sciences Research Ethics Committee complies with the SA National Act 61 of 2003 as it pertains to health research and the United States Code of Federal Regulations Title 45 and 46. This committee abides by the ethical norms and principles for research, established by the Declaration of Helsinki, the South African Medical Research Council Guidelines as well as the Guidelines for Ethical Research: Principles Structures and Processes, Second Edition 2015 (Department of Health).

pharmaceuticals

MDPI

Review

Introducing HDAC-Targeting Radiopharmaceuticals for Glioblastoma Imaging and Therapy

Liesbeth Everix [1], Elsie Neo Seane [2], Thomas Ebenhan [3,4,5], Ingeborg Goethals [6] and Julie Bolcaen [7,*]

[1] Molecular Imaging Center Antwerp (MICA), University of Antwerp, 2610 Antwerpen, Belgium
[2] Department of Medical Imaging and Therapeutic Sciences, Cape Peninsula University of Technology, Cape Town 7530, South Africa
[3] Pre-Clinical Imaging Facility (PCIF), (NuMeRI) NPC, Pretoria 0001, South Africa
[4] Department of Science and Technology/Preclinical Drug Development Platform (PCDDP), North West University, Potchefstroom 2520, South Africa
[5] Nuclear Medicine, University of Pretoria, Pretoria 0001, South Africa
[6] Department of Nuclear Medicine, Ghent University Hospital, 9000 Ghent, Belgium
[7] Radiation Biophysics Division, SSC laboratory, iThemba LABS, Cape Town 7131, South Africa
* Correspondence: jbolcaen@tlabs.ac.za; Tel.: +27(0)218431217

Abstract: Despite recent advances in multimodality therapy for glioblastoma (GB) incorporating surgery, radiotherapy, chemotherapy and targeted therapy, the overall prognosis remains poor. One of the interesting targets for GB therapy is the histone deacetylase family (HDAC). Due to their pleiotropic effects on, e.g., DNA repair, cell proliferation, differentiation, apoptosis and cell cycle, HDAC inhibitors have gained a lot of attention in the last decade as anti-cancer agents. Despite their known underlying mechanism, their therapeutic activity is not well-defined. In this review, an extensive overview is given of the current status of HDAC inhibitors for GB therapy, followed by an overview of current HDAC-targeting radiopharmaceuticals. Imaging HDAC expression or activity could provide key insights regarding the role of HDAC enzymes in gliomagenesis, thus identifying patients likely to benefit from HDACi-targeted therapy.

Keywords: glioblastoma; histone deacetylases inhibitors; radiopharmaceuticals; theranostics

Citation: Everix, L.; Seane, E.N.; Ebenhan, T.; Goethals, I.; Bolcaen, J. Introducing HDAC-Targeting Radiopharmaceuticals for Glioblastoma Imaging and Therapy. *Pharmaceuticals* **2023**, *16*, 227. https://doi.org/10.3390/ph16020227

Academic Editors: Martina Benešová and Gábor Bakos

Received: 20 December 2022
Revised: 24 January 2023
Accepted: 26 January 2023
Published: 1 February 2023

1. Introduction

Glioblastoma multiforme (GB) is the most malignant tumor in the central nervous system (CNS). Despite recent advances in multimodality therapy for GB incorporating surgery, radiotherapy (RT), chemotherapy and targeted therapy, the overall prognosis remains poor. Almost all tumors recur with a more aggressive form, and there is no standard of care for recurrent GB. The survival rate at 5 years postdiagnosis remains at only 5.8% [1–3]. Novel molecular markers were identified improving GB classification and providing powerful prognostic information [4]. However, therapy resistance remains a hurdle. Precision oncology incorporating personalized targeted therapy holds much promise in developing more efficacious and tolerable therapies [3]. One of the interesting targets for GB-targeted therapy is the histone deacetylase family (HDAC). Due to their pleiotropic effects on, e.g., DNA repair, cell proliferation, differentiation, apoptosis and senescence, they have gained a lot of attention in the last decade as anti-cancer agents. In addition, HDAC inhibitors (HDACi) have been applied for the treatment of metabolic disorders and psychiatric or neurodegenerative diseases [5]. The HDAC family contains 18 family members, categorized as following: class I (HDAC1,2,3,8), IIa (HDAC 4,5,7,9), IIb (HDAC 6,10), III (nicotinamide adenine dinucleotide (NAD+)-dependent sirtuins (SIRTs) and IV (HDAC11) [6,7]. Two groups of enzymes control the acetylation and deacetylation of histones: histone acetyltransferase (HAT) and HDACs. The transfer or removal of acetyl groups by HATs and HDACs induce a more open and accessible chromatin structure or

ANNEXURE C: Certificate of Presentation

CERTIFICATE

OF PRESENTATION

This Certificate is Proudly Present to

Neo Seane

For giving an oral presentation
at
ISRRT World Congress 2024
in conjunction with
Hong Kong Radiographers and Radiation Therapists Conference
on
6 - 9 June 2024

Vincent W. S. Leung, PhD
ISRRT WORLD CONGRESS 2024 CONVENER

ANNEXURE D: Proof of manuscript submission

From: susy@mdpi.com on behalf of Editorial Office
To: Elsie Seane
Cc: Shankari Nair; Charlot Vandevoorde; Alessandra Bisio; Anna Joubert
Subject: [EXTERNAL] [Cancers] Manuscript ID: cancers-3324761 - Submission Received
Date: Monday, November 04, 2024 17:12:21

This message originated from outside your

organization Dear Ms. Seane,

Thank you very much for uploading the following manuscript to the MDPI submission system. One of our editors will be in touch with you soon.

Journal name: Cancers
Manuscript ID: cancers-3324761 Type of manuscript: Article
Title: CUDC-101 and proton irradiation reduces migration and invasion capacity of triple negative breast cell line
Authors: Elsie Neo Seane *, Shankari Nair, Charlot Vandevoorde, Alessandra Bisio, Anna Joubert
Received: 4 Nov 2024
E-mails: seanee@cput.ac.za, shankari.nair.dr@gmail.com, c.vandevoorde@gsi.de, alessandra.bisio@unitn.it, annie.joubert@up.ac.za
Cancer Metastasis
https://www.mdpi.com/journal/cancers/sections/Cancer_Metastasis

We encourage you to provide an Author Biography on this publication's webpage. Please click the following link to find the corresponding instructions and decide whether to accept our invitation:
https://susy.mdpi.com/user/manuscript/author_biography/ef957417671bcaeb0af6a79c0bb020e7

You can follow progress of your manuscript at the following link (login required):
https://susy.mdpi.com/user/manuscripts/review_info/ef957417671bcaeb0af6a79c0bb020e7

The following points were confirmed during submission:
1. Cancers is an open access journal with publishing fees of 2900 CHF for an accepted paper (see https://www.mdpi.com/about/apc/ for details). This manuscript, if accepted, will be published under an open access Creative Commons CC BY license (https://creativecommons.org/licenses/by/4.0/), and I agree to pay the Article Processing Charges as described on the journal webpage (https://www.mdpi.com/journal/cancers/apc). See https://www.mdpi.com/about/openaccess for more information about open access publishing.

Please note that you may be entitled to a discount if you have previously received a discount code, if your institute is participating in the MDPI Institutional Open Access Program (IOAP)(https://www.mdpi.com/about/ioap), or if a society you are a member of is part of our affiliation program(https://www.mdpi.com/societies_partnership). If you have been granted any other special discounts for your submission, please contact the Cancers editorial office.

Annexure E: Statistician letter

Date: 28 / 10 / 2021

LETTER OF CLEARANCE FROM THE BIOSTATISTICIAN

This letter is to confirm that, Elsie Neo Seane from UP

discussed with me the study titled: Radiosensitising efficacy of histone deacetylase inhibitors CUDC-101 and SAHA in breast cell lines

I hereby confirm that I am aware of the project and also undertake to assist, if possible, with the Statistical analysis of the data generated from the project.

The analytical tool(s) that will be used is(are): Parameters from the clonogenic, MTT, Lactate dehyragenase, apoptosis, gamma-H2AX and wound healing assays are continuous and will be summarised by reporting, but may not be limited to, descriptive statistics mean, standard deviation, median and 95%confidence intervals. These parameters will be analysed using an appropriate ANOVA or regression analysis for the observations derived from the 2x6x5 factorial experiments. *Post hoc* analyses will employ the powerful 'margins' statements if data is analysed in Stata Release 17 or late. Should a nonparametric data analysis be necessary ANOVA for ranks may be considered. A suitable transformation may also be sought so as to still do a parametric analysis. Testing will be done at the 0.05 level of significance.
The study will follow an experimental approach using a 2X6X5 factorial design with main effects being the HDCAi, different concentrations of HDACi, and radiation with three repeats and 180 observations. The analysis of variance (ANOVA) will assess the three main effects (HDACi, concentrations, radiations) along with the possible first order interactions and the single second order interaction. The residual mean squares degrees of freedom is 120 and since this exceeds the norm of 30 degrees of freedom; the sample size is adequate.

Signature 

PJ Becker (Tel: 012-319-2203)

Research Office, Faculty of Health Sciences